Hydrophobic Modification of siRNA to Improve Delivery and Efficacy of RNAi Therapeutics

By

Samantha Sarett

Dissertation
Submitted to the Faculty of the
Graduate School of Vanderbilt University
in partial fulfillment of the requirements
for the degree of

DOCTOR OF PHILOSOPHY
in

Biomedical Engineering
May, 2017
Nashville, Tennessee

Approved:

Craig Duvall, Ph.D.

Todd Giorgio, Ph.D.

Jeffrey Davidson, Ph.D.

Scott Geulcher, Ph.D.

Dana Brantley-Sieders, Ph.D.

Copyright © 2017 by Samantha Sarett
All Rights Reserved

ACKNOWLEDGEMENTS

I would like to thank my advisor, Dr. Craig Duvall, whose ideas and expertise shaped this work and whose guidance was central to my progress. I am also grateful for the constant help and encouragement of the members of the Advanced Therapeutics Laboratory at Vanderbilt University. The collaboration and friendship with past and current labmates and peers has been an amazing aspect of my time at Vanderbilt. In particular, accomplishing this work would not have been possible without my co-authors, all of whom have offered invaluable contributions to experiments and scientific discussion. In addition, I would like to thank Dr. Todd Giorgio, Dr. Dana Brantley-Sieders, Dr. Jeffrey Davidson, and Dr. Scott Guelcher as well as the members of their groups for their expertise, guidance, and assistance in my research.

I am grateful to the National Institutes of Health (NIH NIBIB R21EB012750 and R01EB019409) and the National Science Foundation (NSF CAREER BMAT 1349604) for financial support of these studies. I am also thankful for the financial support provided by the National Science Foundation Graduate Research Fellowship Program. I would like to acknowledge the cores and facilities in which portions of this work were performed, including the Vanderbilt Institute for Nanoscale Science and Engineering (VINSE).

TABLE OF CONTENTS

Page

ACKNOWLEDGEMENTS iii

LIST OF TABLES iv

LIST OF FIGURES v

Chapter

1. Introduction 1

1.1 Motivation 1

1.2 Approach: siRNA hydrophobization 3
1.3 Innovation 5
1.4 Specific aims 7

1.5 Outline 10

2. Background 12

2.1 siRNA mechanism 13
2.2 General delivery barriers 14
2.3 Modifications and carriers 15
2.4 siRNA conjugates 18
2.5 Local delivery considerations 23
2.6 Local siRNA delivery for chronic wound treatment 29
2.7 Systemic delivery considerations 35
2.8 Systemic siRNA delivery for cancer treatment 43

3. Conjugation of palmitic acid improves potency and longevity of siRNA delivered via endosomolytic polymer nanoparticles 49

3.1 Abstract 49
3.2 Introduction 50
3.3 Experimental methods 52
3.4 Results 56
3.5 Discussion 64

4. Hydrophobic interactions between polymeric carrier and palmitic acid-conjugated siRNA improve PEGylated polyplex stability and enhance *in vivo* pharmacokinetics and tumor gene silencing 70

4.1 Abstract 70
4.2 Introduction 71
4.3 Experimental methods 75
4.4 Results and discussion 83
4.5 Conclusions 95

5. Lipophilic siRNA targets albumin *in situ* and promotes bioavailability, tumor penetration, and carrier-free gene silencing 97

5.1 Abstract 97
5.2 Significance 98

5.3 Introduction 98
5.4 Methods 102
5.5 Results 110
5.6 Discussion 122

6. Toward development of a hydrophobic siRNA conjugate for local treatment of chronic wounds 126

6.1 Introduction 126
6.2 Materials and methods 128
6.3 Results and discussion 133
6.4 Conclusions 138

7. Synopsis and significance 139

7.1 Summary 139
7.2 Concerns and Limitations 143
7.3 Significance 145
7.4 Future Directions 146
7.5 Conclusion 147

Appendix

A. Supplementary Figures 148
B. Protocols 164

REFERENCES 169

LIST OF TABLES

Table Page

5.1 Key comparisons of siRNA-L_2 vs. siRNA 113

5.2 Key comparisons of siRNA-L_2 vs. *in vivo* jetPEI.....117

S4.1 Table of pharmacokinetic equations used for evaluation of si-NPs and siPA-NPs.....151

S4.2 EC50 values of heparin-dependent si-NP/siPA-NP dissociation 153

S4.3 Table of oligonucleotide sequences used with si-NPs, si-PA NPs.....154

LIST OF FIGURES

Figure Page

2.1 Graphical depiction of selected current siRNA delivery strategies 23

2.2 Schematic depiction of PHD2 activity in normoxia and hypoxia.....31

2.3 Sustained silencing of PHD2 increases angiogenesis within PEUR tissue scaffolds.....34

2.4 Depiction of siRNA-loaded NP interaction with the glomerular basement membrane.....39

2.5 siRNA-loaded NPs often exhibit poor penetration of tumor architecture 47

3.1. Purification of PA-conjugated oligonucleotide 56

3.2 The siRNA-PA conjugate loads into NPs at a lower N:P ratio than unmodified siRNA 57

3.3 siRNA-PA NPs have a larger hydrodynamic diameter than siRNA NPs.....57

3.4 Superior luciferase silencing at a lower N:P ratio with luc-PA siRNA NPs 58

3.5 Luc-PA NPs exhibited superior luciferase silencing vs. luc NPs at a range of doses 59

3.6 PHD2-PA NPs exhibited superior silencing vs. PHD2 siRNA NPs at a range of doses.....60

3.7 siRNA-PA NPs exhibit superior cellular uptake and retention 62

3.8 Uptake of siRNA-PA NPs strongly depends upon macropinocytosis 63

3.9 Luc-PA NPs silenced more effectively and over an increased duration.....64

4.1 Synthesis of siPA and polyplex NPs and schematic of siPA-NP formation 84

4.2 siPA is packaged more efficiently and stably with 50B polymer than unmodified siRNA 85

4.3 *In vitro* characterization of siPA-NPs vs. si-NPs.....87

4.4 Higher stability of siPA-NPs corresponds to greater circulation time, tumor accumulation...91

4.5 siPA-NPs silence luciferase in an orthotopic tumor model, cause no significant toxicity 94

5.1 Successfully synthesized and purified siRNA-L_2 conjugate binds to albumin.....111

5.2 Conjugation of L_2 to siRNA increases circulation half-life, reduces renal clearance 113

5.3. Schematic showing the advantages of siRNA-L_2 over traditional NPs.....114

5.4 siRNA-L_2 achieves superior delivery to PDX snfd orthotopic tumors.....118

5.5 siRNA-L_2 penetrates tumors, is internalized by tumor cells, resulting in gene silencing 121

6.1 Evaluation of PA-modified siRNA as a local RNAi therapeutic for wound healing 134

6.2 “Grafting-to” synthesis of a multivalently hydrophobic siRNA-polymer conjugate 135

6.3 Synthesis efficacy of a multivalently hydrophobic DNA-polymer conjugate.....136

6.4 “Grafting-from” synthesis of a multivalently hydrophobic siRNA-polymer conjugate.....137

S3.1 DNA vs. DNA-PA NPs showed no difference in membrane-disruptive activity.....148

S3.2 Significant increase in cytotoxicity for siRNA NPs using an N:P ratio of 6:1 vs. 4:1.....149

S3.3 No background fluorescence observed in untreated fibroblasts.....149

S4.1 Characterization of 50B polymer.....150

S4.2 DLS size characterization of siPA-NPs vs. si-NPs at a range of N:P ratios.....150

S4.3 Cell internalization of si-NPs and siPA-NPs at N:P = 10:1 151

S4.4 Stability of si-NPs and siPA-NPs in the presence of FBS.....152

S4.5 Comprehensive panel of FRET-based heparin challenge assay.....152

S4.6 PA-modified siRNA improved stability of 50B polyplexes but not 0B polyplexes.....153

S4.7 Enhanced circulation time depends on hydrophobic interactions between siPA and NPs..154

S5.1 Synthesis scheme and HPLC purification of siRNA-L_2.....155

S5.2 *In vitro* characterization of siRNA-L_2 155

S5.3 Albumin binding and degradation characteristics of siRNA-L_2.....156

S5.4 Blood chemistry panel, body weight of mice injected with siRNA-L_2, *in vivo* jetPEI 157

S5.5 Representative images of biodistribution to the organs in tumor-bearing mice.....158

S5.6 In an orthotopic tumor model, absolute radiance per each organ over time.....159

S5.7 In an orthotopic tumor model, fraction of total radiance per each organ over time.....159

S5.8 In a PDX tumor model, biodistribution and liver:tumor ratio evaluation 160

S5.9 Tumor spheroid penetration and cellular uptake of siRNA, siRNA-L_2, *in vivo* jetPEI.....160

S5.10 Representative images and mouse body weight of treated, tumor-bearing mice 161

S6.1. siRNA-loaded polymer nanoparticles induce an inflammatory response 162

S6.2 Confirmation of synthesis of azide-functionalized RAFT CTA.....163

S6.3 NMR spectra showing RAFT polymerization of a p(MPC-co-PFPA).....163

S6.4 NMR spectra confirming modification of p(MPC-co-PFPA) with dodecylamine.....163

CHAPTER 1

INTRODUCTION

Text partially adapted from:

Sarett SM, Nelson CE, Duvall CL (2015). Technologies for controlled, local delivery of siRNA. *Journal of Controlled Release, 218*.

Sarett SM (2014). Conjugation of palmitic acid improves potency and longevity of siRNA delivered via endosomolytic polymer nanoparticles. Unpublished master's thesis, Vanderbilt University, Nashville, Tennessee.

1.1 Motivation

The discovery that double stranded RNA (dsRNA) can trigger catalytic degradation of messenger RNA (mRNA) has inspired more than two decades of research aimed at understanding and harnessing this mechanism[1]. Because well-designed RNA interference (RNAi) therapeutics can potently and specifically suppress translation of any gene, including intracellular targets traditionally considered "undruggable", they have been heavily studied as a potential new class of pharmaceutics that can modulate drug targets that are inaccessible by conventional small molecule inhibitors and antibody drugs[2]. The pathologies of chronic wounds and cancers are particularly well-suited to modulation with RNAi.

Chronic, non-healing wounds are a potentially high-impact target because sites of impaired healing are characterized by widespread changes in gene expression and the extracellular milieu relative to those of normally healing wounds[3-5]. Manipulation of a master

regulator gene, such as that encoding a transcription factor, offers the opportunity to broadly influence the environment at the wound, allowing for a healing and wound closure. Addressing this pathology necessitates localized delivery of RNAi effectors.

Alternatively, cancer is a powerful target for gene silencing because cancer is a wildly heterogenous and rapidly evolving disease[6]. RNAi strategies are extremely versatile because they can be readily adapted to target any genetic sequence[7]. Therefore, these strategies can be easily altered to address cancer's genetic diversity and capacity for drug resistance. Facile treatment of the majority of cancers requires systemic, intravenous delivery of RNAi mediators.

In the development of gene silencing therapeutics, synthetic, double-stranded small interfering RNA (siRNA) has emerged as a leading candidate[8, 9]. siRNA is potentially advantageous in comparison to other RNAi approaches because it can directly load into the RNA induced silencing complex (RISC) machinery, simplifying dosing control and circumventing the requirement for delivery into the nucleus (e.g., as required with shRNA-encoding vectors)[10, 11]. However, emergence of translational siRNA therapies has remained slow, with the primary challenge being the formidable anatomical and physiological barriers that must be overcome to deliver siRNA to its intracellular site of action in target cell types[2].

These barriers are particularly daunting given siRNA's poor pharmacokinetic properties; siRNA has a short half-life *in vivo* due to nuclease degradation, is incapable of effectively translocating the cellular membrane, and faces lysosomal degradation upon endocytosis. Strategies to address these issues are diverse, encompassing a wide range of carriers and conjugates[12]. However, siRNA delivery strategies are accompanied by associated side effects and drawbacks[13]. Identification of effective, potent, and biocompatible siRNA delivery strategies remains a significant challenge, as evidenced by the fact that an siRNA therapeutic has yet to

achieve clinical approval. Thus, investigation of alternative and novel strategies to improve siRNA's pharmacokinetic profile is a highly impactful pursuit.

1.2 Approach: siRNA hydrophobization

Optimized polymeric and lipid carriers can protect the siRNA against degradation and transport it into the cell[14], and the incorporation of endosomolytic moieties in these systems can also facilitate endosomal escape[15]. Encapsulation of siRNA into nanocarrier delivery vehicles is typically driven by electrostatic condensation of anionic siRNA with polycationic polymers or lipids. These polyelectrolyte formulations are hampered by poor stability *in vivo*, as they are prone to disassembly in the presence of serum proteins and during renal filtration[16-18]. Additionally, these carrier systems can elicit an immune response and cytotoxicity at high concentrations[13]. Increasing gene silencing potency and enabling the use of lower doses of the delivery system enhances the likelihood of siRNA's therapeutic application. A promising strategy to accomplish this aim is via hydrophobization of the carrier or of the siRNA itself.

Increasing the hydrophobicity of cationic polymer-based siRNA delivery systems has been shown to correspond to improvements in gene silencing. Hydrophobization of the cationic carrier poly(ethylene imine) (PEI) via conjugation of lipids to the polymer maintains silencing efficacy while reducing cytotoxicity, although the lipid chains begin to negatively impact gene silencing at a threshold chain length[19]. Additionally, more hydrophobic poly(β-amino ester) (PBAE)-based delivery vehicles were shown to achieve greater transfection than comparable counterparts[20]. Further, optimizing the ratio of hydrophobic and cationic content of an siRNA-loaded polymer nanoparticle conferred enhanced nanoparticle stability and gene silencing potency[21]. These studies demonstrate that incorporating hydrophobic components within the

nanocarrier, thereby facilitating hydrophobic interactions within the delivery vehicle, can allow for improved therapeutic efficacy. A logical extension of incorporation of hydrophobic moieties into the nanocarrier is to hydrophobize the siRNA cargo.

Hydrophobic modification of the siRNA cargo allows enhanced loading into nanocarriers, as encapsulation is driven not solely by electrostatic interactions but also by hydrophobic interactions between the siRNA molecules or with hydrophobic carrier components. Incorporation of siRNA conjugated to cholesterol into cationic lipoplexes resulted in lipoplexes with improved loading efficiency, stability, and circulation time compared to lipoplexes loaded with unmodified siRNA[22]. The potential benefits derived from dual hydrophobization of siRNA cargo and delivery vehicle components have yet to be fully explored. Most strategies of this nature exclusively explore siRNA-cholesterol, and modulation of the hydrophobic moiety is an attractive area for investigation.

Hydrophobization of the siRNA has also shown therapeutic efficacy without a nanocarrier delivery system. The drawbacks of conventional cationic nanocarriers, including toxicity at high doses, preferential uptake and clearance by the mononuclear phagocyte system (MPS), and a large size that limits broad tissue penetration, have prompted investigation of siRNA conjugates that enable reduction or elimination of the nanocarrier component. Lipid-conjugated siRNA has been explored as a means of gene silencing without an additional carrier[23, 24]. Hydrophobic modification of siRNA with lipidic moieties imparts resistance to degradation by nucleases and facilitates increased interaction with the cellular membrane, improving siRNA uptake[25, 26]. Additionally, the biocompatibility and physiological relevance of lipids allows modified siRNA to leverage endogenous lipid trafficking mechanisms. For example, cholesterol-siRNA associates with high and low density lipoproteins in serum, which naturally distribute to

the liver, and carrier-free hepatic gene silencing has been achieved with siRNA-cholesterol conjugates[27, 28].

Palmitic acid (PA) conjugation was found to be a superior modification for siRNA compared to cholesterol, various aromatic groups, and additional lipidic moieties[29, 30]. Specifically, PA conferred increased stability to siRNA while also enhancing cellular penetration and gene silencing beyond that achieved via other hydrophobic modifications[25, 26]. While siRNA-PA exhibited some silencing activity without a carrier system, it was most efficacious in combination with the commercial lipidic vector Lipofectamine 2000. Importantly, the development of siRNA conjugates that effect potent gene silencing in non-hepatic tissues remains an unmet need. Evaluation of a more diverse set of hydrophobic molecules for siRNA conjugation will provide further insight and allow development of more successful therapeutic approaches.

1.3 Innovation

To date, exploration of siRNA conjugates has been less extensive than investigation into nanocarrier-based delivery strategies. As discussed, achieving silencing in non-hepatic targets remains a significant challenge and limits the applicability of previously reported siRNA conjugates. Investigation of novel, strategically chosen hydrophobic moieties for siRNA modification will allow development of superior siRNA conjugates for 1) local delivery from biomaterial scaffolds for regenerative medicine applications and 2) systemic, intravenous delivery for cancer therapies.

Effective local siRNA delivery from a biomaterial scaffold requires an siRNA conjugate system that impacts potent gene silencing, maintains high biocompatibility, and exhibits

sustained release from the scaffold. As mentioned, monovalent hydrophobic modification of siRNA with PA improves stability, cellular uptake, and silencing potency beyond unmodified siRNA[25]. Additionally, PA modification is expected to enable greater retention of siRNA in partially hydrophobic biomaterial scaffolds. Thus, siRNA-PA is a promising candidate for a local, scaffold-based delivery application. However, monovalent hydrophobic modification of siRNA may not be sufficient to induce potent carrier-free silencing; previous reports utilized a high (micromolar dose) in *in vitro* studies. Combination of siRNA-PA with a polymer nanocarrier system is a unique alternative to its carrier-free use that could improve the potency of the delivery system. Alternatively, a rational strategy to address the potential shortcoming of monovalently hydrophobic siRNA-PA is a multivalently hydrophobic siRNA conjugate, which to date has never been evaluated. A multivalently hydrophobic siRNA conjugate is hypothesized to facilitate stronger hydrophobic interactions with the cell membrane and the biomaterial scaffold, promoting enhanced cellular uptake and scaffold retention, respectively. Development of a multivalently hydrophobic siRNA conjugate is a wholly novel approach that could have broad utility in local, scaffold-based RNAi therapies, which currently show immense promise in regenerative medicine.

Designing an optimal siRNA conjugate for intravenous administration requires consideration of the delivery challenges unique to systemic delivery. Of particular concern is the rapid renal clearance of unmodified siRNA, which has a circulation half-life of less than 2 minutes. Leveraging endogenous proteins as chaperons for siRNA could extend the circulation half-life of siRNA. It has been noted that cholesterol- and α-tocopherol-modified siRNA associates with serum lipoproteins[24, 27], whose physiological role is transportation of these molecules. While lipoproteins deliver their cargo primarily to the liver, the most abundant serum

protein albumin, a natural fatty acid carrier, does not target a specific organ. Thus, albumin's extremely prolonged circulation time (on the order of weeks)[31] could facilitate distribution of siRNA to a non-hepatic target. We have identified a hydrophobic moiety that binds albumin with high affinity, and hypothesize that conjugation of the albumin-binding moiety to siRNA will broadly enhance its pharmacokinetic properties. Albumin has been investigated extensively as a carrier and a conjugate for small molecules as well as protein therapeutics; albumin-based therapeutics like Abraxane, Levemir, and Optison have achieved clinical relevance[31, 32], demonstrating the translatability of this approach. However, no one has investigated non-covalent, *in situ* targeting of siRNA to albumin for non-hepatic delivery. The application of albumin-binding siRNA to cancer is particularly promising due to the unique tumor microenvironment and the propensity for rapidly-growing tumor cells to internalize albumin[33]. An albumin-binding siRNA conjugate is anticipated to allow for the first demonstration of *in vivo*, carrier-free gene silencing at a non-hepatic target site.

Taken together, the proposed mono- or multivalently hydrophobic siRNA conjugate for local delivery and albumin-binding siRNA conjugate for systemic delivery are unique approaches to address the delivery barriers limiting RNAi therapy development. Development and investigation of these conjugates carrier-free and in concert with polymer nanocarriers will be a strong contribution to a growing knowledge base that will enable the translation of siRNA therapeutics to the clinic.

1.4 Specific aims

The overall goal of this project is to broaden the therapeutic index of small interfering RNA (siRNA) therapies by developing siRNA conjugates that enable potent and sustained gene

silencing while maintaining high treatment biocompatibility. We hypothesize that siRNA conjugation with mono- or multivalent hydrophobic moieties will improve siRNA's pharmacokinetic properties, notably stability, cellular uptake, bioavailability, and potency/longevity, resulting in enhanced therapeutic efficacy and facilitating clinical translation of RNAi therapies. We evaluate this hypothesis through completion of the following aims:

Specific Aim 1: *Synthesize an siRNA-palmitic acid (PA) conjugate and evaluate in combination with nanoparticle carriers* in vitro *for application to local, systemic delivery strategies.* Conjugation of siRNA to palmitic acid (PA) has been found to be superior to various aromatic groups and additional lipidic moieties in potentiating siRNA gene silencing efficacy and cellular internalization. siRNA conjugated to PA or unmodified siRNA will be packaged into our established polymer nanoparticle (NP) systems optimized for local or systemic delivery. We will evaluate cellular uptake and gene silencing in cells relevant to local delivery-focused, regenerative medicine applications (mouse fibroblasts (NIH-3T3s) and mesenchymal stem cells (MSCs)) as well as in cells relevant to systemic delivery-focused, cancer treatment applications (the triple negative human breast cancer cells MDA-MB-231s and MCF7s). Additionally, we will investigate the loading capacity and resistance to disassembly of NPs incorporating siRNA-PA. We anticipate that siRNA-PA will act synergistically with polymer NP systems to enhance silencing potency and longevity overall while reducing the required polymer dose, thereby broadening the therapeutic index of these treatment strategies.

Specific Aim 2: *Synthesize siRNA conjugated to strategically-chosen hydrophobic moieties and evaluate carrier-free* in vitro *for application to local, systemic delivery strategies.* Both lipidic

vectors and cationic polymers can provoke the induction of inflammatory cytokines and interferon responses, and cationic delivery vehicles are known to cause toxicity associated with their high surface charge. Reducing or eliminating the need for a nanocarrier is thus a highly impactful pursuit. For local delivery applications, we propose to conjugate siRNA to a copolymer containing the reactive group pentafluorophenyl acrylate (PFPA), which allows for decoration of the polymer with multiple hydrophobic moieties. In contrast to the single PA molecule on siRNA-PA, the higher concentration of hydrophobic molecules on the polymer-siRNA conjugate is anticipated to facilitate greater and sustained interaction with the cellular and endolysosomal membranes. We will synthesize and characterize the multivalent siRNA-polymer conjugate. For systemic delivery applications, we have identified a divalent lipid moiety that binds to albumin. We hypothesize that conjugation to this albumin-binding moiety will allow siRNA to leverage albumin as an endogenous nanocarrier and enhance its pharmacokinetic properties. We will evaluate albumin-binding siRNA's stability, *in vitro* cellular uptake in MDA-MB-231s and MCF7s, and circulation half-life and biodistribution in CD31 mice. The studies described in aims 1 and 2 will result in identification of lead siRNA conjugate systems for both local and systemic delivery applications.

Specific Aim 3: *Investigate lead siRNA conjugate systems* in vivo *in therapeutically-relevant models for local, scaffold-based delivery at sites of impaired wound healing and systemic, intravenous delivery to tumors.* In the local delivery setting, siRNA designed against prolyl hydroxylase 2 (PHD2) and delivered in nanoparticles from a biodegradable scaffold has shown promise for treatment of chronic wounds. Additionally, we have previously established the capacity of poly(thioketal) urethane (PTK-UR) scaffolds to promote wound healing. After

identifying a lead siRNA conjugate-based therapeutic for local delivery, we will incorporate the therapeutic into PTK-UR scaffolds, and assess its efficacy *in vivo* in previously established models of impaired wound healing (rat ischemic wound models). We will evaluate PHD2 silencing via real time RT-PCR and blood vessel development and tissue ingrowth via histological staining. In the systemic delivery setting, nanocarrier-based delivery of RNAi cancer therapies has proven complex and challenging. We will identify a lead siRNA conjugate for systemic delivery and assess it *in vivo* in orthotopic and patient-derived xenograft triple negative breast cancer models in mice. We will evaluate silencing of a model gene, distribution to tumors, and penetration and uptake at the site of tumors. These investigations will yield valuable insight into the therapeutic efficacy and translatability of our siRNA conjugate-based therapies in the pathologies of chronic wounds and cancer.

In summary, the principal goal of this work is to develop siRNA conjugate-based delivery systems that are optimized for 1) local, biomaterial scaffold-based delivery for treatment of chronic wounds or 2) systemic, intravenous delivery for cancer treatment. We anticipate that these siRNA conjugate-based systems will reduce immunogenic effects related to conventional siRNA transfection strategies while maintaining potent and sustained gene silencing. This combination will broaden the therapeutic index of the RNAi therapies, enhancing the probability of clinical success and translation.

1.5 Outline

This dissertation describes the development of hydrophobically-modified siRNA conjugates and their evaluation for therapeutic efficacy in local and systemic delivery platforms.

Chapter 1 provides the motivation for this work and brief introductory information and outlines the specific aims that will be addressed. Chapter 2 details comprehensive background information on the characteristics and mechanism of action of siRNA, barriers that impede siRNA's delivery to its target site (encompassing general barriers as well as those specific to local and systemic delivery), and existing strategies to improve siRNA's delivery. Background is also given on the two therapeutic focuses of this work, chronic wounds and cancer. Chapter 3 describes the evaluation of siRNA modified with the lipid palmitic acid (siRNA-PA) in combination with a polymer nanoparticle carrier system tailored to local delivery applications for gene silencing potency and longevity. Chapter 4 expands upon the utility of siRNA-PA through investigation in concert with nanoparticles designed for intravenous administration, with a focus on pharmacokinetics, physiological stability, and gene silencing in tumors. Chapter 5 details the development of a novel albumin-binding, lipid-based siRNA conjugate (siRNA-L_2) and its evaluation carrier-free as a potentially transformative oncological therapeutic. Chapter 6 explains the strategy and progress in synthesis of siRNA conjugated to a multivalently hydrophobic polymer for use in local RNAi therapies. Finally, Chapter 7 concludes this work with a broad summary and assessments of its significance, possible limitations, and promising futures directions.

CHAPTER 2

BACKGROUND

Text partially adapted from:

Sarett SM, Nelson CE, Duvall CL (2015). Technologies for Controlled, Local Delivery Of siRNA. *Journal of Controlled Release, 218.*

Sarett SM (2014). Conjugation of Palmitic Acid Improves Potency and Longevity of siRNA Delivered via Endosomolytic Polymer Nanoparticles. Unpublished master's thesis, Vanderbilt University, Nashville, Tennessee.

Sarett SM, Werfel TA, Jackson MA, Kilchrist KV, Brantley-Sieders D, Duvall CL (2017). Lipophilic siRNA Targets Albumin in Situ and Promotes Bioavailability, Tumor Penetration, and Carrier-Free Gene Silencing. *PNAS, Under review.*

Sarett SM, Werfel TA, Chandra I, Jackson MA, Kavanaugh TE, Hattaway ME, Giorgio TD, Duvall CL (2016). Hydrophobic Interactions between Polymeric Carrier and Palmitic Acid-Conjugated siRNA Improve PEGylated Polyplex Stability and Enhance *In Vivo* Pharmacokinetics and Tumor Gene Silencing, *Biomaterials, 97.*

Sarett, SM, Kilchrist, KV, Miteva, M, Duvall, CL (2015). Conjugation of Palmitic Acid Improves Potency and Longevity of siRNA Delivered via Endosomolytic Polymer Nanoparticles. *Journal of Biomedical Materials Research Part A, 103*.

2.1 siRNA mechanism

The molecular phenomenon of RNAi-based post-transcriptional gene silencing, first termed "reversible co-suppression", was unraveled following the unexpected observation by Napoli et al. in 1990 that introduction of a transgene intended to overexpress chalcone synthase (CHS, a gene for flower pigmentation) yielded more white flowers and was associated with a 50-fold reduction of CHS mRNA[34]. The gene silencing capability of antisense oligodeoxynucleotides (ODNs) was first elucidated, but it was discovered soon thereafter that double-stranded RNA (dsRNA) are capable of achieving 100 to 1000-fold more potent gene suppression than ODNs[35]. The delivery of dsRNA of varying lengths, siRNA, short hairpin RNA (shRNA), and plasmids expressing shRNA can trigger gene-specific silencing, which is optimal when there is full complementarity between the guide strand and the target mRNA sequence[9, 36]. These synthetic dsRNA molecules are more effective than ODNs because they "hijack" the catalytically-active gene silencing machinery that is integral to endogenous, negative feedback pathways utilized by naturally expressed microRNA (miRNA)[9, 37, 38].

When larger dsRNA are delivered to the cellular cytoplasm, they are cleaved by the enzyme Dicer into siRNA, which are 19-21 nucleotides in length and characterized by 3' nucleotide overhangs. The siRNA strands are then separated, and the antisense or guide strand, recognized by a less stable 5' end, is incorporated into the RNA-induced silencing complex (RISC)[39]. The activated RISC loaded with the siRNA guide strand binds to complementary mRNA and initiates its degradation. When siRNA binds completely to mRNA, it facilitates RISC-mediated cleavage of the mRNA. However, if siRNA binds partially to the mRNA it can block translation to protein without mediating cleavage[7, 40]. Fully complementary binding is important because the activated RISC has enzymatic activity, enabling a single siRNA to elicit

the degradation of multiple mRNAs[41]. In contrast, synthetic microRNA (miRNA) often modulate multiple mRNA targets with partial complementarity and thus can influence larger systems of genes[42]. While the coordinated control of multiple, related genes through miRNA therapeutics is a powerful strategy, properly designed siRNA-based therapeutics are desirable because they offer more predictable functional effects based on modulation of specific genes.

2.2 General delivery barriers

While discovery and development of small molecule drugs for clinical use remains an enormous challenge, the translation of siRNA therapeutics is fully unchartered. Thus, in addition to traditional drug development challenges, the "normal" pipeline for development of an siRNA drug for FDA clearance has yet to be established[43, 44]. The major difficulty faced when designing siRNA therapeutics is that of delivery to its site of action; synthetic dsRNA or siRNA molecules have relatively poor pharmacokinetic properties and thus face more formidable extracellular and intracellular delivery challenges relative to small molecule drugs. Oral bioavailability of siRNA molecules is very poor because they are relatively large, hydrophilic, and susceptible to degradation, and systemic, intravenous delivery of siRNA results in rapid renal filtration and clearance through the urine[14]. siRNA also has a short half-life *in vivo* and can be degraded by nucleases, especially if optimized chemical modifications are not incorporated onto the siRNA molecule[45]. Furthermore, siRNA does not readily translocate lipid bilayers, such as those that constitute the outer cellular membrane and the endo-lysosomal intracellular vesicles. The latter can cause siRNA that has been internalized by target cells to be degraded within lysosomes or exocytosed, rather than becoming bioavailable for interaction with the RISC machinery in the

cytosol[14, 46, 47]. For example, in the absence of a mechanism for endosomal escape, only 1-2% of the siRNA delivered by lipid nanoparticles is believed to be released into the cytosol and to be bioavailable for RISC loading and target gene silencing. There are a variety of delivery systems under development for overcoming these systemic and general delivery barriers[14], but there remains a need to optimize the biocompatibility and therapeutic efficacy of these systems.

Utilization of siRNA therapeutically is complicated by the potential for toxicity and immunogenicity of both the siRNA molecules and the carriers used. siRNA molecules can activate Toll-like receptors (TLRs), which are a part of the innate immune system that recognizes and mounts an immune response against microbial invaders[48-52]. Additionally, siRNA can elicit off-target effects due to partial sequence complementarity to unintended genes or by saturating the cell's RISC machinery, altering endogenous miRNA gene regulatory processes[51, 53, 54]. Furthermore, systems used to deliver siRNA can induce toxic and immunogenic consequences[14]. These inadvertent effects can override therapeutic benefits and convolute interpretation of experiments designed to test the functional significance of siRNA therapeutics[55]. These challenges highlight the need for diverse approaches to siRNA delivery that facilitate isolation of confounding variables.

2.3 Modifications and carriers

A variety of chemical modifications, conjugation strategies, and lipid/polymer carriers have been identified to address the challenges inherent to siRNA therapies. A commonly-utilized chemical modification to siRNA molecules is replacement of phosphodiester linkages with phosphorothioate linkages at select locations on the backbone, which confers improved

resistance of siRNA to nuclease degradation[45, 56, 57]. Further, modifications to the siRNA backbone at the 2' position, such as 2'-O-methyl, endow siRNA molecules with greater stability and eliminate the TLR-driven immune response without impacting silencing efficacy[45, 56, 58, 59]. Careful siRNA sequence selection can also aid in avoiding modulation of non-targeted genes and enhance the activity at the targeted gene. Systematic, computer-aided optimization of siRNA sequence and design has become standard practice and accelerates identification of siRNA sequences likely to exhibit high target gene silencing with minimal off-target effects and immunogenicity[45, 51].

While optimization of siRNA sequence and chemical modifications can improve upon safety and efficacy, siRNA activity benefits from delivery via a carrier system in most applications. These carriers typically improve stability against nucleases and enhance cellular penetration capacity and/or endosomal escape; thus, siRNA formulation into nanocarriers is often utilized synergistically with systems for localized, sustained delivery[14]. siRNA carriers vary widely but commonly consist of lipids/liposomes, polymers, or viral constructs[12, 14, 60-62]. Transfection with lipids/liposomes is the most broadly utilized technique, with a variety of commercial reagents available that can facilitate fusion with and transport across cellular membranes[12, 14, 63]. Similarly, cationic polymers and dendrimers are conventionally used for siRNA packaging, protection, and delivery. Synthetic polymers such as linear or branched PEI, poly(L-lysine), poly(amidoamine) (PAMAM) dendrimers, PBAEs, poly(dimethylaminoethylmethacrylate) (pDMAEMA), and histidine and/or imidazole containing copolymers, as well as natural polymers like atelocollagen and chitosan, are among the most extensively utilized[14, 64-70]. These cationic polymers electrostatically package/protect siRNA and

in some cases, contain secondary and tertiary amines that enable endosomal escape via the proton sponge effect[64].

Other polymers have also been developed that have active membrane-disruptive behavior triggered by the slightly acidic pH of the endo-lysosomal pathway. These polymer-based systems have been utilized primarily to form siRNA nano-formulations with actively endosomolytic cores and have been combined with a variety of micelle/polyplex surface chemistries[21, 70-73]. Several of these systems leverage a poly(DMAEMA-*co*-butyl methacrylate-*co*-propylacrylic acid (PAA) polymer block that is approximately charge-neutral and forms a stable micelle core at physiologic pH. When exposed to a more acidic pH, the DMAEMA and PAA monomers become concurrently more protonated, yielding a net cationic state that triggers micelle destabilization and endo-lysosomal membrane interaction/disruption[70].

Cationic lipids and polymers have a number of shortcomings that are gradually being addressed through both rational design and high throughput synthesis/screening approaches. Traditional cationic transfection reagents generally provoke the induction of inflammatory cytokines and interferon responses, especially at high concentrations, resulting in cytotoxicity. Additionally, these carriers often suffer loss of activity in serum and salt-containing environments. Adsorption of proteins to the particle surface prompts aggregation and/or clearance by cells of the MPS, and the presence of counterions destabilizes polyelectrolyte nanoparticles, inducing their disassembly. Additionally, while the nanocarrier should remain stable in the extracellular environment, the siRNA must be released from the packaging system intracellularly in order to ensure efficient incorporation into the RISC complex[14, 17]. Recent and ongoing research addresses these concerns; bioreducible, biodegradable, and environmentally-responsive polymers and PEGylation strategies can be utilized both to reduce cytotoxicity and to

incorporate mechanisms of siRNA release[14, 66, 73-75]. While these strategies have led to dramatic improvements in efficacy compared to early generation nanocarriers, their synthetic complexity presents another substantial barrier to clinical translation.

2.4 siRNA conjugates

Direct conjugation to molecules such as polymers, peptides, lipids, antibodies, and aptamers is another strategy for facilitating siRNA silencing efficacy in a non-toxic manner[12, 60, 76]. Conjugation of targeting ligands, antibodies, or aptamers to siRNA has shown promise as a means to facilitate receptor-mediated, cell-specific uptake. For example, Alnylam demonstrated the *in vivo* silencing efficacy of trivalent *N*-acetylgalactosamine (GalNAc) siRNA conjugates and showed hepatocyte-specific uptake when delivering the conjugates carrier-free[77, 78]. Akin to Alnylam's other therapies, this siRNA conjugate relies upon the natural trafficking of injected therapeutics to the liver and is not readily translatable to non-hepatic pathologies.

With respect to antibodies, the bulk of prior research has concentrated on conjugation to the siRNA delivery vehicle[79, 80]; however, Cuellar et al. focused on direct antibody conjugation to siRNA. Their studies comprehensively evaluated seven siRNA-antibody conjugates, investigating each with and without a delivery carrier, with reducible and non-reducible linkage sites, and in cell lines with a range of antigen expression[81]. Of those investigated, only two exhibited carrier-free silencing at doses up to 500 nM, and the silencing achieved was lower than that achieved in conjunction with a lipid-based carrier. Lack of an endosomal escape mechanism was identified as a critical barrier to vector-free siRNA-antibody efficacy. Aptamers are an alternate targeting strategy, and aptamers directly fused to siRNA showed increased stability and

moderate gene silencing at sub-micromolar doses without the use of a transfection reagent[82]. Notably, this approach requires complex production methods, limiting its potential utility.

Another option for siRNA conjugation is that of cell-penetrating peptides (CPPs). CPPs, like the HIV-derived Tat peptide and penetratin, have emerged as potent cellular membrane translocators, but they are also associated with concerns regarding cytotoxicity and immunogenicity[83, 84 85-87]. Additionally, the positive charge on CPPs can complicate their use as a conjugation-based strategy for siRNA due to the formation of aggregates that act as vectors similar to larger carrier vehicles. This phenomenon also convolutes gene silencing effects attributed to distinct CPP-siRNA conjugates.

The strategy of coupling a peptide ligand to siRNA avoids many of the problems associated with CPP-conjugated siRNA, and the conjugation of siRNA to the cell-binding motif RGD was shown to both increase cellular uptake and facilitate gene silencing at low siRNA doses [88]. However, the gene silencing efficacy of RGD-modified siRNA was explored solely in a melanoma cell line engineered to overexpress the αvβ3 receptor that RGD bind; it would be crucial to confirm this conjugate's efficacy in cells expressing physiologically relevant levels of αvβ3. αvβ3 is of interest due to its high binding affinity for RGD and its common overexpression on cancerous cells[89]. Significantly, siRNA conjugated to divalent RGD was ineffective at silencing gene expression, while siRNA conjugated to tri- and tetravalent RGD had similar and impressive silencing effects. As cellular uptake was similar between di- and multivalent conjugates, the reason for this difference is undetermined but is perhaps linked to cellular internalization[88]. These results indicate the significant impact of valency on cellular association and other physiological interactions. Distinct from both CPP- and integrin-based approaches is identification of a peptide with desired cellular specificity and penetration via phage display, as

was accomplished by Hsu et al.; their siRNA-peptide conjugate penetrated the skin and achieved *in vivo* silencing of >40% at 10 μM in a mouse model. While the capability to penetrate skin is exciting, the high dose requirement is a drawback[90].

siRNA conjugation has also been achieved with more complex biologic molecules, such as cationic moieties and polymers. Unfortunately, siRNA modified with cationic moieties, for example oligospermine, induces charge-based toxicity at higher doses[91]. While a combination of both oligospermine and cholesterol was effective at improving biocompatibility, synthesis of these conjugates requires multiple steps resulting in low yield[92]. Improved synthesis and purification methods for cationic siRNAs allowed for silencing at lower doses and therefore limited toxic side effects; however, these measures add further steps before obtaining the final product and again result in a low final yield[93]. The potential for toxicity, the low yields, and the complications and expense associated with cation-conjugated siRNA present major barriers to their widespread use.

Another effective, though complex, approach was described for the conjugation of siRNA to a synthetic anionic polymer via a maleic acid amide (MAA) linkage that enabled endosomal disruption and release of single siRNA molecules into the cytoplasm[94]. siRNA was conjugated to maleic acid amide at a very high efficiency using a one-step reaction, and siRNA release was triggered at acidic pH via hydrolysis of MAA[94], directly addressing the endosomal escape barrier. However, the siRNA-polyanion constructs required packaging with a polycation into a polyion complex to achieve gene silencing[94]. Additionally, in this system the hydrolysis of MAA would yield a free amine group; while no cellular toxicity was seen at the doses used, this could pose a problem at higher concentrations. siRNA conjugated to a diverse range of PEG architectures has also been explored in conjunction with a range of cationic delivery agents[95-97].

These approaches demonstrate the feasibility and potential utility of polymer-siRNA conjugates. However, those investigated to date have necessitated combination with a transfection aid to achieve potent gene knockdown.

A leading strategy for siRNA modification is conjugation with lipid-like moieties such as cholesterol, α-tocopherol, and palmitic acid. These modifications hydrophobize the siRNA and can dramatically improve its pharmacokinetic properties, resulting in enhanced silencing activity when coupled to nanocarriers or delivered carrier-free[24, 25, 98]. These conjugations increase siRNA nuclease resistance and enhance cellular internalization (by facilitating interaction with the cellular membrane) without detrimentally impacting gene silencing activity[25, 30]. Conjugation to cholesterol and α-tocopherol have demonstrated some potential for use without a cationic delivery agent, as these modifications improve stability against nuclease degradation as well as cellular internalization. Notably, a variant of cholesterol-conjugated siRNA is commercially marketed as a gene-silencing agent for use without a transfection reagent[23, 24, 26, 27, 85, 99]. However, cholesterol and α-tocopherol-conjugated siRNA require high doses (micromolar) before a gene silencing effect can be observed, and the gene silencing of these conjugates can depend on pre-incubation with lipoproteins that associate with the lipophilic moieties of the siRNA to facilitate uptake [27, 100, 101]. The lipoproteins naturally distribute to the liver, limiting the relevance of these conjugates for non-hepatic pathologies.

Conjugation of palmitic acid (PA) to siRNA has shown particular promise as a modification strategy to improve siRNA stability, cellular penetration, and gene silencing[30]. PA is an endogenous post-transcriptional modification commonly found on membrane-associated signaling proteins; while PA is involved in a wide variety of cellular functions, it is especially believed to influence protein-membrane interactions as well as protein uptake and intracellular

trafficking[102-104]. Motivated by the inherent effects of PA on membrane binding and translocation, PA-modified siRNA has been recently tested as an approach to enhance gene silencing in comparison to unmodified siRNA or siRNA conjugated to cholesterol in cancer cell lines *in vitro*[25, 30]. In these studies, PA conjugation was demonstrated to enhance knockdown of siRNA delivered via Lipofectamine 2000 (a commercial transfection reagent with established cytotoxicity) and also to enable some gene silencing in the absence of a transfection reagent at high (micromolar) doses[13, 25]. The superior cellular internalization and gene silencing efficacy of siRNA-PA relative to siRNA conjugated with cholesterol and various aromatic and lipidic moieties[29, 30] makes PA a logical choice for further investigation of hydrophobized siRNA.

Lastly, a unique strategy for *in situ* conjugation of siRNA has been described by Lau et. al., in which maleimide-functionalized siRNA binds endogenously to circulating albumin. This conjugation strategy is notable for its simplicity and for its capacity to improve the circulation half-life compared to non-functionalized siRNA. However, this strategy for intravenous RNAi was not applied to a particular pathology and in proof-of-concept work elicited moderate (~35%) gene silencing solely in the heart after four 1 mg/kg doses (the liver, spleen, and aorta were also investigated but displayed no significant silencing). This study is highly significant, as it is the first to demonstrate *in vivo*, non-hepatic, carrier-free siRNA silencing. It reveals the immense promise of leveraging albumin as an endogenous chaperone for siRNA and motivates further investigation tailored to a therapeutic application.

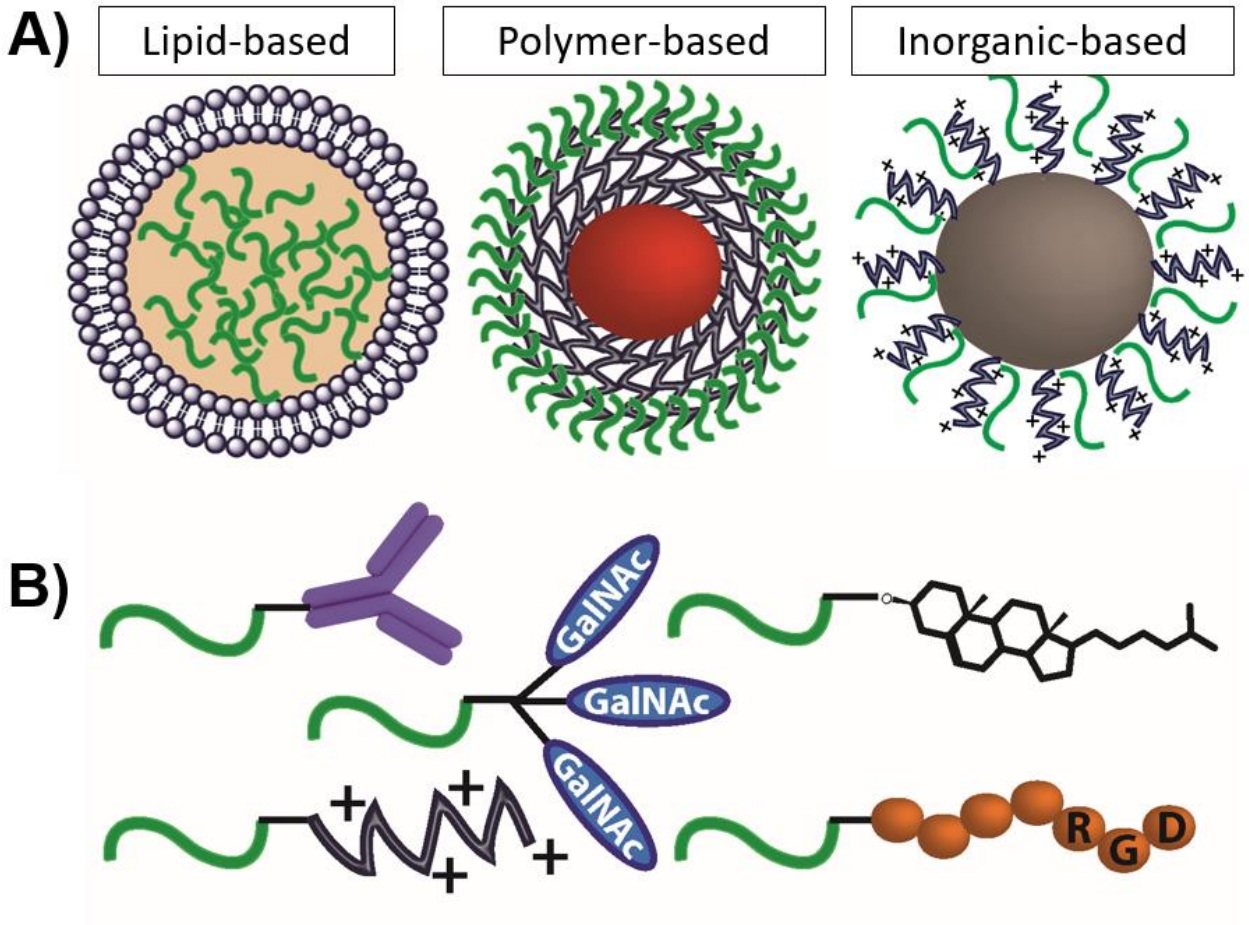

Figure 2.1. A) Depiction of common cationic delivery vehicles; from left to right, depiction of a liposome as a lipid-based carrier, depiction of a polymer nanoparticle as a polymer-based carrier, and depiction of a polymer-decorated iron oxide nanoparticle as an inorganic-based carrier. B) Depiction of several siRNA conjugates in development; top left: siRNA-antibody, middle: siRNA-GalNAc, top right: siRNA-cholesterol, bottom left: siRNA-cationic polymer, bottom right: siRNA-RGD.

2.5 Local delivery considerations

The broad delivery challenges of siRNA, as well as leading strategies to circumvent these challenges, have been discussed above. The proposed development of siRNA conjugates for 1) local and 2) systemic delivery necessitates further elucidation of the particular barriers and advantages characteristic of each situation.

Local delivery of siRNA emerged as a logical aim for the first forays into therapeutic application of siRNA. Delivering siRNA directly to its site of action circumvents substantial systemic delivery barriers, ensures that a sufficient dose reaches the target tissue, and lessens the potential for off-target side effects[43]. For these reasons, many of the first therapeutic applications of siRNA tested clinically involved local delivery (primarily topical or injection-based). However, initial clinical trials involving local siRNA delivery were largely disappointing and did not meet the high expectations of the scientific and medical communities[44, 105]. These studies revealed unexpected concerns regarding siRNA safety (e.g., therapies based on naked siRNA triggered immune responses) and pharmacokinetics[43, 44, 55, 105, 106]. The advancement of siRNA molecular design principles and improved delivery systems have increased the number of candidate siRNA therapeutics entering the clinical pipeline, but there is currently a dearth of locally delivered siRNA therapeutics in testing relative to systemically delivered formulations[43, 44]. An enormous opportunity exists to develop sustained-release, local delivery systems that enable both spatial and temporal control of gene silencing.

Localized siRNA delivery obviates many of the systemic delivery barriers but also raises unique challenges. In topical strategies, epithelial surfaces like the skin act as delivery barriers to target cells[107]. Most depot systems eliminate the dermal barrier by maintaining direct contact exists between the local delivery reservoir and the target cells. This scenario highlights a key concern for local delivery platforms, that of controlled release. A primary design interest is to control the kinetics of siRNA release such that duration of gene silencing can be temporally controlled and/or sustained without repeated treatments. Without a mechanism for controlled release from the delivery system, siRNA activity has a finite half-life and its activity will diminish over time. This is especially important in applications where the siRNA dose cannot be

easily reapplied, including delivery from the surface of an implanted device, delivery to sites that are not easily accessible and/or would require assistance from a health care professional, or delivery from depots that also serve as biodegradable tissue engineering scaffolds[108]. At sites of tissue repair, there is the added challenge of rapid cellular turnover and proliferation as the different phases of regeneration proceed; when transfected cells undergo mitosis, the siRNA dose is diluted amongst the daughter cells. In this challenging environment, siRNA gene suppression has been shown to be maximal at approximately two days post-transfection and to disappear almost entirely after one week[2, 109]. By creating delivery platforms with tunable release profiles, gene silencing can be customized for specific therapeutic applications and for sustained effect in tissues that are remodeling and/or regenerating.

Local siRNA delivery systems and their degradation products must also be non-cytotoxic and should not interfere with the desired therapeutic response. Materials that degrade into biocompatible, resorbable byproducts eliminate the need for physical removal of the delivery system. For some systems, the rate at which the material degrades can be used to tune the temporal release profile of the siRNA[110, 111]. Altering the kinetics for diffusion-based release is also possible, for example by regulating the delivery system's crosslinking density and/or porosity via synthesis techniques[112-114]. Of particular interest for regenerative medicine and tissue engineering are multifunctional, porous biomaterials that enable controlled siRNA release, support cellular ingrowth, and degrade at rates that match *de novo* tissue formation[115-118]. Therefore, many delivery systems are fabricated using materials with inherent *in vivo* degradation mechanisms; for example, scaffold and microparticle systems are commonly based on hydrolytically degradable polyesters such as poly(lactic-co-glycolic acid) (PLGA)[112, 113, 117, 119]. However, the degradation products of PLGA acidify the local environment and can result in

inflammation, creating impetus for the exploration of other biodegradable systems[120, 121]. Environmentally-responsive systems that respond to cellular stimuli like proteases or reactive oxygen species (ROS) offer a promising alternative. For instance, biomaterials incorporating polythioketal crosslinkers confer ROS-dependent degradation that produces non-acidic, cytocompatible byproducts[122, 123]. The material choice for a local delivery depot determines not only the degradation rate but also the adherence of cells, their viability and their phenotype. In addition, the affinity of an siRNA therapeutic for the material influences release and cellular uptake characteristics[111]. All of these concerns should be considered, with the goal of designing a system in which the reservoir and siRNA therapeutic work synergistically to elicit the desired cellular response.

Another approach to engineering delivery systems for spatially confined, efficient cellular uptake is to leverage the phenomenon of substrate-mediated uptake[118, 124]. Substrate-mediated uptake or "reverse transfection" occurs when nucleic acids immobilized on a material surface are internalized by cells adherent to that surface rather than being internalized via solution phase endocytosis or pinocytosis. Substrate-mediated delivery concentrates the therapeutic at the cell-material interface and can enhance transfection efficiency by 10- to 100-fold[111, 118, 124]. This reduces diffusion of the siRNA away from the target site and is also especially relevant for tissue regenerative applications where cells adhere and grow within a biomaterial that possesses dual functions as a delivery depot and tissue template.

In most cases, localized, sustained delivery of siRNA carriers and conjugates requires an additional construct to serve as a depot for release of the siRNA therapeutic. To this aim, polymer scaffold-based delivery has emerged as a particularly promising option. The use of polymer scaffolds to facilitate sustained release of siRNA is a potentially transformative strategy

to influence local cellular behavior in tissue regenerative applications. An extensive array of polymers and polymer combinations has been explored for scaffold fabrication. Naturally-derived polymers, such as physiological extracellular matrix (ECM) components and polysaccharides (commonly anionic alginate, agarose, dextran, and hyaluronic acid (HA) and cationic chitosan), are often utilized because they have inherent cell-adhesion and degradation mechanisms. Collagen is a particularly popular ECM biomaterial because it is a fibrous extracellular matrix component that is enzymatically degradable[125]. One of the earliest studies that investigated scaffold-mediated delivery as a means to control siRNA release kinetics utilized collagen scaffolds loaded with siRNA formulated with provokeM dendrimers[126]. These scaffolds achieved greater than 50% gene silencing at 7 days (using a 200 nM siRNA dose) in *in vitro* studies with fibroblasts, demonstrating the potential for sustained silencing via scaffold-based local delivery.

While natural polymers offer advantages in terms of host cell recognition, using synthetic materials enables greater control over a range of scaffold properties, including the pore structure, degradation mechanism/rate, and mechanical stiffness/strength. PLGA offers the distinct advantage of highly tunable degradation rates, and PLGA scaffolds have been shown to promote cellular ingrowth and produce localized and long-term nucleic acid transfection in numerous applications[118, 127]. Poly(ester urethane) (PEUR) scaffolds formed from non-toxic isocyanates, such as lysine triisocyanate (LTI), have also been successfully adapted for the sustained delivery of a variety of biomacromolecules[128-130]. Another promising scaffold type is that comprised of ROS-responsive poly(thioketal)-urethane (PTK-UR), which have been shown to mediate improved tissue ingrowth in comparison to hydrolytically-degradable PEUR versions[122].

For all scaffold-based delivery applications, it is vital that the vehicle for siRNA's intracellular delivery can be readily incorporated into the bulk delivery depot without significant loss of gene silencing activity. Lyophilization of siRNA-loaded poly- and lipo-plexes can reduce their activity, primarily because extensive particle aggregation occurs at high concentrations. Several stabilization strategies have been developed to maintain gene silencing efficacy post-fabrication into local delivery systems[108, 131-133]. For example, siRNA nanoparticles were shown to have a 50% activity loss when directly incorporated into PEUR scaffolds. However, when the natural sugar trehalose was used as a stabilizing agent, nanoparticle size and activity were retained relative to fresh siRNA formulations[108, 134]. Additionally, siRNA complexed with either chitosan or Transit TKO transfection reagent and lyophilized onto the surface of tissue culture plates maintained transfection efficiency only when sucrose was utilized as a lyoprotectant[132]. Sucrose stabilization showed similar efficacy as a lyoprotectant of polyplexes of DNA and PEI[133]. These results demonstrate the necessity of carefully optimizing the integration of the siRNA intracellular delivery system with the bulk scaffold/depot fabrication method and chemistry.

While local delivery presents novel challenges, it also has inherent advantages over systemic delivery that make it the logical choice for translation of siRNA therapies to a subset of pathologies. In particular, local delivery of siRNA therapies from a biomaterial scaffold has emerged as a promising strategy for applications in regenerative medicine, such as the treatment of chronic wounds.

2.6 Local siRNA delivery for chronic wound treatment

Impaired wound healing is a significant healthcare problem in the United States that affects more than 6.5 million people[135]. Patients with diabetes are ten times more likely to suffer amputation due to non-healing wounds, and the Center for Disease Control estimates that 1 in 3 of today's children will develop diabetes in their lifetime[136, 137]. It is anticipated that the prevalence of problematic skin wounds will parallel the expanding diabetes pandemic. Thus, there is an established, growing, and unmet clinical need for improved treatment of chronic wounds.

In normal wound healing, a coordinated combination of cellular infiltration, proliferation, and extracellular matrix deposition directs a transition from the initial inflammatory response at a site of injury to the process of tissue regeneration[138, 139]. Chronic wounds do not complete this progression and are often characterized by excessive inflammation, reduced vascularization (leading to an ischemic environment), rapid degradation of regenerated tissue, and lack of a coordinated cellular response, resulting in incomplete healing[4]. Impaired wound healing is a common long-term complication of diabetes due to a myriad of factors including inferior peripheral circulation and a reduction of the levels and response to growth factors[5].

Two cell types that are particularly relevant to wound healing are fibroblasts and mesenchymal stem cells. Fibroblasts play a key role in wound remodeling via their proliferation, secretion of growth factors, extracellular matrix production, and promotion of angiogenesis[138]. However, fibroblasts isolated from chronic wounds show a decrease in proliferation rate and a diminished response to various cytokines[138, 140]. While the mechanism for this alteration in fibroblast behavior has not been identified, this indicates that mere delivery of growth factors will be insufficient to fully restore normal fibroblast behavior at the site of chronic wounds.

MSCs are central regulators of wound healing; they modulate the inflammatory response and release bioactive factors that influence the migration, proliferation, and phenotype of nearby cells. Additionally, the capacity of MSCs to differentiate into various tissue-forming cell types endows them with particular value in functional tissue regeneration[139]. Modulating the characteristics and activities of cells essential to the wound healing process, such as fibroblasts and MSCs, is a potentially high-impact strategy for chronic wound treatment.

Due to the complex nature of wound healing, a variety of physiological abnormalities can contribute to impaired healing. However, the formation of functional vessel networks is essential to the healing process following injury, and dysfunctional wound healing is often characterized by delayed or absent angiogenesis[3], as the development of stable, functional blood vessels is essential to delivering oxygen and nutrients to cells and facilitating long-term tissue viability[125, 138]. Plasmids encoding platelet-derived growth factor (PDGF) or VEGF can promote angiogenesis when delivered from PLGA scaffolds, but there is evidence that the upregulation of a single growth factor will not be sufficient to stimulate both sprouting and maturation of vessels[118, 141-143]. While delivery of combinations of multiple growth factors can more closely recapitulate an environment that stimulates functional vessel formation, these strategies are typically complex and expensive[144]. siRNA provides an attractive alternative because by silencing one gene it can influence activity of multiple downstream targets.

Several functional targets for stimulation of angiogenesis via genetic repression have been identified, the most promising among them that of prolyl hydroxylase domain 2 (PHD2). PHD2 is an endogenous negative regulator of the transcription factor hypoxia-inducible factor-1α (HIF-1α)[145]. Potent inhibition of PHD2 results in a large up-regulation of HIF-1α and its downstream genes VEGF, fibroblast growth factor 2 (FGF-2), endothelial nitric oxide synthase

(eNOS), angiopoietin (ANGPT), and stromal cell-derived factor 1 (SDF-1)[146, 147] (Figure 2.2). These factors orchestrate both formation and maturation of vessels and, in the case of SDF-1, recruit endothelial progenitors that further promote local vasculogenesis[148]. Because PHD2 deficiency stimulates mature blood vessel formation, silencing its expression is of interest both in broad tissue engineering applications and in chronic, ischemic skin wounds[149].

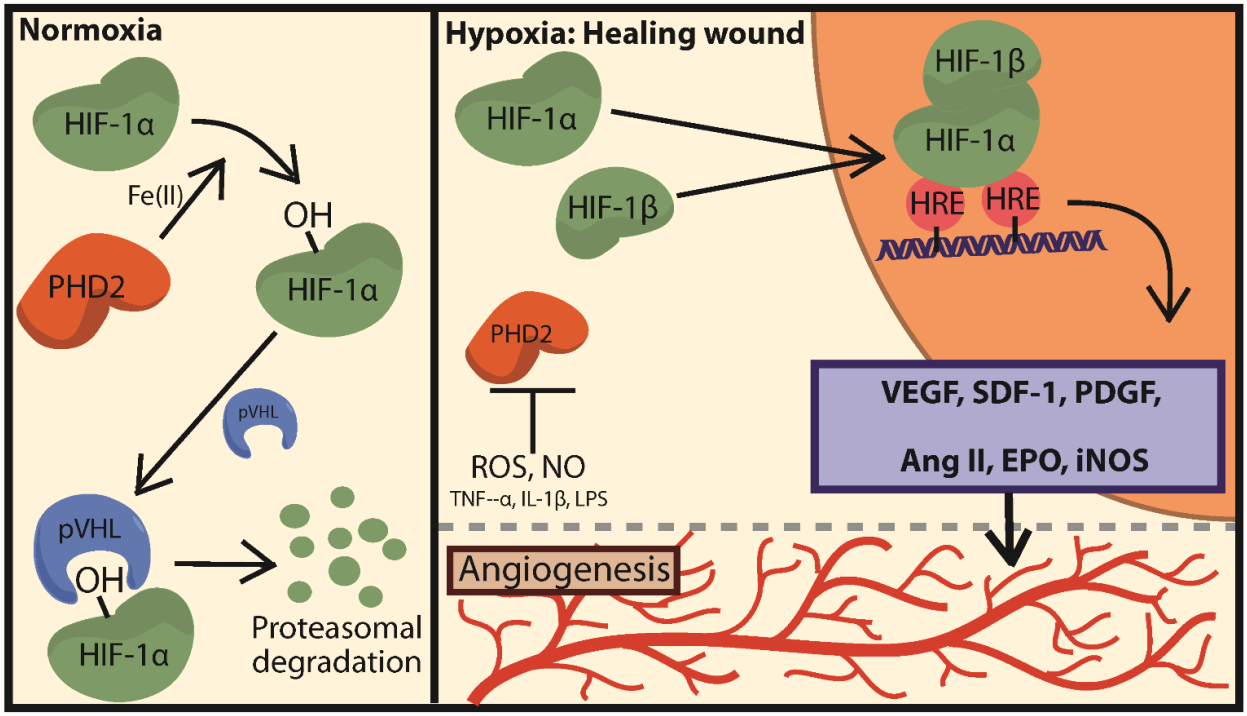

Figure 2.2. Schematic depiction of prolyl hydroxylase 2 (PHD2) activity in normoxia (left) and hypoxia (right) in a normally healing wound. HIF-1: hypoxia inducible factor 1, pVHL = von Hippel Lindau protein, HRE = hypoxia responsive element, VEGF = vascular endothelial growth factor, SDF-1 = stromal-derived growth factor 1, PDGF = platelet derived growth factor, Ang II = angiotensin II, EPO = erythropoietin, iNOS = inducible nitric oxide synthase.

siRNA's potential role as a broad effector of angiogenesis has prompted its investigation as a wound healing therapeutic. The Saadeh group demonstrated proof-of concept work for

localized gene silencing in a wound model via an agarose matrix system containing 20 pmols of liposomal siRNA transfection complexes[150]. In this study, therapeutically relevant siRNA were not investigated and the ubiquitously expressed, essential mitogen-activated protein kinase 1 and lamin A/C genes were used as model targets. Targeting these genes facilitated demonstration of the localized nature of the matrix-based silencing and established that the delivery system in itself had no adverse effects on the wound healing process. siRNA complexes distributed in the agarose matrix were applied to a mouse wound and allowed to gel, then removed at 5 days and replaced at 7 days. At day 14, 50-60% silencing of model genes was observed specifically at the wound site, with protein-level knockdown observed via immunological staining and Western blots at day 14 and 21. However, the necessity for repeated dosing suggests that further optimization of the release kinetics could improve this system's utility. This work demonstrated the feasibility of scaffold systems to regulate gene expression locally at wound sites as well as other targets[150]. The Saadeh group leveraged this proof-of-concept work in subsequent studies, discussed in detail in later sections, that target relevant genes for therapeutic applications in wound healing and related pathologies[151-154].

Previous work in our lab by Nelson et. al. used a PEUR scaffold loaded with siRNA/polymer nanoparticle complexes to investigate the impact of silencing PHD2 in a subcutaneous model of wound healing[108, 134]. The system has proven promising due to its capacity for tunable, sustained release and prolonged gene silencing. Tuning the release rate was possible by adjusting the type of isocyanate used and the amount of excipient added during scaffold formulation. Lysine triisocyanate (LTI) contributed to faster release than hexamethylene diisocyanate trimer (HDIt), and increasing the percentage of the excipient trehalose (0-5% incorporated trehalose was investigated) also promoted faster release[108]. A broad range of release

rates could thus be achieved, with *in vitro* results showing scaffolds incorporating LTI and 5% trehalose released all siRNA nanoparticles in 5 days while scaffolds incorporating HDIt and 0% trehalose released only ~5% siRNA nanoparticles over 20 days. Modulating the release rate elicited corresponding changes in the *in vivo* silencing profile. Silencing of a model gene in a mouse subcutaneous implant model (with 0.5 nmols siRNA/nanoparticle complexes per scaffold) peaked at >90%; scaffolds incorporating LTI and 0% trehalose exhibited silencing at this level at 35 days but scaffolds incorporating LTI and 5% trehalose resulted in a silencing peak at 5 days and <50% silencing at 35 days. To prove the therapeutic utility of this system, siRNA against PHD2 was investigated in scaffolds utilizing LTI and 5% trehalose. At 14 days, 80% silencing of PHD2 was observed, resulting in greater than 2-fold upregulation of downstream pro-angiogenic markers VEGF and fibroblast growth factor (FGF). Silencing PHD2 also increased vascular volume within the scaffolds by more than 2-fold and increased mean vascular thickness, suggesting that PHD2 silencing may support both angiogenesis and vessel enlargement and maturation (Figure 2.3)[108]. This approach to local PHD2 siRNA delivery shows promise as a means of promoting angiogenesis in wound healing and tissue regeneration applications. Additionally, the sustained and controllable release from the PEUR scaffolds provides motivation to investigate this delivery system in other localized pathologies.

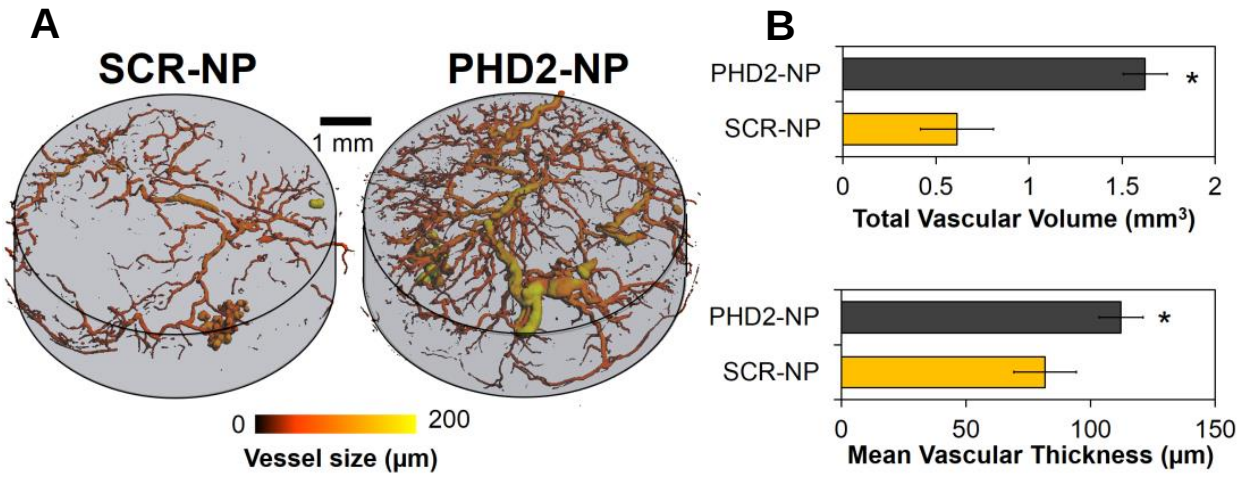

Figure 2.3 Sustained silencing of PHD2 increases angiogenesis within PEUR tissue scaffolds. A) Micro-CT images visually demonstrate the increased vasculature within the PHD2-NP scaffolds. B) Quantitative analysis of 3D micro-CT vessel images reveals a significant increase in vascular volume within PHD2-NP-loaded scaffolds relative to control scaffolds containing scrambled (SCR) siRNA. *$p<0.05$.

Vandegrift et. al. subsequently investigated PHD2 silencing as a means to promote angiogenesis[151]. They aimed to improve upon the success rate of acellular dermal matrix (ADM) implantation for dermal replacement and reconstruction by promoting incorporation of the ADM into the host tissue via vascularization. ADM was loaded with 20 pmol siRNA by soaking in siRNA solution. *In vitro* release of siRNA from ADM occurred almost immediately, with 70% released after 1 hour and a maximum of 80% release achieved. However, in a mouse model of a cutaneous dorsum wound, siRNA-loaded ADM silenced PHD2 by about 70% at 7 days and 93% at 14 days. While the sustained silencing contrasted with the burst release profile, further validation of PHD2 silencing was observed based on upregulation of VEGF and FGF mRNA expression by 2.3-fold and 4.7-fold, respectively, at 7 days, and VEGF and SDF-1 protein expression by 4-fold and 2-fold, respectively, at 14 days. The ADM integration was improved

but not significant; however, this local delivery system further validates the promise of PHD2 silencing with siRNA as a pro-angiogenic therapy for wound healing.

The reported therapeutic promise of PHD2 siRNA motivates its further investigation in local delivery systems to treat chronic wounds. Establishing effective and long-term gene silencing of PHD2 from biomaterial scaffolds while minimizing immunogenic effects is a promising approach to improving wound healing outcomes, and scaffold-based delivery of an siRNA conjugate has never been investigated. Development of a hydrophobic siRNA conjugate that enhances release kinetics and gene silencing from biomaterial scaffolds for applications in regenerative medicine and impaired wound healing is a unique and potentially high-impact pursuit.

2.7 Systemic delivery considerations

While local delivery may be a superior strategy for chronic wounds and other suitable pathologies, treatment of many disease states necessitates systemic delivery. For example, addressing metastatic carcinomas and systemic infections requires broad therapeutic distribution[155]. Additionally, systemic delivery strategies are generally less invasive and more easily administered than local therapies, which confer significant advantages in the transition to clinical relevancy. However, the obstacles to development of an effective, systemic siRNA therapy are numerous and challenging to address.

First, naked siRNA has extremely poor pharmacokinetic properties for systemic administration. The typical systemic delivery route for RNAi therapies is intravenous injection; however, injection of unmodified siRNA results in rapid clearance from the bloodstream (naked

siRNA has a circulation half-life of less than 2 minutes)[73]. The short half-life of siRNA is attributed primarily to immediate renal filtration, which occurs through the pores of the glomerular membrane for molecules of a size less than approximately 5 nm[16, 156]. siRNA, with a hydrodynamic diameter of around 2 nm, is almost completely cleared in its first pass through the kidneys and excreted in the urine. Avoiding rapid clearance and prolonging the circulation half-life is critical to the efficacy of systemic siRNA therapies, as enhancing circulation persistence directly increases bioavailability. Further limiting the utility of naked siRNA is its rapid degradation by serum nucleases and poor capacity to translocate the cellular membrane. As mentioned, unmodified siRNA is unstable and generally incapable of eliciting cellular uptake. Therefore, siRNA that avoids rapid clearance remains relatively impotent. There is a myriad of intelligently-designed and effective siRNA delivery strategies intended to specifically to enhance siRNA's therapeutic utility in systemic applications, but there remain notable drawbacks to these systems.

By far the most widely investigated, prevalent, and successful strategy for systemic delivery of siRNA is that of nanocarrier-mediated delivery. Nanocarriers, which are generally of sizes ranging from 20 to hundreds of nanometers, are too large to readily pass through the pore of the glomerular membrane and therefore avoid the swift renal clearance characteristic of siRNA[157]. Nanocarriers can also protect siRNA from degradation, and mediate its cellular internalization and endosomal escape[17, 21, 158]. Unfortunately, these distinct advantages are associated with significant drawbacks.

Intravenously-administered siRNA nanocarriers are prone to opsonization by serum proteins and activation of the complement cascade, resulting in an innate immune response and phagocytosis by monocytes and macrophages[159, 160]. Compounding this undesirable and rapid

clearance, activation of the immune system triggers production of inflammatory cytokines and interferons that can lead to undesirable side effects. Cationic surfaces favor rapid protein adsorption and therefore are particularly poorly suited for systemic delivery[161]. Because efficient siRNA loading often requires incorporation with a cationic moiety, generation of a neutral or anionic outer layer that shields the cationic carrier from serum proteins has emerged as the most promising strategy to produce siRNA nanocarriers that can evade recognition by the immune system. The gold standard for preparation of "stealthy" nanocarriers is surface modification with PEG chains[162-166]. PEG is an anionic, extremely hydrophilic polymer that adopts an extended conformation at the nanocarrier surface and effectively resists protein adsorption. PEGylation of both nanoparticles and liposomes has been shown to dramatically enhance their circulation time. The optimal PEG length and density varies depending on carrier type; for liposomes, an optimal PEG density balances stealth properties with liposomal stability, and longer PEG chains (20 kDa) were shown to enhance circulation half-life of siRNA micelles relative to shorter chains (5k and 10k)[167]. Tuning the nature of a PEG coating is essential to confer effective shielding. For example, PEGylation of siRNA matrix nanoparticles did not confer pharmacokinetic benefits, likely due to inconsistent or incomplete PEG covering[163]. Notably, while PEGylation prolongs circulation persistence and reduces immune activation, PEGylated nanocarriers exhibit reduced cellular internalization and capacity to induce endosomal escape, essential properties for an siRNA delivery vehicle[167]. This dilemma inspired the development of nanoparticles that can shed their PEG layer in response to strategically-chosen external stimuli[72]. It also motivated the investigation of alternative stealth coatings, such as anionic linear polysaccharides and zwitterions[166]. While immense progress has been made in developing design parameters that

yield effective and non-immunogenic nanocarriers for systemic delivery, development of a fully non-immunogenic nanoparticle delivery vehicle is a challenging and as yet unsolved problem.

In addition, siRNA nanocarriers are subject to destabilization and disassociation in the challenging *in vivo* environment. siRNA association with delivery vehicles is typically driven by electrostatic forces. The presence of charged serum proteins and salts in the bloodstream can destabilize nanocarriers over time, and the renal glomerular basement membrane presents a particularly stringent stability challenge[156, 168]. The glomerular basement membrane is characterized by a profusion of negatively charged proteoglycans, like heparan sulfate, that can rapidly destabilize polyelectrolyte siRNA nanocarriers, resulting in release and clearance of siRNA cargo. This challenge has been addressed through modification and optimization of delivery vehicle design[21, 161]. Incorporation of hydrophobic components into siRNA nanocarriers has emerged as a capable strategy to improve carrier stability, cellular uptake, and cytocompatibility[169, 170]. For example, siRNA polymer nanoparticles that leverage hydrophobic interactions in addition to electrostatic forces demonstrate superior stability, circulation time, and gene silencing efficacy[21] (Figure 2.4). The ratio of hydrophobic and cationic content was a key determinant of these properties. Distinct from hydrophobic modification of the nanocarrier, Oe et al. proved that hydrophobization of the siRNA cargo through cholesterol conjugation facilitates siRNA loading and enhances the stability of polyion complex micelles[22]. A promising, but as yet uninvestigated, approach to further enhance nanocarrier stability is the combination of hydrophobized siRNA cargo with a partially hydrophobic delivery vehicle.

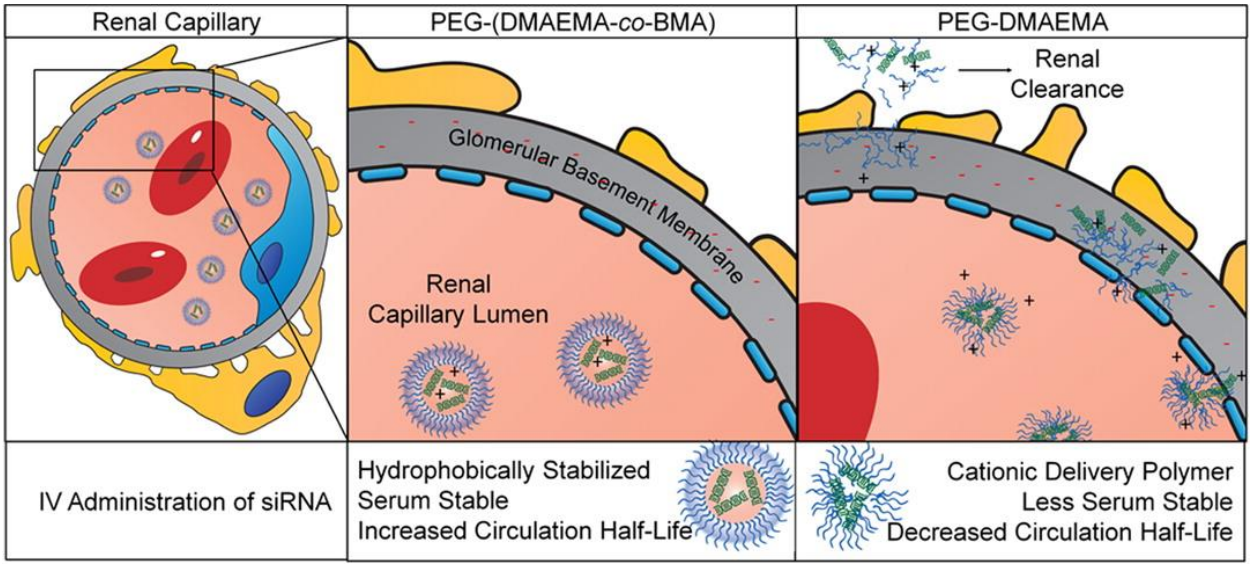

Figure 2.4. Schematic depiction of siRNA-loaded nanoparticle (NP) interaction with the glomerular basement membrane of the kidney. Left: broad view of a renal capillary after intravenous administration of siRNA NPs. Middle: hydrophobically and electrostatically stabilized siRNA NPs resist dissociation. Right: electrostatically stabilized siRNA NPs are destabilized by counterions in the renal membrane. PEG-(DMAEMA-co-BMA) refers to PEGylated nanoparticles incorporating hydrophobic (BMA; butyl methacrylate) and cationic (DMAEMA; dimethylaminoethylmethacrylatez) core components, while PEG-(DMAEMA) refers to PEGylated nanoparticles with a solely cationic core.

An alternative option to improve the stability of siRNA nanocarriers is through compound formulation strategies or the use of inorganic carrier components. siRNA-encapsulating nanoparticles fabricated through water-in-oil-in water (W/O/W) emulsion methods impart significant pharmacokinetic advantages[171] but result in poor loading efficiency, high loss of siRNA during fabrication, exposure of siRNA to potentially damaging organic solvents, and formation of nanoparticles with high weight ratios of carrier polymer(s) relative to siRNA cargo. Covalent crosslinking of nanocarriers subsequent to siRNA loading can also enhance their resistance to disassociation and thus their circulation persistence. Often, crosslinks are comprised

of cleavable or reducible linkages, affording the opportunity to design stimuli-dependent release of siRNA[172, 173]. Nanocarriers based on inorganic materials (e.g. gold, iron oxide, silica) are highly stable and generally avoid the toxicities associated with cationic components of polymeric and lipid nanocarriers[174]. For example, the use of siRNA-coated gold nanoparticles has shown promise as a non-toxic and effective gene silencing mechanism in topical applications[175]. A notable issue is that these inorganic carriers remain in the body post-siRNA delivery and the impact of accumulation and long-term presence of these particles remains uncertain.

Further, while properly designed nanocarriers can diminish rapid renal clearance, they ultimately exhibit preferential accumulation in the MPS organs of the liver and spleen[176]. The cationic components of siRNA nanocarriers are prone to induction of dose-limiting toxicities in these organs[13]. Engineering delivery vehicles to be biodegradable enhances this biocompatibility, as small individual components are amenable to physiological clearance mechanisms. Naturally biodegradable PBAE-based siRNA carriers display low cytotoxicity while maintaining gene silencing efficacy[158]. The high modularity and tunability of synthetic polymers allows incorporation of biodegradable linkages or components that improve carrier biocompatibility. Poly(DMAEMA) is a common component of polymer-based siRNA carriers, and Zhu et al. noted that a triblock polymer with poly(DMAEMA) on terminal ends and biodegradable poly(caprolactone) spanning the middle was a cytocompatible strategy for siRNA delivery[177]. Another strategy to lessen off-target, toxic effects of siRNA nanocarriers is to target them to the specific targeted site. Davis et al. reported the first instance of successful gene silencing in humans by a systemically-delivered siRNA therapy using PEGylated cyclodextrin nanoparticles decorated with targeting ligands for the transferrin protein, which is upregulated in malignant cancer cells[178]. Another study evaluated delivery of siRNA to subctutaneous flank tumors in

mice via PEGylated chitosan nanoparticles $\alpha_v\beta_3$ integrin bearing tripeptide RGD motifs, revealing enhanced therapeutic efficacy for the targeted siRNA nanoparticles[179]. The $\alpha_v\beta_3$ integrin is commonly overexpressed on cancer and nearby endothelial cells and is a typical choice for active tumor targeting. Each of these strategies aimed to diminish the prevalence and extent of toxic side effects by limiting the exposure of siRNA nanoparticles to healthy tissue. However, the transferrin receptor, the $\alpha_v\beta_3$ integrin, and the vast majority of other proteins expressed on cellular surface are not unique to a particular cell type. While protein overexpression in disease states is widespread, lower expression levels of healthy or non-targeted cells will always result in imperfect targeting accuracy.

Nanocarriers also exhibit poor penetration of complex tissue architectures; their larger size limits their capacity to diffuse through extracellular tissue structures and therefore their broad distribution at a target site[180]. As noted, avoiding renal clearance mediated by filtration through pores of the glomerular basement membrane requires a size greater than approximately 5 nm, with sizes greater than 20 nm more effective at fully circumventing this barrier. However, as nanoparticle size increases, nanoparticle capacity to penetrate tissue and achieve internalization in target cells diminishes. Previous work using well-defined spherical latex particles revealed that, for particles 50 to 500 nm in size, cellular uptake was inversely related to particle size[180]. Alternatively, macrophages may preferentially internalize larger nanoparticles for eventual clearance[159]. Additionally, intravenously injected siRNA nanocarriers typically require extravasation to a targeted tissue site. The endothelial barrier in normal vasculature is organized, tight, and contains only small pores; while macromolecules like proteins or naked siRNA can capably extravasate through these pores, even the smaller nanoparticles are generally incapable of doing so[180].

For this reason, systemic delivery of siRNA nanoparticles has often focused on leveraging physiological or pathological variations in the vasculature. In clearance organs like the liver and spleen, in situations of inflammation, and at sites of tumors, variations in the endothelial barrier allow efficient delivery of molecules of nanoparticle size[180]. The power of the endothelial barrier is evident when exploring systemic RNAi therapies currently in clinical trials; all target hepatic pathologies or cancer. Leading the field is Alnylam, which is progressing through late-stage clinical trials with multiple siRNA-based strategies for genetically-based liver diseases. One of the most advanced along the regulatory pathway is a lipid nanoparticle-based siRNA formulation that targets the transthyretin gene for treatment of transthyretin amyloidosis[181, 182], which is currently in Phase III clinical trials. Though clinical trials of Alnylam's trivalent GalNAc siRNA conjugate for the same indication were recently halted, several other clinical trials using this conjugate to address alternate liver disease targets are proceeding as planned.

While Alnylam's conjugate is specifically designed for liver targeting, development of siRNA conjugates capable of circulation persistence could dramatically enhance therapeutic penetration and facilitate broad distribution throughout a desired tissue locale. siRNA conjugates are by nature much smaller than nanocarriers and could prove more proficient at diffusing through pores in the endothelial barrier and through extracellular structures. Unfortunately, exploration of systemically-delivered siRNA conjugates has been largely limited to conjugates engineered for hepatic distribution[23, 183]. The albumin-binding conjugate from Lau et al., despite its lack of a therapeutic target, provides the sole example of an siRNA conjugate eliciting gene silencing in a non-hepatic organ[184]. Further exploration of conjugate-based, systemic RNAi therapies to address a broader range of pathologies is a potentially high-impact pursuit.

The inherent limitations of nanocarrier systems has inspired strategic pursuit of intelligently-designed nanocarriers. Regrettably, improvements in nanocarrier systems are often accompanied by added synthetic complexity and expense. In contrast, a notable feature of clinically-approved nanocarriers is their extreme simplicity. In 1995, Janssen's Doxil was the first nanoparticle delivery vehicle approved for clinical use[185]. Doxil comprises chemotherapeutic Doxorubicin loaded into a PEGylated liposome. Approval of other PEGylated liposomal formulations has followed, and inorganic nanoparticles for iron replacement therapies and use as imaging agents have also achieved clinical relevancy. The only non-liposomal nanoparticle designed for therapeutic delivery is Abraxane, an albumin nanoparticle that binds paclitaxel[31, 186]. These nanoparticles have succeeded by leveraging simple, scalable syntheses and non-toxic components. To achieve translation of siRNA therapies, siRNA nanocarriers must strike a balance, merging a minimalist, translatable approach with marked improvements in siRNA's pharmacokinetic properties and distribution to the target site.

2.8 Systemic siRNA delivery for cancer treatment

The designation of cancer encompasses a multitude of diverse pathologies. While the U.S. has made tremendous progress over the past several decades, reducing overall cancer mortality rates by 23%, cancer remains the second leading cause of death in the nation[187]. President Barack Obama's call for an organized and collaborative scientific initiative to spur development of revolutionary cancer therapies signifies the immense societal benefit of tackling this disease. Because cancer cells are a body's own cells transformed to behave pathologically, cancer is inherently personalized to each patient and variable even amongst similar cancer

subtypes[6]. This presents an extraordinary medical challenge and requires development of diverse and innovative treatment approaches. RNAi cancer therapies are a promising option because they can silence traditionally "undruggable" targets and because they can be easily tuned through sequence modification, addressing the issue of cancer heterogeneity.

Despite the value of oncological RNAi therapies, the poor pharmacokinetic properties of siRNA have severely hindered their successful application. The delivery barriers previously discussed remain relevant, but several aspects of cancer physiology that impact therapeutic delivery are also notable. Tumor cells are characterized by rapid and unchecked proliferation, and their growth can outpace the development and maturation of normal vasculature[188, 189]. For this reason, blood vessels in the vicinity of tumors can be poorly organized, with parts of the tumor lacking access to vessel networks. The lack of consistent blood flow to tumor regions can result in hypoxia and acidity at these locales[190]. Additionally, a tumor's requirement for rapid generation of vascular networks can result in disorganized vessels that contain larger gaps (of 100 to 200 nm in size) in the normally tight endothelial barrier, allowing passage of molecules on the scale of nanoparticles. Similarly, the lymphatic vessels at tumor sites can be ill-formed and dysfunctional as well, resulting in poor drainage of interstitial fluid and macromolecules accumulated therein[189, 191]. The impaired lymphatic drainage coupled with enhanced vascular permeability results in a higher interstitial fluid pressure in tumors compared to the surrounding healthy tissue.

In the 1980s, Maeda et al. noted that the enhanced vascular permeability coupled to the poor lymphatic drainage in tumors allowed chemotherapeutic-loaded nanoparticles to preferentially distribute to and accumulate at the site of cancer[188]. This phenomenon, referred to as the enhanced permeability and retention (EPR) effect, indicates that design of a better

systemic cancer therapy simply requires efficient packaging into a suitably sized (~100 nm) nanocarrier, which passively enables superior delivery to tumor while minimizing accumulation in healthy tissue. However, the EPR phenomenon as a tumor targeting strategy has recently come under intense scrutiny due to the discrepancy observed between pre-clinical and clinical efficacy of nanoparticle-based cancer therapeutics[188, 191, 192]. There is a growing appreciation that amongst wildly heterogeneous human cancers, the EPR effect may be selectively or minimally relevant.

In particular, the widespread "leakiness" of tumor vasculature, a characteristic of simple and rapidly-developing mouse tumor models, has likely been exaggerated. Due to time and budget constraints, initial, pre-clinical research of cancer therapeutics *in vivo* is typically performed in flank or orthotopic mouse tumors models[191]. Subcutaneous flank tumors in particular have proven to be highly permissive and therefore an inaccurate estimator of the therapeutic efficacy of oncological nanotherapies[188]. Orthtopic tumor models provide a more stringent test but the rapid tumor progression characteristic of these models is atypical of human cancers[193]. Another relevant distinction is whether the model is syngeneic or xenograft. Syngeneic tumor models necessitate the use of mouse tumor cells, disqualifying the use of cells derived from human cancers. However, xenograft models require the use of immunocompromised mice to avoid immune rejection; because the immune system is known to play an active role in establishing the tumor microenvironment as well as in nanoparticle clearance, eliminating the innate immune system compromises the ability to fully evaluate the physiological response to a treatment strategy[193]. Alternate mouse tumor models, like that of the patient-derived xenograft (PDX), genetically engineered, or carcinogen-induced models, address a variety of these drawbacks[194, 195]. The PDX model boasts replication of the intratumoral complexity, heterogeneity, and genetic diversity of clinical human cancers, and genetically

engineered or carcinogen-induced models feature spontaneous tumor development that may mitigate differences observed due to excessively rapid tumor growth. However, generation of each of these more complex models is expensive, labor-intensive, and time-consuming. Therefore, the simpler subcutaneous and orthotopic models continue to dominate in preclinical evaluation of cancer therapies.

The limitations of current mouse tumor models and reliance on the EPR effect observed in these models has led to an overestimation of the clinical efficacy of nanoparticle-based cancer therapeutics. Critically, a comprehensive review of the literature noted that on average 0.7% of an injected dose of nanotherapeutic reached the targeted tumor site. The field of nanomedicine has responded to these realizations with efforts to enhance understanding of nanoparticle performance in animal models[52, 196-198], strategies to normalize tumor vasculature[190], and systematic investigations into ideal nanoparticle characteristics[196, 199]. A particular challenge is that of penetration through avascular tumor regions and less permeable tumor vessels. The larger size of most nanocarrier systems severely limits their accumulation in and broad distribution throughout tumor sites[16, 200], resulting in poor and/or inhomogeneous efficacy dependent on vascular architecture and tissue organization (Figure 2.5). This realization has prompted a recent focus on smaller (20-30 nm-sized) nanocarriers[196, 201, 202]. Smaller, conjugate-based therapeutics are another alternative that may allow more homogeneous distribution of therapeutic at the tumor site. Indeed, the apparent tissue permeability of the serum protein albumin (hydrodynamic size ~7.2 nm[31]) is consistently more than 4-fold greater than that of 100 nm liposomes in a variety of mouse models of breast cancer[203].

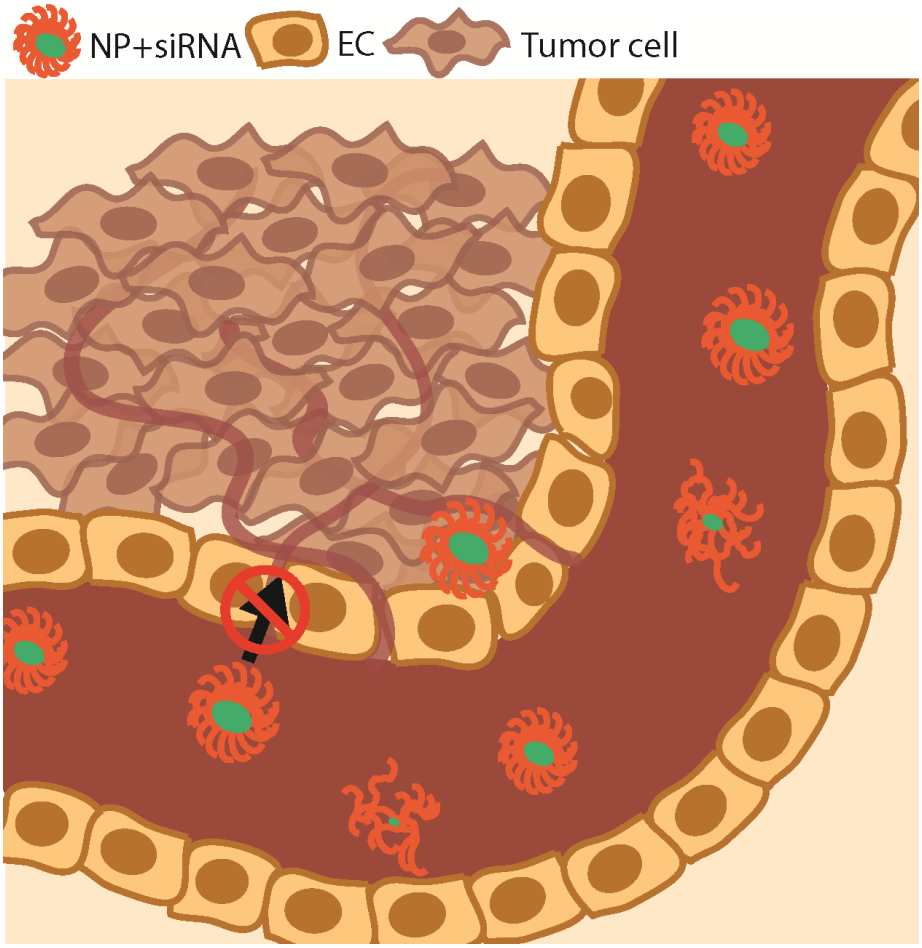

Figure 2.5. siRNA-loaded nanoparticles (NPs) often exhibit poor penetration of tumor architecture due to their large size. siRNA NPs can also exhibit destabilization in the *in vivo* environment.

Characterization of the nature and diversity of cancer pathology is ongoing and essential to development of successful treatment approaches. For systemic siRNA delivery, nanocarrier-based strategies remain the norm, and at least six siRNA-loaded nanoparticle therapies are in Phase I or II clinical trials for cancer treatment[204]. These nanocarrier-based treatments are the only systemically-delivered, oncological siRNA therapies currently in clinical investigation; results to date are inconclusive but unremarkable and dose-limiting toxicities are noted in all cases. The current re-evaluation of how to design and utilize an effective nanoparticle-based

cancer therapy may inspire further improvement of siRNA nanotherapeutics for oncological applications. However, despite the value of improving nanoparticle-based approaches, the diversity of human cancers necessitates equivalently diverse delivery approaches[6, 205]. Smaller, long-circulating siRNA conjugates may offer biocompatible alternatives that facilitate more homogeneous therapeutic distribution within tumors, thereby enhancing therapeutic efficacy.

CHAPTER 3

CONJUGATION OF PALMITIC ACID IMPROVES POTENCY AND LONGEVITY OF SIRNA DELIVERED VIA ENDOSOMOLYTIC POLYMER NANOPARTICLES

Text adapted from:

Sarett, SM, Kilchrist, KV, Miteva, M, Duvall, CL (2015). Conjugation of Palmitic Acid Improves Potency and Longevity of siRNA Delivered via Endosomolytic Polymer Nanoparticles. *Journal of Biomedical Materials Research Part A, 103*.

3.1 Abstract

Clinical translation of siRNA therapeutics has been limited by the inability to effectively overcome the rigorous delivery barriers associated with intracellular-acting biologics. Here, in order to address both potency and longevity of siRNA gene silencing, siRNA conjugated to palmitic acid (siRNA-PA) was paired with pH-responsive micellar nanoparticle (NP) carriers in order to improve siRNA stability and endosomal escape, respectively. Conjugation to hydrophobic PA improved NP loading efficiency relative to unmodified siRNA, enabling complete packaging of siRNA-PA at a lower polymer:siRNA ratio. PA conjugation also increased intracellular uptake of the nucleic acid cargo by 35-fold and produced a 3.1-fold increase in intracellular half-life. The higher uptake and improved retention of siRNA-PA NPs correlated to a 2- to 3-fold decrease in gene silencing IC_{50} in comparison to siRNA NPs in both mouse fibroblasts and mesenchymal stem cells for both the model gene luciferase and the therapeutically relevant gene PHD2. PA conjugation also increased longevity of silencing activity, as indicated by an increase in silencing half-life from 24 hours to 186 hours. Thus,

conjugation of PA to siRNA paired with endosomolytic NPs is a promising approach to enhance the functional efficacy of siRNA in tissue regenerative and other applications.

3.2 Introduction

Therapeutic application of RNA interference provides the potential to potently and specifically suppress transcription factors, subsets of kinases, and other signaling molecules that are traditionally considered "undruggable". Unfortunately, achieving successful *in vivo* delivery of siRNA has proven a complex and difficult challenge, impeding medicinal translation of siRNA therapeutics. siRNA has a short half-life due to nuclease susceptibility, rapid renal clearance if injected intravenously, and an inability to translocate the membranes that make up the outer cell surface and the vesicles of the endolysosomal recycling/degradation pathways[12, 47, 206]. Numerous and varied strategies have been developed in attempts to address these delivery obstacles, including modifications to the siRNA backbone, the use of lipids and polymers as carrier systems, and the conjugation of siRNA to cell-penetrating/cell-binding peptides, antibodies, dendrimers, and lipid-like molecules[12, 19, 70, 109, 207, 208]. Tremendous progress has been made, especially in the application of lipid nanoparticles for delivery of siRNA against hepatic targets, but widespread medicinal application of siRNA remains a distant goal[182, 209]. Thus, there is a continued need to better elucidate the ideal siRNA chemistry and its potential synergism with polymeric- and lipid-based carriers, with the goal of discovering combinations that will expand the therapeutic use of siRNA for a broader set of clinical indications.

Work from our lab and others has focused on diblock copolymers that can package and deliver siRNA to the cytoplasm, facilitated by pH-dependent membrane disruptive activity that promotes endosomal escape[21, 70, 134, 210]. In the current work, we sought to improve the

performance of siRNA formulations with these promising polymers, with the goal of improving efficacy and longevity of action such that functional effects can be achieved at a reduced polymer/siRNA dose. Lessening the dose of the carrier is anticipated to be advantageous in reducing nonspecific side effects, as high doses of both cationic lipids and polymers can induce production of inflammatory cytokines and interferons, global changes in gene expression, and toxicity[12, 13, 98, 207].

Hydrophobization of nucleic acid delivery systems has been demonstrated to enhance carrier stability and transfection efficiency in a broadly applicable manner[19-21, 169]. The conjugation of hydrophobic moieties to siRNA can increase siRNA nuclease resistance and enhance cellular internalization without detrimentally impacting gene silencing activity[25, 30]. Direct conjugation of siRNA to cholesterol and α-tocopherol improves gene silencing efficacy *in vivo*, especially when the target site is the liver and after incubation of the conjugated siRNA with lipoproteins[24, 28, 211]. Conjugation of palmitic acid (PA) to siRNA has shown particular promise as a modification strategy to improve siRNA stability, cellular penetration, and gene silencing[30]. PA is an endogenous post-transcriptional modification commonly found on membrane-associated signaling proteins. While PA is involved in a wide variety of cellular functions, it is especially believed to influence protein-membrane interactions as well as protein uptake and intracellular trafficking[102-104]. Motivated by the inherent effects of PA on membrane binding and translocation, PA-modified siRNA has been recently tested as an approach to enhance gene silencing in comparison to unmodified siRNA or siRNA conjugated to cholesterol in cancer cell lines *in vitro*[25, 30]. In these studies, PA conjugation was demonstrated to enhance knockdown of siRNA delivered via Lipofectamine 2000 (a commercial transfection reagent with

established cytotoxicity) and also to enable some gene silencing in the absence of a transfection reagent at high (micromolar) doses[13, 25].

These promising siRNA conjugate results motivated the current study, which was aimed at testing siRNA-PA conjugates for delivery via endosomolytic polymer-based nanoparticles and at assessing PA conjugates in different cell lines relevant to regenerative medicine applications. The ultimate goal of these studies is to enhance the therapeutic potency in order to minimize the quantity of polymeric carrier and siRNA required, thus reducing the potential for nonspecific effects. We have previously delivered polymeric siRNA nanoparticles from porous, biodegradable polyester urethane (PEUR) scaffolds to achieve tunable and potent gene silencing[108, 134]. This approach for local siRNA delivery has shown tremendous potential in applications for tissue regeneration, especially through local silencing of prolyl hydroxylase domain protein 2 (PHD2) to promote wound healing. PHD2 negatively regulates hypoxia inducible factor 1α, a pro-angiogenic transcription factor, and scaffold-based delivery of PHD2 siRNA activates a pro-angiogenic, pro-proliferation program[108, 212, 213]. The current studies were designed to assess the potential of PA conjugation for enhancing the potency and longevity of gene silencing of siRNA for ultimate application in wound healing.

3.3 Experimental Methods

Materials: Amine-modified single-stranded DNA (modification at 5' end) or Dicer substrate siRNA (modification at 3' end) and complementary single-stranded Cy5-modified DNA or unmodified Dicer substrate siRNA were obtained from Integrated DNA Technologies (Coralville, Iowa). The pGreenFire1-CMV plasmid was obtained from System Biosciences (Mountain View, CA), and packaging plasmids pMDLg/pRRE, pRSV-Rev, and pMD2.G were

purchased from Addgene (Cambridge, MA). Lipofectamine 2000 and NucBlue Fixed Cell ReadyProbes were purchased from Life Technologies (Grand Island, NY). RNEasy spin columns were obtained from Qiagen (Venlo, Netherlands), and the iScript cDNA Synthesis Kit from Bio-Rad (Hercules, CA). NIH-3T3s and HEK-293Ts were obtained from ATCC (Manassas, VA), and mouse marrow stromal cells (C57Bl/6-TgNs) were purchased from Jackson Laboratory (Bar Harbor, ME). Propylacrylic acid was synthesized as previously reported[1,2]. All other reagents were purchased from Sigma-Aldrich (St. Louis, MO).

Oligonucleotide-PA Synthesis and Characterization: Single-stranded amine-modified oligo was reacted with 100-fold molar excess of PA *N*-hydroxysuccinimide ester pre-dissolved at 40 mM in *N*,*N*-dimethylformamide (DMF). The reaction was carried out for 18 hours at room temperature in 45% water, 45% isopropyl alcohol, and 10% DMF. The oligo-PA was purified by reversed-phase HPLC using a Clarity Oligo-RP column (Phenomenex, Torrence, CA) under a linear gradient from 95% water (50 mM triethylammonium acetate), 5% methanol to 100% methanol. The conjugate molecular weight was confirmed using MALDI-TOF mass spectrometry (Voyager-DE STR Workstation, Grand Island, NY) using 50 mg/mL 3-hydroxypicolinic acid in 50% water, 50% acetonitrile with 5 mg/mL ammonium citrate as a matrix. The yield of the oligo-PA was quantified based on absorbance at 260 nm. The purified oligo-PA was annealed to its complementary strand to generate Cy5-modified DNA-PA or siRNA-PA. Conjugation and annealing was also confirmed via agarose gel electrophoresis.

Oligonucleotide-loaded Nanoparticle (NP) Synthesis and Characterization: A diblock copolymer composed of a homopolymer of 2-(dimethylamino) ethyl methacrylate (DMAEMA) blocked with a random copolymer of DMAEMA, 2-propylacrylic acid (PAA), and butyl methacrylate (BMA) was synthesized using reversible addition-fragmentation chain transfer

(RAFT) polymerization as described previously[70, 134]. Assembly of NPs was triggered by dissolving polymer in 100% ethanol, followed by slow addition of PBS or water via syringe pump. siRNA or DNA (with or without PA) was mixed with NPs and allowed to electrostatically condense for 30 minutes. Dynamic light scattering (DLS; Zetasizer Nano-ZS Malvern Instruments Ltd., Worcestershire, U.K.) and transmission electron microscopy (TEM; FEI Tecnai Osiris, Hillsboro, OR) were used to analyze size and zeta potential of oligo-loaded NPs. Gel electrophoresis was used to test loading efficiency at varied amine:phosphate (N:P) ratios. A red blood cell hemolysis assay[214] was used to determine pH-dependent membrane disruptive activity of oligo NPs as a marker for endosomal escape functionality.

Production of Stable Luciferase-Expressing Cell Lines: To produce lentivirus, the pGreenFire1-CMV plasmid and packaging plasmids pMDLg/pRRE, pRSV-Rev, and pMD2.G were transfected into HEK-293Ts using Lipofectamine 2000. Media was changed after 24 hours and supernatant containing lentivirus was collected at 48 and 72 hours. Viral supernatant was added directly to NIH-3T3s with 6 μg/mL polybrene or mMSCs with 60 μg/mL protamine sulfate. Media was changed after 24 hours. Lentiviral transduction efficiency was evaluated by GFP expression as analyzed by flow cytometry (BD LSR II Flow Cytometer, San Jose, CA).

Luciferase Silencing: NIH-3T3s or mMSCs were treated with siRNA NPs or siRNA-PA NPs; the siRNA was either designed against the luciferase gene (luc siRNA) or was a scrambled sequence (scr siRNA). Cells were treated in 10% serum for 24 hours before imaging with an IVIS 200 imaging system (Caliper Life Sciences, Hopkinton, Massachusetts). Unless otherwise noted, an N:P ratio of 4:1 was used. In the investigation on longevity of luciferase silencing, the media was changed after 12 hours of treatment to 2% serum to prevent cellular overgrowth.

PHD2 Gene Silencing: NIH-3T3s were treated with siRNA NPs or siRNA-PA NPs at an N:P ratio of 4:1 as described above except for using prolyl-hydroxylase 2 (PHD2) siRNA. Cells were treated in 10% serum for 24 hours and then incubated for 24 hours, and the degree of PHD2 knockdown was quantified by real time polymerase chain reaction (RT-PCR) using the ΔΔCt method and normalizing to glyceraldehyde 3-phosphate dehydrogenase (GAPDH).

Cellular Uptake and Retention: NIH-3T3s were treated with Cy5-labeled DNA NPs or DNA-PA NPs in 10% serum for 12 hours at 12.5 nM. To measure retention with minimal dilution effects due to cell proliferation, media was then changed to 2% serum, and cells were cultured for up to an additional 72 hours. Intracellular fluorescence was quantified using flow cytometry at 12, 36, 60, and 84 hours. Extracellular membrane-bound fluorescence was quenched with Trypan Blue. For confocal microscopy imaging studies, NIH-3T3s were treated with 25 nM Cy5-labeled DNA NPs or DNA-PA NPs in 10% serum for 12 hours before media was changed to 2% serum. Cell nuclei were stained with DAPI (using NucBlue Fixed Cell ReadyProbes), and cellular fluorescence was imaged using confocal microscopy at 12, 36, and 60 hours.

To assess the mechanism of uptake of PA-conjugated oligo NPs, NIH-3T3s were pre-treated for 30 minutes with either Dynasore (5 μM), 5-(N-ethyl-N-isopropyl)amiloride (EIPA) (5 μM), or cytochalasin D (50 μM), which are inhibitors of clathrin/caveolin-mediated endocytosis, macropinocytosis, and caveolin-mediated endocytosis/macropinocytosis, respectively. Cy5-labeled DNA-PA NPs were then added at 50 nM, and the cells were incubated with both the inhibitors and NPs for 4 hours in 10% serum. Intracellular fluorescence was then quantified using flow cytometry with extracellular fluorescence quenched with Trypan Blue.

3.4 Results

Synthesis and Characterization of Oligo-PA NPs: PA-conjugated single-stranded oligos were successfully purified from the reactants via HPLC, and the desired products were confirmed by MALDI-TOF analysis (Figure 3.1) and also by an upward shift of the PA-siRNA band in comparison to the unmodified siRNA band on an agarose gel (Figure 3.2). Unmodified siRNA showed full loading into the diblock polymer NPs at an N:P ratio of 6:1, while PA-modified siRNA was fully loaded at a ratio of 4:1 (Figure 3.2). Oligo-PA NPs were ~10 nm larger than unmodified oligo NPs (48 nm vs. 38 nm), as demonstrated by DLS and TEM (Figure 3.3). Zeta potential was equivalent between oligo-PA NPs and unmodified oligo NPs. No difference in pH-dependent membrane disruptive activity (i.e., as a measure of endosomolytic behavior) was detected between unmodified oligo NPs and oligo-PA NPs (Figure S3.1).

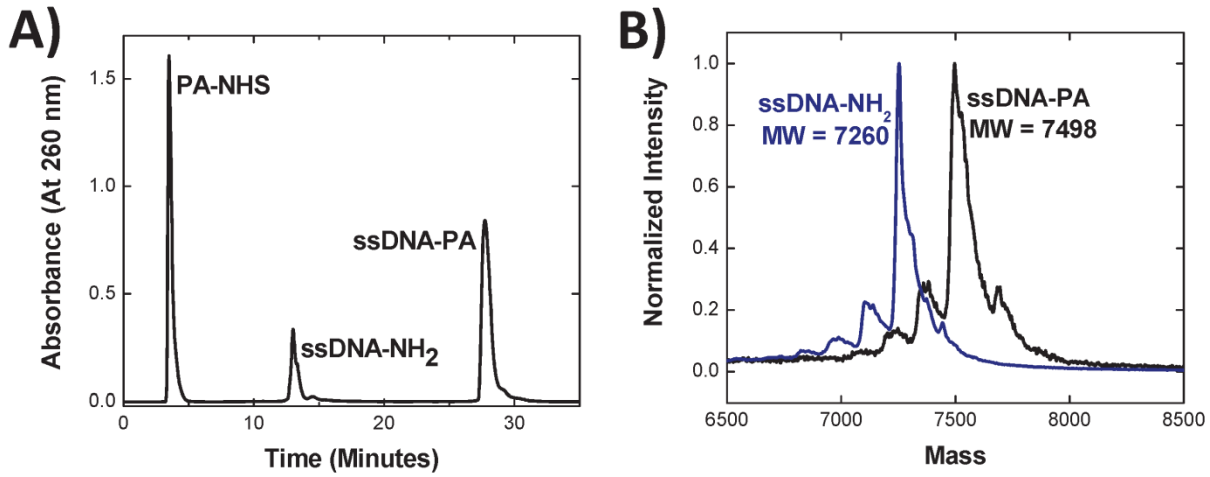

Figure 3.1. Purification of PA-conjugated oligo. A) HPLC separation of PA-conjugated oligo from unreacted oligo, PA-NHS. B) Molecular-weight confirmation by MALDI-TOF mass spectrometry, normalized to maximum intensity for each measurement.

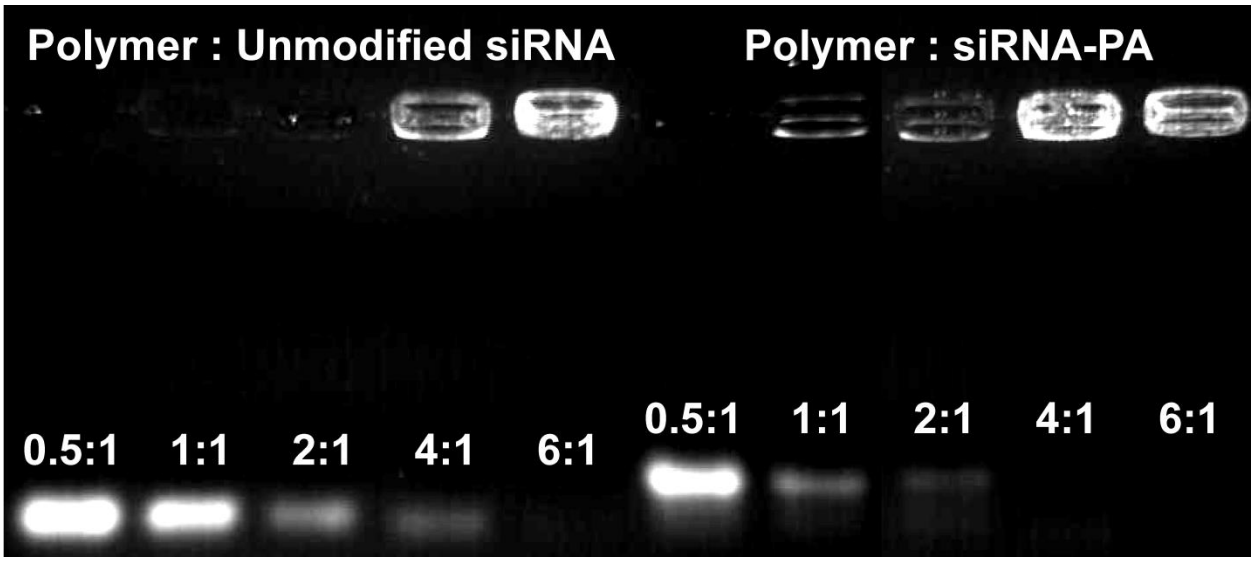

Figure 3.2. The siRNA-PA conjugate efficiently loads into NPs at a lower N:P ratio than unmodified siRNA. siRNA-PA complexed completely at an N:P ratio of 4:1, unmodified siRNA at 6:1. An upward shift in migration time is seen for the PA-modified siRNA, further confirming successful conjugation.

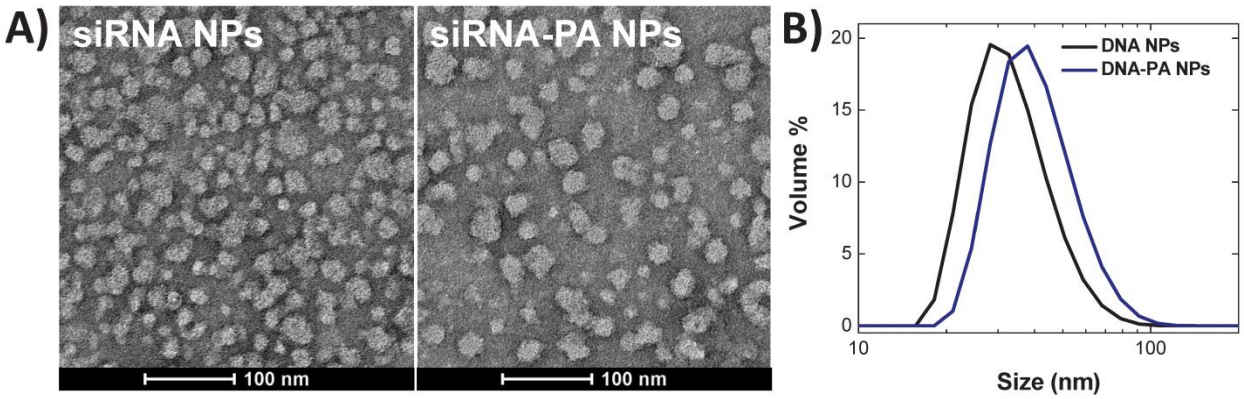

Figure 3.3. Oligo-PA NPs have an approximately 20% larger hydrodynamic diameter than oligo NPs. A) TEM images of siRNA NPs and siRNA-PA NPs. B) DLS measurement of DNA NPs ($z_{average}$ diameter = 40 nm, PDI = 0.10) and DNA-PA NPs ($z_{average}$ diameter = 48 nm, PDI = 0.07).

Gene Silencing Efficacy of siRNA-PA NPs: The influence of the difference in loading efficiency (i.e., N:P ratio required for full packaging) between unmodified and PA-modified siRNA was also investigated for gene silencing. While luc NPs showed a significant increase in luciferase silencing between a ratio of 4:1 and 6:1, no difference was seen in luc-PA NPs between these

two different N:P ratios (Figure 3.4). Greater cytotoxicity, as evaluated by the scrambled controls, was seen at 6:1 in comparison to 4:1 demonstrating the impact of achieving more efficient loading and activity with a smaller quantity of polymeric carrier (Figure S3.2). Superior silencing was detected for luc-PA NPs in comparison to luc NPs at all N:P ratios.

At a fixed N:P ratio of 4:1, increased gene silencing bioactivity of luc-PA NPs over luc NPs was apparent in both mouse fibroblasts (NIH-3T3s) and mMSCs (Figure 3.5). The IC_{50} was calculated based on equation 1 where y is the fraction luciferase activity, x is the concentration in nM, and b is a fit parameter.

$$\textbf{Equation 1}: \; y = \frac{-1}{(1+(\frac{x}{IC_{50}})^{b})} + 1$$

The IC_{50} of luc-PA NPs was 2.2-fold and 3.1-fold lower than that of luc NPs in the fibroblasts and the mMSCs, respectively, indicating that siRNA conjugation to PA significantly improves the gene silencing potency for a given N:P ratio. No significant difference in cytotoxicity was seen in the scr NPs compared to the scr-PA NPs. No significant cytotoxicity was seen below a 40 nM dose of siRNA NPs in the fibroblasts, and no significant cytotoxicity was seen at any of the siRNA NP doses tested in the mMSCs. No cytotoxicity was detected for any siRNA-PA NP doses tested in the fibroblasts or mMSCs.

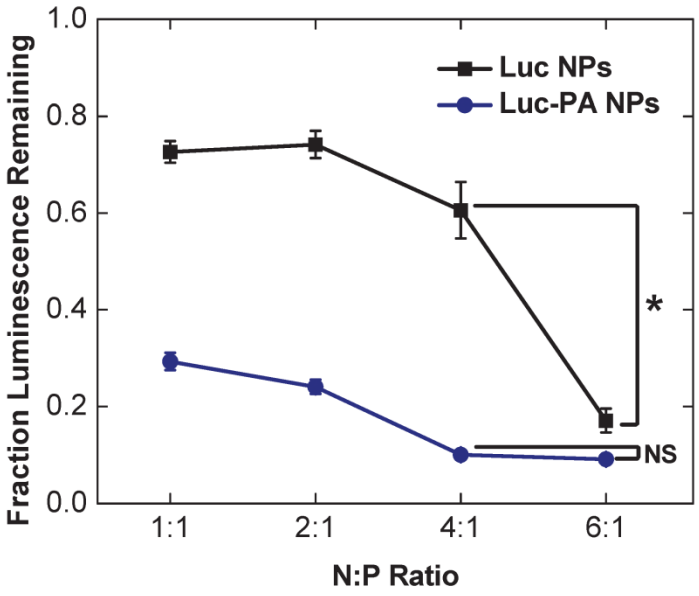

Figure 3.4. Superior luciferase silencing at a lower N:P ratio using luc-PA siRNA vs. luc siRNA NPs. Increasing the N:P ratio above 4:1 did not improve luc-PA NP silencing. These studies were done at 40 nM siRNA treatment for 24 hours in NIH-3T3 fibroblasts. Data are normalized to scrambled controls.

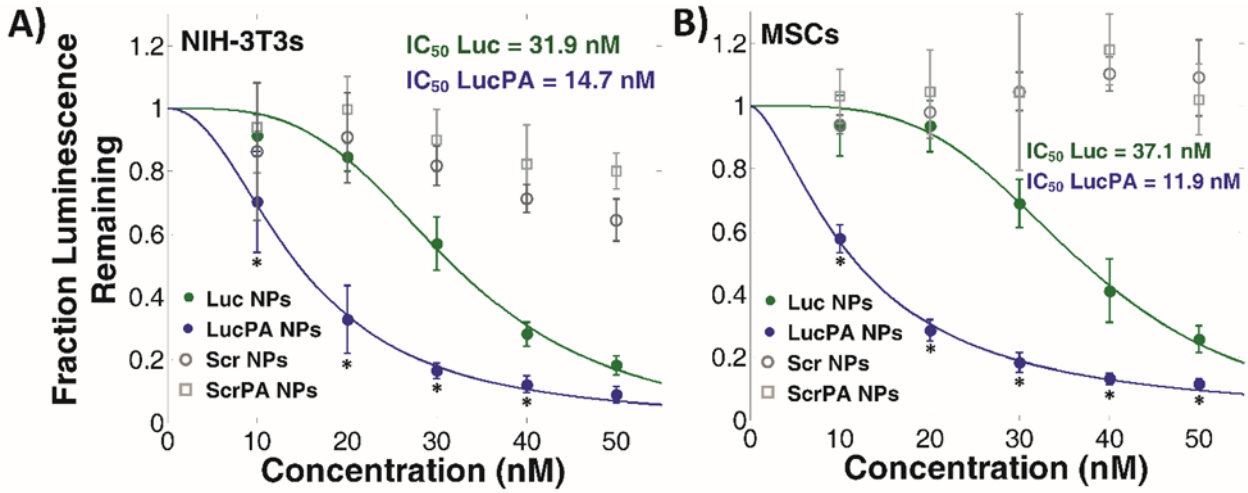

Figure 3.5. Luc-PA NPs exhibited superior luciferase silencing vs. luc NPs at a range of doses. A) In NIH-3T3 fibroblasts, the IC_{50} of luc NPs was 31.9 nM and of luc-PA NPs was 14.7 nM. B) In mouse MSCs, the IC_{50} of luc NPs was 37.1 nM and of luc-PA NPs was 11.9 nM. *$p<0.05$ for luc-PA NP silencing in comparison to luc NP silencing. Data are normalized to untreated cells. Small relative decreases in signal in NIH-3T3s at higher doses of the scr NPs are indicative of mild cytotoxicity.

The impact of PA modification on efficiency of silencing of the therapeutically-relevant gene PHD2 was also investigated. PHD2-PA NPs significantly enhanced gene silencing in comparison to PHD2 NPs when evaluated by RT-PCR (Figure 3.6). In fibroblasts, the IC_{50} of PHD2-PA NPs was 2.3-fold lower than that of PHD2 NPs. These data agree well with the data acquired using luc siRNA, confirming that the bioactivity gained through PA conjugation is consistent across different siRNAs.

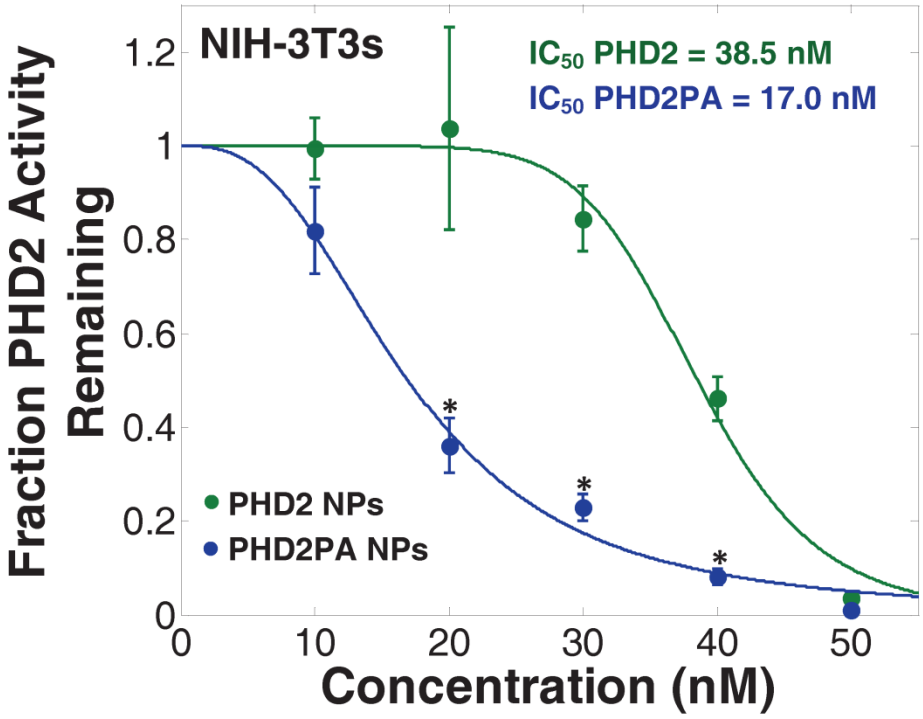

Figure 3.6. PHD2-PA NPs exhibited superior silencing vs. PHD2 siRNA NPs at a range of doses. In NIH-3T3 fibroblasts, the IC_{50} of PHD2 NPs was 38.5 nM and of PHD2-PA NPs was 17.0 nM. *$p<0.05$ for PHD2-PA NP silencing in comparison to PHD2 NP silencing. Data are normalized to scrambled controls.

Cellular Uptake and Retention of Oligo-PA NPs: To mechanistically explore the improved bioactivity achieved through PA conjugation, the cellular uptake and retention of fluorescently

modified DNA NPs or DNA-PA NPs were evaluated by flow cytometry at an N:P of 4:1. The intracellular fluorescent intensity of fibroblasts treated with DNA-PA NPs was 35-fold higher than those treated with the same dose of DNA NPs (Figure 3.7A). The intracellular half-life of the DNA vs. the DNA-PA was also investigated by monitoring the intracellular fluorescence over time after treatment removal and fitting the data to equation 2 where y is the fluorescence, y_0 the initial fluorescence measured at the time of treatment removal, x is the time in hours, and λ is related to the half-life $t_{1/2}$ by equation 3. The intracellular half-life of DNA-PA was found to be 3.1-fold higher than that of unmodified DNA.

Equation 2: $y = y_0(e^{(-\lambda x)})$ **Equation 3**: $t_{1/2} = \frac{\ln(2)}{\lambda}$

In support of the flow cytometry data, confocal microscopy revealed visibly increased fluorescence of fibroblasts treated with DNA-PA NPs in comparison to DNA NPs (Figure 3.7B). The overexposure of the images depicting DNA-PA NP uptake was necessary to demonstrate the uptake of DNA NPs under the same imaging settings and results from the large difference in uptake of the fluorescently labeled siRNA between the two treatments. Additionally, microscopy images at 0, 24, and 48 hours post-removal of treatment supported the flow cytometry results, demonstrating better retention of PA conjugates over time. Importantly, untreated cells showed no fluorescence when imaged using the same microscope settings (Figure S3.3).

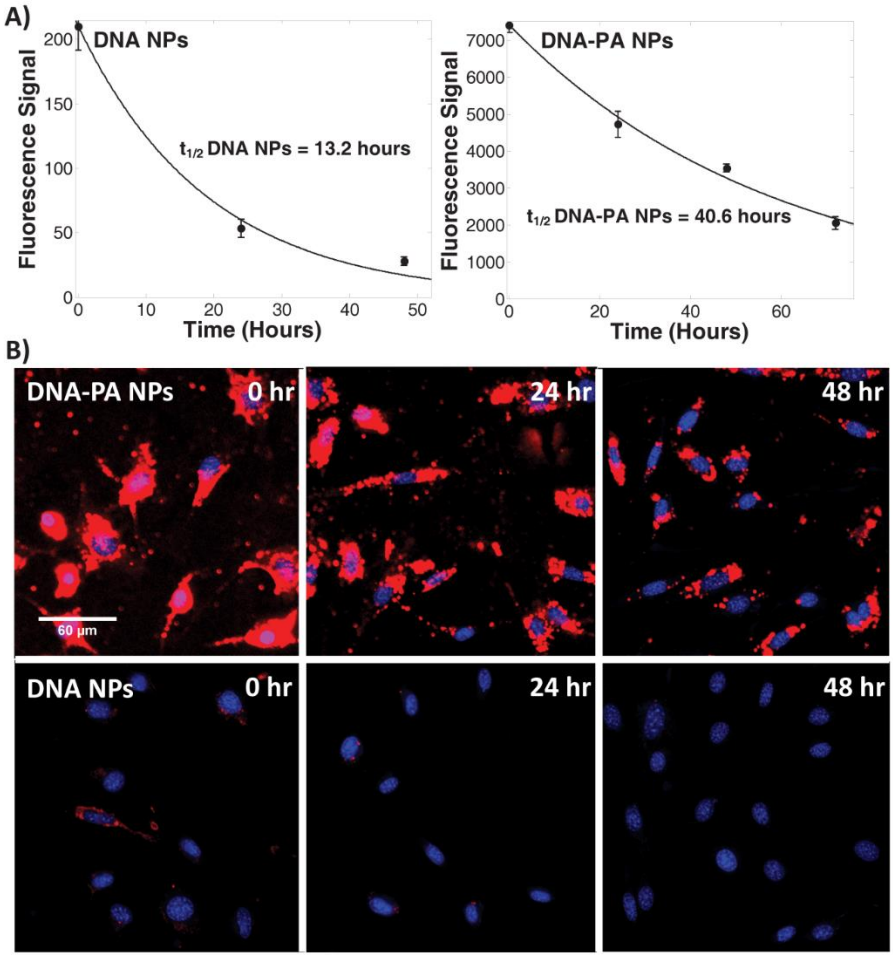

Figure 3.7. A) Intracellular fluorescence was higher and more sustained after treatment with DNA-PA NPs vs. DNA NPs. Quantified by flow cytometry in NIH-3T3s, intracellular half-life of Cy5-labeled DNA NPs is 13.2 hours and of Cy5-labeled DNA-PA NPs is 40.6 hours. Initial fluorescent intensity of DNA-PA NPs is ~35 times that of DNA NPs. Data are normalized to no treatment. B) Confocal microscopy images show increased uptake of DNA-PA NPs vs. DNA NPs. Images are at 0, 24, and 48 hours of incubation post-removal of a 12 hour treatment.

Next uptake pathway inhibitors were used to investigate the uptake mechanism of DNA-PA NPs in fibroblasts. EIPA, an amiloride analog and inhibitor of macropinocytosis, and cytochalasin D, which disrupts actin filament formation and thus impedes both caveolae-mediated uptake and macropinocytosis, significantly inhibited uptake of the DNA-PA NPs

(Figure 3.8). Dynasore, which blocks a dynamin GTPase necessary for formation of all clathrin-coated vesicles and for uptake through caveolae, had no effect on uptake of DNA-PA NPs.

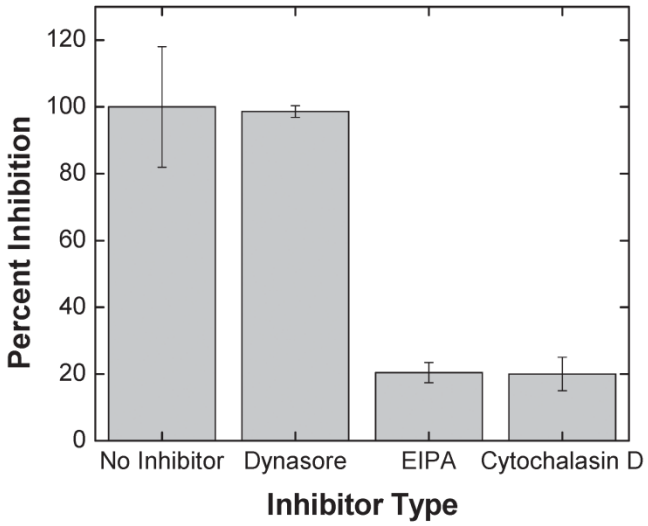

Figure 3.8. Cellular uptake, as measured by intracellular fluorescence, of DNA-PA NPs was inhibited by EIPA and cytochalasin D but not Dynasore. Quantified by flow cytometry in NIH-3T3s and normalized to a no inhibitor control (set to 100%). EIPA- and cyctochalasin D-treated groups were statistically equivalent and significantly different ($p<0.05$) compared to no inhibitor and Dynasore treatment.

Longevity of Gene Silencing of siRNA-PA NPs: The longevity of gene silencing of luc-PA NPs in comparison to unmodified luc NPs was investigated in NIH-3T3 fibroblasts. The duration of luciferase silencing with luc-PA NPs was increased in comparison to luc NPs. In cells treated by luc NPs, luciferase activity returned to equivalent to that of untreated cells by 72 hours, while cells treated with luc-PA NPs exhibited no decrease in silencing between 48 and 72 hours (Figure 3.9). After 7 days, cells treated with luc-PA NPs still showed 40% of the silencing effect detected at 24 hours (28% overall luciferase silencing in comparison to cells treated with scr-PA NPs). Quantification of silencing half-life (based on percentage of silencing measured upon

treatment removal at 24 hours) using Equations 2 and 3 revealed a half-life of 24 hours post-treatment removal for unmodified luc NPs in comparison to 186 hours for luc-PA NPs. This functional longevity of action corresponds to the increased intracellular half-life of DNA-PA compared to unmodified DNA.

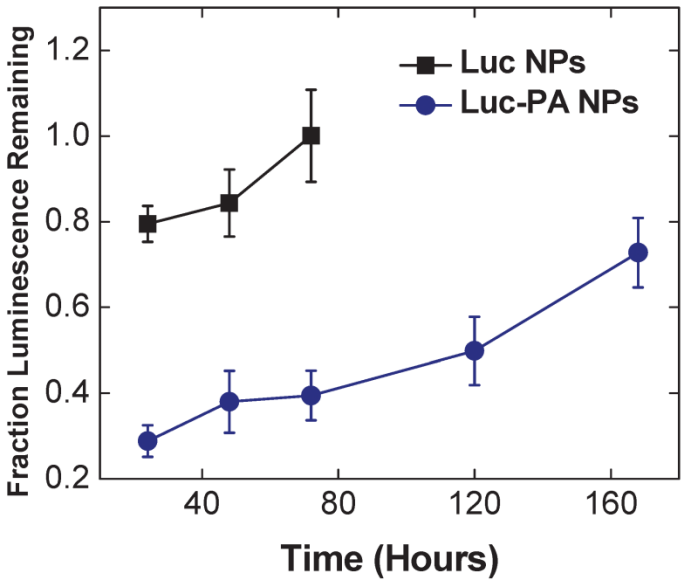

Figure 3.9. Luc-PA NPs silenced more effectively and over an increased duration relative to luc NPs. In NIH-3T3s treated at 30 nM, luc NP-treated cells recovered from luciferase knockdown by 72 hours while at 168 hours, luc-PA NP-treated cells still showed partial silencing. Normalized to scrambled controls. Luc-PA NP treatments elicited statistically greater silencing ($p<0.05$) than luc NP treatments.

3.5 Discussion

Direct conjugation of siRNA to targeting ligands, lipophilic moieties, or carrier molecules is a promising approach to enhancing knockdown efficacy and/or reducing the need for additional transfection reagents[28, 88, 215]. Palmitic acid has shown particular promise for increasing resistance to nuclease degradation, cellular uptake, and gene silencing in initial *in*

vitro tests using commercial lipid-based reagents[30]. Herein, we have characterized the performance of siRNA-PA relative to unmodified siRNA delivered via endosomolytic, polymer-based NPs that have previously demonstrated efficacy both *in vitro* and for local scaffold-based delivery *in vivo*[70, 108]. The goal was to improve the potency and longevity of action of the siRNA and to reduce the potential for negative side effects in ultimate scaffold-based siRNA-NP delivery applications.

The siRNA-PA was successfully synthesized using a one-step reaction and purified using HPLC (Figure 3.1). An important advantage of siRNA-PA over unmodified siRNA was its improved NP packaging. siRNA-PA completely loaded into the NPs at a 4:1 N:P ratio, while unmodified siRNA necessitated a 6:1 ratio for the polymer utilized in these studies (Figure 3.2). These data suggest that hydrophobization of siRNA is an efficient means to improve siRNA cargo loading and stability of NPs[169]. Other reports that nanoparticle carriers loaded with lipid-modified siRNA form particles at lower N:P ratios and with increased stability also support this conclusion[22, 215, 216]. It is posited that interactions among siRNA molecules through the lipophilic moieties increase negative charge density by localizing multiple siRNA molecules; this grouping is proposed to improve loading by cationic agents[215, 217]. Additionally, aggregated lipophilic moieties contribute to micelle stability[216]. Another potential contributing factor, in our NP carriers in particular, is that the PA molecule may help to anchor the siRNA into the hydrophobic micellar nanoparticle core. These hydrophobic interactions could help to reinforce the electrostatic interactions between the siRNA and the poly(DMAEMA)-based NP corona. This hypothesis is supported by the finding that siRNA-PA NPs had larger hydrodynamic diameter than siRNA NPs (Figure 3.3), while unloaded NPs and siRNA NPs were the same size (data not

shown). These data suggest that siRNA-PA impacts the overall NP packing, potentially due to increased interaction with the NP core.

Next, siRNA-PA NP silencing of both the model gene luciferase and of the therapeutically relevant gene PHD2 was benchmarked against siRNA NPs in fibroblasts. Similar studies were also done in MSCs, which have relevance for tissue regenerative applications and represent a cell type that is notoriously challenging to transfect[208, 218]. The first study assessed the effects of the N:P ratio used in the NP formulation on luciferase silencing in fibroblasts. At every N:P ratio tested for an siRNA dose of 40 nM, siRNA-PA NPs produced significantly greater gene silencing than unmodified siRNA NPs (Figure 3.4). The largest improvement in silencing by siRNA-PA occurred at the lower N:P ratios of 1:1, 2:1, and 4:1. Beyond a ratio of 4:1, increasing the amount of polymer had no significant impact on target knockdown for siRNA-PA NPs. Achieving potent silencing with a lower N:P is key to minimizing detrimental treatment effects, as a charge ratio of 6:1 began to cause increased cytoxicity in fibroblasts (Figure S3.2). The siRNA-PA NPs achieved a high level (more than 70%) of silencing efficacy even at an N:P of 1:1, which was superior to unmodified siRNA loaded at a 4:1 N:P ratio (the standard formulation condition for this polymeric NP composition)[70, 134].

Gene silencing potency was also compared for the siRNA-PA NPs and unmodified siRNA NPs formed at a constant N:P of 4:1. In fibroblasts, the dose of siRNA-PA NPs required to achieve 50% gene silencing was consistently two- to three-fold lower than the dose of siRNA NPs needed to achieve this effect. The improved potency of siRNA-PA NPs was apparent both for the model gene luciferase and for the therapeutically-relevant gene PHD2 (Figure 3.5A, 3.6). An even greater increase in gene silencing potency of more than three-fold was observed in MSCs (Figure 3.5B). The polymer NPs used here have been shown to be promising for siRNA

delivery to MSCs[210], while commercial reagents like Lipofectamine and Dharmafect have substantial cytotoxicity and low transfection efficiencies[103, 210]. Our results suggest that there is a synergistic effect between this polymeric carrier and PA-siRNA for transfection of MSCs, which reinforces findings that PA modification of polymeric carriers enhanced MSC plasmid transfection[103]. Unlike strategies to increase bioactivity by increasing the polymer:siRNA N:P ratio, the siRNA conjugated to PA did not have any impact on cell viability. Because the siRNA-PA conjugation decreases the amount of polymer needed and also increases the relative potency of the siRNA, it has the potential to strongly impact the therapeutic index for polymeric NP siRNA formulations.

In order to better understand the mechanism for the improved gene silencing performance of siRNA-PA NPs, cellular uptake and intracellular retention were measured by flow cytometry. The results revealed a 35-fold increase in cellular uptake of DNA-PA NPs relative to DNA NPs in fibroblasts. This effect is attributable to the presence of PA moieties, which may hydrophobically interact with cell membranes. Endogenous PA modification of proteins facilitates membrane binding and endocytotic processes[102, 104], and the number of lipophilic modifications on nucleic acids directly correlates to the level of association with cell membranes[217]. Therefore, the presence of multiple PA moieties on the corona of the NPs may act cooperatively to facilitate uptake, in combination with the positive zeta potential of the NPs. Previous studies of PA-modified siRNA employing Lipofectamine 2000 as a delivery agent showed more modest improvements in cellular uptake relative to the gains achieved herein with polymeric NPs[25]. This discrepancy is likely attributable to differences in the mechanism of siRNA complexation or cellular internalization achieved with each type of reagent. For example, cholesterol-modified siRNA loaded into cationic polymer micelles also demonstrated moderate

cellular uptake enhancement over unmodified siRNA in comparison to the improvement with siRNA-PA over siRNA in our system[22]. However, in this system, lipophilic siRNA was packaged in the core of the micelles, whereas our NP carriers load siRNA/siRNA-PA onto the micelleplex corona, potentially promoting multivalent PA interactions with the cell membrane.

Investigation into the uptake mechanism of PA-conjugated oligo NPs revealed a larger role for macropinocytotic uptake in comparison to clathrin and caveolin-mediated endocytosis, as seen by the lack of uptake inhibition by Dynasore in comparison to EIPA and cytochalasin D (Figure 3.8). It is hypothesized that the PA modification facilitates strong uptake enhancement by preferentially accessing macropinocytotic pathways; this preferential uptake by macropinocytosis could be due to the larger size of the siRNA-PA NPs. Internalization via this pathway may also impact siRNA-PA NP intracellular retention and cytoplasmic bioavailability, as it is accepted that the endocytotic mechanism has a significant impact on the trafficking and ultimate intracellular fate of internalized therapeutics[219, 220]. For example, macropinosomes are believed to be leakier and to provide an easier access point into the cellular cytoplasm[220], which may enhance the efficiency of endosomal escape and intracellular bioavailability of the siRNA-PA NPs. These uptake inhibitor data, combined with the belief that PA conjugation improves siRNA resistance to degradation[25], motivated investigation of intracellular retention (Figure 3.7) and longevity of gene silencing (Figure 3.9). Both of these studies suggested significantly greater persistence for siRNA-PA NPs relative to siRNA NPs. This effect is anticipated to be impactful for regenerative applications where repeat administration of siRNA may not be convenient or feasible.

In conclusion, these studies indicated that siRNA conjugation to PA acts synergistically with endosomolytic polymer NP formulations. PA conjugation reduced the required ratio of

polymer:siRNA and improved silencing potency, which was relevant across multiple genes and cell types relevant to tissue regeneration. Ultimately, the siRNA-PA would significantly reduce the ratio of polymer:siRNA as well as the overall dose of siRNA necessary for functional gene silencing. Furthermore, PA conjugation significantly improved longevity of silencing of siRNA. Thus, utilization of siRNA-PA NPs would facilitate a sustained functional effect with less frequent and/or lower doses, effectively broadening the therapeutic index and enhancing the probability of success for siRNA applications in tissue engineering.

CHAPTER 4

HYDROPHOBIC INTERACTIONS BETWEEN POLYMERIC CARRIER AND PALMITIC ACID-CONJUGATED SIRNA IMPROVE PEGYLATED POLYPLEX STABILITY AND ENHANCE *IN VIVO* PHARMACOKINETICS AND TUMOR GENE SILENCING

Text adapted from:

Sarett SM, Werfel TA, Chandra I, Jackson MA, Kavanaugh TE, Hattaway ME, Giorgio TD, Duvall CL (2016). Hydrophobic Interactions between Polymeric Carrier and Palmitic Acid-Conjugated siRNA Improve PEGylated Polyplex Stability and Enhance *In Vivo* Pharmacokinetics and Tumor Gene Silencing, *Biomaterials, 97.*

4.1 Abstract

Formation of stable, long-circulating siRNA polyplexes is a significant challenge in translation of intravenously-delivered, polymeric RNAi cancer therapies. Here, we report that siRNA hydrophobization through conjugation to palmitic acid (siPA) improves stability, *in vivo* pharmacokinetics, and tumor gene silencing of PEGylated nanopolyplexes (siPA-NPs) with balanced cationic and hydrophobic content in the core (relative to the analogous polyplexes formed with unmodified siRNA, si-NPs). Hydrophobized siPA loaded into the NPs at a lower charge ratio (N^+:P^-) relative to unmodified siRNA, and the siPA-NPs had superior resistance to siRNA cargo unpackaging in comparison to si-NPs upon exposure to the competing polyanion heparin and serum. *In vitro,* siPA-NPs increased uptake in MDA-MB-231 breast cancer cells (100% positive cells vs. 60% positive cells) but exhibited equivalent silencing of the model gene luciferase relative to si-NPs. *In vivo* in a murine model, the circulation half-life of intravenously-injected siPA-NPs was double that of si-NPs, resulting in a >2-fold increase in siRNA biodistribution to orthotopic

MDA-MB-231 mammary tumors. The increased circulation half-life of siPA-NPs was dependent upon the hydrophobic interactions of the siRNA and the NP core component and not just siRNA hydrophobization, as siPA did not contribute to improved circulation time relative to unmodified siRNA when delivered using polyplexes with a fully cationic core. Intravenous delivery of siPA-NPs also achieved significant silencing of the model gene luciferase *in vivo* (~40% at 24 hours after one treatment and ~60% at 48 hours after two treatments) in the murine MDA-MB-231 tumor model, while si-NPs only produced a significant silencing effect after two treatments. These data suggest that stabilization of PEGylated siRNA polyplexes through a combination of hydrophobic and electrostatic interactions between siRNA cargo and the polymeric carrier improves *in vivo* pharmacokinetics and tumor gene silencing relative to conventional formulations comprising only electrostatic interactions.

4.2 Introduction

Small interfering RNA (siRNA) has the potential to become a transformative class of therapeutics due to its ability to potently and specifically silence expression of genes, including targets considered to be "undruggable" by conventional small molecule inhibitors. However, clinical translation of siRNA therapies has been limited, primarily due to the formidable physiological barriers that must be overcome for siRNA to reach its intracellular site of action[12, 43, 47]. When delivered intravenously (e.g., for tumor therapy), siRNA molecules are rapidly cleared through the kidneys[18, 221]. If siRNA reaches target cells, it lacks a mechanism to translocate bilayer membranes, limiting both cellular uptake and endosomal escape. To combat these myriad challenges, lipidic and polymeric carrier systems as well as a variety of siRNA conjugates have been developed that feature mechanisms to improve siRNA pharmacokinetics, stability, cellular uptake, release, endosomal escape, and/or site-specific targeting[21, 22, 24, 25, 70, 72, 76, 78, 88, 222-226].

However, clinical efficacy of these delivery systems remains limited, due in large part to a preferential distribution to and systemic clearance through the hepatic and renal systems. As evidenced by therapies currently in advanced clinical trials, the natural targeting of lipid-based nanoparticles to the liver can be leveraged to successfully modulate gene expression in hepatocytes, but delivery of siRNA to other target tissues remains a challenge[77, 78, 182, 209, 211, 227]. It is thus of high significance to identify systemic siRNA delivery systems that accumulate at other target sites, such as tumors.

Although the magnitude of the enhanced permeability and retention (EPR) effect in spontaneously-formed tumors in humans and large animals is known to be variable, it is accepted that for many tumor types, there is a significant correlation between nanocarrier tumor accumulation and blood circulation persistence (related to avoidance of clearance through organs such as liver and kidney)[162, 228-230]. Likewise, it has been observed that the magnitude of passive tumor uptake of nucleic acid-based nanopolyplexes is directly related to circulation time[231, 232]. Commonly, lipoplex or polyplex nano-formulations designed for intravenous administration are PEGylated to impart colloidal stability and to reduce opsonization and clearance by the mononuclear phagocyte system (MPS)[73, 165, 233, 234]. However, siRNA delivered by polyplexes that are stabilized solely through electrostatic interactions with polyplex core-forming cationic polymers is susceptible to rapid clearance through the kidney. This clearance is due to polyplex disassembly triggered by the competing interactions between the cationic polymer and the polyanionic heparan sulfates of the glomerular basement membrane (GBM). As a result, electrostatically-stabilized or polyion complex nanoparticle formulations impart only minor differences in pharmacokinetics (i.e., blood persistence half-life) relative to free siRNA ($t_{1/2}$ siRNA ~1 – 2 min, $t_{1/2}$ siRNA nanoparticles ~3 – 5 min)[18, 221, 234-236]. While siRNA-encapsulating

nanoparticles fabricated through water-in-oil-in water (W/O/W) emulsion methods impart significant pharmacokinetic advantages[171], loading of highly anionic and hydrophilic siRNA into a hydrophobic core nanoparticle formulation is not very efficient, resulting in loss of expensive siRNA during fabrication, exposure of siRNA to potentially damaging organic solvents, and formation of nanoparticles with high weight ratios of carrier polymer(s) relative to siRNA cargo. The aim of the current report was to increase the stability of PEGylated siRNA polyplexes against polyanion-induced disassembly, limiting removal of intravenously-delivered polyplexes from the circulation while obviating complex and inefficient siRNA-loaded nanoparticle formulation processes.

Here, we sought to improve pharmacokinetics for tumor applications by developing a PEGylated nanopolyplex formulation that is core-stabilized by both electrostatic and hydrophobic interactions between the polymeric carrier and the siRNA cargo. We recently developed PEGylated, core-loaded siRNA nanopolyplexes (si-NPs) with a combination of both electrostatic and hydrophobic stabilization due to the optimized balance of cationic and hydrophobic content within the polymer block that forms the polyplex core[237]. These si-NP formulations comprised unmodified siRNA and the diblock polymer poly(ethylene glycol)-*b*-poly(dimethylaminoethyl methacrylate-*co*-butyl methacrylate) (PEG-*b*-p(DMAEMA-*co*-BMA)) with 50 mole percent of both cationic DMAEMA and hydrophobic BMA monomer in the core-forming block (polymer termed "50B"). Relative to the analogous PEG-*b*-p(DMAEMA) diblock polymer (termed "0B" and characterized by a fully cationic core), the 50B formulation exhibited improved resistance to disassembly by heparin sulfates, circulation time, and endosomal escape, as well as superior gene silencing bioactivity both *in vitro* and *in vivo*. Here, we utilized the 50B polymer for packaging

and delivery of hydrophobized siRNA to evaluate the impact of providing both electrostatic and hydrophobic interactions between the polymeric carrier and the siRNA cargo.

To test the hypothesis that a combination of electrostatic and hydrophobic interactions between the 50B polymer and siRNA cargo increases formulation stability and performance, we compared pharmacokinetics and bioactivity of 50B-based nanopolyplexes loaded with unmodified siRNA to those loaded with siRNA conjugated to the hydrocarbon palmitic acid (PA). Conjugation of siRNA to lipid-like moieties (e.g. cholesterol, α-tocopherol, and palmitic acid) improves stability and enhances cellular uptake of siRNA by increasing the hydrophobicity of the siRNA molecule[23, 24, 26]. Furthermore, conjugation to hydrophobic molecules such as cholesterol or palmitic acid (PA) can make siRNA more effective when delivered via polymeric delivery carriers[22, 23, 25, 101, 238]. Similarly, incorporation of hydrophobic components into the polymer carrier has been proven to enhance polyplex stability and cellular uptake and transfection of unmodified nucleic acids[19-21, 169, 216, 239, 240]. The Kataoka group has specifically illustrated improvements in stability of a polyplex micelle delivery system via separate investigations into cholesterol modification of the siRNA molecule or micellar components. The approach in the current work is unique in that we investigate the interplay between hydrophobized siRNA and a partially hydrophobic polymer nanocarrier (50B), facilitating hydrophobic as well as electrostatic interactions between cargo and carrier. To isolate the pharmacokinetic significance of hydrophobic interactions between hydrophobized siRNA and the 50B polyplex core versus hydrophobization of each component individually, both the 0B (purely cationic) polymer and unmodified siRNA were used as controls for *in vivo* pharmacokinetics studies. This experimental design elucidates the functional benefit of dual hydrophobization for improving *in vivo* stability and target gene silencing in an orthotopic triple negative breast cancer (MDA-MB-231) model.

4.3 Experimental Methods

Materials. Amine-modified single-stranded DNA (modification at 5' end) or RNA (modification at 3' end) and complementary single-stranded Cy5-, Alexa Fluor 488- or Alexa Fluor 546-modified DNA or unmodified RNA were all obtained from Integrated DNA Technologies (Coralville, Iowa). The pGreenFire1-CMV plasmid was obtained from System Biosciences (Mountain View, CA), and packaging plasmids pMDLg/pRRE, pRSV-Rev, and pMD2.G were purchased from Addgene (Cambridge, MA). Lipofectamine 2000 and NucBlue Fixed Cell ReadyProbes were purchased from Life Technologies (Grand Island, NY). CytoTox-ONE Homogeneous Membrane Integrity Assay (a lactate dehydrogenase (LDH) assay) was purchased from Promega (Madison, WI). PD10 desalting columns were purchased from GE Healthcare (Waukesha, WI). Quant-iT RiboGreen RNA Assay Kit was purchased from ThermoFisher Scientific (Waltham, MA). All other reagents were purchased from Sigma-Aldrich (St. Louis, MO).

Synthesis of 4-Cyano-4-(ethylsulfanylthiocarbonyl)sulfanylpentanoic Acid (ECT) and PEG-ECT. The RAFT chain transfer agent ECT was synthesized as previously described, and the R-group of the CTA was subsequently conjugated to PEG[70, 241]. Briefly, dicyclohexylcarbodimide (4 mmol, 0.82 g) was added to the stirring solution of monomethoxy-poly(ethylene glycol) (Mn = 5000, 2 mmol, 10 g), ECT (4 mmol, 1.045 g), and DMAP (10 mg) in 50 mL of dichloromethane. The reaction mixture was stirred for 48 h. The precipitated cyclohexyl urea was removed by filtration, and the dichloromethanane layer was concentrated and precipitated into diethyl ether twice. The

precipitated PEG-ECT was washed three times with diethyl ether and dried under vacuum (yield ~10g). ^{1}H-NMR (400 MHz $CdCl_3$) revealed 91% substitution of the PEG (data not shown)[237].

Polymer Synthesis and Characterization. RAFT polymerization was used to synthesize a 50:50 [BMA]:[DMAEMA] copolymer using the PEG-ECT macro-CTA. The target degree of polymerization was 160, and the monomer plus CTA was 40% weight per volume in dioxane. The polymerization reaction was carried out at 70^{o}C for 24 hours using AIBN as the initiator with a 5:1 [CTA]:[Initiator] molar ratio. A monomer feed ratio of 50:50 mol % or 0:100 mol % [BMA]:[DMAEMA] was used (to generate 50B and 0B respectively), and a double alumna column was utilized to remove inhibitors from DMAEMA and BMA monomers prior to polymerization. The reactions were stopped by removal from heat and exposure of the polymerization solution to air. The resulting polymers were precipitated into a co-solvent of 90% pentane and 10% diethyl ether. The isolated polymers were vacuum-dried, redissolved in water, further purified by dialysis for 24 hours, and lyophilized. Polymers were characterized for composition and molecular weight by ^{1}H-NMR spectroscopy (Bruker 400 MHz spectrometer equipped with a 9.4 T Oxford magnet). Absolute molecular weight and polydispersity of the polymers was determined using DMF mobile phase gel permeation chromatography (GPC, Agilent Technologies, Santa Clara, CA, USA) with inline Agilent refractive index and Wyatt miniDAWN TREOS light scattering detectors (Wyatt Technology Corp., Santa Barabara, CA, USA).

Oligonucleotide-PA Synthesis and Characterization. Single-stranded amine-modified oligo was reacted with 100-fold molar excess of PA *N*-hydroxysuccinimide ester pre-dissolved at 40 mM in

N,*N*-dimethylformamide (DMF). The reaction was carried out for 18 hours at room temperature in 45% water, 45% isopropyl alcohol, and 10% DMF. The oligo-PA was purified by reversed-phase HPLC using a Clarity Oligo-RP column (Phenomenex, Torrence, CA) under a linear gradient from 95% water (50 mM triethylammonium acetate), 5% methanol to 100% methanol. The conjugate molecular weight was confirmed using MALDI-TOF mass spectrometry (Voyager-DE STR Workstation, Grand Island, NY) using 50 mg/mL 3-hydroxypicolinic acid in 50% water, 50% acetonitrile with 5 mg/mL ammonium citrate as a matrix. The yield of the oligo-PA was quantified based on absorbance at 260 nm. The purified oligo-PA was annealed to its complementary strand to generate Cy5-, Alexa Fluor 488- or Alexa Fluor 546-modified DNA-PA or siPA. Conjugation and annealing was also confirmed via agarose gel electrophoresis.

Assembly and Characterization of siRNA- or siPA-Loaded Polyplex NPs. Polyplex NPs loaded with siRNA (si-NPs) or siPA (siPA-NPs) were made by mixing pH 4.0 stock solutions of 50B polymer (10 mM buffer, 3.33 mg/mL polymer) and siRNA (50 μM) at N:P ratios of 1, 2, 5, 7, 10, or 20. Control polyplexes comprising the 0B polymer (termed si-0B-NPs and siPA-0B-NPs) were made according to the same procedure. The final charge ratio was calculated as the molar ratio of cationic amines on the DMAEMA (50% are assumed to be protonated at physiologic pH) to the anionic phosphates on the siRNA/siPA. After mixing, these solutions were diluted 5-fold to 100 μL with pH 8.0 phosphate buffer (10 mM) to adjust the final pH to 7.4. After mixing, samples were incubated for 30 min, and 100 ng of siRNA/siPA for each sample was loaded onto a 2% agarose gel containing ethidium bromide to assess siRNA/siPA packaging efficiency. The gels were run at 100 V for 35 min and imaged with a UV transilluminator. Hydrodynamic diameter and zeta potential of the polyplex NPs at the N:P ratios described above were measured in triplicate

using dynamic light scattering (DLS) (Malvern Zetasizer Nano ZS, Malvern, UK). DLS measures were used to evaluate salt stability of polyplex NPs; concentrated NaCl solution was added to si-NP or siPA-NP solutions in 10 mM phosphate buffer to yield final NaCl concentrations of 0, 0.1, 0.5, or 1 M where the final solution was 80% phosphate buffer by volume. For the cell uptake studies (where no functional effects were studied) DNA and DNA-PA was used as a model molecule for siRNA and siPA, respectively. Hereafter, NPs loaded with these molecules are referred to as si-NPs and siPA-NPs to avoid confusion.

Cell Culture. Human epithelial breast cancer cells (MDA-MB-231) were cultured in Dulbecco's modified Eagle's medium (DMEM, Gibco Cell Culture, Carlsbad, CA) supplemented with 10% fetal bovine serum (FBS, Gibco) and 0.1% gentamicin (Gibco).

Production of Stable Luciferase-Expressing MDA-MB-231s. To produce lentivirus, the pGreenFire1-CMV plasmid and packaging plasmids pMDLg/pRRE, pRSV-Rev, and pMD2.G were transfected into HEK-293Ts using Lipofectamine 2000. Media was changed after 24 hours and supernatant containing lentivirus was collected at 48 and 72 hours. Viral supernatant was added directly to MDA-MB-231s with 6 μg/mL polybrene. Media was changed after 24 hours. Lentiviral transduction and was confirmed by GFP expression as analyzed by flow cytometry (BD LSR II Flow Cytometer, San Jose, CA). This was followed by selection with 8 μg/mL puromycin for two weeks to eliminate non-transduced cells.

Cellular Uptake. MDA-MB-231s were seeded at 30,000 cells/well in 24-well plates and allowed to adhere overnight. After adhering, cells were treated with 100 nM Alexa Fluor 488-labeled si-

NPs or siPA-NPs in 10% serum for 24 hours. Lipofectamine was used as a positive control (with treatment at 25 nM to minimize toxicity). After 24 h, media with treatments was removed, cells were washed with PBS (-/-), trypsinized (0.25%), transferred to microcentrifuge tubes, and centrifuged at 420xG for 7 min to pellet the cells. Pellets were re-suspended in 0.4 mL PBS(-/-) with 0.04% trypan blue to quench extracellular fluorescence and monitored by FACS (FACSCalibur, BD Biosciences, Franklin Lakes, NJ, USA) at excitation wavelength of 488 nm and emission wavelength of 519 nm to quantify intracellular delivery.

In Vitro *Gene Silencing.* MDA-MB-231s were treated with si-NPs or siPA-NPs; the siRNA was either designed against the luciferase gene (luc siRNA) or was a scrambled sequence (scr siRNA). Cells were seeded at 2,000 cells/well in 96-well black-walled plates and allowed to adhere overnight. Cells were then treated in 10% serum for 24 hours at a dose of 100 nM siRNA. After 24 h, media was replaced with luciferin-containing media (150 μg/mL) before imaging with an IVIS Lumina III imaging system (Caliper Life Sciences, Hopkinton, Massachusetts) every 24 hours for 10 days. Fresh low serum media (2% FBS) was replaced after each imaging session, and cells were passaged every 3 days. Growth in low serum was used to reduce the confounding influence of proliferation and allowed more direct investigation of gene silencing longevity. To evaluate treatment cytotoxicity, scr siRNA si-NP treatments were removed at 24 hours and cellular bioluminescence was quantified on a Lumina III IVIS (Caliper Life Sciences, Hopkinton, Massachusetts) and compared to no treatment as a measure of relative cell number.

Comparison of siRNA and siPA Polyplex Stability. NPs were loaded with Förster Resonance Energy Transfer (FRET, using Alexa Fluor 488 and Alexa Fluor 546) pair-labeled doubled-

stranded 23mers (FRET-NPs). Fluorescent intensity was measured using a microplate reader (Tecan Infinite F500, Männedorf, Switzerland) with an excitation wavelength of 488 ± 5 nm. Alexa Fluor 488 emission was collected at 519 ± 5 nm, and Alexa Fluor 546 emission was obtained at 573 ± 5 nm. FRET was calculated as a ratio of the fluorescent intensity as follows:

$$\text{FRET} = \frac{I_{573}}{I_{519}}$$

Because siRNA decomplexation by heparan sulfate-containing glomerular basement membrane in the kidney is a primary cause for rapid systemic clearance of polycation-siRNA nanoparticles, the stability of FRET-NPs was measured in the presence of 2 to 100 U/mL of heparin sodium salt in DPBS[18, 221]. The fluorescence emission was measured over time following addition of heparin sodium salt. The heparin concentration at which the FRET signal was reduced 50% (EC50) for siRNA and siPA polyplexes was calculated as according to the following equation where y is the FRET ratio, x is the heparin concentration, and b is a fit parameter.

$$y = \frac{-1}{1 + \left(\frac{x}{EC50}\right)^{b}} + 1$$

The same assay was performed in the presence or absence of 10, 40, and 50% of FBS as well. In this study, si-NPs and siPA-NPs were prepared as described above and incubated with either FBS or an equal volume of PBS. FRET was calculated according to the equation above, and %FRET was calculated at each time point by dividing the FRET ratio of FBS-treated NPs by PBS-treated controls. The Quant-iT RiboGreen RNA Assay Kit was used to quantify the amount of unpackaged siRNA before and after addition of 100 U/mL heparin for si-NPs, siPA-NPs, si-0B-NPs, and siPA-0B-NPs.

Blood Plasma Pharmacokinetics. Fluorescent (Cy-5-labeled) si-NPs and siPA-NPs were formed at an N:P ratio of 10:1 As a comparison, siRNA and siPA were loaded into 0B at a ratio of 10:1. NPs were injected into the tail vein of CD-1 mice (4-6 weeks old, Charles Rivers Laboratories, Wilmington, MA, USA) at 1 mg/kg. Blood was collected retro-orbitally at 5 min and 10 min post-injection, not exceeding two collections per animal. After 20 min, animals were sacrificed, and blood was immediately collected via cardiac puncture. Blood samples were centrifuged at 2000 G for 5 min and 5 μL of plasma was taken from the supernatant and diluted into 95 μL PBS (-/-). Fluorescence was measured and quantified on an IVIS Lumina III imaging system (Xenogen Corporation, Alameda, CA, USA) at excitation wavelength of 620 ± 5 nm and emission wavelength of 670 ± 5 nm (n = 6). A standard curve was generated by measuring the fluorescence of the initial fluorescent polyplex solution in PBS (-/-) over the range of 200% to 1.5% of the injected dose. The standard curve was utilized in order to calculate the percent of injected dose in each blood sample, and the calculated values were used to determine siRNA concentration in the plasma at each time point as well as area under the curve (AUC) values (see Table S4.1 for equations).

Biodistribution in Tumor-bearing Mice. Athymic nude female mice (4-6 weeks old, Jackson Laboratory, Bar Harbor, ME, USA) were injected in each mammary fat pad with 1 x 10^6 MDA-MB-231 cells in DMEM:Matrigel (50:50). After 17 days, tumor-bearing mice were injected via the tail vein with 1 mg/kg (nucleic acid dose) of fluorescent siNPs or siPA-NPs. After 20 minutes, animals were sacrificed and the organs of interest (heart, lungs, liver, spleen, kidneys, and tumors) were excised. The fluorescence intensity in the organs was quantified on an IVIS Lumina III

imaging system (Xenogen Corporation, Alameda, CA, USA) at excitation wavelength of 620 ± 5 nm and emission wavelength of 670 ± 5 nm (n = 3 animals, n = 6 tumors).

Target Gene Silencing After Intravenous (I.V.) Injection. Athymic nude female mice (4-6 weeks old, Jackson Laboratory, Bar Harbor, ME, USA) were injected in each mammary fat pad with 1 x 10^6 MDA-MB-231 cells in DMEM:Matrigel (50:50). After 17 days, tumor-bearing mice were injected i.p. with luciferin substrate (150 mg/kg) and imaged for bioluminescence on an IVIS Lumina III imaging system (Xenogen Corporation, Alameda, CA, USA) 20 minutes post-injection. Next, the mice were injected via the tail vein with 1 mg/kg (siRNA dose) NPs containing either luc siRNA / siPA, a scr siRNA / siPA, or saline. Mice were imaged and treated at days 17 and 18 following tumor cell inoculation and imaged on day 19. Relative luminescence was determined by measuring the raw luminescent intensity of each tumor on each day and comparing to the initial signal at day 17 (n =10 tumors per group).

Acute Toxicity in Liver and Kidney. Tumor-bearing mice used for *in vivo* luciferase silencing studies were sacrificed on day 20 following tumor cell inoculation (and following treatment with 1 mg/kg siRNA on days 17 and 18). Blood was collected by cardiac puncture and then centrifuged at 2000 G for 5 min. Then, plasma was harvested and tested by the Vanderbilt Translational Pathology Shared Resource (TPSR) for systemic levels of alanine aminotransferase (ALT), aspartate aminotransferase (AST), and blood urea nitrogen (BUN).

Statistical Methods. The treatment groups were statistically compared using a one way ANOVA test coupled with a Tukey means comparison test; a p-value < 0.05 was deemed representative of

a significant difference between groups. For all data shown, the arithmetic mean and standard error are reported, and the sample size (n) is indicated.

Ethics Statement. The animal studies were conducted with adherence to the guidelines for the care and use of laboratory animals of the National Institutes of Health (NIH). All experiments with animals were approved by Vanderbilt University's Institutional Animal Care and Use Committee (IACUC).

4.4 Results and Discussion

Polymer and siPA Conjugate Synthesis. A previously reported RAFT polymerization scheme was used to synthesize the 50B polymer from a 5 kDa PEG-ECT macro-CTA[237]. The scheme is desirable for its simplicity and scalability, and it consistently yields polymers at target molecular weight (MW) with low polydispersity index (PDI). The 50B polymer used here was synthesized from the macro-CTA with a final degree of polymerization (DP) of 152 (Target DP: 160) and PDI of 1.03 as determined by ^{1}H-NMR and GPC, respectively (Figure 4.1). The RAFT-polymerized block monomer composition and MW were quantified by ^{1}H-NMR using characteristic peaks from PEG (-O-C**H$_2$**C**H$_2$**-, δ 3.65s), BMA (-O-C**H$_2$**CH$_2$-, δ 3.95s), and DMAEMA (-O-C**H$_2$**CH$_2$-, δ 4.05s), showing 49:51 (BMA:DMAEMA) mol% ratio in the polyplex core-forming block and total MW of 27,800 Da (including 5kDa PEG). The control 0B polymer was synthesized by the same 5route and had a 110 DP, 1.16 PDI, 0:100 mol% ratio, an0 d 22,300 Da MW (data not shown).

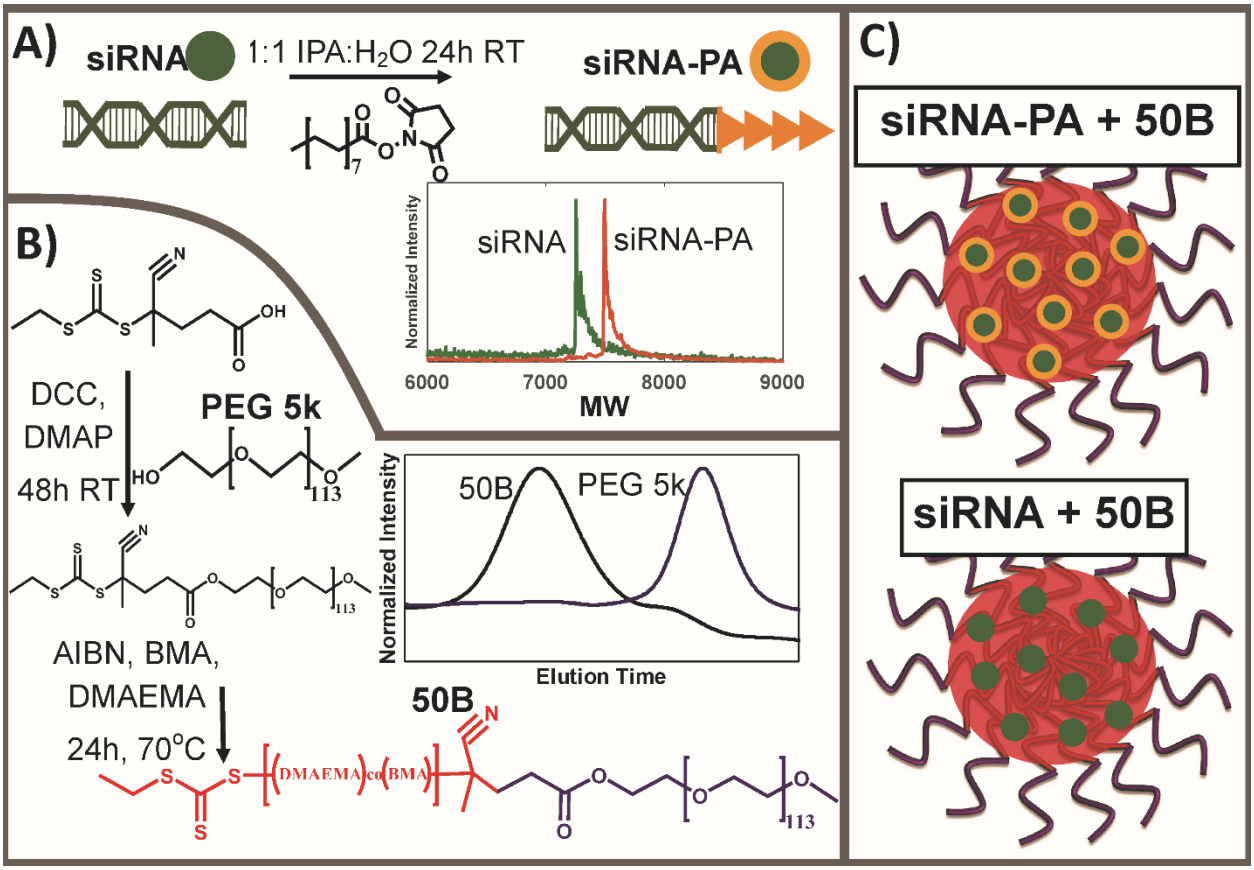

Figure 4.1. A) Synthesis of siPA and product confirmation via MALDI-TOF. B) Synthesis of 50B and GPC analysis. C) Schematic of core-loaded siPA-NP and si-NP polyplexes.

Synthesis of siPA-NPs. Single-stranded DNA or RNA was successfully conjugated with PA in a one-step reaction and purified from the reactants via HPLC. Isolation of the desired products was confirmed by MALDI-TOF analysis (Figure 4.1) and also by shift upward of the free siPA band in comparison to the unmodified siRNA band in a gel retardation assay (Figure 4.2).

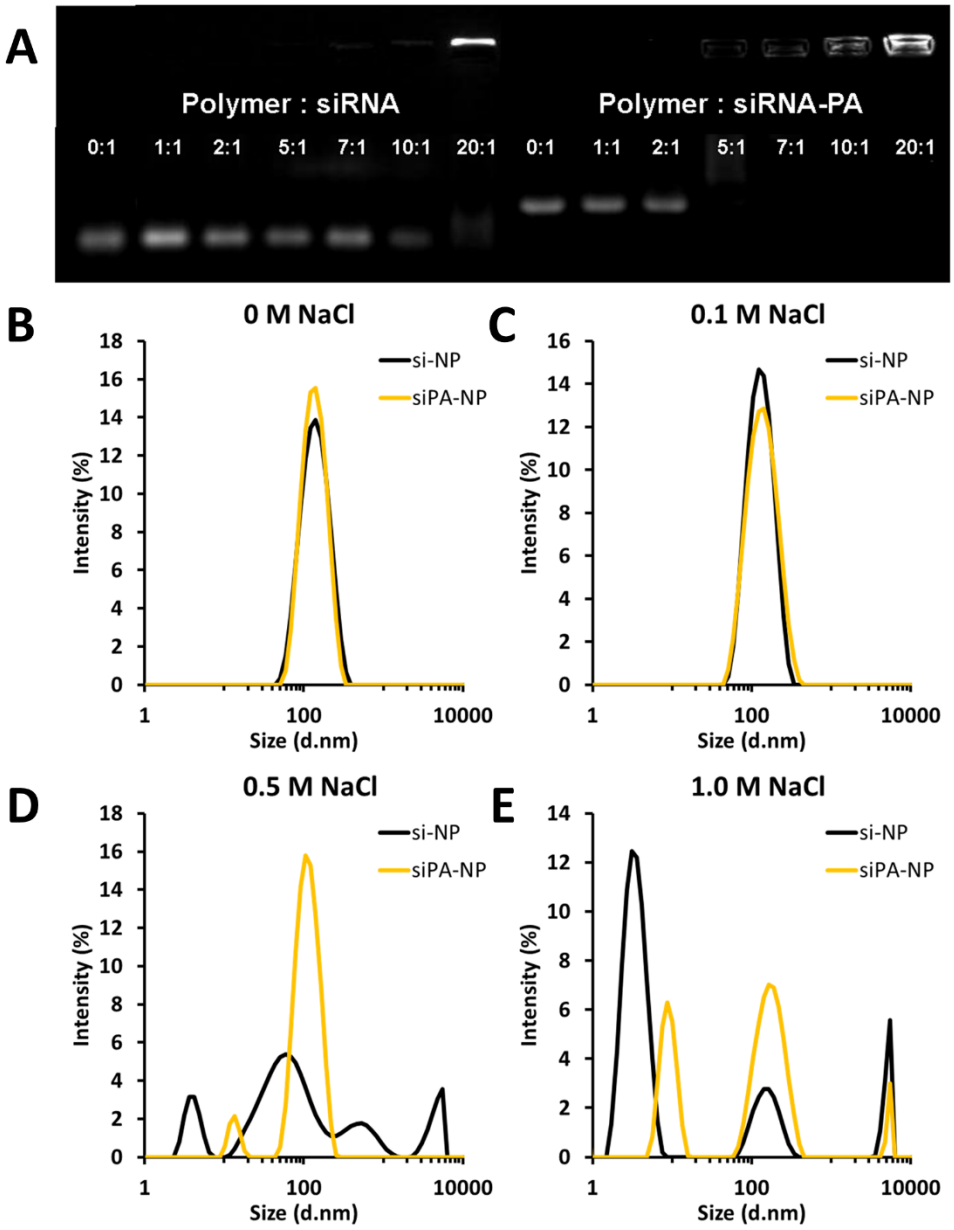

Figure 4.2. siPA is packaged more efficiently and stably with 50B polymer than unmodified siRNA. A) As evaluated by gel retardation assay, siPA loads fully at a lower N:P ratio than unmodified siRNA; note that the upward shift of siPA compared to siRNA also confirms PA conjugation. B-D) As evaluated by dynamic light scattering, siPA-NPs are more stable to elevated salt concentrations (approximately 25 nm smaller) than si-NPs at N:P = 10:1.

Characterization of si-NPs/siPA-NPs. Unmodified siRNA completely loaded into the PEGylated nanopolyplexes at an N:P ratio of 20:1, while siPA was fully loaded at a ratio of 5:1, as characterized by gel retardation assays (Figure 4.2A). This result suggests that hydrophobization of the siRNA molecule enhances interactions with 50B and improves efficiency of loading into NPs. DLS measurements reveal that siPA-NPs are of equivalent size and exhibit enhanced stability to elevated salt concentration relative to si-NPs (Figure 4.2B and S4.2). The zeta potential does not differ significantly between siPA-NPs and si-NPs, with each displaying a slight negative charge which is optimal for intravenous administration (data not shown).

This result is in agreement with previous reports from our group and others showing that lipid-modified siRNA loads more efficiently into nanocarrier systems with completely electrostatically-driven siRNA complexation mechanisms[22, 215, 238]. However, the siPA-NP system is unique in that it is the first to elucidate the importance of hydrophobic interactions between lipid-modified siRNA and hydrophobized cationic polymer components. We posit that the hydrophobization of the siRNA stabilizes the nanoparticles by introducing interaction between the lipophilic moieties on different siRNA molecules and, unique to the siPA-NPs, with the hydrophobic BMA monomer which is ~50 mol% of the core-forming block of the carrier polymer in the current system. This overall result indicates that a combination of electrostatic and hydrophobic interactions between siPA and 50B improved its loading efficiency and stability in the presence of competing polyelectrolytes (akin to those encountered in systemic administration), motivating further characterization of the stability and function of siPA-NPs in biological contexts.

In vitro *validation of si-NPs/siPA-NPs.* After establishing the improved loading efficiency of siPA relative to unmodified siRNA, we characterized the performance of si-NPs and siPA-NPs *in vitro*

(Figure 4.3). Evaluation of the cytotoxicity of each demonstrated greater than 80% cell viability at all N:P ratios examined after 24 h (Figure 4.3A), with a trend toward decreased cell number for higher N:P ratios. This result confirms that the nanopolyplex system is generally well-tolerated but also emphasizes the translational significance of reducing the amount of polymer necessary to achieve a therapeutic effect, for example through improved siRNA loading and delivery using a lower N:P ratio.

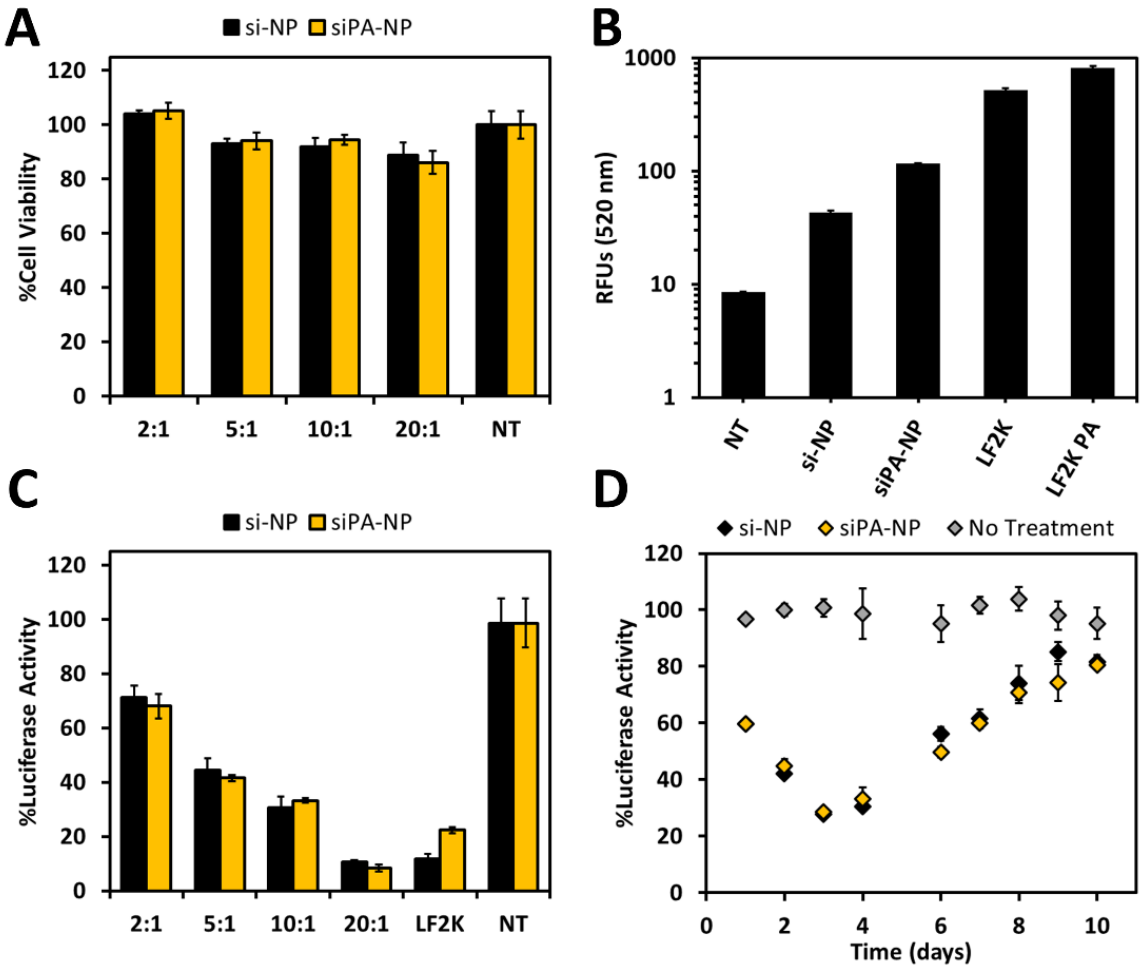

Figure 4.3. *In vitro* characterization of siPA-NPs vs. si-NPs. A) Both formulations exhibit >80% cell viability at all N:P ratios investigated as evaluated by percent difference in luciferase signal from that of no treatment (n = 4). No treatments were statistically significantly different from NT. B) siPA-NPs are internalized by cells ~2-fold more than si-NPs after 24 hours of treatment (N:P = 10:1, n = 3). Each treatment group is statistically different from all

other treatment groups ($p<0.05$). C) siPA-NPs and si-NPs exhibit increasing luciferase silencing at higher N:P ratios but are not significantly different from each other. (n = 4). No statistically significant differences between si-NP and siPA-NP treatment at each ratio. D) Both siPA-NPs and si-NPs show prolonged luciferase silencing (over 10 days) at an N:P ratio of 10:1 (n = 3). No statistically significant differences between si-NP and siPA-NP treatment at each timepoint. For C) and D), all treatment groups are normalized to analogous scrambled siRNA controls to account for treatment effect on cell viability; no treatment is averaged each day by measuring luminescent signal of untreated cells (n = 3).

Next, the cellular uptake of siPA-NPs was compared to si-NPs. After treatment with siPA-NPs, nearly 100% of cells were positive for the fluorescently-tagged nucleic acid (Figure S4.3). This was equivalent to the percentage positive cells observed after treatment with Lipofectamine® 2000, a commercial transfection reagent. The corresponding treatment of si-NPs resulted in a cell population 60% positive (Figure S4.3), revealing that PA conjugation increased NP cellular internalization. This is corroborated by evaluation of the mean fluorescent intensity of treated cells, which was approximately 2-fold higher for siPA-NPs compared to si-NPs (Figure 4.3B). Many physicochemical and biological factors such as particle size[242, 243], surface charge[242], shape[244], PEG density[245], particle elasticity[246], internalization and trafficking route[247, 248], etc., can contribute to differences in particle uptake. In our studies, the most obvious difference between the si-NPs and siPA-NPs was enhanced stability of siPA-NPs in the presence of serum (Figure S4.4). Therefore, it is likely that increased siPA-NP stability in the presence of serum contributes to the observed improvement in uptake, although this result may be multifactorial.

In *in vitro* gene knockdown screens, the si-NPs and siPA-NPs both exhibited potent and sustained silencing in MDA-MB-231 breast cancer cells (Figure 4.3C, D). For each, a higher level of gene silencing was observed as the N:P ratio was increased. Silencing between si-NPs and siPA-NPs did not differ significantly across the N:P ratios screened, despite the small increase in cell

uptake observed for siPA-NPs. This could be due to the enhanced stability of the siPA-NPs, which may impede siRNA unpackaging from nanopolyplexes upon cellular internalization[249]. Although increased polyplex stability may limit siRNA intracellular bioavailability *in vitro*, this potentially negative impact is expected to be outweighed by the benefit gained *in vivo* by increasing circulation half-life and cell uptake. Also of note is the prolonged silencing effect observed in this nanoparticle system, using both unmodified siRNA and siPA (Figure 4.3D). A potential factor in this sustained effect *in vitro* is the inherent endosomolytic capability of the 50B polymer carrier; by avoiding endosomal degradation and/or trafficking from the cell, endosomolytic carriers have been shown to elicit desirable durability of therapeutic action[250]. The prolonged effect of si-NPs and siPA-NPs *in vitro*, with significant silencing out to 10 days post-treatment, suggests that this delivery system achieves a sustained effect that would minimize the need for repeat dosing.

*Pharmacokinetics and Biodistribution***.** Targeting siRNA nanoparticles to cancer targets such as solid tumors *in vivo* is contingent upon the ability to avoid rapid clearance by the liver (phagocytosis) and kidneys (polyanionic disassembly), which extends circulation time and consequently passive tumor uptake by the EPR effect. Disassembly in the kidney, leading to clearance through the urine, is especially detrimental to siRNA polyplex circulation time[18]. We showed previously that 50B-based si-NPs, which have balanced cationic and hydrophobic character in the polymeric block that forms the polyplex core, are more resilient to heparin sulfate disassembly and have longer circulation than strictly cationic analogues[237]. These si-NPs are used as a benchmark to compare siPA-NPs which incorporate hydrophobicity into both the polymer backbone and siRNA molecule.

The siPA-NPs have increased stability upon exposure to heparin compared to si-NPs as monitored by %FRET over time. Neither si-NPs nor siPA-NPs had reduced %FRET in the presence of 2 U/mL heparin, a dose which was previously used to completely disassemble strictly cationic polyplexes (Figure S4.5)[237]. At each dose increasing from 10 – 90 U/mL heparin, siPA-NPs retained higher %FRET compared to si-NPs throughout the entire time course (180 min) (Figure 4.4A and S4.5). Only at the highest heparin dose (100 U/mL) did siPA-NPs and si-NPs have similar kinetics of reduction in %FRET over 180 min. An EC_{50} (indicative of the half maximal concentration of heparin necessary to dissociate polyplexes) was calculated at multiple time points (30, 60, 90, 120, 150, and 180 min) in order to quantify the dose response of heparin-dependent disassembly observed over time. The EC_{50} of siPA-NPs was ~2-fold greater than that of si-NPs at each time point analyzed (Table S4.2), meaning that double the concentration of heparin was required to disassemble siPA-NPs and suggesting that added hydrophobicity of siPA conjugates within siPA-NPs provide increased stability upon exposure to polyanionic challenge such as by heparin sulfates found within the GBM.

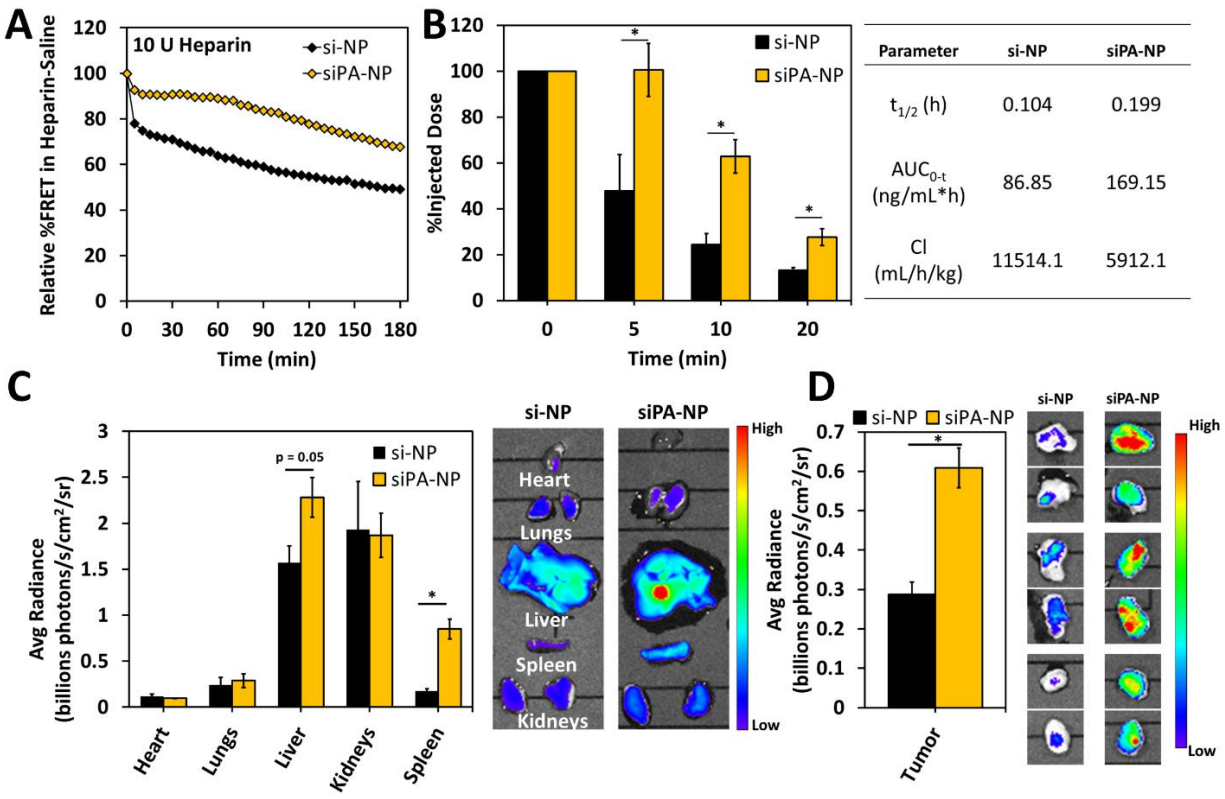

Figure 4.4. Higher stability of siPA-NPs relative to si-NPs corresponds to greater circulation time and increased accumulation in tumor tissue. A) siPA-NPs are more stable than si-NPs in the presence of heparin, as evaluated by FRET measurements. B) siPA-NPs injected intravenously in mice have a longer circulation half-life than si-NPs. C, D) siPA-NPs accumulate more in tumor tissue and in the MPS organs (liver and spleen) than si-NPs in a mouse tumor model at 20 minutes following tail vein injection.

In blood pharmacokinetics experiments, increased fluorescence was detected within blood samples collected at each time point (5, 10, and 20 min) from siPA-NPs compared to si-NPs (Figure 4.4B). The calculated circulation half-life of siPA-NPs (0.199 h) was ~2-fold greater than si-NPs (0.104 h), resulting in ~2-fold increase in area under the curve (AUC), and ~2 fold decrease in blood clearance (CL) (Figure 4.4B). The observation of increased circulation persistence is especially important due to its correlation with passive tumor accumulation, which was studied in athymic nude mice bearing orthotopic xenografts of MDA-MB-231 triple negative breast cancer

cells in the mammary fat pad. Biodistribution in major organs of interest (heart, lungs, liver, kidneys, and spleen) after i.v. administration of 1 mg/kg nanoparticles (siRNA dose) was comparable between siPA-NPs and si-NPs (Figure 4.4C). As a result of decreased renal clearance and consequent increased exposure to other organs and tissues, the siPA-NPs exhibited higher levels of uptake within MPS organs (liver and spleen) than si-NPs. Importantly, a 2-fold increase in tumor uptake was observed by siPA-NPs (Figure 4.4D), confirming that increased circulation time of siPA-NPs translated to increased EPR-based passive tumor uptake. Commonly, active targeting ligands such as folic acid, hyaluronic acid, RGD peptide, or transferrin, are used as a strategy to increase tumor uptake and retention after i.v. administration[236, 251-255]. Herein, tumor uptake was increased by tuning the core chemistry of polyplexes to increase polyplex stability and circulation time. Thus, it is expected that the addition of appropriate targeting ligands in the future will further increase tumor concentration due to improved tumor retention.

The in-depth studies above thoroughly compare the impact of PA-modified vs. unmodified siRNA with the hydrophobized 50B carrier. Conjugation of alkyl chains similar to PA has also been explored as a strategy to improve pharmacokinetics of therapeutics delivered carrier-free by leveraging lipid binding to serum proteins[256]. However, a comprehensive evaluation of lipid-modified siRNAs reveals that PA modification is insufficient to elicit serum protein binding and gene silencing[27]. Based on this prior work, we attributed the pharmacokinetic improvement of siPA-NPs over si-NPs to their enhanced stability due to the impact of the hydrophobic interactions between the PA-modified siRNA and the hydrophobized 50B carrier. To confirm this, we ran a set of control experiments using the fully cationic polymeric carrier 0B. We investigated si-0B-NPs and siPA-0B-NPs in a subset of studies to rule out the possibility that our observations were driven solely by hydrophobization of the siRNA. The degree of siRNA unpackaging in the presence of

heparin was evaluated for si-NPs, siPA-NPs, si-0B-NPs, siPA-0B-NPs. In accordance with previous reports si-NPs and siPA-NPs were more stable in response to heparin than si-0B-NPs and siPA-0B-NPs. siPA-NPs showed an additional enhancement in stability relative to si-NPs that was not observed in si-0B-NPs vs. siPA-0B-NPs (Figure S4.6). Significantly, 0B polyplexes loaded with siPA did not show any increase in blood circulation half-life relative to 0B polyplexes loaded with unmodified siRNA, while siPA increased circulation time approximately 2-fold relative to unmodified siRNA in 50B polyplexes (Figure S4.7). These data confirm that the hydrophobic interactions between siPA and the BMA of the 50B NP core are critical to the enhanced stability and circulation time observed for siPA-NPs.

Target Gene Silencing and Acute Toxicity In Vivo. To measure the impact of the improved pharmacokinetics of siPA-NPs on tumor bioactivity, the *in vivo* bioluminescence was tracked in mice bearing luciferase-expressing MDA-MB-231 orthotopic xenografts of the mammary fat pad after i.v. injection (1mg/kg siRNA dose) on days 17 and 18 after transplantation. The relative luminescence measured by intravital imaging increased steadily over 48 h (up to 2.5-fold) in mice administered saline, si-NP scrambled, and siPA-NP scrambled. Mice administered luciferase si-NPs did not show a treatment response after the first day, but they showed significant reduction in bioluminescence at 48 hours (after 2 consecutive treatments). The mice administered siPA-NPs showed a treatment response at both 24 h (after 1 treatment) and 48 hours (after 2 consecutive treatments), with significant decreases in bioluminescence compared to saline and scrambled controls (Figure 4.5A). Moreover, the bioluminescence of mice administered siPA-NPs did not significantly increase above the baseline measure at 0 hours throughout the time course, indicating complete inhibition of luminescence associated with tumor growth over the 48 h treatment

protocol. These data strongly support the effectiveness of siPA-NPs for effective tumor target gene silencing after a single i.v. administration and confirms the functional significance of the increased stability, circulation time, and tumor uptake of siPA-NPs. This increase in efficacy is expected to be impactful for knockdown of pathological genes, with these results suggesting that siPA-NPs would achieve a therapeutic response with a lower dose or fewer administrations relative to si-NPs.

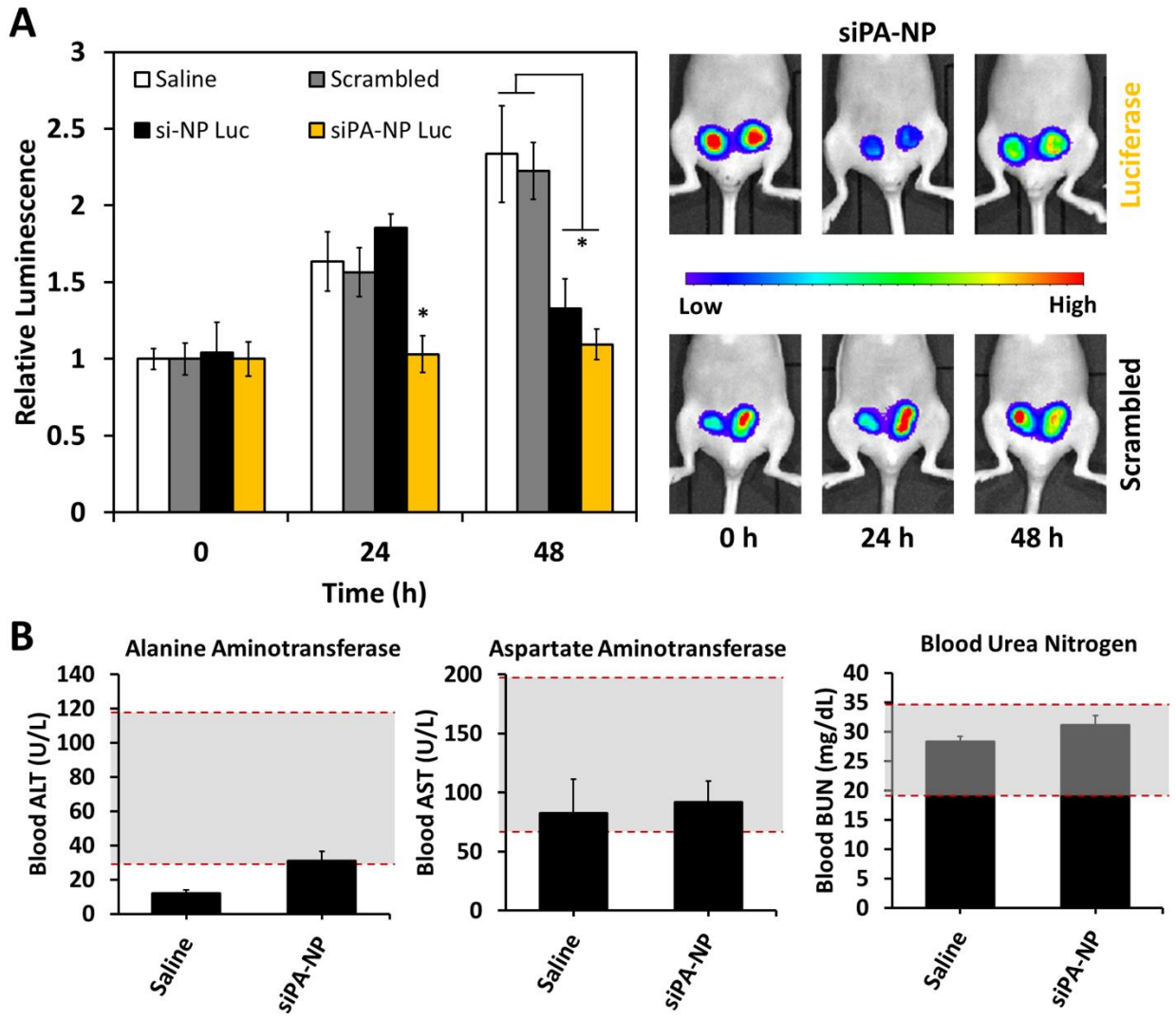

Figure 4.5. siPA-NPs delivered intravenously silence luciferase in an orthotopic MDA-MB-231 tumor model more effectively than si-NPs and cause no significant liver and kidney toxicity. A) Luciferase silencing, compared to

scrambled siRNA controls. B) Measurements of liver (ALT and AST) and kidney (BUN) toxicity for si-NP and siPA-NPs 48 h after treatments.

Because there was significant accumulation of siPA-NPs in the liver and kidneys, ALT and AST (indicators of liver function / toxicity) and BUN (indicator of kidney function / toxicity) were assessed in the treated mice. Blood collected from mice at the time of euthanasia (48 hours after the last treatment) showed that systemic levels of ALT, AST, and BUN were not significantly elevated by the treatment protocol of si-NPs or siPA-NPs utilized. ALT and AST was increased in si-NPs above the mean levels of saline and siPA-NPs, but the increase was not statistically significant (Figure 4.5B).

4.5 Conclusions

The performance of PEG-*b*-p(DMAEMA-*co*-BMA) "50B", which forms siRNA-loaded NPs with balanced cationic and hydrophobic core content, can be improved through pairing with siPA hydrophobized siRNA. The hydrophobicity of both the polymer and siPA molecule was essential to improved polyplex stability, which can be attributed to increased van der Waals interactions between carrier and cargo. These interactions facilitated more efficient siPA loading into NPs and siPA-NP polyplexes were also more resilient to heparin sulfate-induced destabilization. Increased siPA-NP stability, when compared to our benchmark si-NPs, resulted in increased blood circulation time and EPR-driven passive uptake into orthotopic tumor xenografts after intravenous polyplex injections. The enhanced pharmacokinetics of siPA-NPs translated to increased bioactivity of siRNA, as assessed by target gene silencing of the model gene luciferase within orthotopic triple negative breast cancer (MDA-MB-231) tumors. Our results demonstrate that increasing the strength of associative forces, rather than solely utilizing

electrostatic forces that are traditionally leveraged to drive polyplex assembly, can increase both polyplex stability and bioactivity *in vivo*. The data support continued efforts to stabilize siRNA NP systems to improve pharmacokinetics and pharmacodynamics of siRNA and increase clinical translatability for cancer applications.

CHAPTER 5

LIPOPHILIC SIRNA TARGETS ALBUMIN *IN SITU* AND PROMOTES BIOAVAILABILITY, TUMOR PENETRATION, AND CARRIER-FREE GENE SILENCING

Text adapted from:

Sarett SM, Werfel TA, Jackson MA, Kilchrist KV, Brantley-Sieders D, Duvall CL (2017). Lipophilic siRNA Targets Albumin in Situ and Promotes Bioavailability, Tumor Penetration, and Carrier-Free Gene Silencing. PNAS. *Under review.*

5.1 Abstract

Clinical translation of therapies based on small interfering RNA (siRNA) is hampered by its comprehensively poor pharmacokinetic properties that necessitate molecule modifications and complex delivery strategies. Here, we sought an alternative approach to nanoparticle carriers by leveraging the long-lived endogenous serum protein albumin as an siRNA carrier. We synthesized siRNA conjugated to a diacyl lipid moiety (siRNA-L_2), that rapidly binds albumin *in situ*. siRNA-L_2, in comparison to unmodified siRNA, exhibited a 5.7-fold increase in circulation half-life corresponding to an 8.6-fold increase in bioavailability and markedly reduced renal clearance. Benchmarked against leading commercial siRNA nanocarrier (*in vivo* jetPEI), siRNA-L_2 achieved 19-fold greater tumor accumulation and a 46-fold increase in tumor cell uptake in a mouse orthotopic model of human triple negative breast cancer. siRNA-L_2 penetrated tumor tissue rapidly and homogeneously; 30 minutes after intravenous injection, siRNA-L_2 achieved uptake in 99% of tumor cells, compared to 60% for jetPEI. Remarkably, siRNA-L_2 displayed a tumor:liver accumulation ratio of greater than 40:1 vs. less than 3:1 for jetPEI. The improved pharmacokinetic properties of siRNA-L_2 facilitated significant tumor gene silencing for 10 days after two intravenous doses. Proof-of-concept was established in a patient-derived xenograft model, in

which jetPEI tumor accumulation was reduced 4-fold relative to the same formulation in the orthotopic model. The siRNA-L_2 tumor accumulation diminished only 2-fold, suggesting that the superior tumor distribution of the conjugate over nanoparticles will be accentuated in clinical situations. These data reveal the immense promise of *in situ* albumin targeting for development of translational, carrier-free RNAi-based cancer therapies.

5.2 Significance

Small interfering RNA (siRNA) has the capacity to silence traditionally undruggable targets, but *in vivo* delivery barriers limit clinical translation of siRNA, especially for non-hepatic targets. To date, delivery strategies for RNAi cancer therapies have focused on synthetic nanocarriers, but their shortcomings include limited delivery to and variable distribution throughout the target site and small therapeutic indices due to non-specific, carrier-associated toxicities. A diacyl lipid-modified siRNA can leverage albumin as an endogenous carrier, resulting in comprehensively enhanced pharmacokinetic properties that translate to greater quantity and homogeneity of tumor accumulation relative to nanocarriers. The albumin-binding siRNA conjugate strategy is synthetically simple and safe at high doses, and thus is a translatable and potentially transformative option for RNAi oncology therapies.

5.3 Introduction

Harnessing the therapeutic potential of small interfering RNA (siRNA) hinges upon enhancing its pharmacokinetic properties to overcome *in vivo* delivery barriers. Unmodified siRNA exhibits rapid renal clearance from circulation, leading to removal through the urine[28] and allowing minimal bioavailability in target tissues. Improving delivery of siRNA via encapsulation

in nanoparticulate carrier systems has been the principal strategy employed by the field. Nanocarriers can improve circulation half-life, resistance to degradation, intracellular uptake, and ultimately gene silencing potency[22, 73, 178, 257]. However, commonly-utilized cationic lipid/polymer formulations are complex and expensive to synthesize and can be toxic and/or immunogenic[13, 258]. Additionally, their preferential uptake by clearance organs such as the liver and spleen hinders delivery to target tissues[73, 159]. siRNA conjugates have emerged as an alternative to nanocarrier-mediated delivery[25, 27, 259-262], offering the possibility of improving siRNA pharmacokinetics without requiring a more complex delivery vehicle. Alnylam Pharmaceuticals has demonstrated high gene silencing potency of a trivalent N-Acetylgalactosamine (GalNAc) siRNA conjugate, which binds with high specificity and affinity to the asialoglycoprotein receptor on liver cells[77, 78]. Carrier-free gene silencing has also been achieved in the liver with siRNA-cholesterol conjugates[27, 28], but the development of siRNA conjugates that efficiently deliver to non-hepatic tissues is an unmet need. Here, we developed an siRNA conjugate that leverages endogenous albumin as a chaperone. We anticipate that albumin-associated siRNA will show particular promise as a cancer therapeutic by extending the circulation time of siRNA, enabling efficient tumor tissue penetration, and leveraging the propensity of tumor cells to internalize albumin[263, 264].

The enhanced permeability and retention (EPR) effect, based upon the high vascular permeability and diminished lymphatic drainage at tumor sites, suggests a preferential tumor accumulation of particles of nanocarrier size (~100 nm). However, the EPR phenomenon as a tumor targeting strategy has recently come under intense scrutiny due to the discrepancy observed between pre-clinical and clinical efficacy of nanoparticle-based cancer therapeutics[188, 189, 191, 192]. There is a growing appreciation that amongst wildly heterogeneous human cancers, the EPR effect may be only relevant in select tumor or patient subsets. In particular, the widespread “leakiness”

of tumor vasculature, a characteristic of rapidly-developing mouse tumor models, has likely been exaggerated in its relevance to slower-forming human lesions[205]. The field of nanomedicine has responded to these realizations with efforts to enhance understanding of nanoparticle performance in animal models[52, 196-198], strategies to normalize tumor vasculature[190], systematic investigations into ideal nanoparticle characteristics[196, 199], and a focus on smaller (20-30 nm-sized) nanocarriers[196, 201, 202]. Despite the promise of these approaches, the diversity of human cancers necessitates equivalently diverse delivery approaches[6, 205] and opportunity for improvement remains, particularly in the area of enhancing uniformity of tumor distribution. Nanoparticles typically exhibit concentration of dose near leaky vessels but not within more avascular tumor regions[16, 200], resulting in inhomogeneous efficacy and higher potential for incomplete remission and recurrence. Smaller, long-circulating siRNA conjugates may offer an alternative that creates more homogeneous therapeutic distribution within tumors. Indeed, the apparent tissue permeability of the serum protein albumin (hydrodynamic size ~7.2 nm[31]) is consistently more than 4-fold greater than that of 100 nm liposomes in a variety of mouse models of breast cancer[203]. Here, we sought to design an siRNA conjugate that 'hitchhikes' on long-circulating albumin to confer siRNA molecules with an unprecedented combination of circulation persistence and high tissue penetration to enable systemic, carrier-free delivery of siRNA for oncological applications.

In situ targeting of albumin following intravenous delivery is a viable strategy because endogenous albumin is the most abundant serum protein (>40 mg/mL) and has a circulation half-life of about 20 days[33]. It is also a natural carrier of and has a high affinity for poorly soluble lipids[31, 33]. Albumin has been investigated extensively as a carrier and a conjugate for small molecules as well as protein therapeutics; albumin-based therapeutics like Abraxane, Levemir, and Optison have achieved clinical relevance[31, 32], demonstrating the translatability of this approach.

However, to our knowledge, no one has investigated non-covalent, *in situ* targeting of siRNA to albumin for non-hepatic delivery. Previous work has established the utility of interaction of high and low density lipoproteins with cholesterol-conjugated siRNA[27, 100, 101, 183, 211], but the natural trafficking of these lipoproteins concentrates the therapy in the hepatocytes of the liver. The potential of albumin-bound siRNA has been minimally explored[183, 184] and to our knowledge, albumin-bound siRNA has never been investigated as an oncological therapy. In our unique strategy, we exploit the capacity of albumin to bind fatty acids by modifying siRNA with a lipidic moiety designed for high-affinity albumin binding. The Irvine lab developed and previously utilized this hydrophobic modification for *in situ* albumin targeting of CpG-DNA to promote delivery to lymph nodes for vaccine applications[265]. We pursued modification of siRNA with a lipidic albumin-targeting agent rather than alternative albumin-binding molecules like peptide domains[266] and a truncated Evans blue molecule[267] because hydrophobically-modified siRNA exhibits improved resistance to nucleases and enhanced cellular internalization[25]. Thus, the strategic choice of modification with an albumin-binding lipid has the potential to confer additional advantages in siRNA stability and cell membrane interactions for uptake and endosomal escape in addition to circulation persistence, tissue penetration, and biodistribution. To investigate the clinical potential of our siRNA conjugate, we examined its efficacy as a systemic RNAi cancer therapeutic by evaluating delivery and gene silencing in translationally relevant models of human triple negative breast cancer.

5.4 Methods

Materials. Amine-modified single-stranded DNA (modification at 5' end) or RNA (modification at 3' end) and complementary single-stranded Cy5-, unmodified DNA or unmodified RNA were

obtained from Integrated DNA Technologies (Coralville, Iowa) (for DNA) or GE Dharmacon (Lafayette, CO). The pGreenFire1-CMV plasmid was obtained from System Biosciences (Mountain View, CA), and packaging plasmids pMDLg/pRRE, pRSV-Rev, and pMD2.G were purchased from Addgene (Cambridge, MA). *In vivo* jetPEI was purchased from VWR International (Radnor, PA). 1,2-distearoyl-sn-glycero-3-phosphoethanolamine-*N*-[azido(polyethylene glycol)-2000] (DSPE-PEG_{2000}-azide) was purchased from Avanti Polar Lipids (Alabaster, AL). NucBlue Fixed Cell ReadyProbes were purchased from Life Technologies (Grand Island, NY). NAP-25 filtration columns were purchased from Fisher Scientific. All other reagents were purchased from Sigma-Aldrich (St. Louis, MO).

Oligonucleotide-L_2 Synthesis. Single-stranded amine-modified oligo was reacted with 10-fold molar excess of dibenzocyclooctyne-PEG_4-N-hydroxysuccinimidyl ester (DBCO-PEG_4-NHS)) pre-dissolved at 25 mM in DMSO. The reaction was carried out for 18 hours at room temperature at a 1 mM oligonucleotide concentration in 30% dimethylsulfoxide (DMSO) and 70% phosphate buffered saline (PBS) with 8 mM TEA. The product was diluted 3-fold in water and filtered twice through NAP-25 columns, lyophilized, and then reacted with 5-fold molar excess of DSPE-PEG_{2000}-azide for 24 hours at a 0.1 mM oligonucleotide concentration in 50% methanol, 50% water. The reaction was dilution and filtered one time through a NAP-25 column and then purified with reversed-phase HPLC using a Clarity Oligo-RP column (Phenomenex, Torrence, CA) under a linear gradient from 95% water (50 mM triethylammonium acetate), 5% methanol to 100% methanol. The conjugate molecular weight was confirmed using MALDI-TOF mass spectrometry (Voyager-DE STR Workstation, Grand Island, NY) using 50 mg/mL 3-hydroxypicolinic acid in 50% water, 50% acetonitrile with 5 mg/mL ammonium citrate as a matrix. The yield of the oligo-

L_2 was quantified based on absorbance at 260 nm. The purified oligo-L_2 was annealed to its complementary strand to generate Cy5-, unmodified DNA-L_2 or siRNA-L_2. Conjugation and annealing was also confirmed via agarose gel electrophoresis.

DNA was used as a cost-effective analog for siRNA in imaging studies, and is referred to as siRNA/siRNA-L_2 in the main text and supplemental figures for simplicity and cohesion (except where the figure is intended to show DNA's comparability to siRNA). DNA/siRNA and DNA-L_2/siRNA-L_2 exhibited degradation on similar time scales (Figure S5.3C-D) and DNA-L_2 exhibits similar albumin binding (Figure S5.2B), validating its use as a model for siRNA-L_2.

Oligonucleotide-L_2 Characterization.

Critical micelle concentration of oligo-L_2 was assessed fluorescently using Nile red, as described previously[268, 269]. Briefly, different dilutions were prepared from a 1 mg/mL stock solution to obtain micelle samples ranging in concentration from 0.0001 to 1 mg/mL. Then, 10 μL of a 1 mg/mL Nile red stock solution in methanol was added to 1 mL of each sample and incubated overnight in the dark at room temperature. The next day, samples were filtered with a 0.45 μm syringe filter, and Nile red fluorescence was measured in 96 well plates using a micro plate reader (Tecan In- finite 500, Tecan Group Ltd., Mannedorf, Switzerland) at an excitation wavelength of 535± 20 nm and an emission wavelength of 612± 25 nm. The CMC was defined, as previously described[270], as the intersection point on the plot of the Nile red fluorescence versus the copolymer concentration.

Degradation of siRNA and siRNA-L_2 was assessed by incubation in 60% fetal bovine serum (FBS) for 4 hours, 2 hours, 1 hour, 30 minutes, or 15 minutes and evaluation by agarose gel electrophoresis with comparison to a control sample in water.

Evaluation of Albumin-Binding to Oligo-L_2 *In Vitro*.

PAGE gel migration assay was used to assess binding of oligo-L_2 to bovine serum albumin (BSA). 4-20% Mini-Protean TGX Precast Gel were run in the Tetra Blotting Module (BioRad, Hercules, CA). siRNA, siRNA-L_2, DNA, and DNA-L_2 were incubated with varying amounts of BSA for 15 minutes. PAGE gels were stained using GelRed Nucleic Acid Stain (Biotium, Fremont, CA) according to manufacturer protocol and imaged under ultraviolet light for visualization of nucleic acid migration. Gels were subsequently stained with Coomassie blue to evaluate BSA migration.

PAGE gel migration assay was used to assess binding of oligo-L_2 to albumin in serum. siRNA or siRNA-L_2 was incubated at 9-fold, 13-fold molar excess BSA and 50%, 75% FBS for approximate matching of mass of protein loaded per well. siRNA and siRNA-L_2 were imaged under ultraviolet light after post-staining with GelRed. Serum proteins were stained with Coomassie blue.

Cell Culture. Human epithelial breast cancer cells (MDA-MB-231) were cultured in Dulbecco's modified Eagle's medium (DMEM, Gibco Cell Culture, Carlsbad, CA) supplemented with 10% fetal bovine serum (FBS, Gibco) and 0.1% gentamicin (Gibco). Luciferase-Expressing MDA-MB-231s were generated as previously described[257].

***In Vitro* Gene Silencing.** MDA-MB-231s were treated with siRNA or siRNA-L_2 complexed with *in vivo* jetPEI according to manufacturer protocol. The siRNA was either designed against the luciferase gene (luc siRNA) or was a scrambled sequence (scr siRNA). Cells were seeded at 2,000 cells/well in 96-well black-walled plates and allowed to adhere overnight. Cells were then treated

in 10% serum for 24 hours at a dose of 100 or 50 nM siRNA. After 24 h, media was replaced with luciferin-containing media (150 μg/mL) before imaging with an IVIS Lumina III imaging system at 24 and 48 hours.

Evaluation of Albumin-Binding to Oligo-L_2 *In Vivo*.

Fluorescent (Cy-5-labeled) DNA and DNA-L_2 was injected into the tail vein of CD-1 mice (4-6 weeks old, Charles Rivers Laboratories, Wilmington, MA, USA) at 1 mg/kg. Blood was collected at 20 minutes post-injection, and serum was isolated. Serum from mice injected with DNA, DNA-L_2, or saline was evaluated via PAGE gel migration assay was used to assess binding of oligo-L_2 to albumin *in vivo*.

Tumor Spheroid Penetration *In Vitro*.

MCF7 cells (ATCC) were cultured in DMEM supplemented with 1% penicillin-streptomycin and 10% FBS. Three-dimensional MCF7 spheroid cultures were established as described previously[271, 272]. Briefly, cells were grown to 50% confluence in two-dimensional culture. Cells were washed twice with trypsin (0.05%, Gibco), trypsin was aspirated, and cells were incubated at 37°C for 10-15 minutes. Cells were resuspended in growth medium, pipetted to generate single cell suspensions, and counted (Bio-Rad TC20 Automated Cell Counter). Single cell suspensions (7,500 cells/500 μl) were seeded in 8 well chamber slides (Nunc Lab-Tek II) pre-coated with 10 ul growth factor-reduced Matrigel (BD Biosciences) in growth media containing 2% growth factor-reduced Matrigel and cultured for 5 days. On day 5, cultures were treated with 100-500 nM Cy5-labeled DNA, DNA-L_2, or DNA complexed with *in vivo* jetPEI for 4 hours in fresh growth medium. Cultures were washed once in PBS and fixed for 2 minutes with BD Cyotfix/Cytoperm solution

(BD Biosciences). After aspirating fixative and removing plastic chamber, cultures on slides were mounted with ProLong Gold Antifade with DAPI (Molecular Probes) and secured by coverslip. Slides were stored at 4^{o}C degrees prior to confocal imaging. Confocal imaging was performed using the Nikon C1si+ system on a Nikon Eclipse Ti-0E inverted microscopy base. The PMT HV gain, laser power, and display settings were set for maximal SNR based on control biological samples such that negative control samples lacking label had no background fluorescence and treatment samples had no saturated pixels. Image acquisition and analysis were performed using Nikon NIS-Elements AR version 4.30.01.

Blood Plasma Pharmacokinetics. Fluorescent (Cy-5-labeled) DNA and DNA-L_2 was injected into the tail vein of CD-1 mice (4-6 weeks old, Charles Rivers Laboratories, Wilmington, MA, USA) at 1 mg/kg. Prior to injection, the mouse ear was placed on a coverslip on the Nikon C1si+ confocal microscope system. An artery within the ear was set in focus and upon injection images of the artery were automatically collected every 2 seconds for 30 minutes. After 30 minutes, animals were sacrificed. Maximum initial fluorescence of the artery was set to a time of 0 seconds. Artery fluorescence was evaluated by quantifying a circular ROI entirely within the vessel. Data were fit to a one-phase exponential decay model (equation below) and half-life and area under the curve was determined from these fits.

$$\boldsymbol{Fluorescence_{blood} = Fluor_0 * e^{-kt}}$$

Biodistribution in Tumor-bearing Mice. For the orthotopic mouse tumor model, athymic nude female mice (4-6 weeks old, Jackson Laboratory, Bar Harbor, ME, USA) were injected in each mammary fat pad with 1 x 10^6 MDA-MB-231 cells in DMEM:Matrigel (50:50). After 21 days,

tumor-bearing mice were injected via the tail vein with 1 mg/kg (nucleic acid dose) of fluorescent DNA, DNA-L_2 or DNA loaded in *in vivo* jetPEI. After 30 minutes, 24 hours, and 48 hours, animals were sacrificed and the organs of interest (heart, lungs, liver, spleen, kidneys, and tumors) were excised. The fluorescence intensity in the organs was quantified on an IVIS Lumina III imaging system at excitation wavelength of 620 ± 5 nm and emission wavelength of 670 ± 5 nm (n = 3 animals, n = 6 tumors). Tumor radiance data were fit to a one-phase exponential decay model (equation below) and area under the curve was determined from these fits.

$$\boldsymbol{Radiance_{tumor} = Radiance_0 * e^{-kt}}$$

For the patient-derived xenograft (PDX) mouse tumor model triple-negative line HCI-010 was transplanted into one inguinal mammary fat pad (surgically cleared of endogenous epithelium) of NOD-SCID (Jackson Laboratory) female mice of 3-4 weeks of age[194]. After approximately 8 weeks, PDX tumors were harvested, cut to 4 mm x 2 mm pieces, serially transplanted into the cleared inguinal mammary fat pads of a new cohort of NOD-SCID female mice, and grown to a volume of 300-500 mm^3 Tumor-bearing mice were injected via the tail vein with 1 mg/kg (nucleic acid dose) of fluorescent DNA-L_2 or DNA loaded in *in vivo* jetPEI. After 24 hours, animals were sacrificed and the organs of interest (heart, lungs, liver, spleen, kidneys, and tumors) were excised. The fluorescence intensity in the organs was quantified on an IVIS Lumina III imaging system at excitation wavelength of 620 ± 5 nm and emission wavelength of 670 ± 5 nm (n = 2 animals, n = 2 tumors).

Acute Toxicity in Liver and Kidney. CD31 mice were injected with siRNA-L_2 (10 mg/kg) or *in vivo* jetPEI-loaded siRNA (1, 2 mg/kg). After 24 hours, blood was collected by cardiac puncture and then centrifuged at 2000 G for 5 min. Then, plasma was harvested and tested by the Vanderbilt

Translational Pathology Shared Resource (TPSR) for systemic levels of alanine aminotransferase (ALT), aspartate aminotransferase (AST), blood urea nitrogen (BUN), and creatinine. Organs were fixed in formalin, sectioned, and imaged for histological evaluation.

Tumor Distribution *In Vivo* After Intravenous (*i.v.*) Injection. For the orthotopic tumor model, athymic nude female mice (4-6 weeks old, Jackson Laboratory, Bar Harbor, ME, USA) were injected in each mammary fat pad with 1 x 10^6 MDA-MB-231 cells in DMEM:Matrigel (50:50). After 21 days, tumor-bearing mice were injected via the tail vein with saline, 1 or 10 mg/kg fluorescent DNA-L_2, or 1 mg/kg DNA loaded in *in vivo* jetPEI. Tumors were excised, and cells were isolated from each tumor. A mixture of collagenase and DNAse was used to dissociate cells and ammonium-chloride-potassium lysing buffer was used to lyse red blood cells. Uptake of fluorescent DNA or DNA-L_2 was evaluated by flow cytometry (n = 4 animals, n = 8 tumors). Tumor cells were identified as the cell population expressing green fluorescent protein (GFP), while the GFP-negative cell population corresponded to native mouse cells.

Target Gene Silencing After *i.v.* Injection. Athymic nude female mice (4-6 weeks old, Jackson Laboratory, Bar Harbor, ME, USA) were injected in each mammary fat pad with 1 x 10^6 MDA-MB-231 cells in DMEM:Matrigel (50:50). After tumors reached a size of 50 mm^2, tumor-bearing mice were injected i.p. with luciferin substrate (150 mg/kg) and imaged for bioluminescence on an IVIS Lumina III imaging system 30 minutes post-injection. Next, the mice were injected via the tail vein with 10 mg/kg (based on siRNA dose) luciferase-targeting (luc) siRNA or siRNA-L_2 or a scrambled sequence (scr) siRNA-L_2. Mice were imaged and treated at days 0 and 1 following tumor cell inoculation and imaged on day 2, 3, 4, 7, and 10. Relative luminescence was determined

by measuring the raw luminescent intensity of each tumor on each day and comparing to the initial signal at day 7 (n =10 tumors per group). Mouse body weight was evaluated at each of these timepoints to investigate treatment toxicity.

Statistical Methods. The treatment groups were statistically compared using a one way ANOVA test (for non-repeated measures) or a two way ANOVA (for measures repeated at multiple time points) coupled with a Tukey means comparison test; a p-value < 0.05 was deemed representative of a significant difference between groups. For all data shown, the arithmetic mean and standard error are reported, and the sample size (n) is indicated.

Ethics Statement. The animal studies were conducted with adherence to the guidelines for the care and use of laboratory animals of the National Institutes of Health (NIH). All experiments with animals were approved by Vanderbilt University's Institutional Animal Care and Use Committee (IACUC).

5.5 Results

Purified siRNA-L_2 conjugate binds to albumin. To synthesize siRNA-L_2, a single-stranded amine-modified siRNA was reacted with an NHS ester/octyne heterobifunctional crosslinker and subsequently conjugated with 1,2-distearoyl-sn-glycero-3-phosphoethanolamine-N-[azido(polyethylene glycol)-2000] (DSPE-PEG_{2000}-azide) to generate siRNA-L_2 **(**Figure 5.1A, S5.1A). The fully purified L_2 conjugates were obtained by reverse phase chromatography and

purity was confirmed by mass spectrometry (Figure 5.1B, S5.1B). Following purification, sense strand siRNA-L_2 was annealed to the corresponding antisense strand (for imaging studies, the antisense strand was Cy5-labeled). It was confirmed that conjugation of the L_2 moiety to siRNA did not significantly impact its inherent gene silencing activity, as demonstrated by *in vitro* knockdown evaluation of siRNA and siRNA-L_2 delivered via the commercial transfection reagent *in vivo* jetPEI (Figure S5.2A).

The albumin-binding capacity of siRNA-L_2 was confirmed using a non-denaturing PAGE gel migration assay (Figure 5.1C, S5.2B). siRNA-L_2 alone migrates above the albumin band because it exists as a micellar population at the concentration loaded into the gel (0.05 mg/mL, while critical micelle concentration is 1.4 µg/mL, Figure S5.2C). As the albumin:siRNA-L_2 ratio increases, more siRNA-L_2 binds to and migrates with albumin. Unmodified siRNA does not bind to albumin to any degree at any of the concentrations tested. Binding of L_2 conjugates to albumin in the presence of complete serum was also evaluated by gel migration assay, revealing preferential binding to the albumin component of serum (Figure S5.3A).

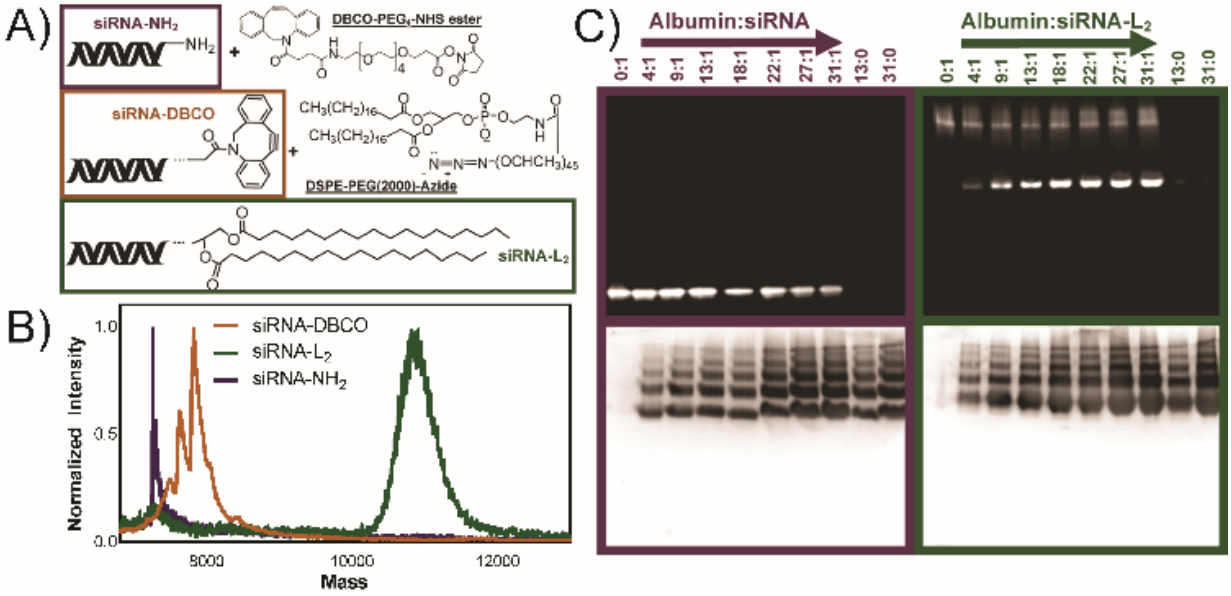

Figure 5.1. Successfully synthesized and purified siRNA-L_2 conjugate binds to albumin. A) Abbreviated structures of reactants and final oligonucleotide-L_2 conjugate. B) MALDI-TOF mass spectrometry of the original amine-modified siRNA, the DBCO intermediate, and the L_2 conjugate. C) Albumin binding measured by gel stained for siRNA (top) and protein (bottom). siRNA-L_2 migrates as a micellar population alone and co-migrates with albumin, while unmodified siRNA does not migrate with albumin. Note that albumin shows up as multiple bands due to running in non-denaturing, native gel conditions.

Albumin-binding of siRNA-L_2 enhances circulation time and reduces rapid renal clearance. To characterize the *in vivo* pharmacokinetics of siRNA-L_2 in comparison to unmodified siRNA, circulation persistence was evaluated in real time using intravital confocal microscopy following intravenous (*i.v.*) injection (see Methods). The circulation half-life ($t_{1/2}$) of siRNA-L_2 was 5.7-fold longer than unmodified siRNA (Figure 5.2A-B, Table 5.1). Additionally, the area under the curve, a measure of bioavailability of systemically-delivered therapeutics, was 8.6-fold greater for the L_2-conjugate compared to unmodified oligonucleotide. To evaluate *in situ* albumin binding, serum samples from mice injected with siRNA-L_2 (blood collection at 20 minutes post-injection) were evaluated via PAGE gel migration assay and revealed the presence of albumin-bound siRNA-L_2 (Figure S5.3B). These data confirm that albumin acts as a chaperone for siRNA-L_2 *in vivo* and establish that siRNA-L_2 association with albumin confers significant improvements in siRNA pharmacokinetics. To support these studies, the time scale of degradation of unmodified and L_2-modified oligonucleotides was investigated. siRNA and siRNA-L_2 showed resistance to degradation in serum over the pharmacokinetic time frame assessed, and L_2 modification imparted a slight improvement in resistance to serum degradation (Figure S5.3C-D).

Biodistribution of siRNA vs. siRNA-L_2 was evaluated in excised organs at 20 minutes post-injection. For *in vivo* studies, siRNA-L_2 exhibited increased accumulation in almost all

organs, likely due to its prolonged circulation time and reduced clearance into the urine in comparison to unmodified siRNA (Figure 5.2C). The kidneys were the sole exception, showing significantly more unmodified siRNA accumulation (a 1.6-fold greater fraction of the total organ radiance) at this early timepoint. This illustrates that using albumin as a natural carrier for siRNA-L_2 allows reduction of acute clearance through the renal route.

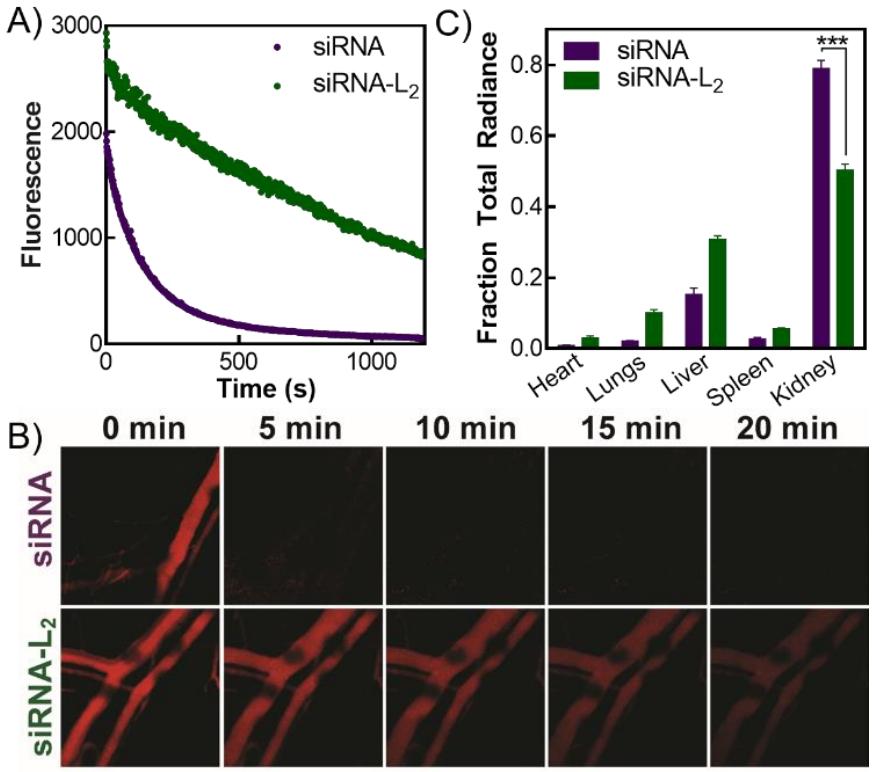

Figure 5.2. Conjugation of diacyl lipid to oligonucleotides increases circulation half-life and reduces renal clearance. A) Cy5-labeled siRNA-L_2 and siRNA fluorescence in the blood measured in real time intravitally by confocal microscopy after *i.v.* injection of CD1 mice. B) Representative images of fluorescence in mouse blood vessels over time. C) Organ biodistribution of siRNA and siRNA-L_2 at 20 minutes. n of 3, standard error shown; *** = $p<0.001$.

Parameter	siRNA	siRNA-L_2	p-value
$t_{1/2}$, circulation (min)	2.3 ± 0.2	13.1 ± 1.6	0.0023
$AUC_{circ, 0-\infty}$ (fluor. intensity*min)	5,500 ± 800	47,300 ± 6,700	0.0034
Fraction kidney radiance	0.790 ± 0.018	0.503 ± 0.014	<0.0001

Table 5.1. Key comparisons of siRNA-L_2 vs. siRNA.

siRNA-L_2 outperforms a leading *in vivo* nanoparticle carrier in safety and tumor accumulation. The reduction in kidney accumulation and prolonged circulation half-life of siRNA-L_2 motivated a comparison to commercially available *in vivo* nanoparticles. Of particular interest is the biodistribution profile of siRNA-L_2 in comparison to typical nanocarriers, as high uptake by mononuclear phagocytic system organs (the liver and the spleen) can result in minimal dose accumulation at the target site[176]. Compared to nanoparticles, siRNA-L_2 is expected to avoid this off-target accumulation and to more readily penetrate tumor tissue (Figure 5.3)

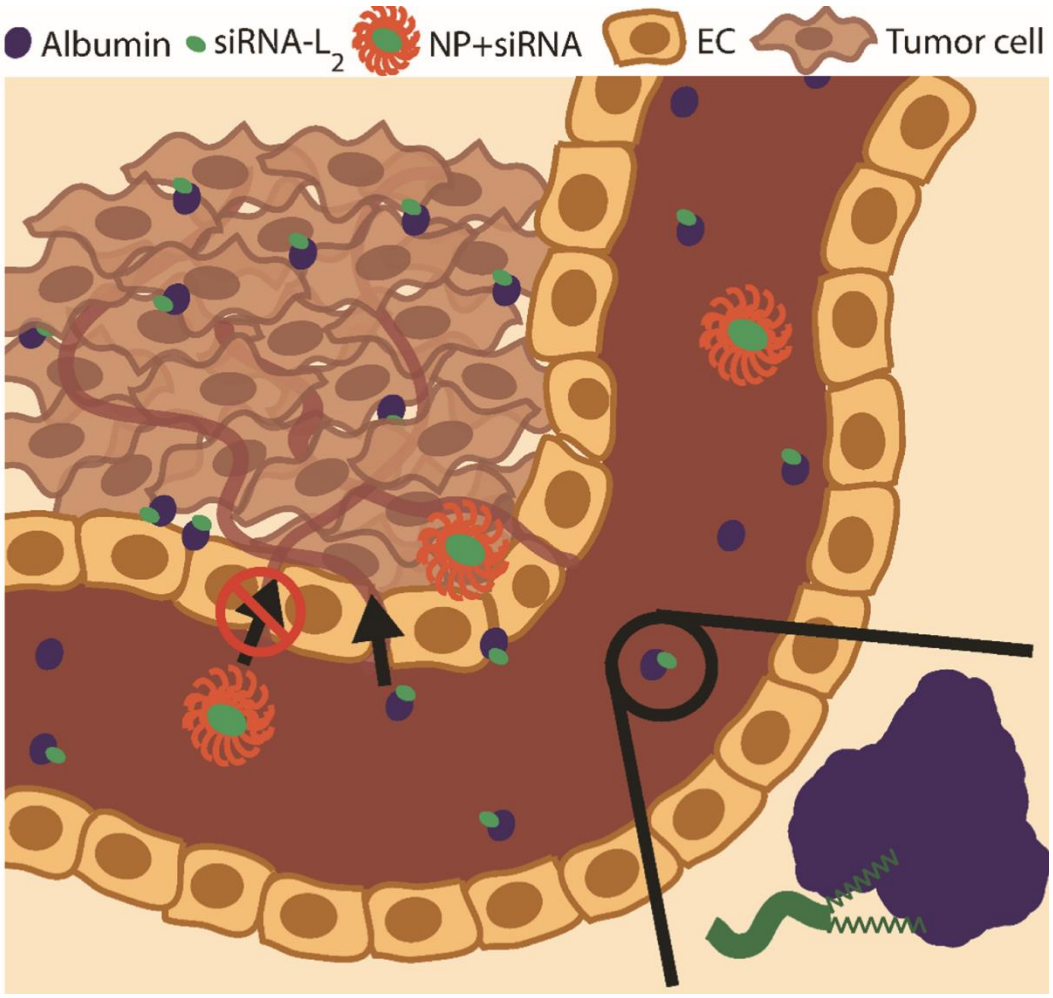

Figure 5.3. Schematic showing the advantages of diacyl lipid-modified siRNA over traditional nanoparticles (NPs) in penetration and accumulation in tumors.

siRNA-L_2 was compared to a leading formulation for nanoparticle-based *in vivo* nucleic acid delivery, *in vivo* jetPEI. *In vivo* jetPEI nanoparticles (jetPEI NPs) have been used in clinical trials and this comparison is a stringent test for therapeutic potential[273]. Prior to *in vivo* biodistribution studies, non-toxic doses were determined for siRNA-L_2 and jetPEI NPs. siRNA-L_2 is expected to avoid the toxic side effects associated with high doses of cationic nanocarriers, permitting safe use at higher dosages and potentially expanding the ultimate therapeutic index of siRNA drugs. Toxicity was investigated by monitoring mouse body weight and quantifying blood

chemistry markers of liver (alanine aminotransferase (ALT) and aspartate aminotransferase (AST)) and kidney (blood urea nitrogen (BUN) and creatinine) toxicity. Mice injected with an siRNA-L_2 dose of 10 mg/kg exhibited normal levels statistically equivalent to those of saline-injected mice and no change in body weight (Figure S5.4A-E). jetPEI NPs at a dose of 1 mg/kg showed no signs of toxicity, but doubling that dose to 2 mg/kg resulted in mortality for 3 of 4 mice and showed marked hepatic and renal toxicity in the surviving mouse. These data suggest that siRNA-L_2 is a safer alternative to nanocarrier-based delivery with the potential for a much broader therapeutic index. The maximum tolerated dose (MTD) of 1 mg/kg for *in vivo* jetPEI and a well-tolerated dose of 10 mg/kg for siRNA-L_2 were used in subsequent studies (MTD not determined for siRNA-L_2).

The biodistribution profile of the L_2 conjugate vs. jetPEI NPs was evaluated in a mouse orthotopic xenograft tumor model. siRNA-L_2 or jetPEI NPs were injected intravenously into tumor-bearing mice and organs were evaluated for siRNA accumulation. Comparing the absolute radiance in the organs over time from mice treated with jetPEI NPs or siRNA-L_2, it is evident that the 10 mg/kg treatment of siRNA-L_2 significantly enhances accumulation in all of the organs at an acute (30 minute) time point (Figure 5.4A, S5.5, S5.6A). Notably, the vast majority of siRNA-L_2 was cleared from all organs excepting the kidneys and tumors by 24 hours (Figure 5.4A, S5.6-7). jetPEI NPs, in contrast, create higher proportional delivery to and retention within the mononuclear phagocyte system (MPS) clearance organs (the liver and spleen) (Figure 5.4B).

The *in vivo* tolerability of high siRNA-L_2 doses enables a remarkable increase in tumor accumulation (Figure 5.4C, D). The area under the curve of the therapeutic within the tumor was 19.3-fold higher for siRNA-L_2 at 10 mg/kg than for the maximum tolerated dose of jetPEI NPs (Table 5.2). Dose-matched siRNA-L_2 at 1 mg/kg also outperforms jetPEI NPs in this measure of

tumor accumulation by 2.4-fold. Additionally, the fraction of the total organ radiance in the tumors is consistently higher for siRNA-L_2 at both doses compared to jetPEI NPs, indicating more preferential tumor accumulation with siRNA-L2 relative to jetPEI NPs.

To further annotate the ability of siRNA-L_2 to avoid the typical MPS organ accumulation of nanoparticles and accumulate preferentially within tumors, we evaluated the tumor:liver radiance ratio. At the 10 mg/kg siRNA-L_2 dose, a remarkable tumor:liver accumulation of more than 40:1 was observed at both 24 and 48 hours, indicating successful accumulation at a non-hepatic site (Figure 5.4E, F, Table 5.2). In contrast, jetPEI NPs displayed a tumor:liver ratio of below 3:1, a more than 15-fold decrease compared to siRNA-L_2 at 10 mg/kg and also lower than that observed for siRNA-L_2 at 1 mg/kg (which achieved tumor liver ratio of approximately 15:1).

The clear superiority of siRNA-L_2 in the orthotopic model motivated investigation in a more clinically-relevant patient-derived xenograft (PDX) model of triple negative breast cancer. Dose-matched siRNA-L_2 and *in vivo* jetPEI NPs at 1 mg/kg were injected intravenously and biodistribution was evaluated at 24 hours. siRNA-L_2 attained 4.0-fold greater tumor distribution in the PDX model than jetPEI NPs (whereas there was a 2.2-fold increased tumor delivery in the dose-matched orthotopic model) at 24 hours (Figure 5.4G-H, S5.8A). Compared to the orthotopic model, achieving tumor accumulation in the PDX model was more challenging. The added challenge of PDX tumors was more detrimental for jetPEI NPs than siRNA-L_2. Total tumor accumulation in PDX tumors was 4.3-fold lower than orthotopic tumors for jetPEI NPs while it was only reduced by 2.4 fold for siRNA-L_2. The lower MPS accumulation of siRNA-L_2 relative to NPs was consistent in the PDX model, with siRNA-L_2 again showing a marked improvement in tumor:liver ratio (8:1 vs. 1:1) (Figure S5.8B).

Parameter	jetPEI NPs	siRNA-L_2 (1)	siRNA-L_2 (10)	p-value$_{L2(1)}$	p-value$_{L2(10)}$
$AUC_{tumor,\ 0.5\text{-}48h}$ (radiance*hr)	$1.48*10^{10}$	$3.61*10^{10}$	$2.90*10^{11}$		
Liver:tumor $ratio_{24\ hrs,\ orthotopic}$	2.6 ± 0.2	15.4 ± 5.0	40.7 ± 5.2	0.1117	0.0007
Liver:tumor $ratio_{24\ hrs,\ PDX}$	1.5 ± 0.4	7.8 ± 1.8		0.1357	
Liver:tumor $ratio_{48\ hrs,\ orthotopic}$	2.8 ± 0.2	6.2 ± 2.6	43.1 ± 2.7	0.1739	0.0007
Fold tumor cell uptake, 30 min	7.2 ± 0.6	34.7 ± 4.7	325.2 ± 29.0	0.0001	<0.0001
Fold tumor cell uptake, 24 hr	16.7 ± 1.0	31.0 ± 3.6	326.8 ± 16.0	0.0032	<0.0001

Table 5.2. Key comparisons of siRNA-L_2 vs. *in vivo* jetPEI.

siRNA-L_2 exhibits homogeneous distribution and high cellular internalization at the tumor site. The small size of albumin-bound siRNA-L_2 is expected to increase tissue penetration and homogeneity of distribution over nanoparticles. Using an *in vitro* tumor spheroid model, the penetration and distribution of siRNA-L_2 vs. jetPEI NPs throughout 3D tumor architecture was evaluated. The siRNA-L_2 showed homogeneous and substantial cell uptake throughout the entirety of spheroids, while jetPEI NPs remained localized largely around the edges of the spheroid (Figure 5.5A). Unmodified siRNA showed improved penetration into the interstitial spaces compared to the jetPEI complexes, but exhibited lower overall fluorescence than siRNA-L_2 (Figure S5.9A). To complement these results, flow cytometry was used to measure uptake per cell (as quantified by mean intracellular fluorescence) in tumor spheroids following siRNA formulation treatment. The cellular internalization of siRNA-L_2 was 2-fold higher than that of unmodified siRNA, evidencing an uptake benefit derived from hydrophobic modification (Figure 5.9B). Compared to jetPEI NPs, siRNA-L_2 exhibited a greater than 5-fold uptake increase (Figure 5.5B), with 84% of siRNA-L_2-treated cells positive for uptake compared to 27% of jetPEI NP-treated cells (Figure 5.9C-D).

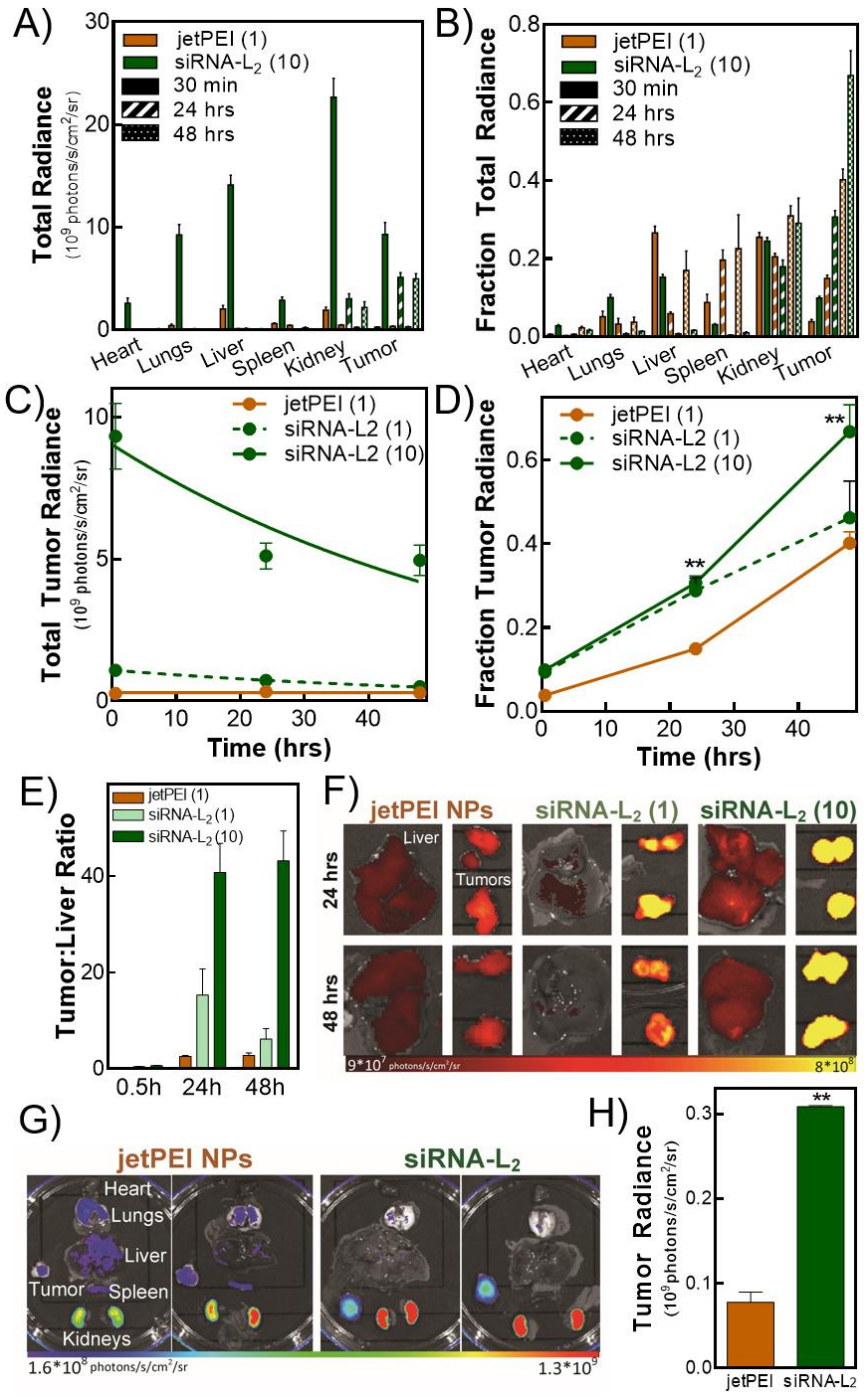

Figure 5.4. siRNA-L_2 achieves superior delivery to PDX snfd orthotopic tumors. Biodistribution was evaluated using a non-toxic dose of 1, 10 mg/kg of siRNA-L_2 and the MTD of 1 mg/kg jetPEI NPs. A-F) Orthotopic model: A) Absolute organ radiance for siRNA-L_2 (10 mg/kg), jet PEI NPs (1 mg/kg). B) Fraction organ radiance for siRNA-L_2, jetPEI NPs. C) Absolute tumor radiance; exponential decay fits plotted. All treatments are statistically different at all timepoints ($p<0.05$) except that siRNA-L_2 (1 mg/kg) does not differ from jetPEI at 48 hours. D)

Fraction tumor radiance; ** = $p<0.01$. E) Tumor:liver ratio reveals a lower proportion in the liver for siRNA-L_2 in comparison to jetPEI NPs. n = 4, standard error plotted. Ratio for siRNA-L_2 at 10 mg/kg is statistically greater than jetPEI at 24, 48 hours. F) Representative images depicting accumulation in liver, tumors. G-H) PDX model: G) Biodistribution and H) plotted tumor radiance (n = 2) of dose-matched jetPEI NPs and siRNA-L_2 at 24 hours. Radiance units are photons/s/cm^2/sr.

These *in vitro* tumor spheroid results inspired an investigation of tumor penetration and homogeneity of internalization by cells within orthotopic breast tumors *in vivo*. Following intravenous injection of siRNA-L_2 or jetPEI NPs, cells were isolated from excised tumors and evaluated by flow cytometry for cellular internalization. Tumor cells were identified by expression of green fluorescent protein (GFP). siRNA-L_2 outperformed jetPEI NPs at both 30 minutes and 24 hours, with siRNA-L_2 at 1 mg/kg displaying 5- and 2-fold increased uptake at respective time points and siRNA-L_2 at 10 mg/kg showing 45- and 20-fold increased uptake (Figure 5.5C-D, Table 5.2). At 30 minutes, mice treated with siRNA-L_2 at either dose displayed uptake in more than 96% of tumor cells, while jetPEI NP-treated mice showed uptake in only 60% of cells (Figure S5.9E). The preferential and homogeneous distribution of siRNA-L_2 to tumor sites and high uptake by tumor cells makes it ideally suited for cancer therapies.

siRNA-L_2 elicits sustained silencing in an *in vivo* tumor model. The promising tumor penetration characteristics of siRNA-L_2 inspired examination of its gene silencing efficacy *in vivo* in an orthotopic mouse tumor model. After treatment with luciferase-targeted siRNA or siRNA-L_2 at days 0 and 1, luminescence was evaluated over 10 days, where an increase in luminescence indicates tumor growth and successful luciferase silencing abrogates the increase in luminescent signal. siRNA-L_2-treated tumors exhibited significantly reduced tumor luminescence in

comparison to tumors treated with unmodified luciferase-targeting siRNA or inactive, control siRNA-L_2 sequences (Figure 5.4D, S5.10A). Comparing to the scrambled siRNA-L_2 control, maximum silencing was more than 60% at day 1, with nearly 50% silencing sustained at days 7 and 10, revealing the prolonged gene silencing capacity of siRNA-L_2. No change in mouse body weight was observed over the course of treatment, further indicating that siRNA-L_2 treatment is well-tolerated (Figure S5.10B).

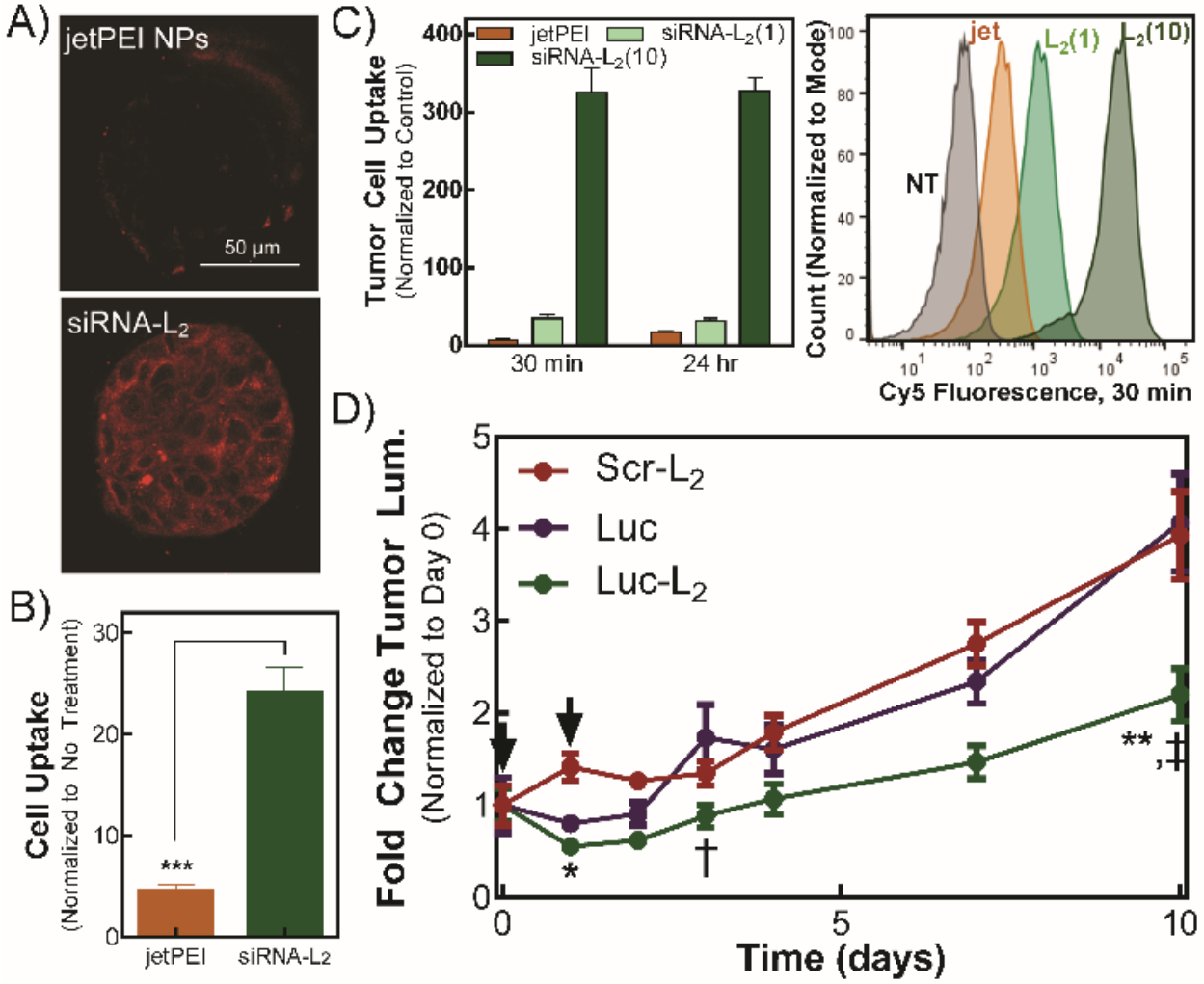

Figure 5.5. siRNA-L2 penetrates tumors and is internalized by tumor cells, resulting in sustained gene silencing in a mouse tumor model. A) Representative confocal microscopy images of tumor spheroid penetration and internalization. B) Cellular internalization of Cy5-labeled siRNA-L_2 or jetPEI NPs loaded with Cy5 siRNA in MCF-7 tumor spheroids. Treatment at 100 nM, quantified by flow cytometry; n=3, standard error plotted, *** = $p<0.001$.

C) Cellular internalization in tumor cells isolated from orthotopic xenograft mouse tumors after injection of jetPEI NPs at 1 mg/kg or siRNA-L_2 at 1, 10 mg/kg; n of 6 to 8 tumors. siRNA-L_2 treatment at 10 mg/kg exhibited statistically greater uptake than all other treatment groups. D) Gene silencing of luciferase-targeted siRNA-L_2 compared to unmodified siRNA in an orthotopic xenograft mouse tumor model; treatment at day 0 and 1 (as indicated by arrows) at 10 mg/kg, n of 10. * = $p<0.05$, ** = $p<0.01$: Luc-L_2 vs. Scr-L_2, † = $p<0.05$, ‡ = $p<0.01$: Luc-L_2 vs. Luc. Standard error plotted.

5.6 Discussion

Simple conjugation of a hydrophobic albumin-binding diacyl lipid moiety to siRNA is a powerful delivery strategy to improve siRNA pharmacokinetic properties. L_2 conjugation increases circulation half-life, cellular internalization capacity, and tumor penetration and retention of siRNA while simultaneously reducing accumulation in clearance organs. These myriad benefits lead to enhanced and prolonged *in vivo* gene silencing in tumors, supporting siRNA-L_2's potential as a cancer therapy that can act on currently undruggable targets.

Leveraging albumin as an endogenous nanocarrier is a relatively recent but extremely promising strategy to extend the circulation persistence of therapeutics. Clinically relevant examples range from Abraxane, an albumin-based nanoparticle that encapsulates Taxol, to Levemir, a therapeutic peptide modified to associate non-covalently with endogenous albumin[31]. siRNA, with its high potential medical impact but characteristically short circulation half-life, is an ideal candidate to develop with albumin as an in vivo chaperone. Inducing high-affinity binding of siRNA to albumin via modification with a lipidic moiety is a logical strategy. Previous work has shown siRNA amenable to lipid modifications, which often confer improvements in nuclease resistance and cellular internalization without impacting gene silencing[23, 25, 27, 238]. Conjugation with L_2 therefore has potential benefits on enhancing molecule stability and uptake while also

prompting *in situ* albumin binding. Notably, this binding is non-covalent and dynamic. In its physiological role as a fatty acid carrier, albumin facilitates the cellular uptake of lipids, likely through a variety of mechanisms that employ receptors for both albumin and lipid domains[274, 275]. Conjugation of L_2 could allow siRNA-L_2 to hijack these natural pathways. Additionally, the hydrophobic interaction of the L_2 moiety with the cellular membrane could encourage siRNA-L_2 to be internalized independent of albumin.

L_2 modification as an albumin targeting approach is desirable for achieving pharmacokinetic improvements while maintaining simplicity and safety. Despite the synthetic complexity of nanoparticle systems, siRNA-L_2 possesses a circulation half-life above that of non-crosslinked polyion nanoparticles[18, 73] and nearly equivalent to that observed in a relatively intricate crosslinked micelle system employing cholesterol-modified siRNA[22]. Perhaps more striking is the complete lack of toxicity observed for siRNA-L_2 at doses of 10 mg/kg, which sharply contrasts with the reported toxicity and immunogenicity of nanoparticulate carriers and our direct evaluation of *in vivo* jetPEI[17, 52]. siRNA-L_2 couples an improved circulation half-life with a lack of dose-limiting side effects, and therefore is anticipated to enable very broad therapeutic windows when developed against specific targets. Additionally, we expect that the efficacy of siRNA-L_2 could be further optimized through modifications to enhance *in vivo* stability and through identification of siRNA sequences with extremely potent silencing[45, 207].

Another associated challenge with nanoparticle delivery systems is their preferential accumulation within clearance organs, specifically the liver and spleen[159]. Accumulation of synthetic and toxic/immunogenic nanoparticle components in these organs is the typical cause of dose-limiting toxicities. However, siRNA-L_2 avoids retention in the MPS organs while also exhibiting a significant reduction in the kidney accumulation at 20 minutes, an indicator of rapid

renal clearance, associated with unmodified siRNA delivery. This is exemplified by the tumor:liver accumulation ratio of more than 40:1 achieved by siRNA-L_2. The disparity between *in vivo* jetPEI, with a ratio of less than 3:1, is pronounced. The lack of siRNA-L_2 retention in the liver is a key advantage over nanoparticulate delivery systems and will allow a greater percentage of the injected dose to be retained at its site of action in tumors. The lower tumor:liver ratio observed with *in vivo* jetPEI and nanoparticle systems in the literature is consistent with reported challenges in achieving efficient nanoparticle delivery to tumor sites; in a comprehensive analysis of nanoparticle delivery to solid tumors, the median injected dose delivered to the tumor site was 0.7%[176]. It is notable that even in recent, advanced, and promising nanoparticle systems, including those that employ modifications for "stealth" or targeting mechanisms, the ratio of tumor:liver accumulation is consistently close to or below 1:1[22, 174, 257, 276-280]. The marked improvement of siRNA-L_2 in relative tumor accumulation supports its translational promise.

There is also a significant tumor penetration benefit of siRNA-L_2, likely due to its small size relative to nanoparticle carriers. While *in vivo* jetPEI displays poor penetration of tumor tissue, siRNA-L_2 distributes homogeneously throughout tumor tissue and achieves consistently high uptake in tumor cells. The capacity of siRNA-L_2 to offer superior tumor penetration is particularly significant given the highly inconsistent nature of clinical tumor vasculature and tissue morphology which limits consistent nanoparticle distribution[176, 281]. Here, we note that the PDX mouse model is less permissive than the orthotopic model. PDX models are considered more clinically relevant, as they preserve the native tissue architecture of the primary tumor through multiple *in vivo* passages and consistently recapitulate histopathologic and molecular characteristics, including drug responses and metastatic potential[194]. The more challenging nature of the PDX model relative to the orthotopic model (which is considered more stringent than the

flank model[191]) aligns with recent discussion suggesting that the permeable nature of commonly-used mouse tumor models has led to an overestimation of the EPR effect[188, 192]. While nanocarriers like *in vivo* jetPEI may achieve efficacy in highly vascularized or non-solid tumors[188], they lack the ability to diffuse throughout the bulk of tumor architecture. Faced with a more difficult delivery challenge in the PDX model, siRNA-L_2 maintains tumor accumulation better than does *in vivo* jetPEI. As the majority of human solid tumors contain regions of poor vascularization and display disparity in vessel permeability[188, 191], siRNA-L_2's characteristics and performance imply applicability to a much broader range of cancers. A recognition of the limitations of the EPR effect and a developing understanding of tumor heterogeneity calls for innovative solutions for systemic RNAi cancer therapies. siRNA-L_2 deviates enormously from the standard nanoparticle format, and its notable advantages should inspire further research into similar conjugate-based strategies.

In situ targeting of albumin as an endogenous carrier is a powerful strategy to enhance the bioavailability of siRNA and avoid the issues associated with synthetic nanocarriers. siRNA-L_2 surpasses conventional delivery systems in circulation persistence, safety, biodistribution profile, and tumor penetration and cellular internalization. Ultimately, siRNA-L_2 achieves sustained gene silencing in tumors *in vivo*, providing strong proof-of-concept for therapeutic efficacy. This work highlights the immense value of the siRNA-L_2 conjugate as a translational and potentially transformative approach to improve *i.v.* RNAi cancer therapies.

CHAPTER 6

TOWARD DEVELOPMENT OF A HYDROPHOBIC SIRNA CONJUGATE FOR LOCAL TREATMENT OF CHRONIC WOUNDS

Text partially adapted from:

Sarett SM, Nelson CE, Duvall CL (2015). Technologies for controlled, local delivery of siRNA. *Journal of Controlled Release*, *218*.

Sarett SM (2014). Conjugation of palmitic acid improves potency and longevity of siRNA delivered via endosomolytic polymer nanoparticles. Unpublished master's thesis, Vanderbilt University, Nashville, Tennessee.

Sarett, SM, Kilchrist, KV, Miteva, M, Duvall, CL (2015). Conjugation of Palmitic Acid Improves Potency and Longevity of siRNA Delivered via Endosomolytic Polymer Nanoparticles. *Journal of Biomedical Materials Research Part A, 103*.

6.1 Introduction

Due to the complex nature of wound healing, a variety of physiological abnormalities can contribute to impaired healing. However, inadequate angiogenesis and the resulting deficiencies in oxygen and nutrient delivery to developing tissue have been identified as key problems in

chronic wounds. For complex pathologies like impaired wound healing, physiological gene inhibition presents a powerful alternative to typical small molecule drugs, as the suppression of a strategically selected gene allows for simultaneous modulation of a myriad of downstream targets and facilitates a broad and coordinated therapeutic effect. The inhibition of prolyl hydroxylase 2 (PHD2) in cells recruited to the site of wound healing has emerged as a powerful strategy to promote angiogenesis due to PHD2's role as a regulator of hypoxia inducible factor-1α (HIF-1α) activity. Silencing the regulator gene PHD2 through application of PHD2-targeted siRNA aids in restoration of a pro-healing environment at sites of impaired wound healing.

However, development of an effective RNAi-based therapy for local application has been frustrated by barriers to siRNA's cytoplasmic delivery. Previously, our group has established long-term and potent *in vivo* silencing efficacy of PHD2-targeted siRNA delivered from polymeric nanoparticles (NPs) loaded into polyester urethane (PEUR) biomaterial scaffolds[108, 134]. This delivery platform leverages the advantages of localized and sustained therapeutic release to achieve tunable gene silencing that resulted in upregulation of pro-angiogenic genes and enhanced blood vessel formation. However, there is a need to optimize this therapeutic strategy due to anti-angiogeneic, pro-inflammatory side effects derived from the NP carrier (Figure S6.1). These side effects are particularly undesirable at sites of chronic wounds (which are often characterized by a state of pathologically increased inflammation) but typical of cationic NP carriers. We established that conjugation of palmitic acid (PA) to siRNA reduces the dose of cationic nanocarrier required for effective and prolonged gene silencing, endowing siRNA-PA NPs with a broader therapeutic index than unmodified siRNA NPs. We will continue our evaluation of siRNA-PA NPs, benchmarked against siRNA NPs and delivered from polyurethane scaffolds, in a rat model of impaired wound healing.

While siRNA-PA NPs are a more biocompatible option than siRNA NPs, the ideal siRNA conjugate eliminates the need for a nanocarrier and will likely facilitate more homogeneous distribution throughout the site of chronic wounds. A multivalently hydrophobic siRNA conjugate is expected to potentiate cellular uptake through multiple simultaneous interactions with the cellular membrane; indeed, we have shown that a divalently hydrophobic siRNA conjugate achieved higher internalization than the monovalent siRNA-PA molecule. Current strategies for coating cell membranes involve "anchoring" to the lipid bilayer via hydrophobic interactions, and multivalent interactions have been shown to be far more potent than similar monovalent interactions[282, 283]. We will investigate several strategies for conjugation of siRNA to a multivalently hydrophobic polymer, notably "grafting-to" and "grafting-from" approaches using reversible addition-fragmentation chain transfer (RAFT) polymerization techniques. The novel siRNA-polymer conjugates developed will leverage hydrophobic modification of siRNA as a non-toxic strategy to improve siRNA's pharmacokinetics, advancing development of a biocompatible RNAi therapeutic for treatment of chronic wounds.

6.2 Materials and methods

Materials: Amine-modified single-stranded DNA (modification at 5' end) or Dicer substrate siRNA (modification at 3' end) and complementary single-stranded Cy5-modified DNA or unmodified Dicer substrate siRNA were obtained from Integrated DNA Technologies (Coralville, Iowa). Lipofectamine 2000 was purchased from Life Technologies (Grand Island, NY). RNEasy spin columns were obtained from Qiagen (Venlo, Netherlands), and the iScript cDNA Synthesis Kit from Bio-Rad (Hercules, CA). Macro-Prep High Q Support anionic resin was also purchased from Bio-Rad. NIH-3T3s were purchased from Jackson Laboratory (Bar

Harbor, ME). Propylacrylic acid was synthesized as previously reported[1,2]. All other reagents were purchased from Sigma-Aldrich (St. Louis, MO).

Oligonucleotide-PA Synthesis and Characterization: Single-stranded amine-modified oligo was reacted with 100-fold molar excess of PA *N*-hydroxysuccinimide ester pre-dissolved at 40 mM in *N*,*N*-dimethylformamide (DMF). The reaction was carried out for 18 hours at room temperature in 45% water, 45% isopropyl alcohol, and 10% DMF. The oligo-PA was purified by reversed-phase HPLC using a Clarity Oligo-RP column (Phenomenex, Torrence, CA) under a linear gradient from 95% water (50 mM triethylammonium acetate), 5% methanol to 100% methanol. The conjugate molecular weight was confirmed using MALDI-TOF mass spectrometry (Voyager-DE STR Workstation, Grand Island, NY) using 50 mg/mL 3-hydroxypicolinic acid in 50% water, 50% acetonitrile with 5 mg/mL ammonium citrate as a matrix. The yield of the oligo-PA was quantified based on absorbance at 260 nm. The purified oligo-PA was annealed to its complementary strand to generate Cy5-modified DNA-PA or siRNA-PA. Conjugation and annealing was also confirmed via agarose gel electrophoresis.

Oligonucleotide-loaded Nanoparticle (NP) Synthesis: A diblock copolymer composed of a homopolymer of 2-(dimethylamino) ethyl methacrylate (DMAEMA) blocked with a random copolymer of DMAEMA, 2-propylacrylic acid (PAA), and butyl methacrylate (BMA) was synthesized using reversible addition-fragmentation chain transfer (RAFT) polymerization as described previously[70, 134]. Assembly of NPs was triggered by dissolving polymer in 100% ethanol, followed by slow addition of water or PBS via syringe pump. siRNA or DNA (with or without PA) was mixed with NPs and allowed to electrostatically condense for 30 minutes. NPs were used at this stage directly for cellular uptake studies. For scaffold encapsulation, the

excipient trehalose was added at a 60:1 weight ratio to siRNA and incubated with the NPs for 30 minutes. NPs were then frozen and lyophilized.

Cellular Uptake: NIH-3T3s were treated with Cy5-labeled DNA or DNA-PA in 10% serum for 24 hours at 500 nM and with Cy5-labeled DNA or DNA-PA complexed with Lipofectamine 2000 (according to manufacturer protocol) for 24 hours at 50 nM. Intracellular fluorescence was quantified using flow cytometry at 12, 36, 60, and 84 hours. Extracellular membrane-bound fluorescence was quenched with Trypan Blue.

Poly(thioketal urethane) (PTK-UR) Scaffold Synthesis: 100 mg PTK-UR scaffold were prepared using reactive liquid molding. Poly(thioketal) polyol[284] was added to water, TEGOAMIN33 catalyst, and the pore opener calcium stearate. These components were then mixed for 30 seconds at 3300 rpm in a Hauschild DAC 150 FVZ-K SpeedMixer (FlackTek, Inc., Landrum, SC). This mixture was added to a micro-centrifuge tube containing the lyophilized siRNA/siRNA-PA NPs; siRNA was designed to target PHD2 or was a non-targeted (scrambled) control sequence. A homogenous mixture was obtained through another 30 seconds of mixing. Next, lysine triisocyanate (LTI) was added and the components were mixed for an additional 30 seconds. The tubes were exposed to air and the reaction mixture allowed to freely rise and harden for at least 2 hours. The targeted index (ratio of isocyanate to hydroxyl equivalents times 100) was 115, where the number of OH equivalents is calculated from the poly(thioketal) polyol's molecular weight. The amounts of each component for the respective scaffold formulations, given as equivalent amounts in parts per hundred parts polyol (PPHP), are 1.5, 2.3, 4.0, and 36.1 for water, TEGOAMIN33, calcium stearate, and LTI, respectively.

Diabetic Rat Excisional Wound Model: All surgical procedures are reviewed and approved by Vanderbilt University's Institutional Animal Care and Use Committee. As previously described[284], for these animal studies, adult male Sprague-Dawley rats (~350g) will be treated with streptozotocin (STZ) at 50mg drug/kg rat and allowed to develop diabetes for 10 days, with a blood glucose concentration greater than 300 mg/dL confirming the diabetic state. PTK-UR scaffolds loaded with PHD2 or PHD2-PA siRNA NPs will then be implanted in full-dorsal excisional wounds, which are used to mimic chronic diabetic ulcers. Scaffolds will be excised from euthanized animals at days 4 and 7 to be processed for histology and gene expression quantification.

Evaluation of PHD2 Gene Silencing: Approximately half of each scaffold excised at 4, 7 day was stored in RNAlater to preserve mRNA content. RNA was isolated directly from these scaffold sections, transcribed into cDNA, and the degree of PHD2 knockdown was quantified by real time polymerase chain reaction (RT-PCR) using the ΔΔCt method and normalizing to glyceraldehyde 3-phosphate dehydrogenase (GAPDH) and peptidyl-prolyl cis-trans isomerase B (PPIB).

Synthesis of azide-functionalized chain transfer agent (CTA): The RAFT CTA 4-Cyano-4-(ethylsulfanylthiocarbonyl)sulfanylpentanoic Acid (ECT*)* was synthesized as previously described[70, 241]. Azidoethanol was synthesized through reaction of sodium azide (2.4 M in water) with 2-bromoethanol (3:1 excess of sodium azide). Azidoethanol was extracted in diethyl ether and isolated by rotary evaporation. Immediately following rotary evaporation, azidoethanol was coupled to ECT via N-(3-Dimethylaminopropyl)-N′-ethylcarbodiimide (EDC) HCl/4-Dimethylaminopyridine (DMAP) coupling. Azidoethanol:ECT ratio was 1.25:1; EDC HCl was at a 2-fold molar excess and DMAP was 7.5% of the molar amount of EDC HCl. Reaction was

achieved in dichloromethane (DCM) and ECT-azide was isolated through washing with water three times and synthesis was confirmed by H NMR evaluation.

Polymer synthesis from ECT-azide: ECT-azide was used as a CTA in RAFT polymerization of 2-methacryloyloxyethyl phosphorylcholine (MPC) and pentafluorophenyl acrylate (PFPA). ECT-azide was at a ratio of 5:1 to free radical initiator AIBN. The solvent was methanol and monomer concentration was 20% of the total reaction volume. The combination of ECT-azide, AIBN, MPC, PFPA, and trioxane in methanol was nitrogen purged and polymerized for 24 hours at 65^{o}C. The characteristic trioxane H NMR peak (5.2 ppm) was used to evaluate reaction monomer efficiency through comparison of monomer peak area pre- and post-polymerization. p(MPC-co-PFPA) polymers were characterized by H NMR and F NMR, where F NMR revealed the successful incorporation of PFPA.

Synthesis of DNA-DBCO: Synthesis of DNA-DBCO is previously described; briefly, single-stranded DNA-NH_2 was reacted with 10-fold molar excess of DBCO-PEG_4-NHS in 30% dimethylsulfoxide (DMSO) and 70% phosphate buffered saline (PBS) with 8 mM TEA. The product was purified by NAP-25 column filtration.

Reaction of PFPA to dodecylamine: p(MPC-co-PFPA) was dissolved in water and dodecylamine was dissolved in DMSO in equal volumes. Solutions were combined, with dodecylamine at a 50-fold excess to PFPA groups in the polymer. p(MPC-co-12C) was characterized by H NMR and F NMR, where disappearance of the F NMR peaks revealed elimination of the PFPA moieties.

Reaction and purification of p(MPC-co-12C) to DNA-DBCO: DNA-DBCO dissolved in water at a 100 μM concentration was reacted to p(MPC-co-12C) dissolved in an equal volume of methanol. p(MPC-co-12C) was at a 50-fold excess to DNA-DBCO. The reaction was evaluated

through agarose gel electrophoresis, staining with ethidium bromide. The crude reaction mixture was purified to eliminate excess polymer through mixing with Macro-Prep High Q Support anionic resin chromatography beads. Resin and crude reaction were incubated in water for 30 minutes on the shaker. Mixture was centrifuged at 3,000 G for 5 minutes and supernatant was removed. Bound DNA-DBCO or DNA-p(MPC-co-12C) was eluted from the beads through washing with 3 M NaCl. This eluent was filtered through a NAP25 desalting column and lyophilized. This product was then purified further through HPLC purification in the Clarity Oligo RP column as previously described.

Reaction of ECT-azide to DNA-DBCO: DNA-DBCO dissolved in water at a 100 μM concentration was reacted to ECT-azide dissolved in an equal volume of methanol. ECT-azide was at a 50-fold excess to DNA-DBCO. Reaction was evaluated through MALDI mass spectrometry.

6.3 Results and discussion

In pursuit of a hydrophobic siRNA conjugate for carrier-free efficacy in local, scaffold-based delivery, we initially investigated siRNA-PA. Given the facile synthesis of siRNA-PA and its higher stability relative to unmodified siRNA, we investigated whether the monovalent PA modification would be sufficient to induce cellular uptake. Unfortunately, oligonucleotide modification with PA was incapable of promoting substantial cellular internalization carrier-free even at high (500 nM) doses (Figure 6.1A). Additionally, siRNA-PA in the absence of a nanocarrier elicited no significant gene silencing in *in vitro* evaluations at doses up to 5 μM. These results motivated our choice of siRNA-PA NPs, rather than siRNA-PA carrier-free, for investigation *in vivo*.

siRNA or siRNA-PA NPs, targeted to the PHD2 gene, were loaded into PTK-UR biomaterial scaffolds; the PTK-UR scaffold formulation was chosen because of its proven capacity to facilitate and support tissue ingrowth and wound healing[122, 284]. Loaded scaffolds were implanted at the site of excisional wounds in diabetic rats. Diabetic rats display defective closure of excisional wounds, highlighting the importance of diabetic complications in wound healing and making this a challenging wound model that replicates aspects of the well-documented clinical connection of diabetes to impaired wound healing[4, 5]. In this stringent *in vivo* model, NPs loaded with PA-modified PHD2 siRNA elicited more sustained gene silencing than those loaded with unmodified PHD2 siRNA (Figure 6.1B). This promising result confirms the greater longevity of siRNA-PA NPs. However, there remains an impetus for establishment of potent silencing without the use of a polymer nanocarrier.

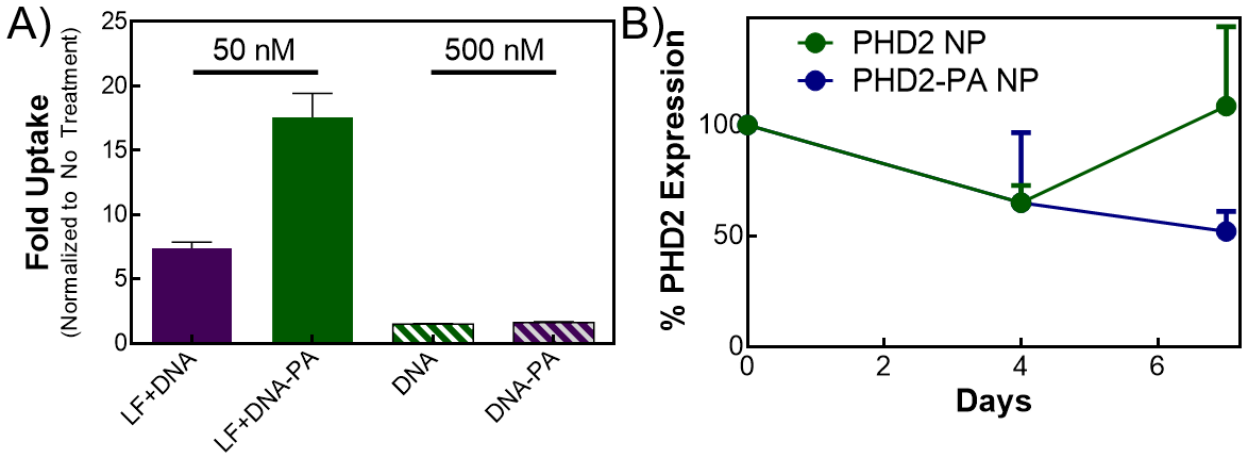

Figure 6.1. A) In combination with Lipofectamine 2000 (LF), PA conjugation results in enhanced substantial cellular uptake at a 50 nM dose. Carrier-free DNA-PA is not effective at inducing cellular uptake at a dose of 500 nM (not statistically greater than DNA, while both DNA and DNA-PA carrier-free were statistically lower than both LF treatments. B) In a rat diabetic excisional wound model, scaffolds loaded with NPs of PA-modified siRNA-PA elicited more prolonged gene silencing compared to those using unmodified PHD2 siRNA (no differences were statistically significant).

A multivalently hydrophobic siRNA-polymer conjugate is expected to facilitate enhanced interaction with the cellular membrane, leading to improved internalization and therefore gene silencing. However, the conjugation of two large macromolecules, like that of siRNA to a polymer, is often hampered by low reaction efficiencies and challenging purification procedures [285, 286]. Further complicating the synthesis of a multivalently hydrophobic siRNA-polymer conjugate is the solubility disparity that exists between a partially hydrophobic polymer and hydrophilic siRNA. Recognition of these difficulties motivated development of a strategy for siRNA-polymer synthesis based on efficient "click" conjugation chemistry, a "grafting-to" approach (Figure 6.2).

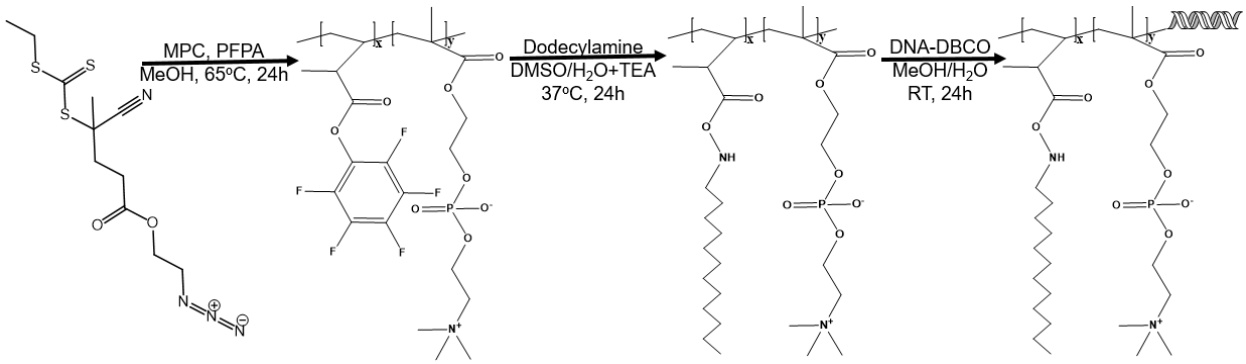

Figure 6.2 "Grafting-to" approach for synthesis of a multivalently hydrophobic siRNA-polymer conjugate. An azide-functionalized RAFT CTA is used to generate a co-polymer of MPC and PFPA, and the PFPA moieties are subsequently replaced with a 12-carbon chain. The polymer, end-functionalized with the azide, is conjugated to siRNA-DBCO,

Our approach leverages RAFT co-polymerization of a hydrophilic, zwitterionic monomer (MPC) with an amine-reactive monomer (PFPA). The MPC imparts aqueous solubility to the polymer while the PFPA can be modified post-polymerization with amine-functionalized lipids, endowing the polymer with multiple hydrophobic groups. An azide-functionalized RAFT CTA

was synthesized (Figure S6.2) to provide a controlled site for reaction with DBCO-functionalized siRNA (Figure 5.1, S5.1).

The first step is RAFT polymerization from the azide-functionalized CTA. Measurement of monomer consumption pre- and post-polymerization allows estimation of the polymer composition and molecular weight (Figure S6.3). The prototypical polymer candidate was characterized to have a molecular weight of ~12,000, with about 80% MPC composition and 20% PFPA composition (corresponding to 9 reactive sites per polymer). The polymer was subsequently reacted to an amine-functionalized 12-carbon lipid, resulting in an azide-functionalized multivalently hydrophobic polymer (Figure S6.4). This polymer is amenable to reaction with the previously-described DBCO-functionalized oligonucleotides. Conjugation of DNA-DBCO to the polymer was achieved (Figure 6.4A), though the reaction could not be driven to completion and significant conjugate yield necessitated high (50-fold) excesses of the polymer. The high polymer excess caused issues in purification of the siRNA-conjugate; the similar molecular weights of siRNA and the polymer precluded size-based isolation, and HPLC purification methods, while effective at separating DNA-DBCO from DNA-polymer (Figure 6.4B) did not eliminate residual polymer.

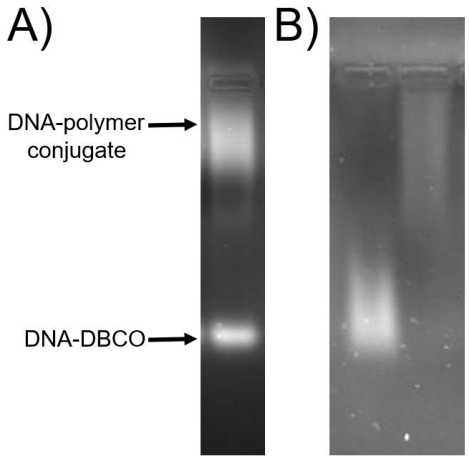

Figure 6.3. A "grafting-to" approach allows synthesis of a multivalently hydrophobic DNA-polymer conjugate, as evidenced by gels stained for nucleic acids. A) Crude reaction of DNA-DBCO to azide-functionalized polymer; the DNA-polymer conjugate migrates much more slowly than DNA-DBCO. B) Fractions from the two main peaks observed during HPLC purification; DNA-DBCO comprises the first peak, while the second is the DNA-polymer conjugate. Both fractions contained substantial residual unreacted polymer.

The moderate efficiency and complex purification of the "grafting-to" strategy motivated exploration of a "grafting-from" approach (Figure 6.4), which is expected to obviate the central purification difficulties. A "grafting-from" approach for siRNA-polymer synthesis has, to date, been accomplished only once; an siRNA-based macroinitiator was used in atom transfer radical polymerization to polymerize a PEG-based monomer[285]. Polymerization of a hydrophobic monomer from an siRNA-based initiator is a wholly novel pursuit. Due to siRNA's poor solubility in organic solvents and its high cost, we identified a recently-developed technique for RAFT polymerization at low volumes in aqueous media as a promising strategy[287]. Synthesis protocols using this technique are in development. Successful implementation of the "grafting-from" approach would eliminate the purification difficulties inherent in the "grafting-to" approach, allowing efficient synthesis of our unique, multivalently hydrophobic siRNA conjugate.

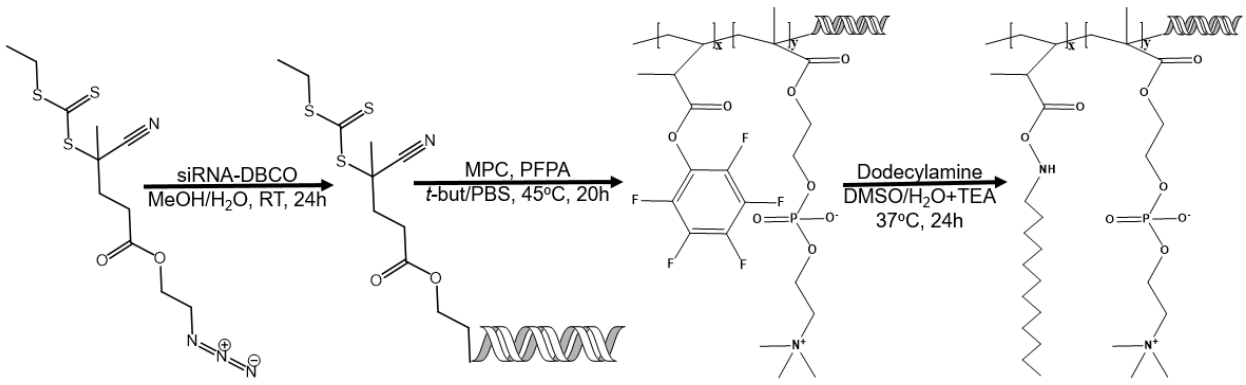

Figure 6.4 "Grafting-from" approach for synthesis of a multivalently hydrophobic siRNA-polymer conjugate. An azide-functionalized RAFT CTA is conjugated to DBCO-functionalized siRNA pre-polymerization. A co-polymer of MPC and PFPA is grown from the siRNA-CTA, and the PFPA moieties are subsequently replaced with a 12-carbon chain.

6.4 Conclusions

Developing a potent siRNA conjugate for local, scaffold-based delivery has the potential to revolutionize the treatment of chronic wounds. Our work demonstrates that a monovalently hydrophobic siRNA conjugate does not induce carrier-free gene silencing efficacy, and polymer nanocarrier options display undesirable inflammatory side effects. We have synthesized a multivalently hydrophobic siRNA-polymer conjugate that could allow for carrier-free gene silencing at sites of impaired wound healing. Further investigation of purification strategies in the "grafting-to" approach and evaluation of synthesis conditions in the "grafting-from" approach will allow characterization of the therapeutic utility of our innovative conjugate in local RNAi applications.

CHAPTER 7

SYNOPSIS AND SIGNIFICANCE

7.1 Summary

Almost three decades have passed since the initial discovery of RNAi[34], and scientific understanding regarding the molecular mechanism and physiological interactions of siRNA, ODNs, LNA, and other RNAi effectors has advanced considerably over that time span[8]. The preclinical value of siRNA has been enormous, allowing facile *in vitro* investigation of the impacts of temporal gene knockdown. However, clinical translation of siRNA and other RNAi therapeutics has proven extremely challenging[288]. While numerous antisense ODN therapies have successfully navigated clinical trials and become valuable treatment options for niche pathologies[289], no siRNA-based therapy has achieved clinical relevancy[290, 291]. Despite the established higher potency of siRNA in comparison to ODNs, the formidable *in vivo* barriers to delivery of siRNA to its site of action have complicated and impeded therapeutic development[14, 43]. The motivation of this work was to improve siRNA's pharmacokinetic properties through covalent conjugation of biocompatible, hydrophobic moieties, improving its potency and therapeutic efficacy when delivered via local or systemic treatment strategies. These studies investigated strategically-chosen siRNA conjugates designed to act synergistically with a delivery platform and with the physiological milieu.

In aim 1, siRNA was hydrophobized with PA and evaluated in combination with polymer nanoparticle carriers. To address local delivery applications, siRNA-PA was encapsulated in nanoparticles of a diblock copolymer with a DMAEMA corona and a core-forming block comprising DMAEMA. PAA, and BMA. The DMAEMA corona condenses anionic siRNA and the copolymer block stabilizes the nanoparticles and endows endosomal escape properties. These nanoparticles are tailored for local delivery applications; the cationic corona promotes cellular internalization but results in aggregation, protein adsorption, and rapid clearance in situations of intravenous delivery. siRNA-PA-loaded nanoparticles (siRNA-PA NPs) were superior to nanoparticles loaded with unmodified siRNA in loading capacity, stability, ability to induce cellular uptake, and gene silencing potency and longevity. siRNA-PA's concentration at the nanoparticle surface facilitated hydrophobic interactions between siRNA-PA molecules and with the cellular membrane, conferring the distinct advantages observed.

To tackle the challenges of systemic siRNA delivery, a PEGylated polymer with equivalent core content of DMAEMA and BMA was utilized. The PEG corona imparts enhanced circulation persistence by shielding the nanoparticles from immune recognition, while the DMAEMA in the corona functions to encapsulate siRNA. The BMA component acts to stabilize the nanoparticles by facilitating hydrophobic forces between polymer strands. In this delivery system, siRNA-PA loads into the nanoparticle core, which allows hydrophobic interactions among siRNA-PA molecules and with the BMA component in addition to the electrostatic attractions between siRNA-PA and the DMAEMA moieties. These dual interactions endow siPA NPs with enhanced loading efficiency, stability in the presence of counterions and serum, and improved cellular internalization. In summary, siRNA-PA has proven advantageous in combination with polymer nanoparticles optimized for local or systemic delivery. These studies demonstrate the broad

pharmacokinetic improvements that can be derived from simple hydrophobic modification of siRNA.

While aim 1 focuses on synergistic combination of hydrophobized siRNA and polymer nanocarriers, aim 2 concentrates on development of hydrophobic siRNA conjugates suited for carrier-free delivery. Unfortunately, siRNA-PA proved incapable of eliciting carrier-free gene silencing even when localized to target tissues. For situations of local delivery, siRNA conjugated to a polymer decorated with multiple hydrophobic moieties is a superior strategy to monovalent modification with PA because it enables multivalent hydrophobic interactions with cellular membranes. However, the published reports of siRNA-polymer conjugates exclusively utilize hydrophilic polymers for siRNA conjugation, with the vast majority of polymers utilized consisting of a PEG derivative. This exemplifies the challenging nature of modifying ~10 kDa siRNA with another large macromolecule, where steric hindrance and solubility differences can create significant issues[285, 286]. Despite the inherent difficulty of this strategy, siRNA-polymer conjugates wherein the polymer is composed of hydrophilic MPC with randomly distributed saturated 12-carbon moieties have been synthesized for ultimate incorporation into a scaffold-based local delivery platform.

An alternate siRNA conjugate was developed to address systemic delivery considerations. siRNA conjugated to the diacyl lipid moiety L_2 emerged as a powerful option due to its capacity to leverage albumin as an endogenous nanocarrier. *In vitro,* siRNA-L_2 exhibited immediate and high-affinity albumin binding as well as enhanced stability, cellular internalization, and penetration of tumor tissue architecture. These studies describe the development of two wholly novel hydrophobic siRNA conjugates for carrier-free therapeutic application. Due to the complexity and toxicity characteristic of nanocarrier systems, conjugate-based strategies are a

potentially high-impact pursuit. This work broadens the scope of this field by investigating the utility of unique hydrophobic moieties.

Aim 3 evaluates the therapeutic potential of leading siRNA conjugate strategies in relevant animal disease models. While the multivalently hydrophobic siRNA-polymer conjugate remains uniquely promising for local, scaffold-based delivery to the site of chronic wounds, to date the challenges in large-scale synthesis and purification of this conjugate have precluded its *in vivo* evaluation. Because siRNA-PA NPs possess a broad therapeutic index in comparison to previously used NP-based strategies, this system was instead investigated. PHD2-PA NPs loaded into a biomaterial scaffold and implanted in diabetic rat excisional wounds imparted enhanced longevity of gene silencing.

siRNA-L_2 was evaluated as a systemic oncological therapy in orthotopic and PDX mouse tumor models of triple negative breast cancer. L_2 conjugation conferred broad improvement of siRNA's pharmacokinetic properties, increasing circulation time and reducing renal clearance. Significantly, siRNA-L_2 exhibited no toxicity at ten-fold the maximum tolerated dose of commercially available *in vivo* siRNA nanocarrier jetPEI. Benchmarked against jetPEI, siRNA-L_2 exhibited higher tumor accumulation and penetration and induced potent and sustained gene silencing. This is the first reported carrier-free, systemic gene silencing using siRNA at a non-hepatic pathological site. This work highlights the clinical potential of hydrophobic siRNA conjugate-based therapies and siRNA-L_2's particular promise as a potentially revolutionary systemic RNAi cancer therapy.

Hydrophobic siRNA conjugates are a powerful tool to endow siRNA with the capacity to overcome the physiological delivery barriers it faces. These conjugates are highly biocompatible and impart stability both in combination with nanocarrier systems and when utilized carrier-free.

This work represents the forefront of an exciting and hopefully fruitful avenue of investigation of divalent and multivalent hydrophobic modifications to siRNA that leverage aspects of the endogenous milieu to confer dramatically enhanced delivery efficacy.

7.2 Concerns and Limitations

Achievement of the described aims represents major progress toward development of effective hydrophobic siRNA conjugates. Yet the stability of the siRNA molecule itself, the lack of an endosomal escape mechanism, and the inability to completely eliminate the nanocarrier in the local delivery platform merit discussion, as these issues could prove limiting factors to therapeutic application of this work.

Molecular modification of the siRNA molecule has become a widespread strategy to improve siRNA's resistance to nuclease degradation and reduce the likelihood of silencing non-targeted genes[45, 59, 207]. Some of the most common modification strategies are substitution of non-bridging phosphate-bound oxygen to sulfur (where replacement of a single oxygen or both oxygens is a phosphorothioate or phosphorodithioate modification, respectively) and substitution of a 2'-OH with a 2'-O-methyl or 2'-fluorine. The impact of these modifications on molecule stability can be dramatic, but their widespread incorporation can also impede gene silencing efficacy. Companies like Alnylam have shown that systematic, high-throughput evaluation of the site and nature of molecular modifications, coupled with sequence optimization, can yield highly potent and stable siRNA molecules[77, 78, 227]. Work by the Sood group highlights the potential to leverage these molecular modifications for enhanced siRNA activity[292], but the optimal choice for siRNA modification can be application- and sequence-dependent. A thorough investigation of ideal

molecule modification is beyond the scope of this work, but the *in vivo* stability of the siRNA used in this project is likely a limiting factor that could be addressed with this strategy.

Further, a requirement for an ideal siRNA therapy that hydrophobization does not directly address is the capacity to induce endosomal escape. While hydrophobic siRNA conjugates have proven capable of translocating the cellular membrane more readily than unmodified siRNA, their ability to disrupt the endosomal membrane and reach the cytoplasm has not been evaluated. The established *in vitro* or *in vivo* gene silencing efficacy of siRNA conjugates delivered carrier-free (e.g. L_2, trivalent RGD, cholesterol, palmitic acid, GalNAc conjugates)[77, 78, 88, 209] indicates that some percentage of these siRNA conjugates achieves delivery to the cytoplasm. However, with the exception of highly potent GalNAc-modified siRNA, establishment of significant gene silencing with carrier-free delivery necessitates high siRNA doses. Although siRNA-L_2 delivery results in more than an order of magnitude higher cellular uptake than an established *in vivo* siRNA nanocarrier, the gene knockdown derived from this uptake may be limited by the lack of an endosomal escape mechanism and the degradation of a majority of the internalized siRNA before it can reach its site of action. Initially, elucidation of the uptake mechanism for siRNA conjugates and their capacity to avoid endosomal degradation is required. Subsequent to this growing understanding, incorporation of an active means of endosomal escape into promising siRNA conjugate-based systems would be a promising avenue of investigation.

Notably, incorporation of hydrophobized siRNA into polymer nanoparticles endows the delivery platform with the ability to escape the endosome. However, the previously described limitations of traditional nanocarriers remain relevant, and the continued need for a polymer nanocarrier, even at a reduced dose, is a limitation of the siRNA-PA-based local therapies. siRNA-PA NPs could not be replaced with a multivalently hydrophobic siRNA-polymer conjugate

because of the significant synthesis challenge posed by generation of this conjugate. While reasonable conjugation efficiency was achieved in a "grafting-to" strategy, purification difficulties confounded further evaluation. A "grafting-from" approach for siRNA-polymer conjugates has to date been accomplished only once and with a hydrophilic PEGMA monomer[285]. A "grafting from" approach to generate the desired multivalently hydrophobic siRNA-polymer conjugate is in development but a fully characterized siRNA-polymer conjugate is not yet available for *in vivo* evaluation for local delivery applications. Thus, complete elimination of the nanocarrier has yet to be validated for treatment of local pathologies.

7.3 Significance

Despite the limitations noted above, this work is both innovative and of high value to researchers developing the next generation of siRNA delivery strategies. We are the first to show the synergistic combination of hydrophobized siRNA and partially hydrophobic polymer nanoparticles, elucidating a means for broadening the therapeutic index of traditional siRNA nanocarriers. Additionally, while monovalent hydrophobic modification of siRNA has been previously investigated, this is the first description of conjugation of divalent and multivalent hydrophobic moieties to siRNA. The siRNA-L_2 and siRNA-polymer we generated are distinct from any previously investigated siRNA conjugates. In particular, siRNA-L_2's capacity to broadly enhance siRNA's carrier-free pharmacokinetic properties provide motivation for evaluation of a greater variety of strategically-chosen hydrophobic moieties for siRNA conjugation.

siRNA-L_2 effected the first reported instance of *in vivo* carrier-free gene silencing at a non-hepatic, desired site. siRNA-L_2's high accumulation, broad penetration, and strong cellular uptake within tumors after systemic, intravenous delivery is unprecedented. It far surpasses typical

nanocarriers and other systemically-delivered siRNA conjugates (e.g. siRNA-cholesterol, siRNA-GalNAc) in its capacity to deliver preferentially to tumors over the liver. These exciting findings position siRNA-L_2 as a leading candidate for systemic, oncological RNAi therapies and we hope that siRNA-L_2's promise inspires further research into siRNA conjugates capable of carrier-free efficacy.

7.4 Future Directions

Development of a multivalently hydrophobic siRNA conjugates is a strong focus of future work. Specifically, current priorities are the identification of an efficient synthesis scheme or purification strategy. Subsequent *in vitro* characterization and evaluation of the siRNA-polymer conjugate for stability, cellular uptake, and gene silencing is vital to assess its potential as a carrier-free therapy.

Additionally, the siRNA-L_2 conjugate, which already exhibits high potency, is amenable to further optimization. The linkage of the siRNA to the divalent lipid moiety is a ~2,000 Da PEG spacer. This spacer imparts aqueous solubility to the hydrophobic moiety, facilitating conjugation with hydrophilic siRNA. It also reduces the stability of the micellar population that siRNA-L_2 spontaneously forms in aqueous media, allowing destabilization of these micelles *in vivo* and effective albumin binding[265]. This linker may further effect the pharmacokinetic properties of siRNA-L_2 and the relative merits and drawbacks of a variety of linker chemistries merit further evaluation. For example, a pH-responsive linker that could impart a capacity for endosomal escape without detrimentally impacting pharmacokinetic properties could have a high impact on siRNA-L_2's gene silencing power.

Moreover, modulation of the two 18-carbon lipid tails that comprise the albumin-binding piece of the L_2 moiety could provide a pharmacokinetic benefit by enabling higher-affinity binding of siRNA-L_2 with albumin. It has been previously shown that shorter fatty acids (lauric, myristic, and palmitic) exhibit preferential binding to albumin over HDL and LDL, while stearic acid (comprising 18 carbons) binds HDL and LDL to a larger degree. The low hepatic accumulation observed indicates that the L_2 moiety preferentially associates with albumin over HDL and LDL; however, it is possible that tuning the length of the diacyl lipids will yield further improvement in albumin binding and circulation persistence.

7.5 Conclusion

Realizing siRNA's clinical potential has proven a daunting challenge. The excitement surrounding RNAi has waxed with predictions of revolutionary medical impacts and waned with the realities of obstacles to clinical translation. Yet scientific understanding of siRNA has continued to grow, and siRNA therapies are poised for a clinical breakthrough. This work reveals that hydrophobization of siRNA is a simple, biocompatible approach to circumvent delivery barriers and broaden the therapeutic index of siRNA therapies. We establish a pivotal role for hydrophobic siRNA conjugates in the advance of siRNA to medical application.

APPENDIX

A. Supplementary figures

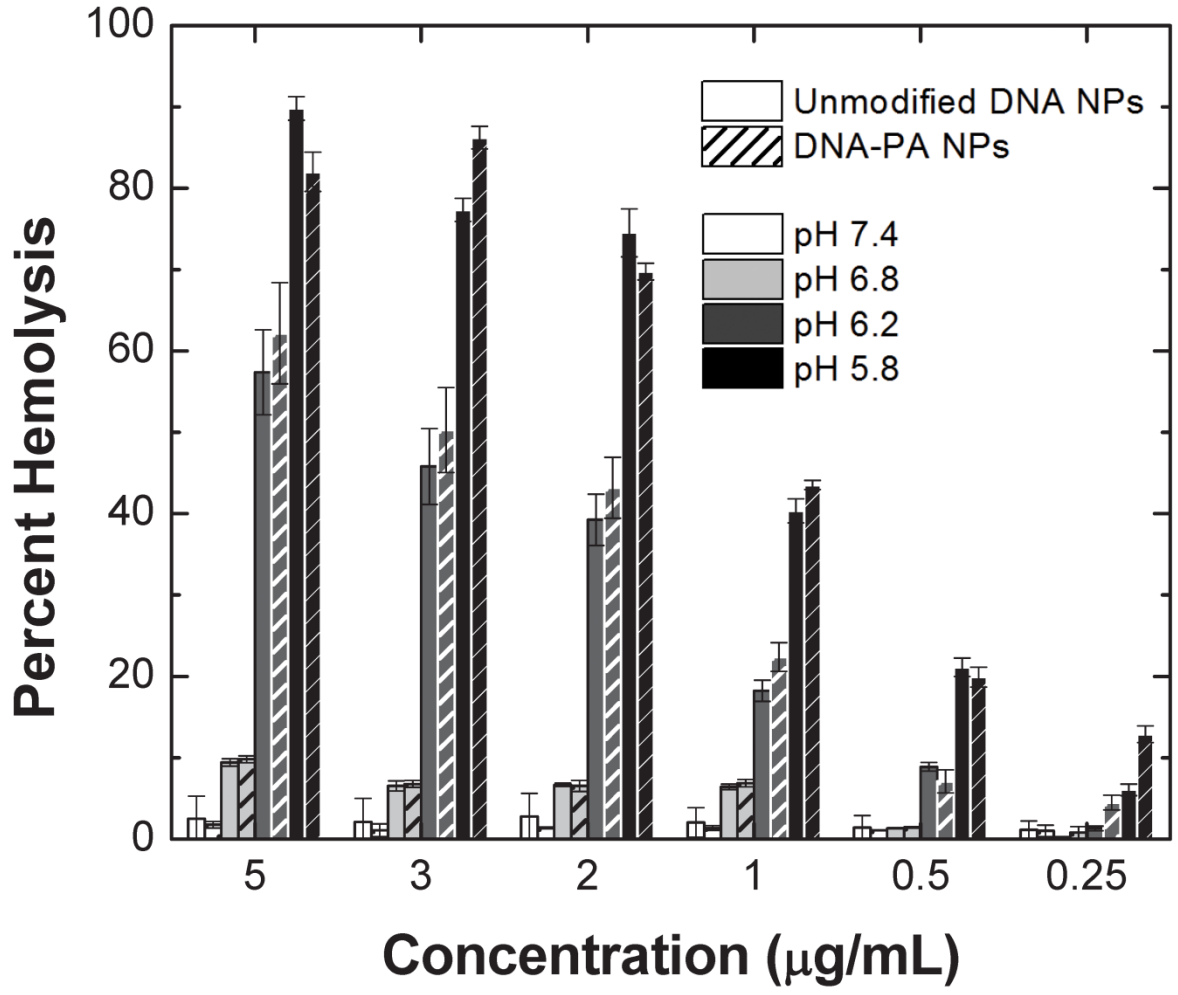

Figure S3.1. DNA vs. DNA-PA NPs showed no significant difference in pH-responsive, membrane-disruptive activity, as determined via red blood cell hemolysis assay.

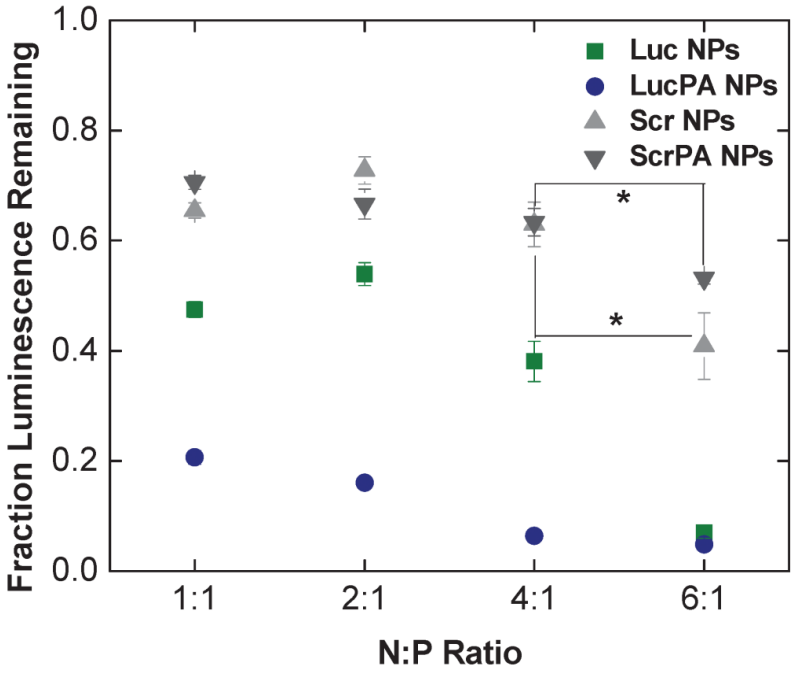

Figure S3.2. Significant increase in cytotoxicity using an N:P ratio of 6:1 vs. 4:1. These studies were done at 40 nM siRNA treatment for 24 hours in NIH-3T3 fibroblasts. Data are normalized to no treatment controls. *p<0.05 for scr, scr-PA NPs at a ratio of 4:1 vs. 6:1.

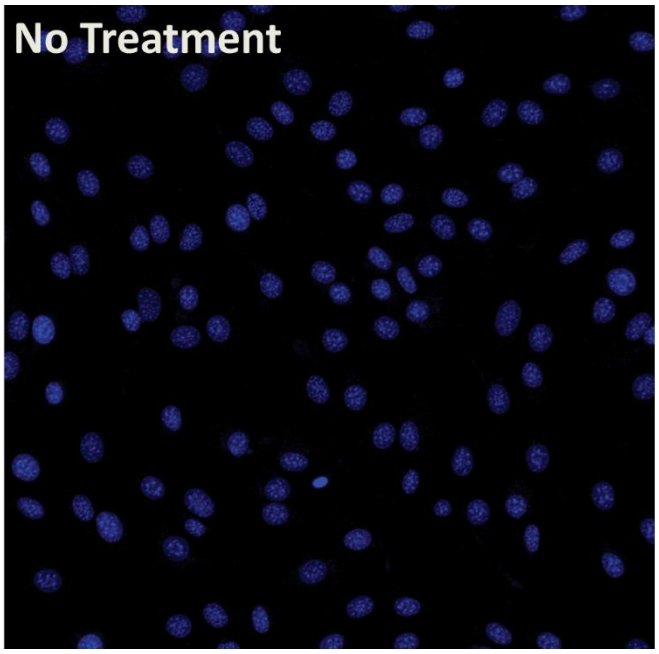

Figure S3.3. No background fluorescence observed in untreated fibroblasts. Shown is an image of untreated fibroblasts using the settings of the reported images showing fluorescence due to DNA NP and DNA-PA NP uptake.

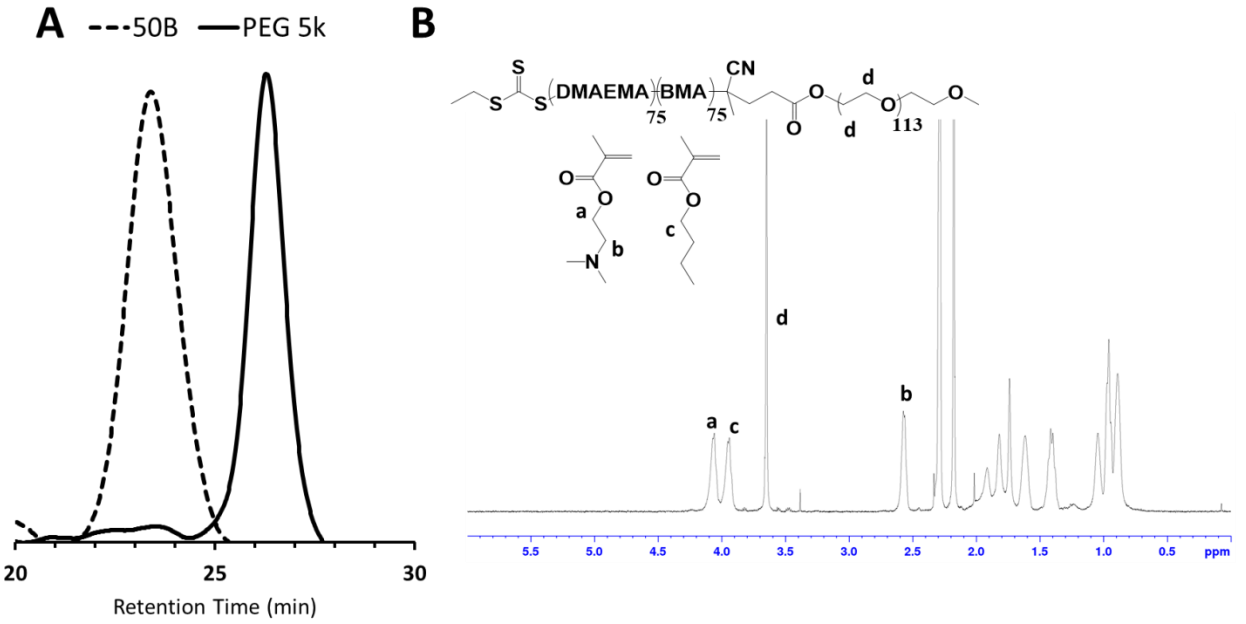

Polymer	RU[a]	%BMA[a]	%DMAEMA[a]	Mn[a]	Mw[b]	PDI[b]
50B	152	49.1	50.9	27800	28060	1.033

Figure S4.1. Characterization of 50B polymer by A) GPC and B) ^{1}H-NMR.

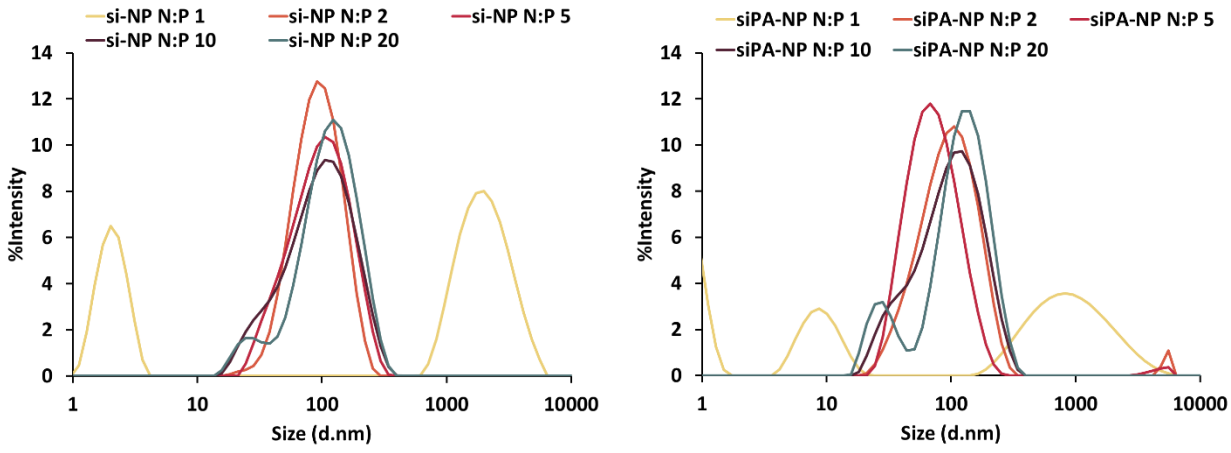

Figure S4.2. DLS size characterization of siPA-NPs vs. si-NPs at a range of N:P ratios.

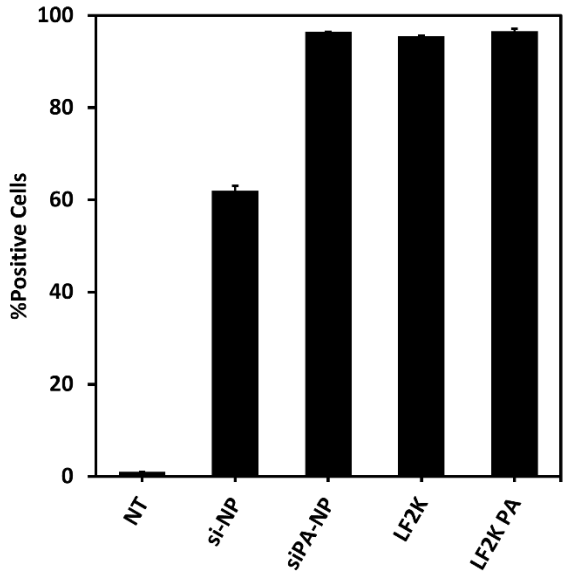

Figure S4.3. Cell internalization of si-NPs and siPA-NPs at N:P = 10:1 plotted as percent positive cells compared to no treatment. Percent positive cells for si-NPs was statistically lower ($p<0.05$) than other treatments groups.

Parameter	Equation
1st Order Model	$C = C_o e^{-k_{el}t}$
$t_{1/2}$	$= \frac{\ln(2)}{k_{el}}$
$AUC_{0\text{-}t}$	$= \int_0^t C\,dt = \frac{C_o e^{-k_{el}t}}{-k_{el}}$
CL	$= \frac{D}{AUC}$

Where, C = Plasma Drug Concentration, C_o = Initial Plasma Drug Concentration, k_{el} = Elimination Constant, t = Time, $t_{1/2}$ = Plasma Half-Life, AUC = Area Under the Curve, CL = Clearance, D = Dose

Table S4.1. Table of pharmacokinetic equations.

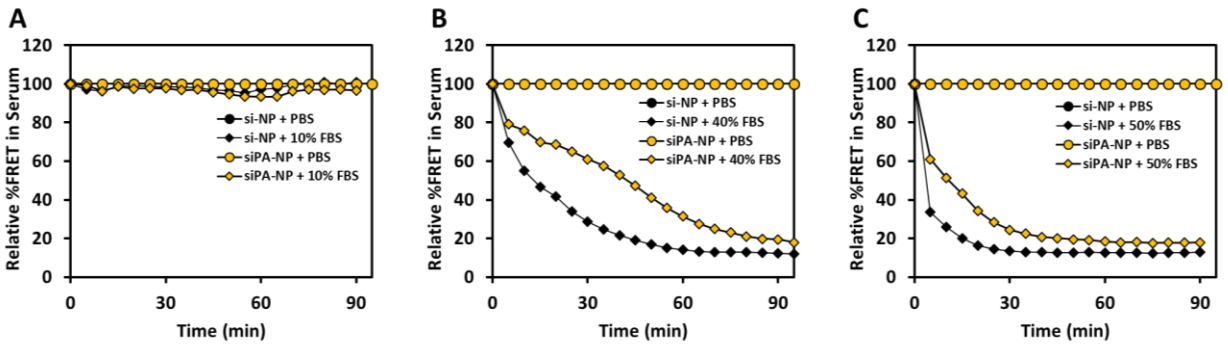

Figure S4.4. Stability of si-NPs and siPA-NPs in (A) 10%, (B) 40%, and (C) 50% fetal bovine serum (FBS) monitored by FRET kinetics.

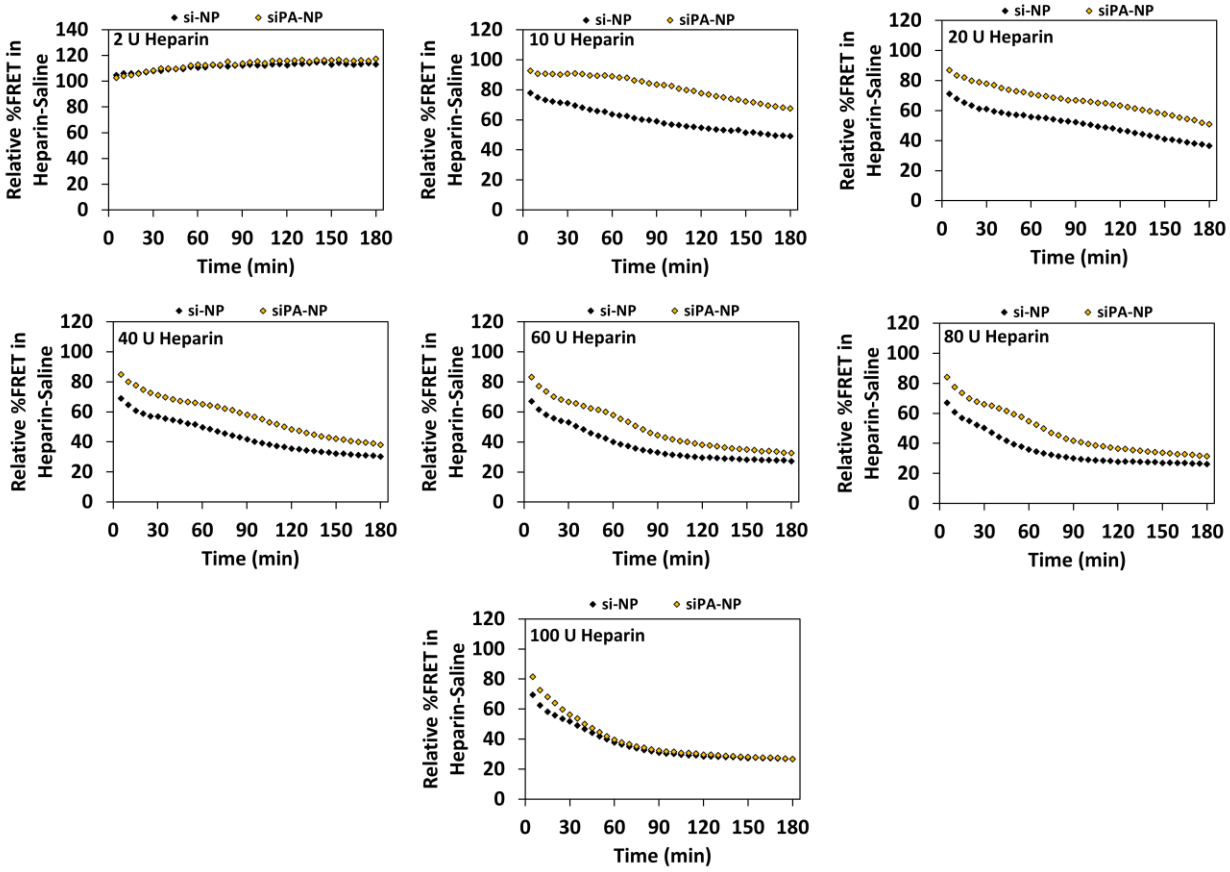

Figure S4.5. Comprehensive panel of FRET-based heparin challenge assay. %FRET signal retained over time after exposure to varying concentrations of heparin saline.

Time (min)	si-NP	siPA-NP
30	73.9	140.6
60	37.0	76.7
90	27.2	50.9
120	22.0	39.9
150	19.1	33.1
180	17.2	28.0

Table S4.2. EC50 values of heparin-dependent si-NP/siPA-NP dissociation as measured by FRET kinetics.

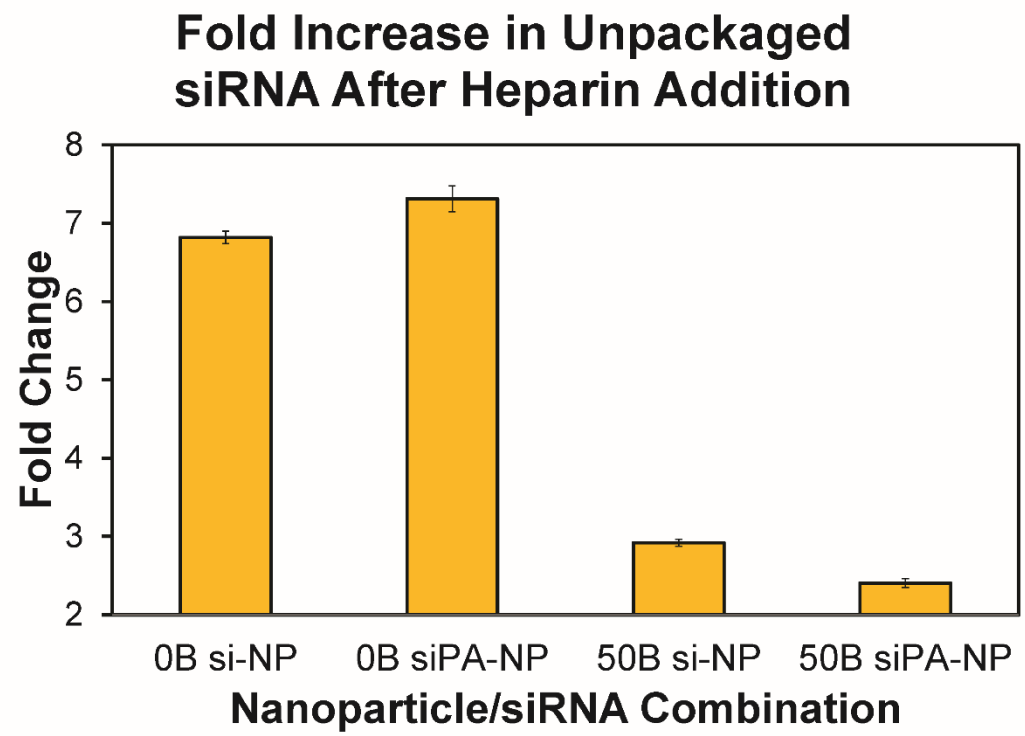

Figure S4.6. PA-modified siRNA contributed to an improvement in stability of 50B polyplexes but not 0B polyplexes. As evaluated by a Ribogreen measure of unpackaged siRNA after 100 U/mL heparin addition and 15 minute incubation time.

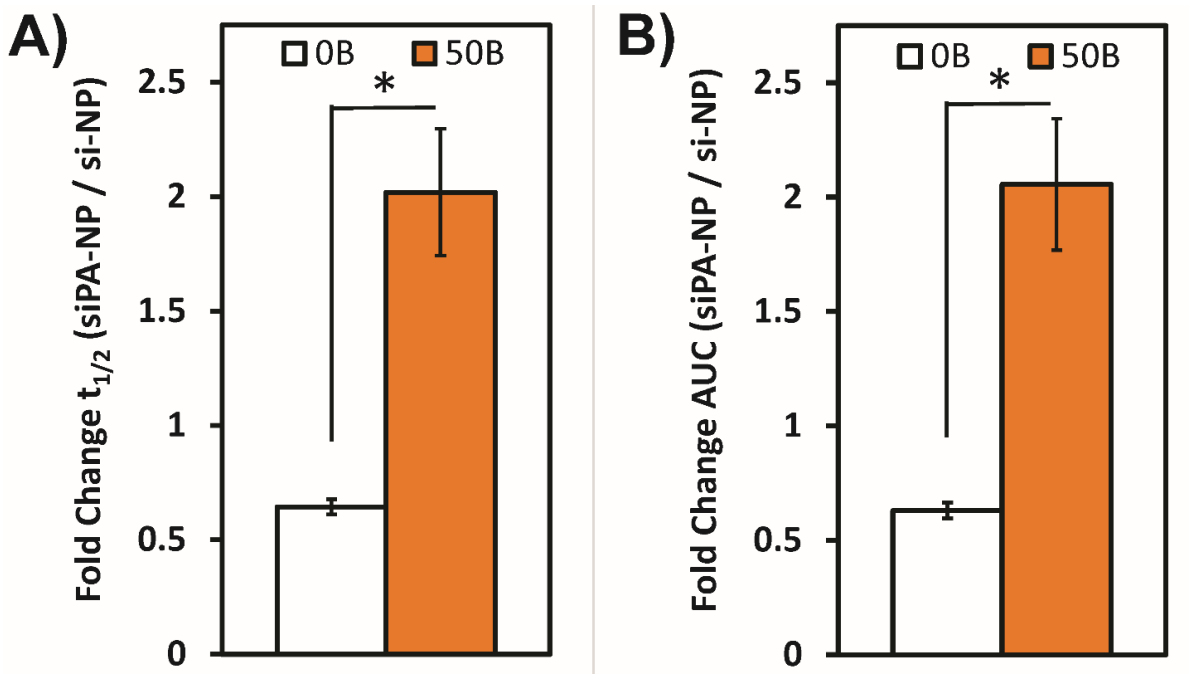

Figure S4.7. Enhanced circulation time depends upon hydrophobic interactions between siPA and polymer NPs. In fully cationic polymer NPs (0B), siPA does not increase A) circulation time half-life or B) area under the curve (AUC) relative to unmodified siRNA, while in 50B NPs an increase in both is observed.

Oligonucleotide	Sequence (5' -> 3')	Source
Alexa488-Sense	GTCAGAAATAGAAACTGGTCATC	IDT
Alexa488-Antisense	[Alexa488]GATGACCAGTTTCTATTTCTGAC	IDT
Alexa546-Sense	GTCAGAAATAGAAACTGGTCATC	IDT
Alexa546-Antisense	[Alexa546]GATGACCAGTTTCTATTTCTGAC	IDT
Cy5-Sense	GTCAGAAATAGAAACTGGTCATC	Sigma
Cy5-Antisense	[Cyanine5]GATGACCAGTTTCTATTTCTGAC	Sigma
Luc-Sense	CAAUUGCACUGAUAAUGAACUCC[dT][dC]	Sigma
Luc-Antisense	GAGGAGUUCA[mU]U[mA]UCAGUGC[mA]A[mU]U[mG][mU][mU]	Sigma
Scr-Sense	CGUUAAUCGCGUAUAAUACGCGU[dA][dT]	Sigma
Scr-Antisense	AUACGCGUAU[mU]A[mU]ACGCGAU[mU]A[mA]C[mG][mA][mC]	Sigma

*Nomenclature: [d] = chiral DNA base, [m] = backbone 2'O-methyl modification

Table S4.3. Table of oligonucleotide sequences.

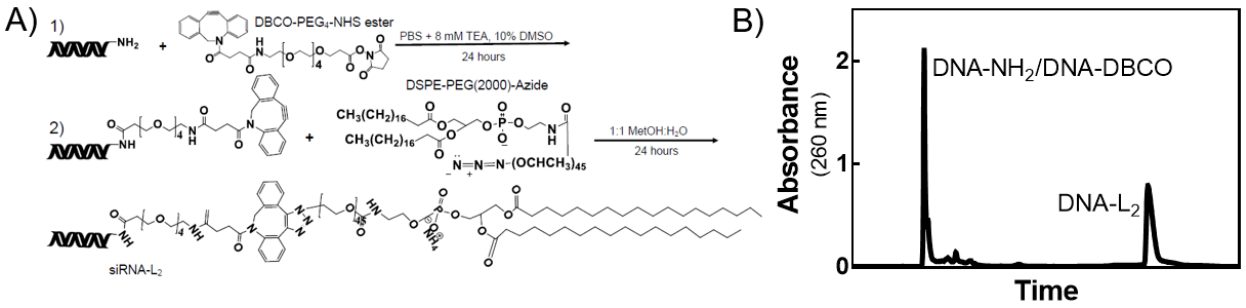

Figure S5.1. A) Full chemical structures of reactants and final product siRNA-L_2. Synthesis scheme is two-step; 1) siRNA-NH_2 + DBCO-PEG_4-NHS ester, 2) siRNA-DBCO + DSPE-PEG(2000)-azide. B) HPLC purification of DNA-L_2 conjugate from reactant precursors.

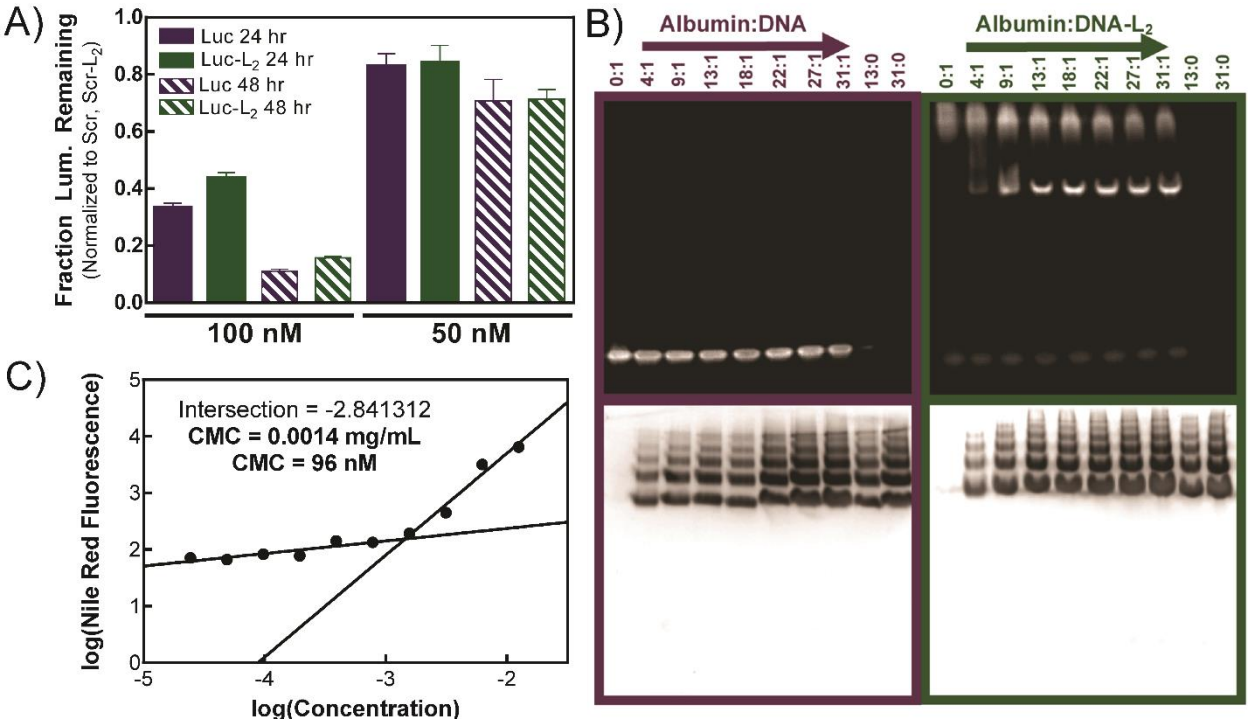

Figure S5.2. A) L_2 conjugation does not impact siRNA silencing efficacy. A comparison of siRNA and siRNA-L_2 silencing from *in vivo* jetPEI at a dose of 100 nM; n of 5, standard error shown. B) Albumin binding of DNA-L_2 as measured by non-denaturing PAGE gel stained for DNA (top) and BSA (bottom). DNA-L_2 migrates as a micellar population alone and co-migrates with albumin. Unmodified siRNA does not migrate with albumin. Molar ratio of albumin:oligo is indicated. C) Critical micelle concentration of siRNA-L_2 as determined via Nile Red assay

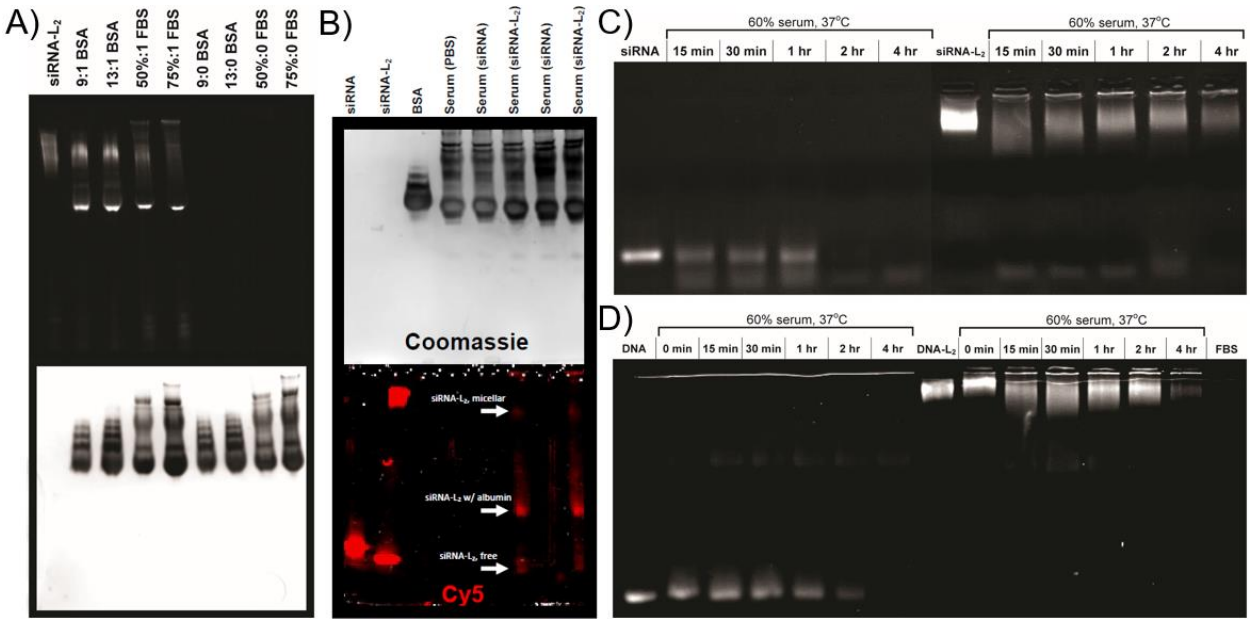

Figure S5.3. A) Evaluation of association of siRNA/siRNA-L_2 with BSA or serum albumin in FBS by PAGE gel retardation assay. siRNA-L_2 alone (far right) migrates as a micellar population. Bound siRNA-L_2 migrates in the same location when mixed with BSA or FBS, suggesting that siRNA-L_2 is associating with the albumin component of FBS. Also shown are protein controls of BSA and FBS (left). B) DNA-L_2 shows association with albumin *in vivo*. Cy5-labeled siRNA-L_2 and siRNA was injected *i.v.* into CD1 mice and blood was collected after 20 minutes. Serum isolated from blood components was evaluated via PAGE gel retardation assay for the presence of Cy5-labeled oligonucleotide. Mice injected with siRNA had no Cy5 signal in the serum, but mice injected with siRNA-L_2 showed faint bands corresponding to the unbound DNA-L_2 and a stronger band corresponding to albumin-bound DNA-L_2. C) siRNA and siRNA-L_2 degrade over time in 60% FBS at 37°C. siRNA-L_2 degrades more slowly than siRNA. D) DNA and DNA-L_2 degrade over time in 60% FBS at 37°C. DNA-L_2 degrades more slowly than DNA.

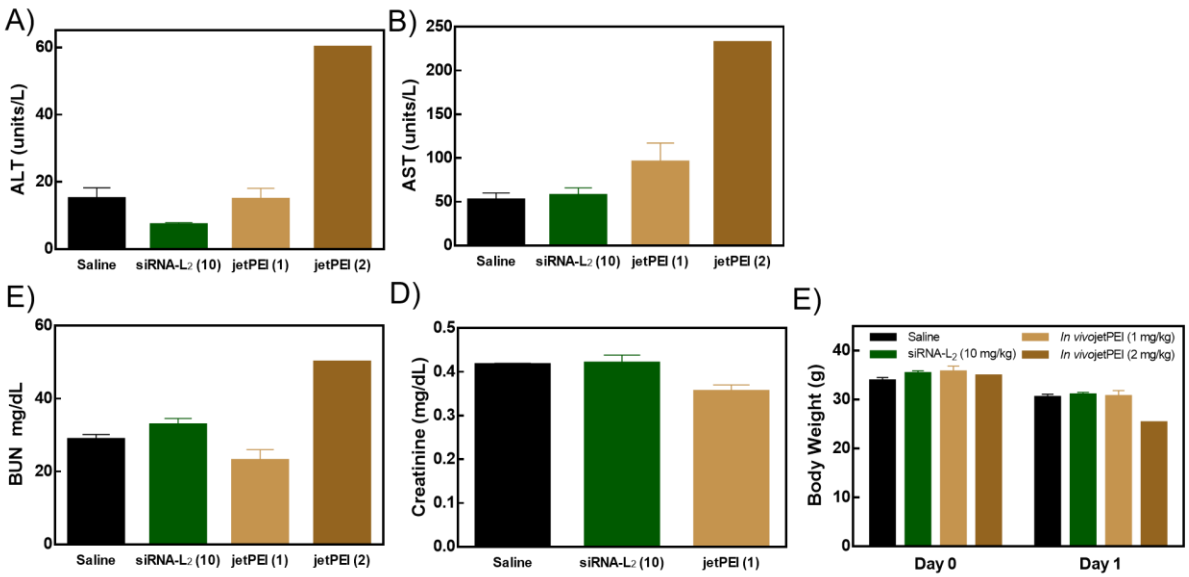

Figure S5.4. Blood chemistry panel and body weight of mice injected with siRNA-L_2 (10 mg/kg) or *in vivo* jetPEI loaded with siRNA (1 mg/kg, 2 mg/kg). A) ALT: alanine aminotransferase; B) AST: aspartate aminotransferase; C) BUN: blood urea nitrogen; D) Creatinine, (reading for *in vivo* jetPEI at 2 mg/kg was not measurable). E) Body weight pre-injection (day 0) and 24 hours post-injection (day 1). n = 4, standard error is plotted. 3 of 4 mice in the 2 mg/kg *in vivo* jetPEI did not survive treatment and could not be included in analysis.

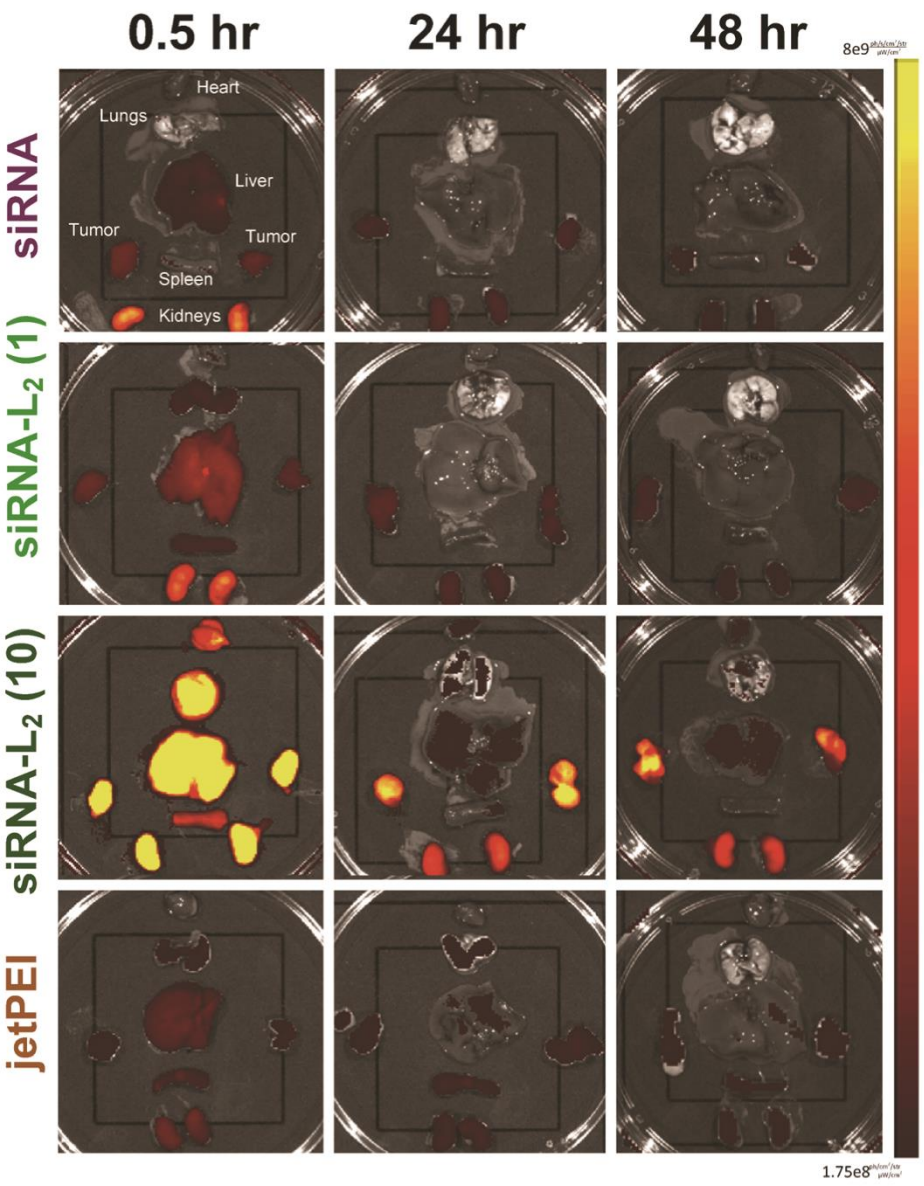

Figure S5.5. Representative images of biodistribution to the organs in orthotopic tumor-bearing mice. siRNA-L_2 was evaluated at 1, 10 mg/kg and jetPEI NPs were evaluated at 1 mg/kg.

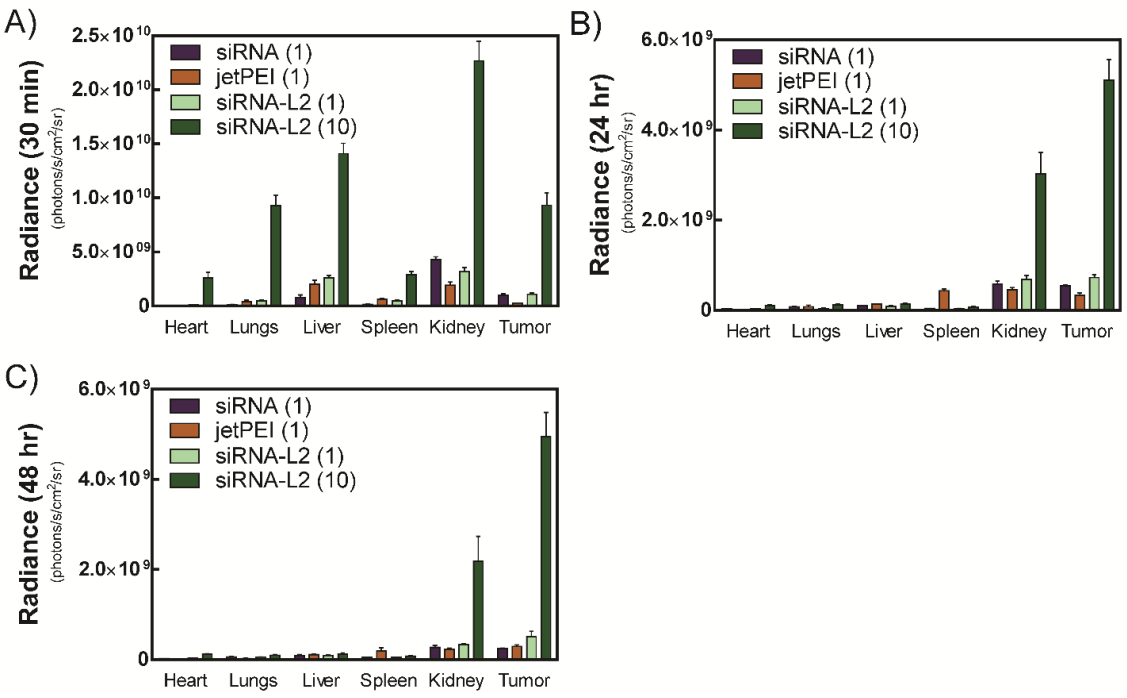

Figure S5.6. In an orthotopic tumor model, absolute radiance per each organ at A) 30 minutes, B) 24 hours, C) 48 hours. n = 4, standard error plotted.

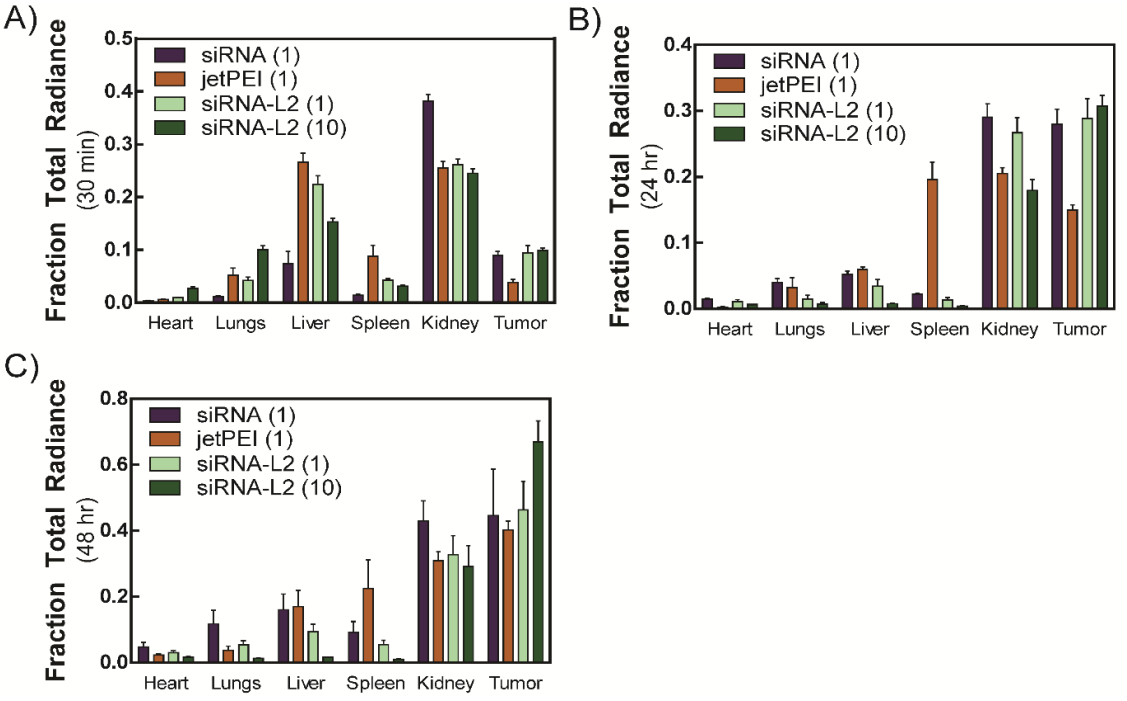

Figure S5.7. In an orthotopic tumor model, fraction of total radiance per each organ at A) 30 minutes, B) 24 hours, C) 48 hours. n = 4, standard error plotted.

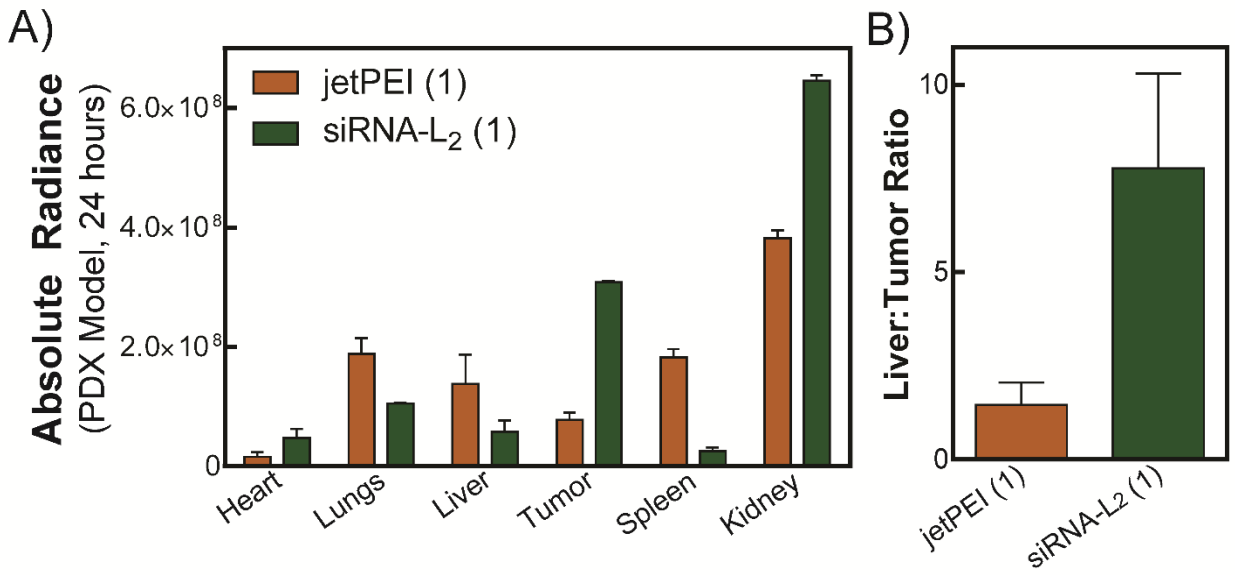

Figure S5.8. In a PDX tumor model, A) absolute radiance per each organ at 24 hours and B) tumor:liver ratio of jetPEI NPs and siRNA-L_2 in a PDX tumor model after intravenous injection at 1 mg/kg. n = 2, standard error plotted.

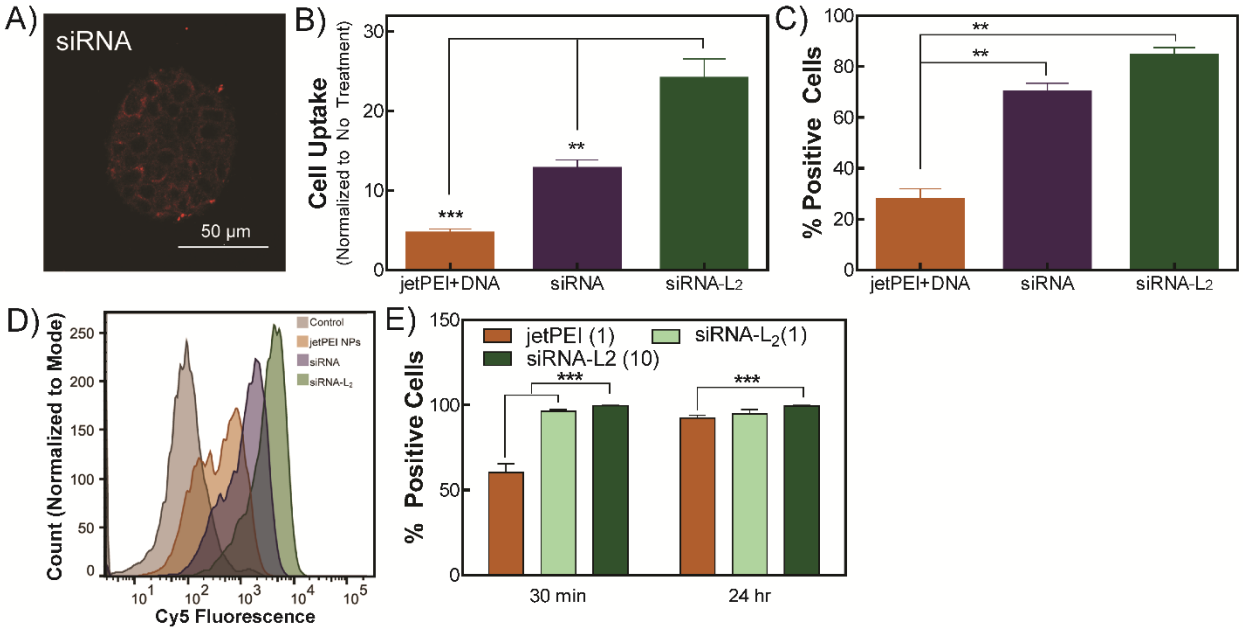

Figure S5.9. A) Representative image of tumor spheroid uptake for siRNA. B) **C**ellular uptake, as evaluated by flow cytometry, of MCF-7 breast cancer cells grown in tumor spheroids. Data are expressed as fold increase in fluorescence relative to untreated cells. Treatment with *in vivo* jetPEI complexes resulted in significantly less uptake

than siRNA, while siRNA-L_2 achieved the highest uptake. C) Percentage positive cells, as evaluated by flow cytometry, of MCF-7 breast cancer cells grown in tumor spheroids. Treatment with *in vivo* jetPEI complexes resulted in significantly fewer positive cells than siRNA and siRNA-L_2, consistent with its poor penetration into the interior of the tumor spheroids. D) Representative histograms of flow cytometric evaluation of Cy5-labeled siRNA uptake by MCF-7 breast cancer cells grown in tumor spheroids. E) Percentage positive cells in tumor cells isolated from orthotopic xenograft mouse tumors. n = 6 to 8. n = 3, standard error plotted; ** = $p<0.01$, ***=$p<0.001$.

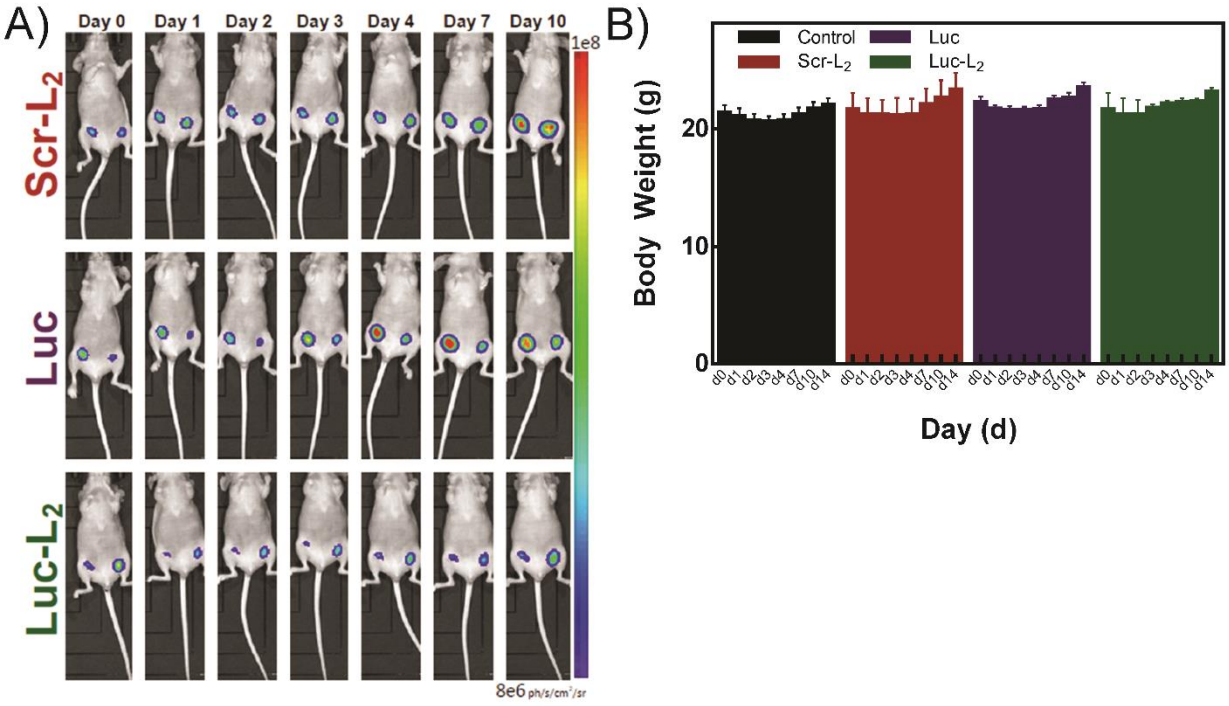

Figure S5.10. Mice with orthotopic luciferase-expressing tumors were treated at 10 mg/kg on day 0 and 1. A) Representative images of tumor luminescence in mice. B) Mouse body weight; body weight is consistent across treatment groups over the course of the experiment. n = 5, standard error is plotted.

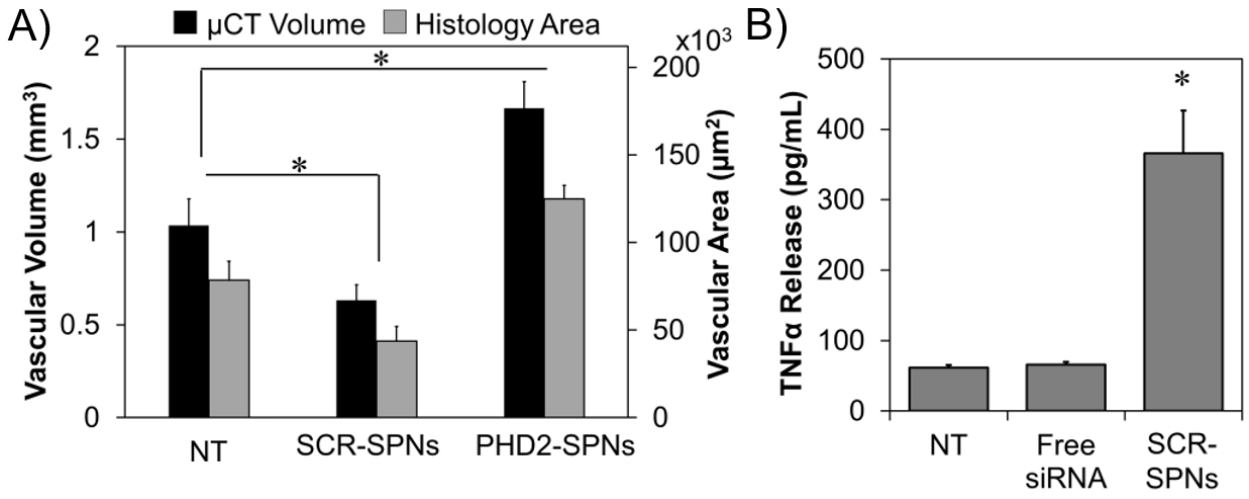

Figure S6.1. siRNA-loaded polymer nanoparticles (SPNs) induce an inflammatory response and impede revascularization. A) While SPNs designed against PHD2 promote higher vascular volume in scaffolds implanted subcutaneously in mice, SPNs with a control, scrambled siRNA sequence negatively effect vascularization. B) Control, scrambled SPNs induce production of inflammatory cytokine TNF-α *in vitro*.

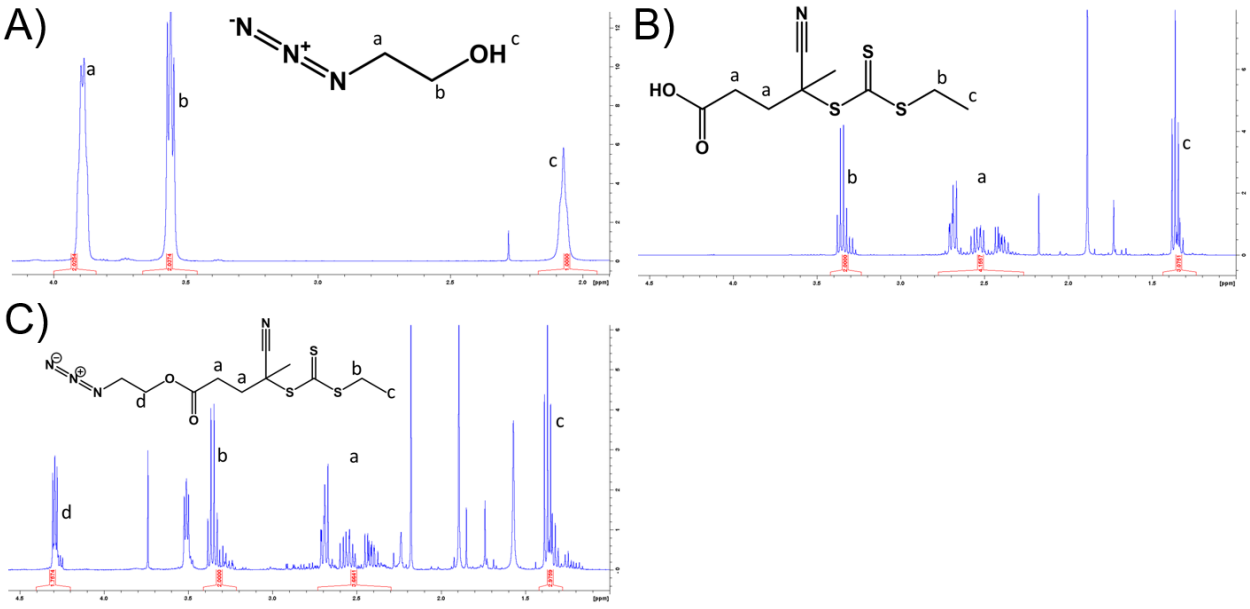

Figure S6.2. Confirmation of synthesis of azide-functionalized RAFT CTA. A) NMR spectrum of precursor azidoethanol. B) NMR spectrum of unmodified RAFT CTA, ECT. C) NMR spectrum of ECT-azide, synthesized via hydroxyl to carboxylic acid coupling of azidoethanol and ECT.

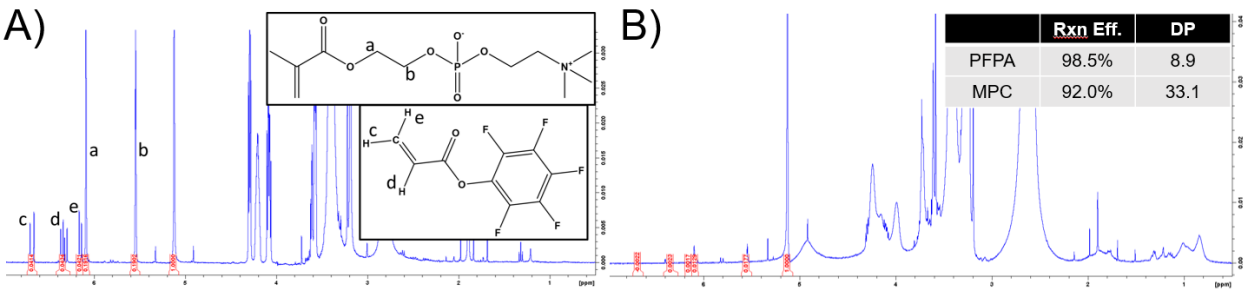

Figure S6.3. NMR spectra pre-RAFT polymerization (A) and post-polymerization (B) of azide-functionalized CTA with MPC and PFPA. Monomer peaks were normalized to trioxane (5.2 ppm) and the disappearance of monomer peaks was used to calculate reaction efficiency.

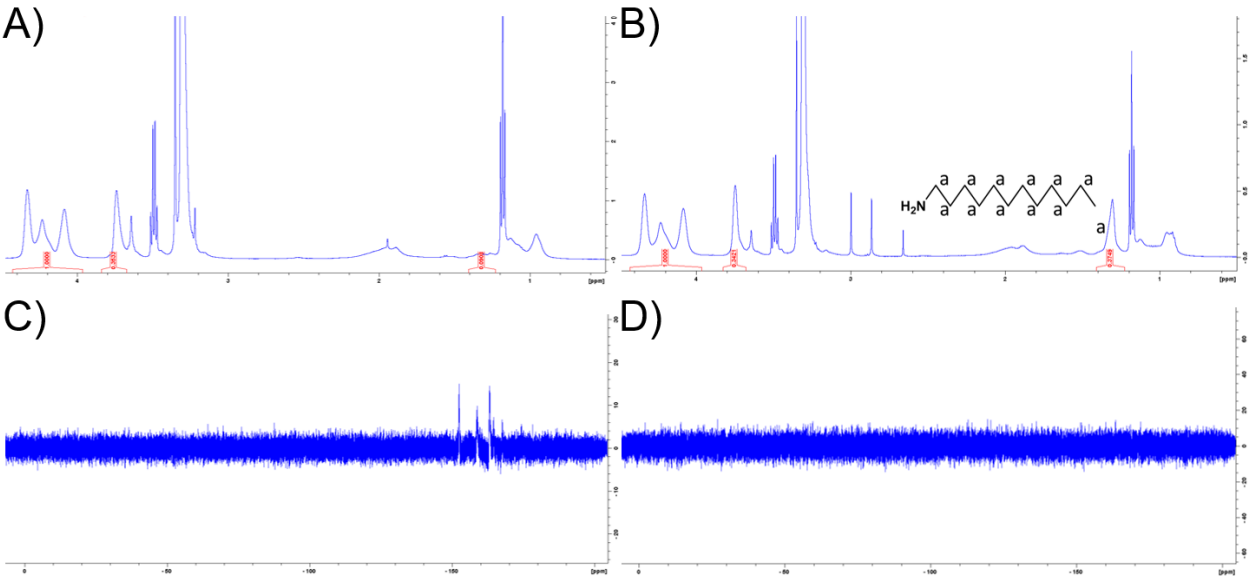

Figure S6.4. NMR spectra confirming modification of azide-functionalized co-polymer of MPC and PFPA with dodecylamine. The original polymer is characterized by H NMR (A) and F NMR (C). The fluorine peaks in C) correspond to the PFPA group. Post-reaction with dodecylamine, the polymer characterized by H NMR (B) shows appearance of a peak corresponding to the 12-carbon backbone. Characterized by F NMR (D), the disappearance of the fluorine peaks indicates expected disappearance of the PFPA moieties.

B. Protocols

Synthesis and validation of siRNA-PA:

1. Prepare palmitic acid *N*-hydroxysuccinimide ester (PA-NHS; stored dry for stability) solution at 10 mM in *N*,*N*-dimethylformamide (DMF; final concentration will be 1 mM in reaction)
2. Dilute siRNA-NH_2 to 10 μM in 50% water, 50% isopropyl alcohol
3. Add PA-NHS solution to the siRNA-NH_2 solution in a volume $1/10^{th}$ that of the total volume of the siRNA-NH_2 solution
    a. Solution may be cloudy

- Add diisopropylethyl amine (DIEA) in a volume $1/100^{th}$ of the total reaction volume

4. Incubate at room temperature overnight
5. Prepare PA solution at 10 mM in DMF (final concentration will be 1 mM in reaction)
6. Add PA solution to the reaction solution in a volume $1/10^{th}$ that of the total volume of the reaction solution
7. Incubate at room temperature overnight
8. Prepare PA solution at 10 mM in DMF (final concentration will be 1 mM in reaction)
9. Add PA solution to the reaction solution in a volume $1/10^{th}$ that of the total volume of the reaction solution
10. Incubate at room temperature overnight
11. Dilute the reaction mixture such that it is less than 10% of the total solution volume in water
12. Spin down at maximum centrifuge speed, preferably at 4^oC, for 5 minutes

13. Take the supernatant and discard the PA collected at the bottom of the tube
14. Run the supernatant through NAP-25 columns **twice**
15. Lyophilize the eluent
16. Measure yield of the siRNA-PA based on absorbance at 260 nm
17. Check for elimination of PA and complete reaction by running a small sample (~10 nmols) on HPLC using the below conditions:
    a. Aqueous mobile phase of 50 mM triethylammonium acetate in water
    b. Organic mobile phase of methanol
    c. Clarity Oligo-RP column
    d. 95% to 0% aqueous phase gradient over 30 minutes
    e. siRNA-PA should elute in a single broad peak between 20-30 minutes; excess PA elutes immediately and siRNA-NH_2 elutes around 14 minutes
18. Verify siRNA-PA purity on MALDI using a matrix of 3-hydroxypicolinic acid in 50% water, 50% acetonitrile with 5 mg/mL ammonium citrate
    a. Spot sample onto the MALDI grid, let it dry completely, and then spot matrix on top and let it dry completely
    b. Molecular weight should be ~7,500

Formation of siRNA-PA NPs using DMAEMA-*b*-DMAEMA-co-PAA-co-BMA:

1. Dissolve polymer (DMAEMA-b-DMAEMA-co-PAA-co-BMA) in a minimal amount of 100% ethanol
    a. Approximately 10 μL ethanol per 1 mg polymer
    b. Ensure complete dissolution by allowing polymer to sit in ethanol for at least 2 hours

2. Add PBS or water at 8 mL/hr using a syringe pump to form nanoparticles
    a. A typical concentration is 1 mg/mL
3. Filter nanoparticle solution using a 0.2 μm sterile filter
4. Spot siRNA-PA in water at 100 μM in an RNAse-free tube
5. Add nanoparticles such that the ratio of positive charge on the polymer (N) to negative charge on the siRNA (P) is at the desired value
6. Allow nanoparticles to condense with siRNA-PA for 30 minutes

Formation of siPA-NPs using PEG-*b*-DMAEMA-co-BMA (50B):

1. Dissolve 50B in a minimal amount of 100% ethanol
    a. Approximately 10 μL ethanol per 1 mg polymer
    b. Ensure complete dissolution by allowing polymer to sit in ethanol for at least 2 hours
2. Dilute 50B to a stock solution of 3.33 mg/mL polymer in 10 mM pH 4.0 phosphate buffer
3. Filter 50B solution using a 0.2 μm sterile filter
4. Spot siRNA-PA in water at 100 μM in an RNAse-free tube
5. Add 50B stock solution such that the ratio of positive charge on the polymer (N) to negative charge on the siRNA (P) is at the desired value
6. Allow polymer to condense with siRNA-PA for 30 minutes
7. Dilute siRNA-PA/50B solution five-fold with10 mM pH 8.0 phosphate buffer to adjust the final pH to 7.4 and form nanoparticles

Synthesis and validation of siRNA-L_2:

1. Dissolve dibenzocyclooctyne-PEG_4-N-hydroxysuccinimidyl ester (DBCO-PEG_4-NHS)) pre-dissolved at 25 mM in dimethyl sulfoxide (DMSO)
2. Dissolve lyophilized siRNA-NH_2 at 1 mM in PBS with 8 mM triethylamine (TEA)
3. Add 30% of the final total solution volume of DBCO-PEG_4-NHS solution in DMSO to the siRNA-NH_2 solution
4. Incubate overnight at room temperature
5. Dilute the reaction at least three-fold in water
6. Filter through NAP-25 columns **twice**
7. Lyophilize the eluent
8. Dissolve lyophilized siRNA-DBCO in water at 200 μM
9. Dissolve DSPE-PEG_{2000}-azide at in methanol at 1 mM
10. Add an equivalent volume of DSPE-PEG_{2000}-azide solution to siRNA-DBCO solution
11. React for 24 hours
12. Add at least 0.5-fold the total reaction volume of water to the reaction solution
13. Filter through a NAP-25 column
14. Purify with reverse-phase HPLC using the following conditions:
    a. Aqueous mobile phase of 50 mM triethylammonium acetate in water
    b. Organic mobile phase of methanol
    c. Clarity Oligo-RP column
        i. Ensure column is clean and a guard column is clean and in place
    d. 95% to 25% aqueous phase gradient over 10 minutes followed by 25% to 0% over 20 minutes

e. siRNA-L_2 should elute in a single broad peak between 25-30 minutes
    i. The micellar nature of siRNA-L_2 can complicate purification; it will "stick" in the column
    ii. This can typically be remedied by repetitive runs from 10% to 0% aqueous phase, throughout which the siRNA-L_2 elutes in "waves"

15. Collect HPLC fractions corresponding to siRNA-L_2
16. Rotovap and lyophilize fractions
17. Measure yield of the siRNA-PA based on absorbance at 260 nm
18. Verify siRNA-L_2 purity on MALDI using a matrix of 3-hydroxypicolinic acid in 50% water, 50% acetonitrile with 5 mg/mL ammonium citrate
    a. Spot sample onto the MALDI grid, let it dry completely, and then spot matrix on top and let it dry completely
    b. Molecular weight should be ~10,000

REFERENCES

1. Matranga C, Tomari Y, Shin C, Bartel DP, Zamore PD. Passenger-strand cleavage facilitates assembly of sirna into ago2-containing rnai enzyme complexes. *Cell*. 2005;123:607-620

2. Dykxhoorn DM, Palliser D, Lieberman J. The silent treatment: Sirnas as small molecule drugs. *Gene therapy*. 2006;13:541-552

3. Brem H, Tomic-Canic M. Cellular and molecular basis of wound healing in diabetes. *The Journal of clinical investigation*. 2007;117:1219-1222

4. Menke NB, Ward KR, Witten TM, Bonchev DG, Diegelmann RF. Impaired wound healing. *Clinics in dermatology*. 2007;25:19-25

5. Davidson JM. Animal models for wound repair. *Arch Dermatol Res*. 1998;290

6. Hammond PT. Shooting for the moon: Nanoscale approaches to cancer. *ACS nano*. 2016;10:1711-1713

7. Judge AD RM, Tavakoli I, Levi J, Hu L, Fronda A, Ambegia E, McClintock K, and MacLachlan I. Confirming the rnai-mediated mechanism of action of sirna-based cancer therapeutics in mice. *The Journal of clinical investigation*. 2009;119

8. Carthew RW, Sontheimer EJ. Origins and mechanisms of mirnas and sirnas. *Cell*. 2009;136:642-655

9. Yao Y, Wang C, Varshney RR, Wang DA. Antisense makes sense in engineered regenerative medicine. *Pharmaceut Res*. 2009;26:263-275

10. Sliva K, Schnierle BS. Selective gene silencing by viral delivery of short hairpin rna. *Virology journal*. 2010;7:248

11. Bartlett DW, Davis ME. Insights into the kinetics of sirna-mediated gene silencing from live-cell and live-animal bioluminescent imaging. *Nucleic Acids Res*. 2006;34:322-333

12. Wang J, Lu Z, Wientjes MG, Au JL. Delivery of sirna therapeutics: Barriers and carriers. *The AAPS journal*. 2010;12:492-503

13. Akhtar S, Benter I. Toxicogenomics of non-viral drug delivery systems for rnai: Potential impact on sirna-mediated gene silencing activity and specificity. *Advanced drug delivery reviews*. 2007;59:164-182

14. Whitehead KA, Langer R, Anderson DG. Knocking down barriers: Advances in sirna delivery. *Nature reviews. Drug discovery*. 2009;8:129-138

15. Murthy N, Campbell J, Fausto N, Hoffman AS, Stayton PS. Design and synthesis of ph-responsive polymeric carriers that target uptake and enhance the intracellular delivery of oligonucleotides. *Journal of Controlled Release*. 2003;89:365-374

16. Ernsting MJ, Murakami M, Roy A, Li SD. Factors controlling the pharmacokinetics, biodistribution and intratumoral penetration of nanoparticles. *Journal of controlled release : official journal of the Controlled Release Society*. 2013;172:782-794

17. Ozpolat B, Sood AK, Lopez-Berestein G. Liposomal sirna nanocarriers for cancer therapy. *Advanced drug delivery reviews*. 2014;66:110-116

18. Zuckerman JE, Choi CH, Han H, Davis ME. Polycation-sirna nanoparticles can disassemble at the kidney glomerular basement membrane. *Proceedings of the National Academy of Sciences of the United States of America*. 2012;109:3137-3142

19. Falamarzian A, Aliabadi HM, Molavi O, Seubert JM, Lai R, Uludag H, Lavasanifar A. Effective down-regulation of signal transducer and activator of transcription 3 (stat3) by polyplexes of sirna and lipid-substituted polyethyleneimine for sensitization of breast tumor cells to conventional chemotherapy. *Journal of biomedical materials research. Part A*. 2014;102:3216-3228

20. Kim J, Sunshine, J. C., Green, J. J. Differential polymer structure tunes mechanism of cellular uptake and transfection routes of poly(β-amino ester) polyplexes in human breast cancer cells. *Bioconjugate chemistry*. 2014;25

21. Nelson CE, Kintzing, R. J., Hanna, A., Shannon, J. M., Gupta, M. K., Duvall, C. L. Balancing cationic and hydrophobic content of pegylated sirna polyplexes enhances endosome escape, stability, blood circulation time, and bioactivity in vivo. *ACS Nano*. 2013;7:8870-8880

22. Oe Y, Christie RJ, Naito M, Low SA, Fukushima S, Toh K, Miura Y, Matsumoto Y, Nishiyama N, Miyata K, Kataoka K. Actively-targeted polyion complex micelles stabilized by cholesterol and disulfide cross-linking for systemic delivery of sirna to solid tumors. *Biomaterials*. 2014;35:7887-7895

23. Ambardekar VV, Han HY, Varney ML, Vinogradov SV, Singh RK, Vetro JA. The modification of sirna with 3' cholesterol to increase nuclease protection and suppression of native mrna by select sirna polyplexes. *Biomaterials*. 2011;32:1404-1411

24. Nishina K, Unno T, Uno Y, Kubodera T, Kanouchi T, Mizusawa H, Yokota T. Efficient in vivo delivery of sirna to the liver by conjugation of alpha-tocopherol. *Molecular therapy : the journal of the American Society of Gene Therapy*. 2008;16:734-740

25. Kubo T, Takei Y, Mihara K, Yanagihara K, Seyama T. Amino-modified and lipid-conjugated dicer-substrate sirna enhances rnai efficacy. *Bioconjugate chemistry*. 2012;23:164-173

26. Kubo T, Yanagihara K, Sato Y, Nishimura Y, Kondo S, Seyama T. Gene-silencing potency of symmetric and asymmetric lipid-conjugated sirnas and its correlation with dicer recognition. *Bioconjugate chemistry*. 2013;24:2045-2057

27. Wolfrum C, Shi S, Jayaprakash KN, Jayaraman M, Wang G, Pandey RK, Rajeev KG, Nakayama T, Charrise K, Ndungo EM, Zimmermann T, Koteliansky V, Manoharan M, Stoffel M. Mechanisms and optimization of in vivo delivery of lipophilic sirnas. *Nature biotechnology*. 2007;25:1149-1157

28. Soutschek J, Akinc, A., Bramlage, B., Charisse, K., Constien, R., Donoghue, M., Elbashir, S., Geick, A., Hadwiger, P., Harborth, J., John, M., Kesavan, K., Lavine, G., Pandey, R. K., Racie, T.,, Rajeev KG, Rohl, I., Toudjarska, I., Wang, G., Wuschko, S., Bumcrot, D., Koteliansky, V., Limmer, S., Manoharan, M., Vornlocher, H. Therapeutic silencing of an endogenous gene by systemic administration of modified sirnas. *Nature*. 2004;432

29. Kubo T, Yanagihara K, Takei Y, Mihara K, Sato Y, Seyama T. Sirnas conjugated with aromatic compounds induce risc-mediated antisense strand selection and strong gene-silencing activity. *Biochemical and biophysical research communications*. 2012;426:571-577

30. Kubo T, Yanagihara K, Takei Y, Mihara K, Sato Y, Seyama T. Lipid-conjugated 27-nucleotide double-stranded rnas with dicer-substrate potency enhance rnai-mediated gene silencing. *Molecular pharmaceutics*. 2012;9:1374-1383

31. Kratz F. Albumin as a drug carrier: Design of prodrugs, drug conjugates and nanoparticles. *Journal of controlled release : official journal of the Controlled Release Society*. 2008;132:171-183

32. Cohen JL CJ, Segar DS, Gillam LD, Gottdiener JS, Hausnerova E, Bruns DE. Improved left ventricular endocardial border delineation and opacification with optison (fs069), a new echocardiographic contrast agent. *Journal of the American College of Cardiology*. 1998;32

33. Neumann E, Frei E, Funk D, Becker MD, Schrenk HH, Muller-Ladner U, Fiehn C. Native albumin for targeted drug delivery. *Expert opinion on drug delivery*. 2010;7:915-925

34. Napoli C LC, Jorgensen R. Lntroduction of a chimeric chalcone synthase gene into petunia results in reversible co-suppression of homologous genes ín trans. *The Plant Cell*. 1990;2

35. Bertrand J, Pottier, M., Vekris, A., Opolon, P., Maksimenko, A., Malvy, C. Comparison of antisense oligonucleotides and sirnas in cell culture and in vivo. *Biochem Biophys Res Commun*. 2002;296

36. Kim DH, Behlke MA, Rose SD, Chang MS, Choi S, Rossi JJ. Synthetic dsrna dicer substrates enhance rnai potency and efficacy. *Nat Biotechnol*. 2005;23:222-226

37. Baker BF. 2'-o-(2-methoxy)ethyl-modified anti-intercellular adhesion molecule 1 (icam-1) oligonucleotides selectively increase the icam-1 mrna level and inhibit formation of the icam-1 translation initiation complex in human umbilical vein endothelial cells. *Journal of Biological Chemistry*. 1997;272:11994-12000

38. Hammond SM, Bernstein, E., Beach, D., Hannon, G. J. An rna-directed nuclease mediates post-transcriptional gene silencing in drosophila cells. *Nature*. 2000;404

39. Bernstein E, Caudy, A. A., Hammond, S. M., Hannon, G. J. Role for a bidentate ribonuclease in the initiation step of rna interference. *Nature*. 2001;409

40. Zamore PD HB. Ribo-gnome: The big world of small rnas. *Science*. 2005;309

41. Haley B, Zamore PD. Kinetic analysis of the rnai enzyme complex. *Nature structural & molecular biology*. 2004;11:599-606

42. Beavers KR, Nelson CE, Duvall CL. Mirna inhibition in tissue engineering and regenerative medicine. *Advanced drug delivery reviews*. 2014

43. Haussecker D. Current issues of rnai therapeutics delivery and development. *Journal of controlled release : official journal of the Controlled Release Society*. 2014;195:49-54

44. Haussecker D. The business of rnai therapeutics in 2012. *Molecular therapy. Nucleic acids*. 2012;1:e8

45. Behlke MA. Chemical modification of sirnas for in vivo use. *Oligonucleotides*. 2008;18:305-319

46. Martinez J, Patkaniowska, A., Urlaub, H., Luhrmann, R., Tuschl, T. Single-stranded antisense sirnas guide target rna cleavage in rnai. *Cell*. 2004;110

47. Gilleron J, Querbes W, Zeigerer A, Borodovsky A, Marsico G, Schubert U, Manygoats K, Seifert S, Andree C, Stoter M, Epstein-Barash H, Zhang L, Koteliansky V, Fitzgerald K, Fava E, Bickle M, Kalaidzidis Y, Akinc A, Maier M, Zerial M. Image-based analysis of lipid nanoparticle-mediated sirna delivery, intracellular trafficking and endosomal escape. *Nature biotechnology*. 2013;31:638-646

48. Elbashir SM, Harborth, J., Lendeckel, W., Yalcin, A., Weber, K., Tuschl, T. Duplexes of 21-nucleotide rnas mediate rna interference in cultured mammalian cells. *Nature*. 2001;411

49. Kariko K, Bhuyan P, Capodici J, Weissman D. Small interfering rnas mediate sequence-independent gene suppression and induce immune activation by signaling through toll-like receptor 3. *The Journal of Immunology*. 2004;172:6545-6549

50. Heil F, Hemmi, H., Hochrein, H., Ampenberger, F., Kirschning, C., Akira, S., Lipford, G., Wagner, H., Bauer, S. Species-specific recognition of single-stranded rna via toll-like receptor 7 and 8. *Science*. 2004;303

51. Jackson AL, Linsley PS. Recognizing and avoiding sirna off-target effects for target identification and therapeutic application. *Nature reviews. Drug discovery*. 2010;9:57-67

52. Zuckerman JE, Gritli I, Tolcher A, Heidel JD, Lim D, Morgan R, Chmielowski B, Ribas A, Davis ME, Yen Y. Correlating animal and human phase ia/ib clinical data with calaa-01, a targeted, polymer-based nanoparticle containing sirna. *Proceedings of the National Academy of Sciences of the United States of America*. 2014;111:11449-11454

53. Yi R, Doehle BP, Qin Y, Macara IG, Cullen BR. Overexpression of exportin 5 enhances rna interference mediated by short hairpin rnas and microrna s. *Rna*. 2005;11:220-226

54. Jackson AL, Bartz, S. R., Schelter, J., Kobayashi, S. V., Burchard, J., Mao, M., Li, B., Cavet, G., Linsley, P. S. Expression profiling reveals off-target gene regulation by rnai. *Nat Biotechnol*. 2003

55. Kleinman ME, Yamada K, Takeda A, Chandrasekaran V, Nozaki M, Baffi JZ, Albuquerque RJ, Yamasaki S, Itaya M, Pan Y, Appukuttan B, Gibbs D, Yang Z, Kariko K, Ambati BK, Wilgus TA, DiPietro LA, Sakurai E, Zhang K, Smith JR, Taylor EW, Ambati J. Sequence- and target-independent angiogenesis suppression by sirna via tlr3. *Nature*. 2008;452:591-597

56. Amarzguioui M, Holen, T., Babaie, E., Prydz, H. Tolerance for mutations and chemical modications in a sirna. *Nucleic Acids Research*. 2003;31

57. Braasch DA, Jensen, S., Liu, Y., Kaur, K., Arar, K., White, M. A., Corey, D. R. Rna interference in mammalian cells by chemically-modified rna. *Biochemistry*. 2003;42

58. Judge A, MacLachlan I. Overcoming the innate immune response to small interfering rna. *Human gene therapy*. 2008;19:111-124

59. Chiu YL. Sirna function in rnai: A chemical modification analysis. *Rna*. 2003;9:1034-1048

60. Kanasty R, Dorkin, J.R., Vegas, A., and Anderson, D. Delivery materials for sirna therapeutics. *Nature Materials*. 2013;12

61. Lee H L-JA, Chen Y., Love KT, Park AI, Karagiannis ED, Sehgal A, Querbes W, Zurenko CS, Jayaraman M, Peng CG, Charisse K, Borodovsky A, Manoharan M, Donahoe JS, Truelove J, Nahrendorf M, Langer R, Anderson DG. Molecularly self-assembled nucleic acid nanoparticles for targeted in vivo sirna delivery. *Nature Nanotechnology*. 2012;7

62. Shen C, Buck AK, Liu X, Winkler M, Reske SN. Gene silencing by adenovirus-delivered sirna. *FEBS Letters*. 2003;539:111-114

63. de Fougerolles A, Vornlocher, H., Maraganore, J., and Lieberman, J. Interfering with disease: A progress report on sirna therapeutics. *Nature Reviews: Drug Discovery*. 2007;6

64. Akinc A, Thomas M, Klibanov AM, Langer R. Exploring polyethylenimine-mediated DNA transfection and the proton sponge hypothesis. *The journal of gene medicine*. 2005;7:657-663

65. Pichon C, Goncalves, C., Midoux, P. Histidine-rich peptides and polymers for nucleic acids delivery. *Advanced drug delivery reviews*. 2001;53

66. Vandenbroucke RE, De Geest BG, Bonne S, Vinken M, Van Haecke T, Heimberg H, Wagner E, Rogiers V, De Smedt SC, Demeester J, Sanders NN. Prolonged gene silencing in hepatoma cells and primary hepatocytes after small interfering rna delivery with biodegradable poly(beta-amino esters). *The journal of gene medicine*. 2008;10:783-794

67. Zauner W, Ogris, M., Wagner, E. Polylysine-based transfection systems utilizing receptor-mediated delivery. *Advanced drug delivery reviews*. 1998;30

68. Noh SM, Han SE, Shim G, Lee KE, Kim CW, Han SS, Choi Y, Kim YK, Kim WK, Oh YK. Tocopheryl oligochitosan-based self assembling oligomersomes for sirna delivery. *Biomaterials*. 2011;32:849-857

69. Takeshita F, Minakuchi Y, Nagahara S, Honma K, Sasaki H, Hirai K, Teratani T, Namatame N, Yamamoto Y, Hanai K, Kato T, Sano A, Ochiya T. Efficient delivery of small interfering rna to bone-metastatic tumors by using atelocollagen in vivo. *Proceedings of the National Academy of Sciences of the United States of America*. 2005;102:12177-12182

70. Convertine AJ, Benoit DS, Duvall CL, Hoffman AS, Stayton PS. Development of a novel endosomolytic diblock copolymer for sirna delivery. *Journal of controlled release : official journal of the Controlled Release Society*. 2009;133:221-229

71. Li H, Yu SS, Miteva M, Nelson CE, Werfel T, Giorgio TD, Duvall CL. Matrix metalloproteinase responsive, proximity-activated polymeric nanoparticles for sirna delivery. *Advanced functional materials*. 2013;23:3040-3052

72. Li H, Miteva M, Kirkbride KC, Cheng MJ, Nelson CE, Simpson EM, Gupta MK, Duvall CL, Giorgio TD. Dual mmp7-proximity-activated and folate receptor-targeted nanoparticles for sirna delivery. *Biomacromolecules*. 2015;16:192-201

73. Miteva M, Kirkbride KC, Kilchrist KV, Werfel TA, Li H, Nelson CE, Gupta MK, Giorgio TD, Duvall CL. Tuning pegylation of mixed micelles to overcome intracellular and systemic sirna delivery barriers. *Biomaterials*. 2015;38:97-107

74. Green MD, Foster, A. A., Greco, C. T., Roy, R., Lehr, R. M. Epps III, T. H., Sullivan, M. O. Catch and release: Photocleavable cationic diblock copolymers as a potential platform for nucleic acid delivery. *Polymer Chemistry*. 2014;5

75. Kozielski KL, Tzeng, S. Y., Hurtado De Mendoza, B. A., Green, J. J. Bioreducible cationic polymer-based nanoparticles for efficient and environmentally triggered cytoplasmic sirna delivery to primary human brain cancer cells. *ACS Nano*. 2015;8

76. Jeong JH, Mok, H., Oh, Y., and Park, T.G. Sirna conjugate delivery systems. *Bioconjugate Chem*. 2009;20:5-14

77. Rajeev KG, Nair JK, Jayaraman M, Charisse K, Taneja N, O'Shea J, Willoughby JL, Yucius K, Nguyen T, Shulga-Morskaya S, Milstein S, Liebow A, Querbes W, Borodovsky A, Fitzgerald K, Maier MA, Manoharan M. Hepatocyte-specific delivery of sirnas conjugated to novel non-nucleosidic trivalent n-acetylgalactosamine elicits robust gene silencing in vivo. *Chembiochem : a European journal of chemical biology*. 2015;16:903-908

78. Matsuda S, Keiser K, Nair JK, Charisse K, Manoharan RM, Kretschmer P, Peng CG, A VKi, Kandasamy P, Willoughby JL, Liebow A, Querbes W, Yucius K, Nguyen T, Milstein S, Maier MA, Rajeev KG, Manoharan M. Sirna conjugates carrying sequentially assembled trivalent n-acetylgalactosamine linked through nucleosides elicit robust gene silencing in vivo in hepatocytes. *ACS chemical biology*. 2015;10:1181-1187

79. Peer DP, E. J., Morishita, Y., Carman, C. V., Shimaoka, M. Systemic leukocyte-directed sirna delivery revealing cyclin d1 as an anti-inflammatory target. *Science*. 2008;319:627-630

80. Lu H, Wang D, Kazane S, Javahishvili T, Tian F, Song F, Sellers A, Barnett B, Schultz PG. Site-specific antibody-polymer conjugates for sirna delivery. *Journal of the American Chemical Society*. 2013;135:13885-13891

81. Cuellar TL, Barnes D, Nelson C, Tanguay J, Yu SF, Wen X, Scales SJ, Gesch J, Davis D, van Brabant Smith A, Leake D, Vandlen R, Siebel CW. Systematic evaluation of antibody-mediated sirna delivery using an industrial platform of thiomab-sirna conjugates. *Nucleic Acids Res*. 2015;43:1189-1203

82. Zhou J, Li H, Li S, Zaia J, Rossi JJ. Novel dual inhibitory function aptamer-sirna delivery system for hiv-1 therapy. *Molecular therapy : the journal of the American Society of Gene Therapy*. 2008;16:1481-1489

83. De Coupade C, Fittipaldi A, Chagnas V, Michel M, Carlier S, Tasciotti E, Darmon A, Ravel D, Kearsey J, Giacca M, Cailler F. Novel human-derived cell-penetrating peptides for specific subcellular delivery of therapeutic biomolecules. *The Biochemical journal*. 2005;390:407-418

84. Holm T, Raagel H, Andaloussi SE, Hein M, Mae M, Pooga M, Langel U. Retro-inversion of certain cell-penetrating peptides causes severe cellular toxicity. *Biochimica et biophysica acta*. 2011;1808:1544-1551

85. Moschos SA, Jones SW, Perry MM, Williams AE, Erjefalt JS, Turner JJ, Barnes PJ, Sproat BS, Gait MJ, Lindsay MA. Lung delivery studies using sirna conjugated to tat(48-60) and penetratin reveal peptide induced reduction in gene expression and induction of innate immunity. *Bioconjugate chemistry*. 2007;18:1450-1459

86. Turner JJ, Jones S, Fabani MM, Ivanova G, Arzumanov AA, Gait MJ. Rna targeting with peptide conjugates of oligonucleotides, sirna and pna. *Blood cells, molecules & diseases*. 2007;38:1-7

87. Detzer A, Overhoff M, Wunsche W, Rompf M, Turner JJ, Ivanova GD, Gait MJ, Sczakiel G. Increased rnai is related to intracellular release of sirna via a covalently attached signal peptide. *Rna*. 2009;15:627-636

88. Alam MR, Ming X, Fisher M, Lackey JG, Rajeev KG, Manoharan M, Juliano RL. Multivalent cyclic rgd conjugates for targeted delivery of small interfering rna. *Bioconjugate chemistry*. 2011;22:1673-1681

89. GC T. Integrins: Molecular targets in cancer therapy. *Current Oncology Reports*. 2006;8

90. Hsu T MS. Delivery of sirna and other macromolecules into skin and cells using a peptide enhancer. *PNAS*. 2011;108

91. Nothisen M, Kotera, M., Voirin, E., Remy, J., Behr, J. Cationic sirnas provide carrier-free gene silencing in animal cells. *JACS Communications*. 2009;131:17730-17731

92. Perche P, Nothisen M, Bagilet J, Behr JP, Kotera M, Remy JS. Cell-penetrating cationic sirna and lipophilic derivatives efficient at nanomolar concentrations in the presence of serum and albumin. *Journal of controlled release : official journal of the Controlled Release Society*. 2013;170:92-98

93. Paris C, Moreau V, Deglane G, Karim L, Couturier B, Bonnet ME, Kedinger V, Messmer M, Bolcato-Bellemin AL, Behr JP, Erbacher P, Lenne-Samuel N. Conjugating

phosphospermines to sirnas for improved stability in serum, intracellular delivery and rnai-mediated gene silencing. *Molecular pharmaceutics*. 2012

94. Takemoto H, Miyata K, Hattori S, Ishii T, Suma T, Uchida S, Nishiyama N, Kataoka K. Acidic ph-responsive sirna conjugate for reversible carrier stability and accelerated endosomal escape with reduced ifnalpha-associated immune response. *Angewandte Chemie*. 2013;52:6218-6221

95. Jung S, Lee SH, Mok H, Chung HJ, Park TG. Gene silencing efficiency of sirna-peg conjugates: Effect of pegylation site and peg molecular weight. *Journal of controlled release : official journal of the Controlled Release Society*. 2010;144:306-313

96. Kim SH, Jeong JH, Lee SH, Kim SW, Park TG. Peg conjugated vegf sirna for anti-angiogenic gene therapy. *Journal of controlled release : official journal of the Controlled Release Society*. 2006;116:123-129

97. Kim HS, Son YJ, Yoo HS. Clustering sirna conjugates for mmp-responsive therapeutics in chronic wounds of diabetic animals. *Nanoscale*. 2016;8:13236-13244

98. Wu SY, McMillan NA. Lipidic systems for in vivo sirna delivery. *The AAPS journal*. 2009;11:639-652

99. Scientific T. Thermo scientific accell sirna delivery. 2013

100. Kuwahara H, Nishina K, Yoshida K, Nishina T, Yamamoto M, Saito Y, Piao W, Yoshida M, Mizusawa H, Yokota T. Efficient in vivo delivery of sirna into brain capillary endothelial cells along with endogenous lipoprotein. *Molecular therapy : the journal of the American Society of Gene Therapy*. 2011;19:2213-2221

101. Uno Y, Piao W, Miyata K, Nishina K, Mizusawa H, Yokota T. High-density lipoprotein facilitates in vivo delivery of alpha-tocopherol-conjugated short-interfering rna to the brain. *Human gene therapy*. 2011;22:711-719

102. Resh MD. Myristylation and palmitylation of src family members: The fats of the matter. *Cell*. 1994;76:411-413

103. Clements BA, Incani, V., Kucharski, C., Lavasanifar, A., Ritchie, B., Uludag, H. A comparative evaluation of poly-l-lysine-palmitic acid and lipofectamine 2000 for plasmid delivery to bone marrow stromal cells. *Biomaterials*. 2007;28:4693-4704

104. Pearce EJ, Magee, A. I., Smithers, S. R., Simpson, A. J. G. Sm25, a major schistosome tegumental glycoprotein, is dependent on palmitic acid for membrane attachment. *The EMBO Journal*. 1991;10:2741-2746

105. Xue HY, Liu S, Wong HL. Nanotoxicity: A key obstacle to clinical translation of sirna-based nanomedicine. *Nanomedicine*. 2014;9:295-312

106. Inoue T, Sugimoto M, Sakurai T, Saito R, Futaki N, Hashimoto Y, Honma Y, Arai I, Nakaike S. Modulation of scratching behavior by silencing an endogenous cyclooxygenase-1 gene in the skin through the administration of sirna. *The journal of gene medicine*. 2007;9:994-1001

107. Vicentini FT, Borgheti-Cardoso LN, Depieri LV, de Macedo Mano D, Abelha TF, Petrilli R, Bentley MV. Delivery systems and local administration routes for therapeutic sirna. *Pharmaceutical research*. 2013;30:915-931

108. Nelson CE, Kim AJ, Adolph EJ, Gupta MK, Yu F, Hocking KM, Davidson JM, Guelcher SA, Duvall CL. Tunable delivery of sirna from a biodegradable scaffold to promote angiogenesis in vivo. *Advanced materials*. 2014;26:607-614, 506

109. Layzer JM. In vivo activity of nuclease-resistant sirnas. *Rna*. 2004;10:766-771

110. Dimitrova M, Affolter C, Meyer F, Nguyen I, Richard DG, Schuster C, Bartenschlager R, Voegel JC, Ogier J, Baumert TF. Sustained delivery of sirnas targeting viral infection by cell-degradable multilayered polyelectrolyte films. *Proceedings of the National Academy of Sciences of the United States of America*. 2008;105:16320-16325

111. Laporte LD, Shea, L. D. Matrices and scaffolds for DNA delivery in tissue engineering. *Advanced drug delivery reviews*. 2007;59

112. Chen M, Gao, S., Dong, M., Song, J., Yang, C., Howard, K. A., Kjems, J., Besenbacher, F. Chitosan/sirna nanoparticles encapsulated in plga nanofibers for sirna delivery. *ACS Nano*. 2012;6

113. Klose D, Siepmann F, Elkharraz K, Krenzlin S, Siepmann J. How porosity and size affect the drug release mechanisms from plga-based microparticles. *International journal of pharmaceutics*. 2006;314:198-206

114. Tai H HD, Takae S, Wang W, Vermonden T, Hennink EW, Stayton PS, Hoffman AS, Endruweit A, Alexander C, Howdle SM, Shakesheff KM. Photo-cross-linked hydrogels from thermoresponsive pegmema-ppgma-egdma copolymers containing multiple methacrylate groups: Mechanical property, swelling, protein release, cytotoxicity. *Biomacromolecules*. 2009;10:2895-2903

115. Mann BK GA, Tsai AT, Schmelen RH, West JL. Smooth muscle cell growth in photopolymerized hydrogels with cell adhesive and proteolytically degradable domains: Synthetic ecm analogs for tissue engineering. *Biomaterials*. 2001;22

116. West JL, Hubbell, J. A. Polymeric biomaterials with degradation sites for proteases involved in cell migration. *Macromolecules*. 1999;32

117. Ma PX. Biomimetic materials for tissue engineering. *Advanced drug delivery reviews*. 2008;60:184-198

118. Shea LD, Smiley, E., Bonadio, J., Mooney, D. J. DNA delivery from polymer matrices for tissue engineering. *Nature biotechnology*. 1999;17

119. De Rosa G, Maiuri, M. C., Ungaro, F., De Stefano, D., Quaglia, F., La Rotonda, M. I., Carnuccio, R. Enhanced intracellular uptake and inhibition of nf-κb activation by decoy oligonucleotide released from plga microspheres. *The journal of gene medicine*. 2005;7

120. Estey T, Kang J, Schwendeman SP, Carpenter JF. Bsa degradation under acidic conditions: A model for protein instability during release from plga delivery systems. *Journal of pharmaceutical sciences*. 2006;95:1626-1639

121. Felix Lanao RP, Leeuwenburgh SC, Wolke JG, Jansen JA. In vitro degradation rate of apatitic calcium phosphate cement with incorporated plga microspheres. *Acta biomaterialia*. 2011;7:3459-3468

122. Martin JR, Gupta MK, Page JM, Yu F, Davidson JM, Guelcher SA, Duvall CL. A porous tissue engineering scaffold selectively degraded by cell-generated reactive oxygen species. *Biomaterials*. 2014;35:3766-3776

123. Wilson DS, Dalmasso, G., Wang, L., Sitaraman, S. V., Merlin, D., Murthy, N. Orally delivered thioketal nanoparticles loaded with tnf-α–sirna target inflammation and inhibit gene expression in the intestines. *Nature Materials*. 2010;9

124. Segura T, Shea, L. D. Surface-tethered DNA complexes for enhanced gene delivery. *Bioconjugate chemistry*. 2002;13

125. Place ES, Evans, N. D., Stevens, M. M. Complexity in biomaterials for tissue engineering. *Nature Materials*. 2009;8

126. Vinas-Castells R, Holladay, C., di Luca, A., Diaz, V. M.,, Pandit, A. Snail1 down-regulation using small interfering rna complexes delivered through collagen scaffolds. *Bioconjugate chemistry*. 2009;20

127. Salvay DM, Zelivyanskaya M, Shea LD. Gene delivery by surface immobilization of plasmid to tissue-engineering scaffolds. *Gene therapy*. 2010;17:1134-1141

128. Guelcher SA. Biodegradable polyurethanes: Synthesis and applications in regenerative medicine. *Tissue engineering. Part B, Reviews*. 2008;14:3-17

129. Hafeman AE, Li B, Yoshii T, Zienkiewicz K, Davidson JM, Guelcher SA. Injectable biodegradable polyurethane scaffolds with release of platelet-derived growth factor for tissue repair and regeneration. *Pharmaceutical research*. 2008;25:2387-2399

130. Li B, Brown KV, Wenke JC, Guelcher SA. Sustained release of vancomycin from polyurethane scaffolds inhibits infection of bone wounds in a rat femoral segmental

defect model. *Journal of controlled release : official journal of the Controlled Release Society*. 2010;145:221-230

131. Lei Y, Rahim M, Ng Q, Segura T. Hyaluronic acid and fibrin hydrogels with concentrated DNA/pei polyplexes for local gene delivery. *Journal of controlled release : official journal of the Controlled Release Society*. 2011;153:255-261

132. Andersen MO, Howard KA, Paludan SR, Besenbacher F, Kjems J. Delivery of sirna from lyophilized polymeric surfaces. *Biomaterials*. 2008;29:506-512

133. Lei Y, Huang S, Sharif-Kashani P, Chen Y, Kavehpour P, Segura T. Incorporation of active DNA/cationic polymer polyplexes into hydrogel scaffolds. *Biomaterials*. 2010;31:9106-9116

134. Nelson CE, Gupta MK, Adolph EJ, Shannon JM, Guelcher SA, Duvall CL. Sustained local delivery of sirna from an injectable scaffold. *Biomaterials*. 2012;33:1154-1161

135. Sen CK, Gordillo GM, Roy S, Kirsner R, Lambert L, Hunt TK, Gottrup F, Gurtner GC, Longaker MT. Human skin wounds: A major and snowballing threat to public health and the economy. *Wound repair and regeneration : official publication of the Wound Healing Society [and] the European Tissue Repair Society*. 2009;17:763-771

136. Duvall CL, Taylor WR, Weiss D, Wojtowicz AM, Guldberg RE. Impaired angiogenesis, early callus formation, and late stage remodeling in fracture healing of osteopontin-deficient mice. *Journal of bone and mineral research : the official journal of the American Society for Bone and Mineral Research*. 2007;22:286-297

137. Duvall CL, Taylor, R. W., Weiss, D., Guldberg, R. E. Quantitative microcomputed tomography analysis of collateral vessel development after ischemic injury. *American Journal of Physiology - Heart and Circulatory Physiology*. 2004;287:H302-H310

138. Falanga V. Wound healing and its impairment in the diabetic foot. *The Lancet*. 2005;366:1736-1743

139. Maxson S, Lopez EA, Yoo D, Danilkovitch-Miagkova A, Leroux MA. Concise review: Role of mesenchymal stem cells in wound repair. *Stem cells translational medicine*. 2012;1:142-149

140. Hehehberger K, Helborn, J. D., Brismar, K., Hansson, A. Inhibited proliferation of fibroblasts derived from chronic diabetic wounds and normal dermal flbroblasts treated with high glucose is associated with increased formation of l-lactate. *Wound Repair and Regeneration*. 1998;6

141. Tokatlian T, Cam C, Segura T. Non-viral DNA delivery from porous hyaluronic acid hydrogels in mice. *Biomaterials*. 2014;35:825-835

142. Jang JH, Rives CB, Shea LD. Plasmid delivery in vivo from porous tissue-engineering scaffolds: Transgene expression and cellular transfection. *Molecular therapy : the journal of the American Society of Gene Therapy*. 2005;12:475-483

143. Alfranca A. Vegf therapy: A timely retreat. *Cardiovascular research*. 2009;83:611-612

144. Brudno Y, Ennett-Shepard AB, Chen RR, Aizenberg M, Mooney DJ. Enhancing microvascular formation and vessel maturation through temporal control over multiple pro-angiogenic and pro-maturation factors. *Biomaterials*. 2013;34:9201-9209

145. Cheema SK, Chen E, Shea LD, Mathur AB. Regulation and guidance of cell behavior for tissue regeneration via the sirna mechanism. *Wound repair and regeneration : official publication of the Wound Healing Society [and] the European Tissue Repair Society*. 2007;15:286-295

146. Semenza GL. Regulation of oxygen homeostasis by hypoxia-inducible factor 1. *Physiology*. 2009;24:97-106

147. Agis H, Watzek G, Gruber R. Prolyl hydroxylase inhibitors increase the production of vascular endothelial growth factor by periodontal fibroblasts. *Journal of periodontal research*. 2012;47:165-173

148. Ceradini DJ, Kulkarni AR, Callaghan MJ, Tepper OM, Bastidas N, Kleinman ME, Capla JM, Galiano RD, Levine JP, Gurtner GC. Progenitor cell trafficking is regulated by hypoxic gradients through hif-1 induction of sdf-1. *Nature medicine*. 2004;10:858-864

149. Mazzone M, Dettori D, Leite de Oliveira R, Loges S, Schmidt T, Jonckx B, Tian YM, Lanahan AA, Pollard P, Ruiz de Almodovar C, De Smet F, Vinckier S, Aragones J, Debackere K, Luttun A, Wyns S, Jordan B, Pisacane A, Gallez B, Lampugnani MG, Dejana E, Simons M, Ratcliffe P, Maxwell P, Carmeliet P. Heterozygous deficiency of phd2 restores tumor oxygenation and inhibits metastasis via endothelial normalization. *Cell*. 2009;136:839-851

150. Thanik VD, Greives, M. R., Lerman, O. Z., Seiser, N., Dec, W., Chang C. C.,, Warren, S. M., Levine, J. P., Saadeh, P. B. Topical matrix-based sirna silences local gene expression in a murine wound model. *Gene therapy*. 2007;14

151. Vandegrift MT, Szpalski C, Knobel D, Weinstein A, Ham M, Ezeamuzie O, Warren SM, Saadeh PB. Acellular dermal matrix-based gene therapy augments graft incorporation. *The Journal of surgical research*. 2015;195:360-367

152. Nguyen PD, Tutela JP, Thanik VD, Knobel D, Allen RJ, Jr., Chang CC, Levine JP, Warren SM, Saadeh PB. Improved diabetic wound healing through topical silencing of p53 is associated with augmented vasculogenic mediators. *Wound repair and regeneration*

: official publication of the Wound Healing Society [and] the European Tissue Repair Society. 2010;18:553-559

153. Lee JW, Tutela, J. P., Zoumalan, R. A., Thanik, V. D., Nguyen, P. D., Varjabedian, L., Warren, S. M., Saadeh, P. B. Inhibition of smad3 expression in radiation-induced fibrosis using a novel method for topical transcutaneous gene therapy. *Arch Otolaryngol Head Neck Surg*. 2010;136

154. Wetterau M, George F, Weinstein A, Nguyen PD, Tutela JP, Knobel D, Cohen Ba O, Warren SM, Saadeh PB. Topical prolyl hydroxylase domain-2 silencing improves diabetic murine wound closure. *Wound repair and regeneration : official publication of the Wound Healing Society [and] the European Tissue Repair Society*. 2011;19:481-486

155. Weiser JR, Saltzman WM. Controlled release for local delivery of drugs: Barriers and models. *Journal of controlled release : official journal of the Controlled Release Society*. 2014;190:664-673

156. Naeye B, Deschout H, Caveliers V, Descamps B, Braeckmans K, Vanhove C, Demeester J, Lahoutte T, De Smedt SC, Raemdonck K. In vivo disassembly of iv administered sirna matrix nanoparticles at the renal filtration barrier. *Biomaterials*. 2013;34:2350-2358

157. Davis ME. Fighting cancer with nanoparticle medicines—the nanoscale matters. *MRS Bulletin*. 2012;37:828-835

158. Jere D, Xu CX, Arote R, Yun CH, Cho MH, Cho CS. Poly(beta-amino ester) as a carrier for si/shrna delivery in lung cancer cells. *Biomaterials*. 2008;29:2535-2547

159. Owens DE, 3rd, Peppas NA. Opsonization, biodistribution, and pharmacokinetics of polymeric nanoparticles. *International journal of pharmaceutics*. 2006;307:93-102

160. Yan X, Scherphof GL, Kamps JAAM. Liposome opsonization. *Journal of Liposome Research*. 2005;15:109-139

161. Poon Z, Lee JB, Morton SW, Hammond PT. Controlling in vivo stability and biodistribution in electrostatically assembled nanoparticles for systemic delivery. *Nano letters*. 2011;11:2096-2103

162. Gabizon A, Shmeeda H, Barenholz Y. Pharmacokinetics of pegylated liposomal doxorubicin. *Clinical Pharmacokinetics*. 2003;42:419-436

163. Godinho B, Ogier JR, Quinlan A, Darcy R, Griffin BT, Cryan JF, O'Driscoll CM. Pegylated cyclodextrins as novel sirna nanosystems: Correlationd between polyethylene glycol length and nanoparticle stability. *International journal of pharmaceutics*. 2014;473

164. Naeye B, Raemdonck K, Remaut K, Sproat B, Demeester J, De Smedt SC. Pegylation of biodegradable dextran nanogels for sirna delivery. *European journal of pharmaceutical sciences : official journal of the European Federation for Pharmaceutical Sciences*. 2010;40:342-351

165. Venkataraman S, Ong WL, Ong ZY, Joachim Loo SC, Rachel Ee PL, Yang YY. The role of peg architecture and molecular weight in the gene transfection performance of pegylated poly(dimethylaminoethyl methacrylate) based cationic polymers. *Biomaterials*. 2011;32:2369-2378

166. Zou H, Wang Z, Feng M. Nanocarriers with tunable surface properties to unblock bottlenecks in systemic drug and gene delivery. *Journal of controlled release : official journal of the Controlled Release Society*. 2015;214:121-133

167. Buyens K DSS, Braekmans K, Demeester J, Peeters L, van Grunsven LA, de Mollerat du Jeu X, Sawant R, Torchilin V, Farkasova K, Ogris M, Sanders NN. Liposome based systems for systemic sirna delivery: Stability in blood sets the requirements for optimal carrier design. *Journal of Controlled Release*. 2012;158

168. Takemoto H, Ishii A, Miyata K, Nakanishi M, Oba M, Ishii T, Yamasaki Y, Nishiyama N, Kataoka K. Polyion complex stability and gene silencing efficiency with a sirna-grafted polymer delivery system. *Biomaterials*. 2010;31:8097-8105

169. Wei H, Volpatti LR, Sellers DL, Maris DO, Andrews IW, Hemphill AS, Chan LW, Chu DS, Horner PJ, Pun SH. Dual responsive, stabilized nanoparticles for efficient in vivo plasmid delivery. *Angewandte Chemie*. 2013;52:5377-5381

170. Kim J, Sunshine JC, Green JJ. Differential polymer structure tunes mechanism of cellular uptake and transfection routes of poly(beta-amino ester) polyplexes in human breast cancer cells. *Bioconjugate chemistry*. 2014;25:43-51

171. Zhu X, Xu Y, Solis LM, Tao W, Wang L, Behrens C, Xu X, Zhao L, Liu D, Wu J, Zhang N, Wistuba II, Farokhzad OC, Zetter BR, Shi J. Long-circulating sirna nanoparticles for validating prohibitin1-targeted non-small cell lung cancer treatment. *Proceedings of the National Academy of Sciences*. 2015;112:7779-7784

172. Jia Z WL, Davis TP, Bulmus V. One-pot conversion of raft-generated multifunctional block copolymers of hpma to doxorubicin conjugated acid- and reductant-sensitive crosslinked micelles. *Biomacromolecules*. 2008;9

173. Matsumoto S CR, Nishiyama N, Miyata K, Ishii A, Oba M, Koyama H, Yamasaki Y, Kataoka K. Environment-responsive block copolymer micelles with a disulfide cross-linked core for enhanced sirna delivery. *Biomacromolecules*. 2009;10

174. Chen Y, Gu H, Zhang DS, Li F, Liu T, Xia W. Highly effective inhibition of lung cancer growth and metastasis by systemic delivery of sirna via multimodal mesoporous silica-based nanocarrier. *Biomaterials*. 2014;35:10058-10069

175. Zheng D, Giljohann D. A., Chen, D. L., Massich, M. D., Wang, X., Iordanov, H, Mirkin, C. A., Paller, A. S. Topical deliery of sirna-based spherical nucleic acid nanoparticle conjugates for gene regulation. *Proc Natl Acad Sci USA*. 2012

176. Wilhelm S, Tavares AJ, Dai Q, Ohta S, Audet J, Dvorak HF, Chan WCW. Analysis of nanoparticle delivery to tumours. *Nature Reviews Materials*. 2016;1:16014

177. Zhu C, Jung S, Luo S, Meng F, Zhu X, Park TG, Zhong Z. Co-delivery of sirna and paclitaxel into cancer cells by biodegradable cationic micelles based on pdmaema-pcl-pdmaema triblock copolymers. *Biomaterials*. 2010;31:2408-2416

178. Davis ME, Zuckerman JE, Choi CH, Seligson D, Tolcher A, Alabi CA, Yen Y, Heidel JD, Ribas A. Evidence of rnai in humans from systemically administered sirna via targeted nanoparticles. *Nature*. 2010;464:1067-1070

179. Corbet C, Ragelle H, Pourcelle V, Vanvarenberg K, Marchand-Brynaert J, Preat V, Feron O. Delivery of sirna targeting tumor metabolism using non-covalent pegylated chitosan nanoparticles: Identification of an optimal combination of ligand structure, linker and grafting method. *Journal of controlled release : official journal of the Controlled Release Society*. 2016;223:53-63

180. Huang L, Sullenger B, Juliano R. The role of carrier size in the pharmacodynamics of antisense and sirna oligonucleotides. *J Drug Target*. 2010;18:567-574

181. Alnylam rnai roundtable: Conjugate delivery. 2012

182. Coelho T, Adams D, Silva A, Lozeron P, Hawkins PN, Mant T, Perez J, Chiesa J, Warrington S, Tranter E, Munisamy M, Falzone R, Harrop J, Cehelsky J, Bettencourt BR, Geissler M, Butler JS, Sehgal A, Meyers RE, Chen Q, Borland T, Hutabarat RM, Clausen VA, Alvarez R, Fitzgerald K, Gamba-Vitalo C, Nochur SV, Vaishnaw AK, Sah DW, Gollob JA, Suhr OB. Safety and efficacy of rnai therapy for transthyretin amyloidosis. *The New England journal of medicine*. 2013;369:819-829

183. Bienk K, Hvam ML, Pakula MM, Dagnaes-Hansen F, Wengel J, Malle BM, Kragh-Hansen U, Cameron J, Bukrinski JT, Howard KA. An albumin-mediated cholesterol design-based strategy for tuning sirna pharmacokinetics and gene silencing. *Journal of controlled release : official journal of the Controlled Release Society*. 2016;232:143-151

184. Lau S, Graham B, Cao N, Boyd BJ, Pouton CW, White PJ. Enhanced extravasation, stability and in vivo cardiac gene silencing via in situ sirna-albumin conjugation. *Molecular pharmaceutics*. 2012;9:71-80

185. Anselmo AC, Mitragotri S. Nanoparticles in the clinic. *Bioengineering & Translational Medicine*. 2016;1:10-29

186. Bhattacharyya J, Bellucci JJ, Weitzhandler I, McDaniel JR, Spasojevic I, Li X, Lin CC, Chi JT, Chilkoti A. A paclitaxel-loaded recombinant polypeptide nanoparticle outperforms abraxane in multiple murine cancer models. *Nature communications*. 2015;6:7939

187. Lowy DR CF. Aiming high — changing the trajectory for cancer. *The New England journal of medicine*. 2016;374

188. Nichols JW, Bae YH. Epr: Evidence and fallacy. *Journal of controlled release : official journal of the Controlled Release Society*. 2014;190:451-464

189. Jain RK, Stylianopoulos T. Delivering nanomedicine to solid tumors. *Nature reviews. Clinical oncology*. 2010;7:653-664

190. Martin JD, Fukumura D, Duda DG, Boucher Y, Jain RK. Reengineering the tumor microenvironment to alleviate hypoxia and overcome cancer heterogeneity. *Cold Spring Harbor perspectives in medicine*. 2016;6

191. Prabhakar U, Maeda H, Jain RK, Sevick-Muraca EM, Zamboni W, Farokhzad OC, Barry ST, Gabizon A, Grodzinski P, Blakey DC. Challenges and key considerations of the enhanced permeability and retention effect for nanomedicine drug delivery in oncology. *Cancer research*. 2013;73:2412-2417

192. Danhier F. To exploit the tumor microenvironment: Since the epr effect fails in the clinic, what is the future of nanomedicine? *Journal of controlled release : official journal of the Controlled Release Society*. 2016;244:108-121

193. Teicher BA. Tumor models for efficacy determination. *Molecular cancer therapeutics*. 2006;5:2435-2443

194. DeRose YS, Gligorich KM, Wang G, Georgelas A, Bowman P, Courdy SJ, Welm AL, Welm BE. Patient-derived models of human breast cancer: Protocols for in vitro and in vivo applications in tumor biology and translational medicine. *Current protocols in pharmacology*. 2013;Chapter 14:Unit14 23

195. Hong AL, Tseng YY, Cowley GS, Jonas O, Cheah JH, Kynnap BD, Doshi MB, Oh C, Meyer SC, Church AJ, Gill S, Bielski CM, Keskula P, Imamovic A, Howell S, Kryukov GV, Clemons PA, Tsherniak A, Vazquez F, Crompton BD, Shamji AF, Rodriguez-Galindo C, Janeway KA, Roberts CW, Stegmaier K, van Hummelen P, Cima MJ, Langer RS, Garraway LA, Schreiber SL, Root DE, Hahn WC, Boehm JS. Integrated genetic and pharmacologic interrogation of rare cancers. *Nature communications*. 2016;7:11987

196. Eliasof S, Lazarus D, Peters CG, Case RI, Cole RO, Hwang J, Schluep T, Chao J, Lin J, Yen Y, Han H, Wiley DT, Zuckerman JE, Davis ME. Correlating preclinical animal studies and human clinical trials of a multifunctional, polymeric nanoparticle. *Proceedings of the National Academy of Sciences of the United States of America*. 2013;110:15127-15132

197. Kai MP, Brighton HE, Fromen CA, Shen TW, Luft JC, Luft YE, Keeler AW, Robbins GR, Ting JP, Zamboni WC, Bear JE, DeSimone JM. Tumor presence induces global immune changes and enhances nanoparticle clearance. *ACS Nano*. 2016;10:861-870

198. Dong Y LK, Dorkin JR, Sirirungruang S, Zhang Y, Chen D, Bogorad RL, Yin H, Chen Y, Vegas AJ, Alabi CA, Sahay G, Olejnik KT, Wang W, Schroeder A, Lytton-Jean AKR, Siegwart DJ, Akin A, Barnes C, Barros SA, Carioto M, Fitzgerald K, Hettinger J, Kumar V, Novobrantseva TI, Qin J, Querbes W, Koteliansky V, Langer R, Anderson DG. Lipopeptide nanoparticles for potent and selective sirna delivery in rodents and nonhuman primates. *PNAS*. 2014;111

199. Reuter KG, Perry JL, Kim D, Luft JC, Liu R, DeSimone JM. Targeted print hydrogels: The role of nanoparticle size and ligand density on cell association, biodistribution, and tumor accumulation. *Nano letters*. 2015;15:6371-6378

200. Wong C ST, Cui J, Martin J, Chauhanb VP, Jiang W, Popovi Z, Jain RK, Bawendi MG, Fukumura D. Multistage nanoparticle delivery system for deep penetration into tumor tissue. *PNAS*. 2011;108

201. Tong R LR. Nanomedicines targeting the tumor microenvironment. *The Cancer Journal*. 2015;21

202. Clark AJ WD, Zuckerman JE, Webster P, Chao J, Lin J, Yen Y, Davis ME. Crlx101 nanoparticles localize in human tumors and not in adjacent, nonneoplastic tissue after intravenous dosing. *PNAS*. 2016;113

203. Qin S, Fite BZ, Gagnon MK, Seo JW, Curry FR, Thorsen F, Ferrara KW. A physiological perspective on the use of imaging to assess the in vivo delivery of therapeutics. *Annals of biomedical engineering*. 2014;42:280-298

204. Barata P SA, Hong DS. Rna-targeted therapeutics in cancer clinical trials: Current status and future directions. *Cancer Treatment Reviews*. 2016;50

205. Bae YH, Park K. Targeted drug delivery to tumors: Myths, reality and possibility. *Journal of controlled release : official journal of the Controlled Release Society*. 2011;153:198-205

206. Tseng YC, Mozumdar S, Huang L. Lipid-based systemic delivery of sirna. *Advanced drug delivery reviews*. 2009;61:721-731

207. Rettig GR, Behlke MA. Progress toward in vivo use of sirnas-ii. *Molecular therapy : the journal of the American Society of Gene Therapy*. 2012;20:483-512

208. Tzeng SY, Hung BP, Grayson WL, Green JJ. Cystamine-terminated poly(beta-amino ester)s for sirna delivery to human mesenchymal stem cells and enhancement of osteogenic differentiation. *Biomaterials*. 2012;33:8142-8151

209. Frank-Kamenetsky M, Grefhorst A, Anderson NN, Racie TS, Bramlage B, Akinc A, Butler D, Charisse K, Dorkin R, Fan Y, Gamba-Vitalo C, Hadwiger P, Jayaraman M, John M, Jayaprakash KN, Maier M, Nechev L, Rajeev KG, Read T, Rohl I, Soutschek J, Tan P, Wong J, Wang G, Zimmermann T, de Fougerolles A, Vornlocher HP, Langer R, Anderson DG, Manoharan M, Koteliansky V, Horton JD, Fitzgerald K. Therapeutic rnai targeting pcsk9 acutely lowers plasma cholesterol in rodents and ldl cholesterol in nonhuman primates. *Proceedings of the National Academy of Sciences of the United States of America*. 2008;105:11915-11920

210. Benoit DS, Boutin ME. Controlling mesenchymal stem cell gene expression using polymer-mediated delivery of sirna. *Biomacromolecules*. 2012;13:3841-3849

211. Nakayama T, Butler JS, Sehgal A, Severgnini M, Racie T, Sharman J, Ding F, Morskaya SS, Brodsky J, Tchangov L, Kosovrasti V, Meys M, Nechev L, Wang G, Peng CG, Fang Y, Maier M, Rajeev KG, Li R, Hettinger J, Barros S, Clausen V, Zhang X, Wang Q, Hutabarat R, Dokholyan NV, Wolfrum C, Manoharan M, Kotelianski V, Stoffel M, Sah DW. Harnessing a physiologic mechanism for sirna delivery with mimetic lipoprotein particles. *Molecular therapy : the journal of the American Society of Gene Therapy*. 2012;20:1582-1589

212. Shen X, Wan, C., Ramaswamy, G., Mavalli, M., Wang, Y., Duvall, C. L., Deng, L. F., Guldberg, R. E., Eberhart, A., Clemens, T. L., Gilbert, S. R. Prolyl hydroxylase inhibitors increase neoangiogenesis and callus formation following femur fracture in mice. *Journal of Orthopaedic Research*. 2009

213. HoWangYin KY, Loinard C, Bakker W, Guerin CL, Vilar J, D'Audigier C, Mauge L, Bruneval P, Emmerich J, Levy BI, Pouyssegur J, Smadja DM, Silvestre JS. Hif-prolyl hydroxylase 2 inhibition enhances the efficiency of mesenchymal stem cell-based therapies for the treatment of critical limb ischemia. *Stem cells*. 2014;32:231-243

214. Evans BC, Nelson CE, Yu SS, Beavers KR, Kim AJ, Li H, Nelson HM, Giorgio TD, Duvall CL. Ex vivo red blood cell hemolysis assay for the evaluation of ph-responsive endosomolytic agents for cytosolic delivery of biomacromolecular drugs. 2013:e50166

215. Liu H, Li Y, Mozhi A, Zhang L, Liu Y, Xu X, Xing J, Liang X, Ma G, Yang J, Zhang X. Sirna-phospholipid conjugates for gene and drug delivery in cancer treatment. *Biomaterials*. 2014;35:6519-6533

216. Oba M, Miyata K, Osada K, Christie RJ, Sanjoh M, Li W, Fukushima S, Ishii T, Kano MR, Nishiyama N, Koyama H, Kataoka K. Polyplex micelles prepared from omega-cholesteryl peg-polycation block copolymers for systemic gene delivery. *Biomaterials*. 2011;32:652-663

217. Schade M, Berti D, Huster D, Herrmann A, Arbuzova A. Lipophilic nucleic acids--a flexible construction kit for organization and functionalization of surfaces. *Advances in colloid and interface science*. 2014;208:235-251

218. Haleem-Smith H, Derfoul, A., Okafor, C., Tuli, R., Olsen, D., Hall, D. J., Tuan, R. S. Optimization of high-efficiency transfection of adult human mesenchymal stem cells in vitro. *Molecular Biotechnology*. 2005;30

219. Reilly MJ, Larsen JD, Sullivan MO. Polyplexes traffic through caveolae to the golgi and endoplasmic reticulum en route to the nucleus. *Molecular pharmaceutics*. 2012;9:1280-1290

220. Khalil IA, Kogure K, Akita H, Harashima H. Uptake pathways and subsequent intracellular trafficking in nonviral gene delivery. *Pharmacological reviews*. 2006;58:32-45

221. Naeye B, Deschout H, Caveliers V, Descamps B, Braeckmans K, Vanhove C, Demeester J, Lahoutte T, De Smedt SC, Raemdonck K. In vivo disassembly of iv administered sirna matrix nanoparticles at the renal filtration barrier. *Biomaterials*. 2013;34:2350-2358

222. Pun SH, Davis ME. Development of a nonviral gene delivery vehicle for systemic application. *Bioconjugate Chemistry*. 2002;13:630-639

223. Yin H, Kanasty RL, Eltoukhy AA, Vegas AJ, Dorkin JR, Anderson DG. Non-viral vectors for gene-based therapy. *Nature reviews. Genetics*. 2014;15:541-555

224. Poon Z, Chang D, Zhao X, Hammond PT. Layer-by-layer nanoparticles with a ph-sheddable layer for in vivo targeting of tumor hypoxia. *ACS Nano*. 2011;5:4284-4292

225. Wei H, Volpatti LR, Sellers DL, Maris DO, Andrews IW, Hemphill AS, Chan LW, Chu DSH, Horner PJ, Pun SH. Dual responsive, stabilized nanoparticles for efficient in vivo plasmid delivery. *Angewandte Chemie International Edition*. 2013;52:5377-5381

226. Foster AA, Greco CT, Green MD, Epps TH, Sullivan MO. Light-mediated activation of sirna release in diblock copolymer assemblies for controlled gene silencing. *Advanced Healthcare Materials*. 2015;4:760-770

227. Yasuda M, Gan L, Chen B, Kadirvel S, Yu C, Phillips JD, New MI, Liebow A, Fitzgerald K, Querbes W, Desnick RJ. Rnai-mediated silencing of hepatic alas1 effectively prevents and treats the induced acute attacks in acute intermittent porphyria mice. *Proceedings of the National Academy of Sciences of the United States of America*. 2014;111:7777-7782

228. Lammers T, Rizzo LY, Storm G, Kiessling F. Personalized nanomedicine. *Clinical Cancer Research*. 2012;18:4889-4894

229. Hansen AE, Petersen AL, Henriksen JR, Boerresen B, Rasmussen P, Elema DR, Rosenschöld PMa, Kristensen AT, Kjær A, Andresen TL. Positron emission

tomography based elucidation of the enhanced permeability and retention effect in dogs with cancer using copper-64 liposomes. *ACS Nano*. 2015;9:6985-6995

230. Papahadjopoulos D, Allen TM, Gabizon A, Mayhew E, Matthay K, Huang SK, Lee KD, Woodle MC, Lasic DD, Redemann C. Sterically stabilized liposomes: Improvements in pharmacokinetics and antitumor therapeutic efficacy. *Proceedings of the National Academy of Sciences*. 1991;88:11460-11464

231. Torchilin V. Tumor delivery of macromolecular drugs based on the epr effect. *Adv Drug Deliv Rev*. 2011;63:131-135

232. Maeda H, Nakamura H, Fang J. The epr effect for macromolecular drug delivery to solid tumors: Improvement of tumor uptake, lowering of systemic toxicity, and distinct tumor imaging in vivo. *Adv Drug Deliv Rev*. 2013;65:71-79

233. Mishra S, Webster P, Davis ME. Pegylation significantly affects cellular uptake and intracellular trafficking of non-viral gene delivery particles. *European Journal of Cell Biology*. 2004;83:97-111

234. Sato A, Choi SW, Hirai M, Yamayoshi A, Moriyama R, Yamano T, Takagi M, Kano A, Shimamoto A, Maruyama A. Polymer brush-stabilized polyplex for a sirna carrier with long circulatory half-life. *Journal of Controlled Release*. 2007;122:209-216

235. Merkel OM, Librizzi D, Pfestroff A, Schurrat T, Buyens K, Sanders NN, De Smedt SC, Béhé M, Kissel T. Stability of sirna polyplexes from poly(ethylenimine) and poly(ethylenimine)-g-poly(ethylene glycol) under in vivo conditions: Effects on pharmacokinetics and biodistribution measured by fluorescence fluctuation spectroscopy and single photon emission computed tomography (spect) imaging. *Journal of Controlled Release*. 2009;138:148-159

236. Deng ZJ, Morton SW, Ben-Akiva E, Dreaden EC, Shopsowitz KE, Hammond PT. Layer-by-layer nanoparticles for systemic codelivery of an anticancer drug and sirna for potential triple-negative breast cancer treatment. *ACS Nano*. 2013;7:9571-9584

237. Nelson CE, Kintzing JR, Hanna A, Shannon JM, Gupta MK, Duvall CL. Balancing cationic and hydrophobic content of pegylated sirna polyplexes enhances endosome escape, stability, blood circulation time, and bioactivity in vivo. *ACS Nano*. 2013;7:8870-8880

238. Sarett SM, Kilchrist KV, Miteva M, Duvall CL. Conjugation of palmitic acid improves potency and longevity of sirna delivered via endosomolytic polymer nanoparticles. *Journal of biomedical materials research. Part A*. 2015

239. Sunshine JC, Akanda MI, Li D, Kozielski KL, Green JJ. Effects of base polymer hydrophobicity and end-group modification on polymeric gene delivery. *Biomacromolecules*. 2011;12:3592-3600

240. Bishop CJ, Abubaker-Sharif B, Guiriba T, Tzeng SY, Green JJ. Gene delivery polymer structure-function relationships elucidated via principal component analysis. *Chemical Communications*. 2015;51:12134-12137

241. Chiefari J, Chong YK, Ercole F, Krstina J, Jeffery J, Le TPT, Mayadunne RTA, Meijs GF, Moad CL, Moad G, Rizzardo E, Thang SH. Living free-radical polymerization by reversible addition−fragmentation chain transfer: The raft process. *Macromolecules*. 1998;31:5559-5562

242. He C, Hu Y, Yin L, Tang C, Yin C. Effects of particle size and surface charge on cellular uptake and biodistribution of polymeric nanoparticles. *Biomaterials*. 2010;31:3657-3666

243. Tang L, Fan TM, Borst LB, Cheng J. Synthesis and biological response of size-specific, monodisperse drug–silica nanoconjugates. *ACS Nano*. 2012;6:3954-3966

244. Gratton SEA, Ropp PA, Pohlhaus PD, Luft JC, Madden VJ, Napier ME, DeSimone JM. The effect of particle design on cellular internalization pathways. *Proceedings of the National Academy of Sciences*. 2008;105:11613-11618

245. Perry JL, Reuter KG, Kai MP, Herlihy KP, Jones SW, Luft JC, Napier M, Bear JE, DeSimone JM. Pegylated print nanoparticles: The impact of peg density on protein binding, macrophage association, biodistribution, and pharmacokinetics. *Nano Letters*. 2012;12:5304-5310

246. Anselmo AC, Zhang M, Kumar S, Vogus DR, Menegatti S, Helgeson ME, Mitragotri S. Elasticity of nanoparticles influences their blood circulation, phagocytosis, endocytosis, and targeting. *ACS Nano*. 2015;9:3169-3177

247. Nam HY, Kwon SM, Chung H, Lee S-Y, Kwon S-H, Jeon H, Kim Y, Park JH, Kim J, Her S, Oh Y-K, Kwon IC, Kim K, Jeong SY. Cellular uptake mechanism and intracellular fate of hydrophobically modified glycol chitosan nanoparticles. *Journal of Controlled Release*. 2009;135:259-267

248. Sahay G, Querbes W, Alabi C, Eltoukhy A, Sarkar S, Zurenko C, Karagiannis E, Love K, Chen D, Zoncu R, Buganim Y, Schroeder A, Langer R, Anderson DG. Efficiency of sirna delivery by lipid nanoparticles is limited by endocytic recycling. *Nat Biotech*. 2013;31:653-658

249. Werfel TA, Swain C, Nelson CE, Kilchrist KV, Evans BC, Miteva M, Duvall CL. Hydrolytic charge-reversal of pegylated polyplexes enhances intracellular un-packaging and activity of sirna. *Journal of Biomedical Materials Research Part A*. 2016;104:917-927

250. Evans BC HK, Osgood MJ, Voskresensky I, Dmowska J, Kilchrist KV, Brophy CM, Duvall, CL. Mk2 inhibitory peptide delivered in nanopolyplexes prevents vascular graft intimal hyperplasia. *Science Translational Medicine*. 2015;7

251. Gabizon A, Shmeeda H, Horowitz AT, Zalipsky S. Tumor cell targeting of liposome-entrapped drugs with phospholipid-anchored folic acid–peg conjugates. *Advanced drug delivery reviews*. 2004;56:1177-1192

252. Choi KY, Chung H, Min KH, Yoon HY, Kim K, Park JH, Kwon IC, Jeong SY. Self-assembled hyaluronic acid nanoparticles for active tumor targeting. *Biomaterials*. 2010;31:106-114

253. Arap W, Pasqualini R, Ruoslahti E. Cancer treatment by targeted drug delivery to tumor vasculature in a mouse model. *Science*. 1998;279:377-380

254. Bellocq NC, Pun SH, Jensen GS, Davis ME. Transferrin-containing, cyclodextrin polymer-based particles for tumor-targeted gene delivery. *Bioconjugate chemistry*. 2003;14:1122-1132

255. Davis ME, Zuckerman JE, Choi CHJ, Seligson D, Tolcher A, Alabi CA, Yen Y, Heidel JD, Ribas A. Evidence of rnai in humans from systemically administered sirna via targeted nanoparticles. *Nature*. 2010;464:1067-1070

256. Pollaro L, Heinis C. Strategies to prolong the plasma residence time of peptide drugs. *MedChemComm*. 2010;1:319

257. Sarett S, Werfel TA, Chandra I, Jackson MA, Kavanaugh TE, Hattaway ME, Giorgio TD, Duvall CL. Hydrophobic interactions between polymeric carrier and palmitic acid-conjugated sirna improve pegylated polyplex stability and enhance in vivo pharmacokinetics and tumor gene silencing. *Biomaterials*.

258. Lv H, Zhang S, Wang B, Cui S, Yan J. Toxicity of cationic lipids and cationic polymers in gene delivery. *Journal of controlled release : official journal of the Controlled Release Society*. 2006;114:100-109

259. Ostergaard ME, Yu J, Kinberger GA, Wan WB, Migawa MT, Vasquez G, Schmidt K, Gaus HJ, Murray HM, Low A, Swayze EE, Prakash TP, Seth PP. Efficient synthesis and biological evaluation of 5'-galnac conjugated antisense oligonucleotides. *Bioconjugate chemistry*. 2015;26:1451-1455

260. Lorenz C, Hadwiger P, John M, Vornlocher HP, Unverzagt C. Steroid and lipid conjugates of sirnas to enhance cellular uptake and gene silencing in liver cells. *Bioorganic & medicinal chemistry letters*. 2004;14:4975-4977

261. Dobrovolskaia MA AP, Hall JB, McNeil SE. Preclinical studies to understand nanoparticle interaction with the immune system and its potential effects on nanoparticle biodistribution. *Molecular pharmaceutics*. 2008;5

262. Shi J XZ, Kamaly N, Farokhzad OC. Self-assembled targeted nanoparticles: Evolution of technologies and bench to bedside transition. *Acc Chem Res*. 2011;44

263. Commisso C, Davidson SM, Soydaner-Azeloglu RG, Parker SJ, Kamphorst JJ, Hackett S, Grabocka E, Nofal M, Drebin JA, Thompson CB, Rabinowitz JD, Metallo CM, Vander Heiden MG, Bar-Sagi D. Macropinocytosis of protein is an amino acid supply route in ras-transformed cells. *Nature*. 2013;497:633-637

264. Kamphorst JJ, Nofal M, Commisso C, Hackett SR, Lu W, Grabocka E, Vander Heiden MG, Miller G, Drebin JA, Bar-Sagi D, Thompson CB, Rabinowitz JD. Human pancreatic cancer tumors are nutrient poor and tumor cells actively scavenge extracellular protein. *Cancer research*. 2015;75:544-553

265. Liu H, Moynihan KD, Zheng Y, Szeto GL, Li AV, Huang B, Van Egeren DS, Park C, Irvine DJ. Structure-based programming of lymph-node targeting in molecular vaccines. *Nature*. 2014;507:519-522

266. Levy OE, Jodka CM, Ren SS, Mamedova L, Sharma A, Samant M, D'Souza LJ, Soares CJ, Yuskin DR, Jin LJ, Parkes DG, Tatarkiewicz K, Ghosh SS. Novel exenatide analogs with peptidic albumin binding domains: Potent anti-diabetic agents with extended duration of action. *PloS one*. 2014;9:e87704

267. Chen H, Wang G, Lang L, Jacobson O, Kiesewetter DO, Liu Y, Ma Y, Zhang X, Wu H, Zhu L, Niu G, Chen X. Chemical conjugation of evans blue derivative: A strategy to develop long-acting therapeutics through albumin binding. *Theranostics*. 2016;6:243-253

268. Gupta MK, Meyer TA, Nelson CE, Duvall CL. Poly(ps-b-dma) micelles for reactive oxygen species triggered drug release. *Journal of controlled release : official journal of the Controlled Release Society*. 2012;162:591-598

269. Fowler SD GP. Application of nile red, a fluorescent hydrophobic probe, for the direction of neutral lipid deposits in tissue sections. *The Journal of Histochemistry and Cytochemistry*. 1985;33

270. Coutinho PJG CE, Ceu Rei M, Real Oliveira MECD. Nile red and dcm fluorescence anisotropy studies in c12e7/dppc mixed systems. *J Phys Chem B*. 2002;106

271. Debnath J, Muthuswamy SK, Brugge JS. Morphogenesis and oncogenesis of mcf-10a mammary epithelial acini grown in three-dimensional basement membrane cultures. *Methods*. 2003;30:256-268

272. Brantley-Sieders DM, Dunaway CM, Rao M, Short S, Hwang Y, Gao Y, Li D, Jiang A, Shyr Y, Wu JY, Chen J. Angiocrine factors modulate tumor proliferation and motility through epha2 repression of slit2 tumor suppressor function in endothelium. *Cancer research*. 2011;71:976-987

273. Sidi AA, Ohana P, Benjamin S, Shalev M, Ransom JH, Lamm D, Hochberg A, Leibovitch I. Phase i/ii marker lesion study of intravesical bc-819 DNA plasmid in h19 over

expressing superficial bladder cancer refractory to bacillus calmette-guerin. *The Journal of urology*. 2008;180:2379-2383

274. McArthur MJ AB, Frolov A, Foxworth WD, Kier AB, Schroeder F. Cellular uptake and intracellular trafficking of long chain fatty acids. *Journal of Lipid Research*. 1999;40

275. Trigatti BL GG. A direct role for serum albumin in the cellular uptake of long-chain fatty acids. *The Biochemical journal*. 1995;306

276. Park J, Park J, Pei Y, Xu J, Yeo Y. Pharmacokinetics and biodistribution of recently-developed sirna nanomedicines. *Advanced drug delivery reviews*. 2016;104:93-109

277. Lee MS, Lee JE, Byun E, Kim NW, Lee K, Lee H, Sim SJ, Lee DS, Jeong JH. Target-specific delivery of sirna by stabilized calcium phosphate nanoparticles using dopa-hyaluronic acid conjugate. *Journal of controlled release : official journal of the Controlled Release Society*. 2014;192:122-130

278. Choi KY SO, Huang X, Min KH, Howard GP, Hida N, Jin AJ, Carvajal N, Lee SW, Hong J, Chen X. Versatile rna interference nanoplatform for systemic delivery of rnas. *ACS Nano*. 2014;8

279. Zhu X, Xu Y, Solis LM, Tao W, Wang L, Behrens C, Xu X, Zhao L, Liu D, Wu J, Zhang N, Wistuba, II, Farokhzad OC, Zetter BR, Shi J. Long-circulating sirna nanoparticles for validating prohibitin1-targeted non-small cell lung cancer treatment. *Proceedings of the National Academy of Sciences of the United States of America*. 2015;112:7779-7784

280. Bartlett DW, Su H, Hildebrandt IJ, Weber WA, Davis ME. Impact of tumor-specific targeting on the biodistribution and efficacy of sirna nanoparticles measured by multimodality in vivo imaging. *Proceedings of the National Academy of Sciences of the United States of America*. 2007;104:15549-15554

281. Nagy JA, Feng D, Vasile E, Wong WH, Shih SC, Dvorak AM, Dvorak HF. Permeability properties of tumor surrogate blood vessels induced by vegf-a. *Laboratory investigation; a journal of technical methods and pathology*. 2006;86:767-780

282. Kane RS. Thermodynamics of multivalent interactions: Influence of the linker. *Langmuir : the ACS journal of surfaces and colloids*. 2010;26:8636-8640

283. Marie E, Sagan S, Cribier S, Tribet C. Amphiphilic macromolecules on cell membranes: From protective layers to controlled permeabilization. *The Journal of membrane biology*. 2014;247:861-881

284. Martin JR, Nelson CE, Gupta MK, Yu F, Sarett SM, Hocking KM, Pollins AC, Nanney LB, Davidson JM, Guelcher SA, Duvall CL. Local delivery of phd2 sirna from ros-degradable scaffolds to promote diabetic wound healing. *Advanced healthcare materials*. 2016;5:2751-2757

285. Lin E-W, Maynard HD. Grafting fromsmall interfering ribonucleic acid (sirna) as an alternative synthesis route to sirna–polymer conjugates. *Macromolecules*. 2015;48:5640-5647

286. Takemoto H, Miyata K, Ishii T, Hattori S, Osawa S, Nishiyama N, Kataoka K. Accelerated polymer-polymer click conjugation by freeze-thaw treatment. *Bioconjugate chemistry*. 2012;23:1503-1506

287. Chapman R GA, Stenzel MH, Stevens MM. Combinatorial low-volume synthesis of well-defined polymers by enzyme degassing. *Angewandte Chemie*. 2016;128

288. Burnett JC, Rossi JJ, Tiemann K. Current progress of sirna/shrna therapeutics in clinical trials. *Biotechnology journal*. 2011;6:1130-1146

289. Bennett CF, Baker BF, Pham N, Swayze E, Geary RS. Pharmacology of antisense drugs. *Annual review of pharmacology and toxicology*. 2017;57:81-105

290. (2008) ADEToaIIoS-iPWSCNCStA-RMDAA.

291. Ozcan G, Ozpolat B, Coleman RL, Sood AK, Lopez-Berestein G. Preclinical and clinical development of sirna-based therapeutics. *Advanced drug delivery reviews*. 2015;87:108-119

292. Wu SY, Yang X, Gharpure KM, Hatakeyama H, Egli M, McGuire MH, Nagaraja AS, Miyake TM, Rupaimoole R, Pecot CV, Taylor M, Pradeep S, Sierant M, Rodriguez-Aguayo C, Choi HJ, Previs RA, Armaiz-Pena GN, Huang L, Martinez C, Hassell T, Ivan C, Sehgal V, Singhania R, Han HD, Su C, Kim JH, Dalton HJ, Kovvali C, Keyomarsi K, McMillan NA, Overwijk WW, Liu J, Lee JS, Baggerly KA, Lopez-Berestein G, Ram PT, Nawrot B, Sood AK. 2'-ome-phosphorodithioate-modified sirnas show increased loading into the risc complex and enhanced anti-tumour activity. *Nature communications*. 2014;5:3459